VIRGINIA POLYTECHNIC INSTITUTE
AND STATE UNIVERSITY

The Charles E. Via, Jr. Department
of Civil and Environmental Engineering
Blacksburg, VA 24061

Structural Engineering and Materials

DEVELOPING AND VALIDATING NEW BOLTED END-PLATE MOMENT CONNECTION CONFIGURATIONS

by
Nonish Jain
Graduate Research Assistant

Matthew R. Eatherton
Assistant Professor

Thomas M. Murray
Emeritus Professor

Report No. CE/VPI-ST-15/08

July 2015

EXECUTIVE SUMMARY

End-plate moment connections are widely used, especially in metal buildings, between rafters (beams) and columns or at splice connections in rafters. References such as the AISC Design Guide 16 entitled "Flush and Extended Multiple-Row Moment End-Plate Connections" present design procedures, supported by physical experiments, to design these connections. It is desirable to develop and validate design procedures for additional end-plate moment connections, particularly those with larger moment capacity.

In this report, four connection configurations are investigated. The selected end-plate configurations include eight-bolt extended four wide, eight-bolt extended stiffened, six bolt flush unstiffened, and twelve bolt extended unstiffened. Design procedures and some previous test data was available for the first two configurations, whereas no prior investigation was found in the literature for the latter two configurations.

Design procedures including yield line analysis and bolt force models were proposed to calculate moment capacity associated with end-plate yielding, moment capacity for bolt rupture with prying action, and moment capacity for bolt rupture without prying action. Similar to the existing design approach for end-plate moment connections found in Design Guide 16, the design procedures are separated into thin end-plate behavior (the end-plate yields and then bolts fracture with prying action) and thick end-plate behavior (where end-plate yielding is prevented and bolts fracture without prying action). Design procedures found in the literature for the eight-bolt extended four wide and eight-bolt extended stiffened configurations were evaluated and modifications were proposed as necessary.

Experimental data found in the literature for the eight-bolt extended four wide and eight-bolt extended stiffened end-plate configurations was analyzed and compared to moment capacities calculated using the proposed design procedures. For the eight-bolt extended four wide configuration, it was found that the experimental data from the literature corroborated the calculated moment capacities for a range of rafter depth and end-plate thickness. It was therefore concluded that no additional tests were required. For

the eight-bolt extended stiffened configuration, reasonable match was found between the reported experimental data and predicted moment capacities, but the previous tested beam specimens did not exceed 36 inches depth. It was decided that two additional tests with deeper rafter sections (56 in. deep) would be useful in validating the design procedures for a wider range of rafter depth.

A full-scale testing program was conducted including ten specimens that used three different end-plate moment connection configurations. Four specimens were designed for each of the two new configurations (six bolt flush unstiffened and twelve bolt multiple row extended unstiffened) such that there was a shallow rafter (36 in.) and deep rafter (60 in.) specimen predicted to exhibit both thin end-plate and a thick end-plate behavior. Also, two deep rafter (56 in.) specimens were tested with the eight-bolt extended stiffened configuration, one with thin end-plate and one with thick end-plate.

The design procedures for all four investigated end-plate moment connection configurations appear reasonable. For the tested configurations, the predicted moment capacity associated with end-plate yielding was 5% smaller than the yield moment obtained during the test (conservative). The predicted moment capacities associated with bolt rupture were an average of 12% less than the experimentally obtained ultimate moment capacities. This conservatism in bolt rupture prediction was in part due to the use of nominal bolt strength in the calculations which is typically notably smaller than actual bolt strength.

ACKNOWLEDGEMENTS

This project was funded by the Metal Building Manufacturers Association (MBMA). The advice and suggestions by the MBMA connection steering committee throughout the project was invaluable. Also, thanks to American Buildings and Bluescope Buildings for donating the test specimens.

Phillip Bellis conducted some of the initial investigation. Valuable assistance in the preparation and conducting of tests was provided by David Mokarem, Dennis Huffman and Brett Farmer. Students that helped with this research include Michael Wood, William McNally, Ebrahim Jumaan, Abhilasha Maurya, Patrick O'Brien, Eric Bianchi, Steve Florig, and Osama Bukhamseen.

TABLE OF CONTENTS

1. INTRODUCTION

1.1.Motivation and Background

In the United States, end-plate moment connections are commonly used in the low rise metal building industry. An end-plate connection is a rigid connection between a rafter and column or between two segments of a rafter (sometimes referred to as a splice plate connection). End-plate connections can be subdivided into extended and flush end-plates depending on whether the end-plate extends beyond the beam flanges or not. Further, end-plates can be either stiffened or unstiffened, where the stiffeners may be located in the web for a flush configuration or outside the flange for an extended configuration.

Over the past three decades, there have been numerous analytical and experimental studies validating the design procedures and behavior of these connections. A partial summary of testing and development of design procedures is presented in (Murray and Shoemaker, 2002) and (Murray, 1988). Based on previous testing and development, the AISC Design Guide 16 (Murray and Shoemaker, 2002) included a total of nine end-plate configurations. For flush end-plate connections, these include the two-bolt unstiffened, four-bolt unstiffened, four-bolt stiffened with web gusset plate between the tension bolt rows, and four-bolt stiffened with web gusset plate outside the tension bolt rows configuration. The extended end-plate configurations include the four-bolt unstiffened, four-bolt stiffened, multiple row 1/2 unstiffened, multiple row 1/3 unstiffened, and the multiple row 1/3 stiffened connection.

More recently, there has been interest by metal building manufacturers in having end-plate connection configurations made available with larger moment capacity. This would allow more flexibility for the pre-engineered metal building industry in the design, detailing, and construction of end-plate connections. This was the motivation for the research described in this report.

1.2.Scope of Research

The objective of this research is to produce validated design procedures for four end-plate connection configurations not currently contained in the AISC Design Guide 16. To achieve this objective, the following work was completed: 1) Previous test data and associated proposed design procedures for two end-plate configurations were evaluated, 2) Design procedures were proposed for these two configurations and two additional configurations, 3) An experimental program was conducted on ten full-scale end-plate moment connection specimens, and 4) The design procedures were validated against experimental data and presented in a form consistent with AISC Design Guide 16.

Selection of End-Plate Configurations

Four end-plate moment connection configurations (shown in Figure 1-1) were selected based on the input of the steering committee organized by MBMA and the literature review of the tests done to date for the extended end-plate moment connections. These four configurations are:

1. Eight Bolt Extended Four Wide Unstiffened (8E-4W)
2. Eight Bolt Extended Stiffened (8ES)
3. Six Bolt Flush Four Wide/Two Wide Unstiffened (6B-4W/2W)
4. Twelve Bolt Multiple Row Extended Four Wide/Two Wide Unstiffened (12B-MRE 1/3-4W/2W)

Sufficient prior test data obtained for the 8E-4W configuration was found to support the design procedures (as described in later chapters) and thus no additional tests were conducted. Prior test data for the 8ES configuration supported the design procedures for rafter depths up to 36 in., but additional tests were conducted as part of this work to examine the behavior for larger rafter depths. The validation of both these configurations based on previous testing is discussed in Chapter 4. No previous testing was found in the literature for the other two configurations (6B-4W/2W and MRE 1/3 4W/2W).

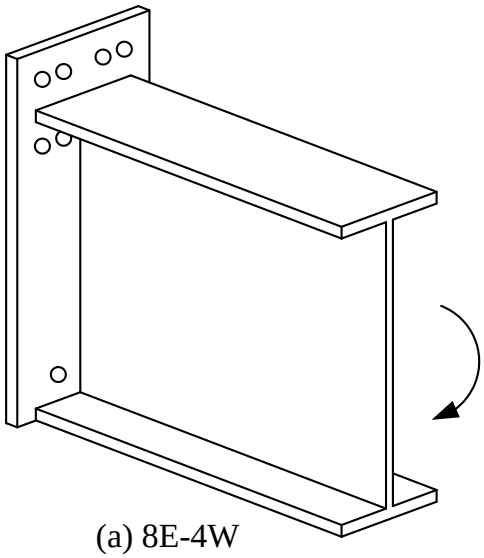

(a) 8E-4W

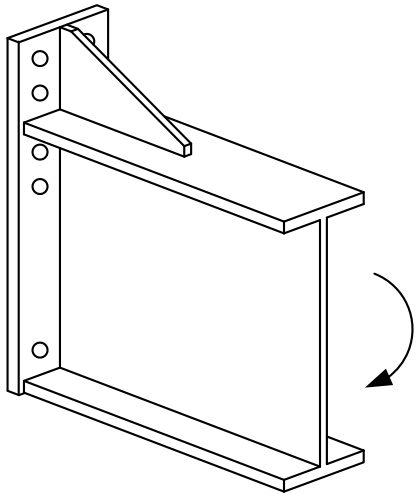

(b) 8ES

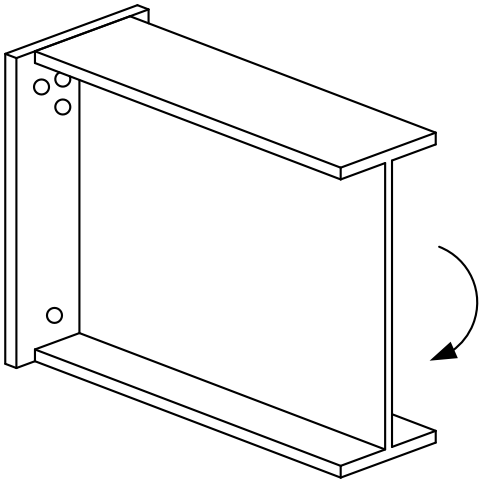

(c) 6B-4W/2W

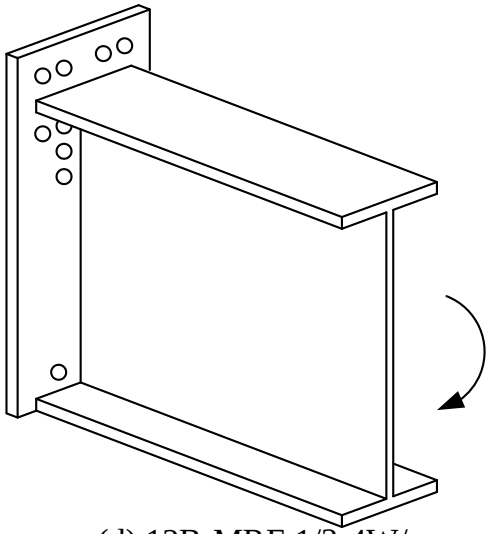

(d) 12B-MRE 1/3-4W/ 2W

Note: Two Bolts shown near the compression flange are just representative. The actual number of bolts will depend on the loading and calculations.

Figure 1-1 Selected Design Configurations

Design Procedures and Limit States

The limit states (and associated variables denoting moment capacity) investigated were: 1) bolt rupture with prying action (M_q), 2) bolt rupture without prying action (M_{np}), and 3) end-plate yielding (M_{pl}). The AISC Design Guide 16 presents two design methodologies, thick end-plate and thin end-plate, that produce different designs and

behavior. The design procedure for thick end-plate behavior prevents end-plate yielding and results in bolt rupture without prying action. The design procedure for thin end-plate behavior, on the other hand, allows end-plate yielding as the primary limit state, followed by bolt rupture with prying action.

For each end-plate configuration, a likely yield line mechanism was identified and related moment capacity associated with end-plate yielding (M_{pl}) was derived. Bolt force models were developed to predict the moment capacity associated with bolt rupture with (M_q) and without (M_{np}) prying action.

For configurations with previous test results (8E-4W and 8ES), the predicted moment capacities for thin plate and thick plate behavior were compared to the experimental results available.

Full-Scale Experimental Program

Ten full-scale tests were conducted including three of the end-plate configurations: four speicmens for 6B-4W/2W, four specimens for 12B-MRE 1/3-4W/2W, and two specimens for the 8ES configuration. Each test specimen consisted of two built-up rafter sections spliced together at midspan using A325 bolts. Each rafter had end-plates welded to both ends so that it could be used for two tests.

The shallow built-up rafter sections were 36 in. deep with 3/4 in. by 12 in. flanges and a 1/4 in. thick web. The deep built-up beams were of two types. For the 6B-4W/2W and 12B-MRE 1/3-4W/2W configuration, the rafter section was 60 in. deep with 3/4 in. by 12 in. flanges and a 3/8 in. thick web. For the 8ES connection, the rafter section was 56 in. deep with 1 in. by 10 in. flanges and a 1/2 in. thick web.

1.3. Report Organization

This report is organized into the following chapters:

- Chapter 1 discusses the motivation for research, the scope of the project and report organization.
- Chapter 2 consists of a brief review of the design procedures for end-plate moment connection configurations included in Design Guide 16.

- Chapter 3 presents the proposed design procedures including yield line analysis and bolt force models derived for the four configurations.
- Chapter 4 examines the validation of connection configurations based on previous test results available from the literature. Two configurations (8E-4W and 8ES) are discussed in this chapter.
- Chapter 5 describes the experimental setup for two new configurations (6B-4W/2W and 12B-MRE 1/3-4W/2W) and for the 8ES configuration. It presents instrumentation, drawings of the setup and tensile coupon test results for the end-plate material.
- Chapter 6 presents the results from the ten tests and these are compared to the predicted moment capacities calculated using the proposed equations from Chapter 3.
- Chapter 7 presents a summary and conclusions of the four test configurations investigated.

2. BACKGROUND

This chapter summarizes the existing end-plate moment connections contained in AISC Design Guide 16, along with the design procedures and typical experimental validation for those connections.

2.1.Design Guide 16 Background

There are nine configurations included in the AISC Design Guide 16 (Murray and Shoemaker, 2002). The scope of the design guide is to provide design procedures for those connection configurations. These configurations are either flush end-plate connections (end-plate stops at the outside of the flange) or extended end-plate configurations (end-plate includes bolts outside the flange). As shown in Figure 2-1, the flush configurations have either two bolts or four bolts on the tension side of the connection and can be stiffened or unstiffened. There are five extended end-plate configurations as shown in Figure 2-2. Again, the end-plate can be stiffened or unstiffened.

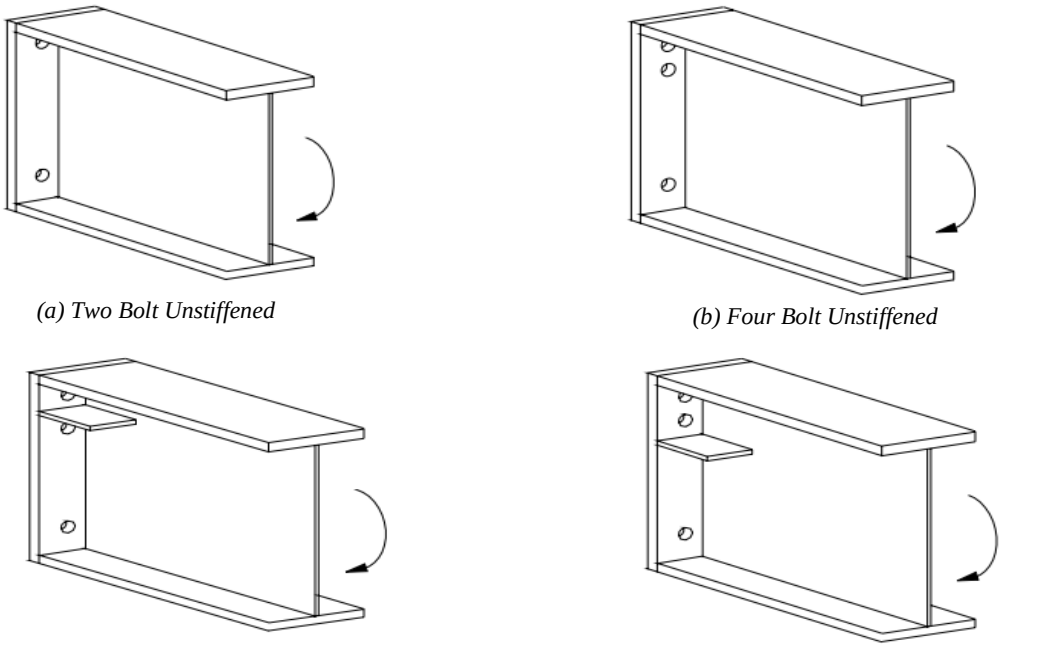

(a) Two Bolt Unstiffened

(b) Four Bolt Unstiffened

(c) Four Bolt Stiffened with web Gusset Plate Between the Tension Bolts

(d) Four Bolt Stiffened with web Gusset Plate Outside the Tension Bolts

Figure 2-1 Flush End-Plate Connections (From Murray and Shoemaker, 2002)

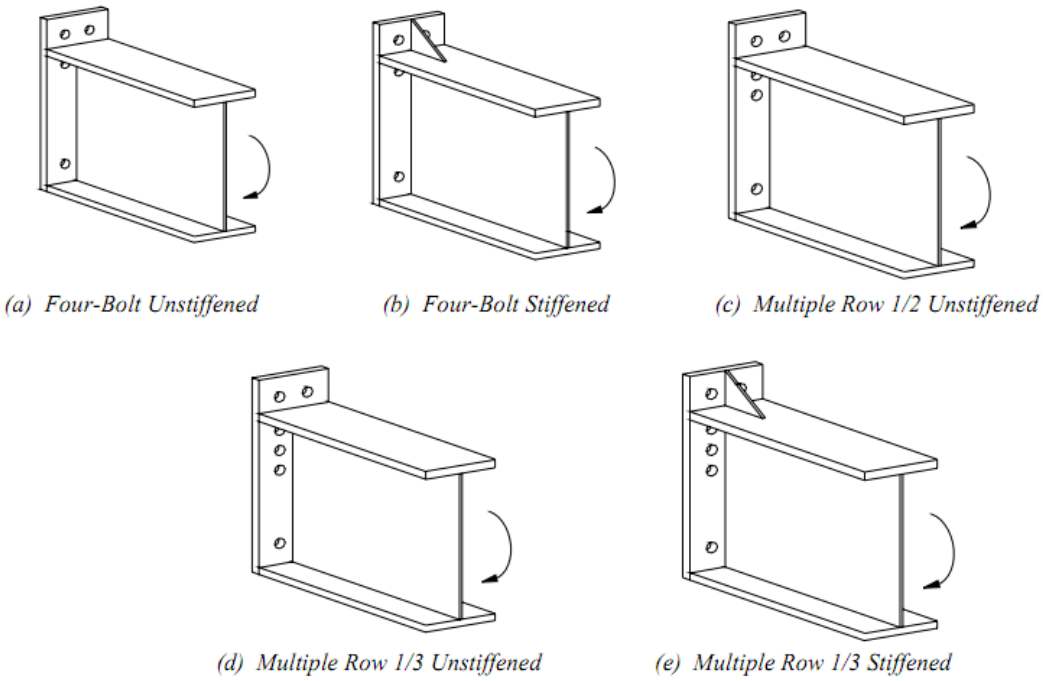

Figure 2-2 Extended End-Plate Connections (From Murray and Shoemaker, 2002)

2.2.Design Methodology

The design procedure as described in section 2.5 of the AISC Design Guide 16 is divided into two categories:

Design Steps for Thick End-Plate Behavior

The design procedure for thick end-plate assumes that bolts rupture without any prying action or end-plate yielding. Thick end-plate design results in thicker end-plate and smaller diameter bolts. The design steps are:

1. Compute the required bolt diameter, $d_{b,reqd} = \sqrt{\frac{2M_u}{\pi\phi F_t\left(\sum d_n\right)}}$, and the moment capacity at bolt rupture without prying action, $M_{np} = \phi\left(2P_t\left(\sum d_n\right)\right)$

   where, $d_{b,reqd}$ = minimum required nominal bolt diameter

   M_u = required flexural strength of the connection

   F_t = nominal tensile strength of the bolt material

d_n = distance from the centerline of the nth tension bolt row to the center of the compression flange

ϕ = 0.75

M_{np} = connection moment capacity based on bolt tension rupture without prying

P_t = Bolt strength given by, $P_t = \pi d_b^2 F_t / 4$

2. Calculate the required thickness of end-plate, $t_{p,reqd} = \sqrt{\frac{\gamma \phi M_{np}}{0.9 \phi_b F_{py} Y}}$, and the moment capacity for end-plate yielding, $M_{pl} = F_{py} t_p^2 Y$

where, ϕ_b = 0.90, bending resistance factor

γ = 1.25 for flush end-plates and 1.0 for extended end-plates

F_{py} = end-plate material yield stress

Y = yield-line mechanism parameter explained in Chapter 3

Design Steps for Thin End-Plate Behavior

The design procedure for thin end-plate assumes that the end-plate yields first and then the bolts rupture with prying action. Thin end-plate design results in thinner end-plate with larger diameter bolts. The design steps are:

1. Compute the required end-plate thickness, $t_{p,reqd} = \sqrt{\frac{\gamma M_u}{\phi_b F_{py} Y}}$ and the end-plate yielding moment, $M_{pl} = F_{py} t_p^2 Y$
2. Select a trial bolt diameter, d_b, and calculate the maximum prying force. A modified version of the Kennedy method (Kennedy, Vinnakota, & Sherbourne, 1981) was used to determine tension bolt forces and prying forces. The Kennedy method uses the split-tee analogy. At a lesser load, the end-plate behaves like a "thick plate", as if no plastic hinges have been formed. As the load increases and assuming the bolts haven't failed yet, plastic hinges are formed at the intersection of the face of the web and centerline of the end-plate at the level of the bolts. This is called as the "intermediate plate behavior". As the connection is loaded even

more and still the bolts haven't ruptured, two additional plastic hinges are formed at the intersection of the bolt centerline and end-plate centerline and after this point the end-plate behaves like a "thin plate". Prying force is generally assumed to be zero at the thick plate limit, increasing in the intermediate stage and then keeping constant in the last stage.

The prying force for bolts depends on whether they are inside the flange or outside the flange. Hence, it is divided into two categories as described below:

Case I: Bolts inside the flange.

This applies to all the bolts in a flush end-plate connection and the interior bolts of an extended end-plate connection. Maximum prying force for this condition is:

$$Q_{\max,i} = \frac{w' t_p^2}{4a_i}\sqrt{F_{py}^2 - 3\left(\frac{F_i'}{w' t_p}\right)^2}$$

where,

$w' = b_p/2 - (d_b + 1/16)$ for two bolts per row

w' = tributary width of the end plate less the bolt hole diameter (including half the distance to adjacent bolts or distance to edge) for more than two bolts per row.

$$a_i = 3.682\left(\frac{t_p}{d_b}\right)^3 - 0.085$$

$$F_i' = \frac{t_p^2 F_{py}\left(0.85w + 0.80w'\right) + \frac{\pi d_b^3 F_t}{8}}{4p_{f,i}}$$

$w = b_p/2$ for two bolts per row

w = tributary width of the end plate (including half the distance to adjacent bolts or distance to edge) for more than two bolts per row.

Case II: Bolts outside the flange.

This applies to the bolts outside the flange in an extended end-plate connection. Maximum prying force for this condition is:

$$Q_{\max,o} = \frac{w' t_p^2}{4a_o}\sqrt{F_{py}^2 - 3\left(\frac{F_o'}{w' t_p}\right)^2}$$

where,

w' = $b_p/2 - (d_b + 1/16)$ for two bolts per row

w' = tributary width of the end plate less the bolt hole diameter (including half the distance to adjacent bolts or distance to edge) for more than two bolts per row.

$$a_o = \min\begin{vmatrix} 3.682\left(\frac{t_p}{d_b}\right)^3 - 0.085 \\ p_{ext} - p_{f,o} \end{vmatrix}$$

$$F_o' = \frac{t_p^2 F_{py}\left(0.85w + 0.80w'\right) + \frac{\pi d_b^3 F_t}{8}}{4p_{f,o}}$$

w = $b_p/2$ for two bolts per row

w = tributary width of the end plate (including half the distance to adjacent bolts or distance to edge) for more than two bolts per row.

3. Calculate the connection design strength for the limit state of bolt rupture with prying action

   a. For a flush connection:

$$\phi M_q = \max\begin{vmatrix} \phi\left[2\left(P_t - Q_{\max,i}\right)\left(d_1 + d_2\right)\right] \\ \phi\left[2\left(T_b\right)\left(d_1 + d_2\right)\right] \end{vmatrix}$$

b. For an extended connection:

$$\phi M_q = \max \begin{vmatrix} \phi\left[2\left(P_t - Q_{\max,o}\right)d_0 + 2\left(P_t - Q_{\max,i}\right)\left(d_1 + d_3\right) + 2T_b d_2\right] \\ \phi\left[2\left(P_t - Q_{\max,o}\right)d_0 + 2T_b\left(d_1 + d_2 + d_3\right)\right] \\ \phi\left[2\left(P_t - Q_{\max,i}\right)\left(d_1 + d_3\right) + 2T_b\left(d_0 + d_2\right)\right] \\ \phi\left[2T_b\left(d_0 + d_1 + d_2 + d_3\right)\right] \end{vmatrix}$$

where, $\varphi = 0.75$

$P_t = \pi d_b^2 F_t / 4$

d_i = distance from the centerline of each tension bolt row to the center of the compression flange

T_b = bolt pretension, for example see minimum bolt pretension specified in Table J3.1 of AISC 360-10

It is noted that while calculating the moment capacity for bolt rupture with prying action, M_q, the maximum value obtained from the different equations is used. This may be counterintuitive, because generally the minimum capacity is used for design purposes. However, in this case it is possible to take advantage of the larger capacity and this can be demonstrated by considering the two possible cases in which a gap opens or does not open behind the end-plate. If the tension force exceeds the bolt pretension and a gap opens, the bolt has additional capacity up to the tension force that causes bolt rupture with prying action. If the bolt pretension is so large that the tension force doesn't exceed the bolt pretension, then no gap will form and prying action cannot develop. Thus, the moment capacity associated with the larger of the two better predicts the actual failure moment than using the minimum of the two.

Another note on the design procedures is that bolt forces (prying or no prying) are calculated assuming the bolts only resist tension associated with connection moment and shear forces are neglected. For design purposes, it is assumed that the bolts on the compression side of the connection resist the shear forces. This may warrant a separate shear check for the compression bolts.

2.3.Typical Experimental Validation for Previous Configurations

The design procedures for each configuration included in the Design Guide 16 were validated by full-scale testing. A configuration was considered validated by examining the test data available in the literature and comparing this data with the calculated moment capacities for the appropriate limit states. For example, the Multiple Row Extended 1/2 Unstiffened (MRE 1/2) configuration was validated against experimental data from eight different tests available in Abel and Murray (1992) and Sumner and Murray (2001). All these tests were subjected to monotonic loading and consisted of two built-up beams spliced together at the midspan. The test specimens covered a wide range of design variables such as the depth of the rafter, bolt pitch, bolt gage etc. At a minimum, the set of specimens used to validate an end-plate design configuration included the following:

- Shallow beam with thin end-plate behavior
- Shallow beam with thick end-plate behavior
- Deep beam with thin end-plate behavior
- Deep beam with thick end-plate behavior

3. PROPOSED DESIGN PROCEDURES

The general design methodology used in the AISC Deign Guide 16 has been presented in Chapter 2. This chapter presents the design procedures specific to the four connection configurations investigated herein. A likely yield line mechanism was identified for each configuration and analyzed to derive the yield line parameter, Y, used to predict moment capacity associated with end-plate yielding. Bolt force models were developed for each configuration to predict the moment capacities associated with bolt rupture with and without prying. The yield line mechanisms and bolt force models for each configuration are presented in the following sections.

3.1. Eight Bolt Extended Four Wide Unstiffened (8E-4W)

Yield Line Analysis

The yield line mechanism considered for the configuration is shown in Figure 3-1. The end-plate has been divided into six panels, formed due to yield lines. The yield line mechanism shown may not be valid if the edge distance is especially large ($e > p_{f,i}$ or $e > s$) in which case an alternate yield line mechanism may control. Similarly, if the rafter is very shallow, the yield lines may overlap with the row of bolts on the compression side, and thus for the yield line mechanism to control it is suggested that $h \gg (2t_f + p_{f,i} + s)$.

The rotation of each panel is given in Table 3-1 and energy associated with plastic hinging of each yield line is provided in Table 3-2. See Figure 3-1 for identification of panel number and yield line number (identified by the two panel numbers between which the yield line resides).

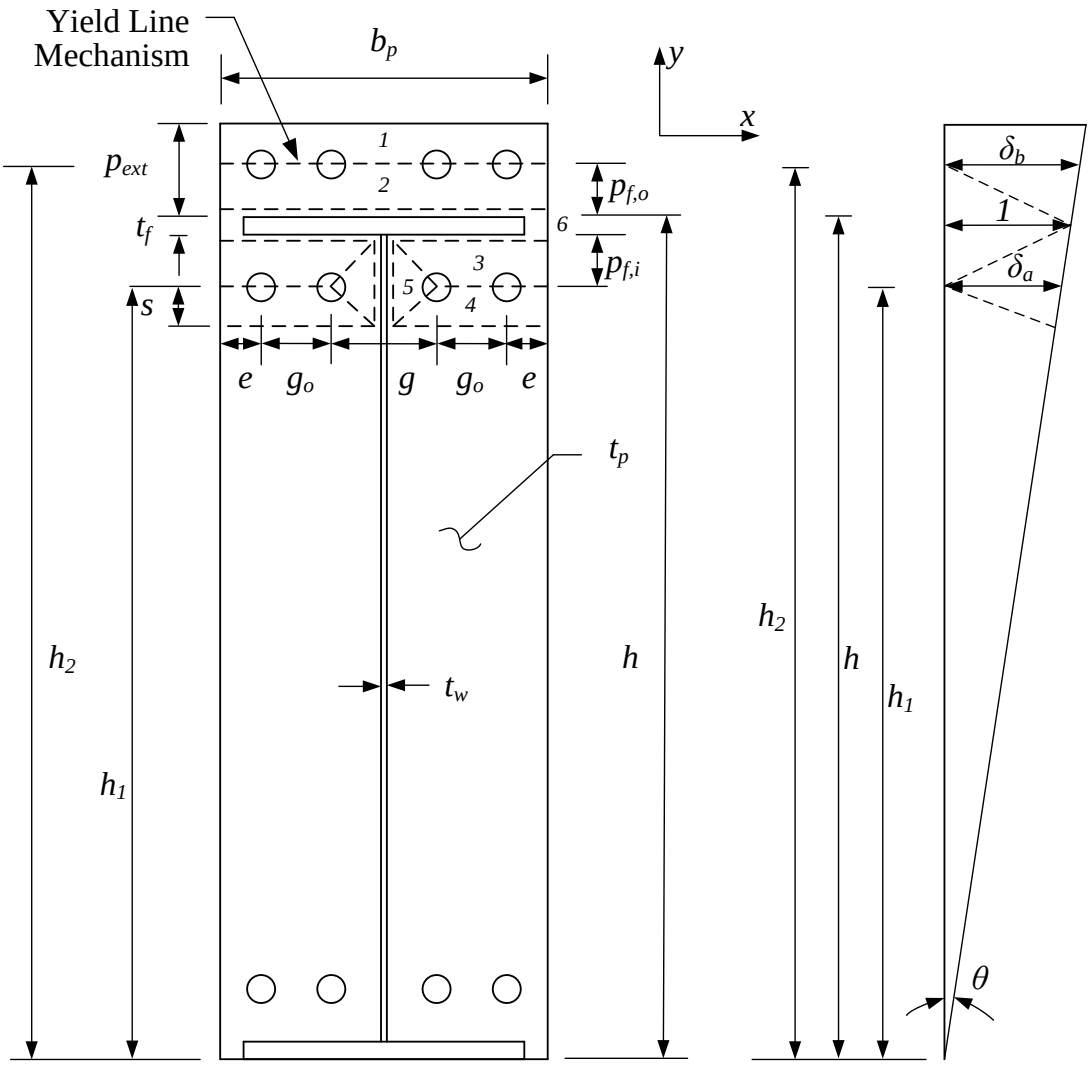

Figure 3-1 Yield Line Mechanism for 8E-4W configuration

Table 3-1 Panel Rotations for 8E-4W configuration

Panel	θ_{nx}	θ_{ny}
1	0	0
2	$\frac{-(\delta_b - \theta(p_{f,o}))}{p_{f,o}}$	0
3	$\frac{-(\delta_a - \theta(p_{f,i}))}{p_{f,i}}$	0
4	$\frac{-(\delta_a - \theta s)}{s}$	0
5	θ	$\frac{2\delta_a - \theta(s - p_{f,i}))}{g}$
6	θ	0

Table 3-2 Energy Stored in Each Yield Line for 8E-4W Configuration

Yield Line	Energy Stored
$W_{i\text{-}1/2}$	$m_p b_p \left(\frac{\delta_b - \theta(p_{f,o})}{p_{f,o}}\right)$
$W_{i\text{-}2/6}$	$m_p b_p \left(\frac{\delta_b - \theta(p_{f,o})}{p_{f,o}} + \theta\right)$
$W_{i\text{-}6/3}$	$m_p \frac{(b_p)}{2}\left(\frac{\delta_a + \theta(p_{f,i})}{p_{f,i}} - \theta\right)$
$W_{i\text{-}3/4}$	$m_p \frac{(b_p - g)}{2}\left(\frac{\delta_a + \theta(p_{f,i})}{p_{f,i}} + \frac{\delta_a - \theta s}{s}\right)$
$W_{i\text{-}3/5}$	$m_p \frac{g}{2}\left(\frac{\delta_a + \theta(p_{f,i})}{p_{f,i}} - \theta\right) + m_p(p_{f,i})\left(\frac{2\delta_a - \theta(s - p_{f,i})}{g}\right)$
$W_{i\text{-}4/5}$	$m_p \frac{g}{2}\left(\theta + \frac{(\delta_a - \theta s)}{s}\right) + m_p(s)\left(\frac{2\delta_a - \theta(s - p_{f,i})}{g}\right)$
$W_{i\text{-}4/6}$	$m_p \frac{(b_p)}{2}\left(\theta + \frac{(\delta_a - \theta s)}{s}\right)$
$W_{i\text{-}5/6}$:	$m_p(p_{f,i} + s)\left(2\delta_a - \theta\frac{(s - p_{f,i})}{g}\right)$

Virtual work was used to solve for the moment that causes plastic hinging along every yield line. The internal work was calculated as the plastic moment, m_p, multiplied by the rotation through which the yield line rotates (see Table 3-2). The sum of the internal work, $\sum W_i$, is calculated as the sum of these values and is given by Equation 3-1:

$$\sum W_i = 2m_p b_p \theta\left(\frac{h_2}{p_{f,o}} + \frac{h_1}{p_{f,i}} + \frac{h_1}{s} - \frac{1}{2}\right) - 2m_p t_w \theta\left(\frac{h_1}{p_{f,i}} + \frac{h_1}{s}\right) + \frac{4m_p\theta}{g}(2h_1 - s - p_{f,i})(p_{f,i} + s) \quad \textbf{(3-1)}$$

To determine the dimension from the interior bolt line to the yield line, *s*, the internal work, $\sum W_i$ is minimized by setting its derivative equal to zero and solving for the related value of *s*. The resulting value of *s* is given by Equation 3-2.

$$\Rightarrow \frac{d(\sum W_i)}{ds} = 0$$

$$\therefore s = \frac{1}{2}\sqrt{b_p g} \qquad \textbf{(3-2)}$$

The moment capacity of the end-plate yielding is found by setting the external work equal to the internal work. The external work, W_e, is given by:

$$W_e = M_{pl}\theta$$

Plugging in the value for end-plate plastic hinge moment capacity, $m_p = F_y \frac{t_p^2}{4}$, and setting external work equal to internal work results in the following:

$$M_{pl} = F_{py} t_p^2 \left[\frac{b_p}{2}\left[\frac{h_2}{p_{f,o}} + \frac{h_1}{p_{f,i}} + \frac{h_1}{s} - \frac{1}{2}\right] + 2(p_{f,i} + s)\left[\frac{h_1}{g}\right]\right]$$

For design, this is simplified into the following:

$$\phi M_{pl} = \phi F_{py} t_p^2 Y, \ \phi = 0.9 \qquad \textbf{(3-3)}$$

$$Y = \frac{b_p}{2}\left[\frac{h_2}{p_{f,o}} + \frac{h_1}{p_{f,i}} + \frac{h_1}{s} - \frac{1}{2}\right] + 2(p_{f,i} + s)\left[\frac{h_1}{g}\right] \qquad \textbf{(3-4)}$$

The yield line parameter, *Y*, presented here matches that presented by Sumner and Murray (2001).

Bolt Force Model

Thick Plate Model

The moment capacity for thick plate behavior (bolt rupture without prying action) is the sum of the nominal tensile strengths of the bolts multiplied by their respective lever arms as given in Equation 3-5. The distances, d_0 and d_1 are shown in Figure 3-2 and the nominal tensile strength of the bolt, P_t, is given in Chapter 2.

$$\phi M_{np} = \phi[4P_t(d_0 + d_1)], \quad \phi = 0.75 \qquad \textbf{(3-5)}$$

Thin Plate Model

The thin end-plate bolt model considers a combination of prying forces at the bolt row levels and since there are two bolt rows which may or not go undergo prying action, four bolt force equations result. Also, it has been experimentally observed that the outer bolts in a row as compared to the inner bolts, contribute less to the moment capacity of the connection. This effect is taken into account by applying bolt distribution factors, α and β, shown in Figure 3-2, which have been calibrated based on experimental results. The equation for moment capacity with prying action, M_q, is given by Equation 3-6.

$$\phi M_q = max \begin{vmatrix} \phi \begin{bmatrix} \{2\alpha_1(P_t - Q_{max,o,1}) + 2\alpha_2(P_t - Q_{max,o,2})\}d_0 + \\ \{2\beta_1(P_t - Q_{max,i,1}) + 2\beta_2(P_t - Q_{max,i,2})\}d_1 \end{bmatrix} \\ \phi[\{2\alpha_1(P_t - Q_{max,o,1}) + 2\alpha_2(P_t - Q_{max,o,2})\}d_0 + \{2T_b(\beta_1 + \beta_2)\}d_1] \\ \phi[\{2T_b(\alpha_1 + \alpha_2)\}d_0 + \{2\beta_1(P_t - Q_{max,i,1}) + 2\beta_2(P_t - Q_{max,i,2})\}d_1] \\ \phi[2T_b\{(\alpha_1 + \alpha_2)d_0 + (\beta_1 + \beta_2)d_1\}] \end{vmatrix}$$

(3-6)

where,

$\phi = 0.75$

T_b = specified bolt pretension load, see Chapter 2

$\alpha_1 = 1.0$ (outside row, inner columns), $\alpha_2 = 0.5$ (outside row, outer columns)

$\beta_1 = 1.0$ (inside row, inner columns), $\beta_2 = 0.75$ (inside row, outer columns)

P_t = nominal bolt strength, see Chapter 2

$Q_{max,o,1}$, $Q_{max,o,2}$, $Q_{max,i,1}$, $Q_{max,i,2}$ = prying force, see Chapter 2.

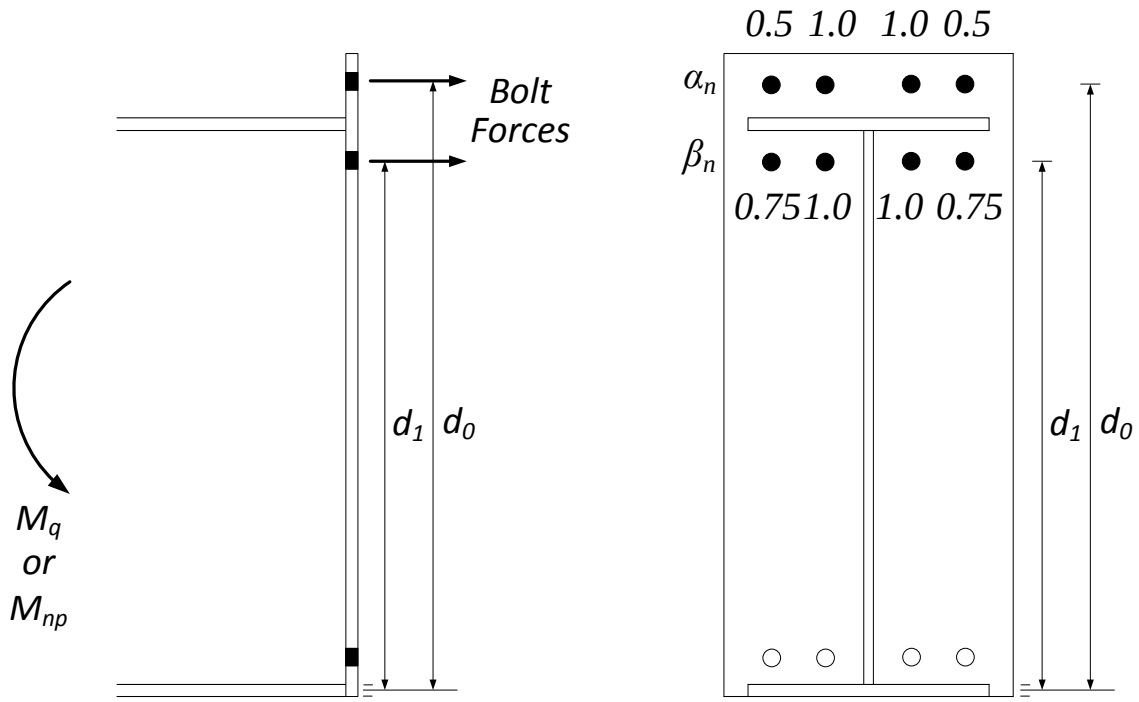

Figure 3-2 Bolt force model and contribution of each bolt for 8E-4W configuration

The bolt force model that is assumed matches that presented by Sumner and Murray (2001). Table 3-3 presents a summary of the design procedures discussed for this configuration.

Table 3-3 Summary of Design Procedures for Eight Bolt Extended Four Wide Unstiffened

Yield Line Mechanism	Bolt Force Model		
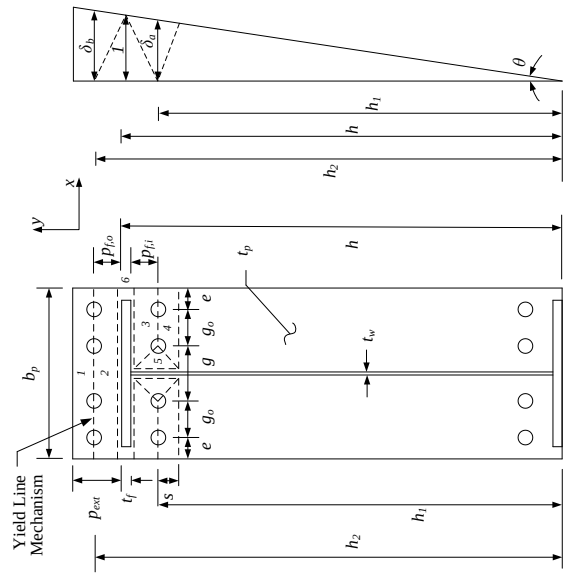	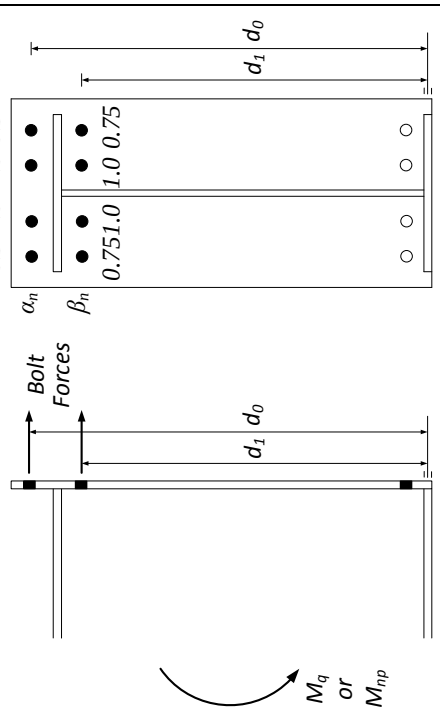	End-Plate Yield	$\phi M_n = \phi M_{pl} = \phi F_{py} t_p^2 Y \qquad \phi = 0.9$ $Y = \frac{b_p}{2}\left[\frac{h_2}{p_{f,o}} + \frac{h_1}{p_{f,i}} + \frac{h_1}{s} - \frac{1}{2}\right] + 2\left(p_{f,i} + s\right)\left[\frac{h_1}{g}\right]$ $s = \frac{1}{2}\sqrt{b_p g}$
		Bolt Rupture with Prying Action	$\phi M_q = max \begin{vmatrix} \phi\left[\begin{matrix}\{2\alpha_1(P_t - Q_{max,o,1}) + 2\alpha_2(P_t - Q_{max,o,2})\}d_0 + \\ \{2\beta_1(P_t - Q_{max,i,1}) + 2\beta_2(P_t - Q_{max,i,2})\}d_1\end{matrix}\right] \\ \phi[\{2T_b(\alpha_1 + \alpha_2)\}d_0 + \{2\beta_1(P_t - Q_{max,i,1}) + 2\beta_2(P_t - Q_{max,i,2})\}d_1] \\ \phi[2T_b\{(\alpha_1 + \alpha_2)d_0 + (\beta_1 + \beta_2)d_1\}] \end{vmatrix}$ $\phi = 0.75,\ \alpha_1 = 1.0,\ \alpha_2 = 0.5, \beta_1 = 1.0,\ \beta_2 = 0.75$
		Bolt Rupture without Prying Action	$\phi M_{np} = \phi[4P_t(d_0 + d_1)], \qquad \phi = 0.75$

3.2.Eight Bolt Extended Stiffened (8ES)

The design procedures presented in this section are similar to Sumner et al. (2000) and are also similar to AISC 358-10 (AISC 2010) with some modifications.

Yield Line Analysis

The yield line mechanism considered is shown in Figure 3-3. The end-plate has been divided into thirteen panels, formed due to yield lines. The rotation of each panel is given in Table 3-4 and the energy associated with each line plastic hinging has been shown in Table 3-5.

The yield line mechanism shown may not be valid if the edge distance is particularly large, $e > (p_{f,i}, p_{f,o},\ p_b\ or\ s)$, in which case an alternate yield line mechanism may control. Also, for the shown yield line mechanism to control, the tension bolts should not be too close to the compression flange, $h \gg (2t_f + p_{f,i} + p_b + s)$, otherwise the yield lines will overlap with the row of bolts on the compression side.

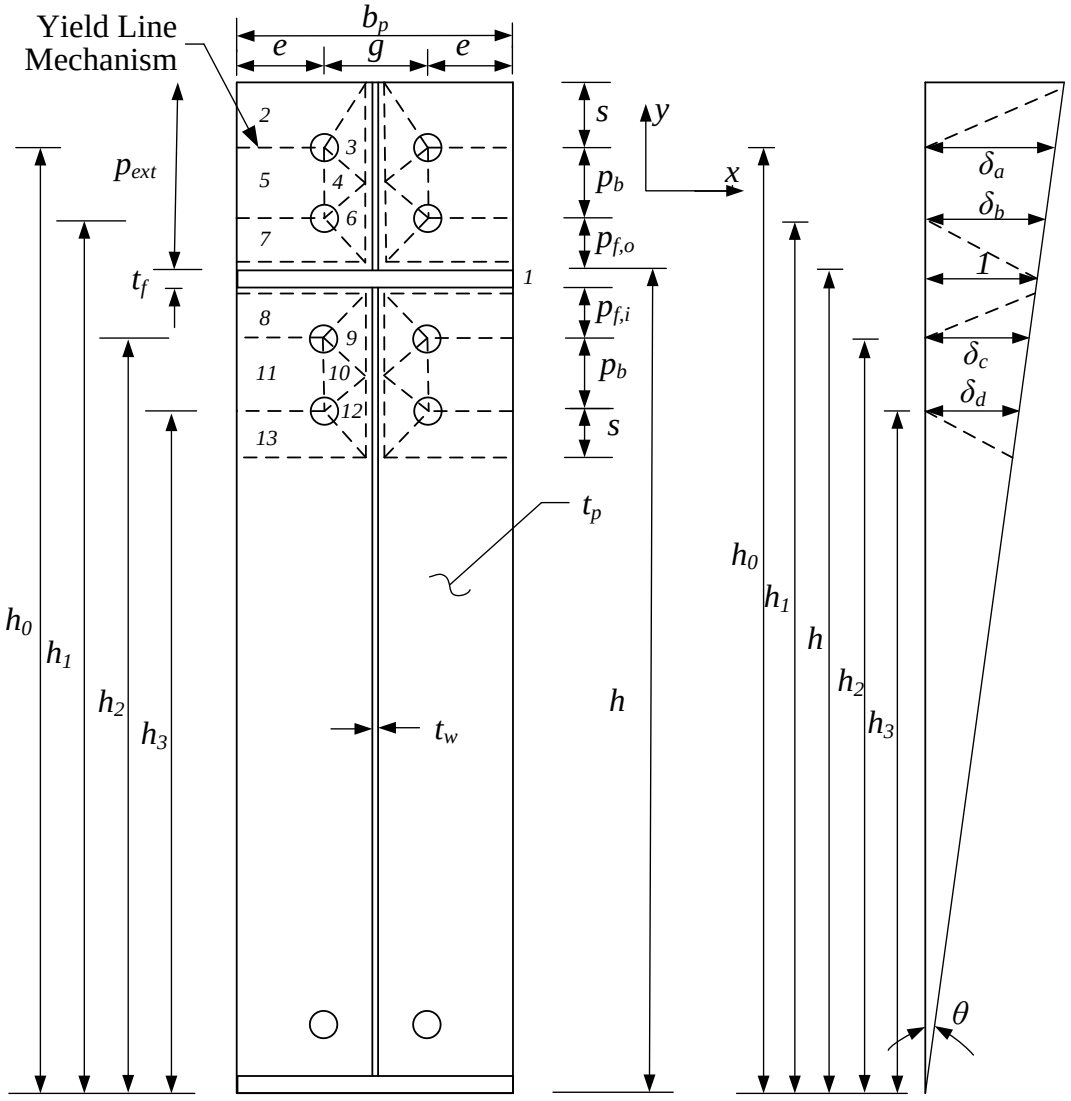

Figure 3-3 Yield Line Mechanism for 8ES Configuration

Table 3-4 Rotation of the Panels for 8ES Configuration

Panel	$\boldsymbol{\theta_{nx}}$	$\boldsymbol{\theta_{ny}}$
1	θ	0
2	$\frac{(\delta_a - s\theta)}{s}$	0
3	θ	$\frac{2\delta_a}{g}$
4	0	$\frac{(\delta_a + \delta_b)}{g}$
5	θ	0
6	θ	$\frac{2\delta_b}{g}$
7	$-\frac{(\delta_b - p_{f,o}\theta)}{p_{f,o}}$	0
8	$\frac{(\delta_c - p_{f,i}\theta)}{p_{f,i}}$	0
9	θ	$\frac{2\delta_c}{g}$
10	0	$\frac{(\delta_c + \delta_d)}{g}$
11	0	0
12	θ	$\frac{2\delta_d}{g}$
13	$-\frac{(\delta_d - s\theta)}{s}$	0

Table 3-5 Energy Stored in Each Yield Line for 8ES Configuration

Yield Line	Energy Stored
$W_{i\text{-}1/2}$	$\frac{m_p b_p}{2}\left(\frac{\delta_a}{s}\right)$
$W_{i\text{-}2/3}$	$\frac{m_p g}{2}\left(\frac{\delta_a}{s}\right) + m_p s\left(\frac{2\delta_a}{g}\right)$
$W_{i\text{-}2/5}$	$m_p\left(\frac{b_p - g}{2}\right)\left(\frac{\delta_a + s\theta}{s}\right)$
$W_{i\text{-}3/1}$	$m_p\left(s + \frac{p_b}{2}\right)\left(\frac{2\delta_a}{g}\right)$
$W_{i\text{-}3/4}$	$\frac{m_p g}{2}(\theta) + \frac{m_p p_b}{2}\left(\frac{\delta_a - \delta_b}{g}\right)$
$W_{i\text{-}4/5}$	$m_p p_b\left(\frac{\delta_a + \delta_b}{g}\right)$
$W_{i\text{-}4/6}$	$\frac{m_p g}{2}(\theta) + \frac{m_p b_p}{2}\left(\frac{\delta_a - \delta_b}{g}\right)$
$W_{i\text{-}6/1}$	$m_p\left(p_{f,o} + \frac{p_b}{2}\right)\left(\frac{2\delta_b}{g}\right)$
$W_{i\text{-}6/7}$	$\frac{m_p g}{2}\left(\frac{\delta_b}{p_{f,o}}\right) + m_p p_{f,o}\left(\frac{2\delta_b}{g}\right)$
$W_{i\text{-}7/5}$	$m_p\left(\frac{b_p - g}{2}\right)\left(\frac{\delta_b + p_{f,o}\theta}{p_{f,o}}\right)$
$W_{i\text{-}7/1}$	$\frac{m_p b_p}{2}\left(\frac{\delta_b}{p_{f,o}}\right)$
$W_{i\text{-}1/8}$	$\frac{m_p b_p}{2}\left(\frac{\delta_c}{p_{f,i}}\right)$
$W_{i\text{-}8/9}$	$\frac{m_p g}{2}\left(\frac{\delta_c}{p_{f,i}}\right) + m_p p_{f,i}\left(\frac{2\delta_c}{g}\right)$
$W_{i\text{-}8/11}$	$m_p\left(\frac{b_p - g}{2}\right)\left(\frac{\delta_c + p_{f,i}\theta}{p_{f,i}}\right)$
$W_{i\text{-}9/1}$	$m_p\left(p_{f,i} + \frac{p_b}{2}\right)\left(\frac{2\delta_c}{g}\right)$

$W_{i\text{-}9/10}$	$\frac{m_p g}{2}(\theta) + \frac{m_p p_b}{2}\left(\frac{\delta_c - \delta_d}{g}\right)$
$W_{i\text{-}10/11}$	$m_p p_b\left(\frac{\delta_c + \delta_d}{g}\right)$
$W_{i\text{-}10/12}$	$\frac{m_p g}{2}(\theta) + \frac{m_p p_b}{2}\left(\frac{\delta_c - \delta_d}{g}\right)$
$W_{i\text{-}11/13}$	$m_p\left(\frac{b_p - g}{2}\right)\left(\frac{\delta_d - s\theta}{s}\right)$
$W_{i\text{-}13/12}$	$\frac{m_p g}{2}\left(\frac{\delta_d}{s}\right) + m_p s\left(\frac{2\delta_d}{g}\right)$
$W_{i\text{-}12/1}$	$m_p\left(\frac{p_b}{2} + s\right)\left(\frac{2\delta_d}{g}\right)$
$W_{i\text{-}13/1}$	$\frac{m_p b_p}{2}\left(\frac{\delta_d}{s}\right)$

The moment that causes plastic hinging of the end-plate was computed using virtual work. The internal work was calculated as the plastic moment, m_p, multiplied by the rotation through which the yield line rotates (see Table 3-5). The sum of the internal work, $\sum W_i$, is calculated as the sum of these values and is given by Equation 3-7:

$$\sum W_i = 2m_p\theta\left[b_p\left(\frac{h_0}{s} + \frac{h_1}{p_{f,o}} + \frac{h_2}{p_{f,i}} + \frac{h_3}{s}\right) + \frac{1}{g}\left(h_0(4s + 3p_b) + h_1\left(4p_{f,o} + p_b\right) + h_2\left(4p_{f,i} + 3p_b\right) + h_3(4s + p_b)\right) + 2g\right] \quad \textbf{(3-7)}$$

To determine the dimension from the interior bolt line to the yield line, *s*, the internal work, $\sum W_i$ is minimized by setting its derivative equal to zero and solving for the related value of *s*. The resulting value of *s* is given by Equation 3-8.

$$\Rightarrow \frac{d(\sum W_i)}{ds} = 0$$
$$\therefore s = \frac{1}{2}\sqrt{b_p g} \quad \textbf{(3-8)}$$

The moment capacity of the end-plate yielding is found by setting the external work equal to the internal work. The external work, W_e, is given by:

$$W_e = M_{pl}\theta$$

Plugging in the value for end-plate plastic hinge moment capacity, $m_p = F_y \frac{t_p^2}{4}$, and setting external work equal to internal work results in the following:

$$M_{pl} = F_{py} t_p^2 \left[\frac{b_p}{2}\left[\frac{h_0}{s} + \frac{h_1}{p_{f,o}} + \frac{h_2}{p_{f,i}} + \frac{h_3}{s}\right] + \frac{2}{g}\left[h_0\left(s + \frac{3p_b}{4}\right) + h_1\left(p_{f,o} + \frac{p_b}{4}\right) + h_2\left(p_{f,i} + \frac{3p_b}{4}\right) + h_3\left(s + \frac{p_b}{4}\right)\right] + g\right]$$

For design, this is simplified into the following:

$$\phi M_{pl} = \phi F_{py} t_p^2 Y, \ \phi = 0.9 \quad \textbf{(3-9)}$$

$$Y = \frac{b_p}{2}\left[\frac{h_0}{s} + \frac{h_1}{p_{f,o}} + \frac{h_2}{p_{f,i}} + \frac{h_3}{s}\right] + \frac{2}{g}\left[h_0\left(s + \frac{3p_b}{4}\right) + h_1\left(p_{f,o} + \frac{p_b}{4}\right) + h_2\left(p_{f,i} + \frac{3p_b}{4}\right) + h_3\left(s + \frac{p_b}{4}\right)\right] + g \quad \textbf{(3-10)}$$

The yield line parameter, *Y*, given in Equation 3-10 does not match the equation presented by Sumner et al. (2000) which is the same equation provided in AISC 358-10 (see Equation 3-11). The terms that appear to be incorrect in the equation from Sumner et al. and AISC 358-10 are identified in Equation 3-11. It is noted that for the specific cases of 8ES connection specimens described in chapters 4 through 6, the values for yield line parameter, *Y*, calculated using Equations 3-10 and 3-11 were nearly the same.

$$Y = \frac{b_p}{2}\left[\frac{h_0}{s} + \frac{h_1}{p_{f,o}} + \frac{h_2}{p_{f,i}} + \frac{h_3}{s}\right] + \frac{2}{g}\left[h_0\left(s + \boxed{\frac{p_b}{4}}\right) + h_1\left(p_{f,o} + \boxed{\frac{3p_b}{4}}\right) + h_2\left(p_{f,i} + \boxed{\frac{p_b}{4}}\right) + h_3\left(s + \boxed{\frac{3p_b}{4}}\right) + \boxed{p_b^{\,2}}\right] + g \quad \textbf{(3-11)}$$

Bolt Force Model

Thick Plate Model

The moment capacity for thick plate behavior (bolt rupture without prying action) is the sum of the bolt nominal tensile strengths multiplied by their respective moment arms (see Figure 3-4 for moment arm dimensions: d_0, d_1, d_2, and d_3). The resulting equation for moment capacity is given by Equation 3-12.

$$\phi M_{np} = \phi[2P_t(d_0 + d_1 + d_2 + d_3)]\,, \qquad \phi = 0.75 \tag{3-12}$$

Thin Plate Model

The thin plate model considers a combination of possible prying forces at the different bolt row levels and there are four bolt rows which may or may not undergo prying action. It is assumed that the rows closest to the flange will likely experience prying action and that the outermost rows won't experience prying action without the rows closest to flange experiencing prying action. Also, there could be a chance that just one of the rows closest to the flange experiences prying and none of the other bolt rows undergo prying action. The resulting five possible scenarios are described by the five options included in Equation 3-13.

$$\phi M_q = max \begin{vmatrix} \phi \begin{bmatrix} 2\alpha_1(P_t - Q_{max,\alpha,1})d_0 + 2\beta_1(P_t - Q_{max,\beta,1})d_1 \\ +2\gamma_1(P_t - Q_{max,\gamma,1})d_2 + 2\delta_1(P_t - Q_{max,\delta,1})d_3 \end{bmatrix} \\ \phi[2\alpha_1 T_b d_0 + 2\beta_1(P_t - Q_{max,\beta,1})d_1 + 2\gamma_1(P_t - Q_{max,\gamma,1})d_2 + 2\delta_1 T_b d_3] \\ \phi[2\alpha_1 T_b d_0 + 2\beta_1(P_t - Q_{max,\beta,1})d_1 + 2\gamma_1 T_b d_2 + 2\delta_1 T_b d_3] \\ \phi[2\alpha_1 T_b d_0 + 2\beta_1 T_b d_1 + 2\gamma_1(P_t - Q_{max,\gamma,1})d_2 + 2\delta_1 T_b d_3] \\ \phi[2T_b(\alpha_1 d_0 + \beta_1 d_1 + \gamma_1 d_2 + \delta_1 d_3)] \end{vmatrix} \tag{3-13}$$

where

$\phi = 0.75$

$\alpha_1 = 1.0$ (outermost row)

$\beta_1 = 1.0$ (outside row closest to flange)

$\gamma_1 = 1.0$ (inside row closest to flange)

$\delta_1 = 1.0$ (innermost row)

The bolt force model presented here matches that of Sumner et al. (2000).

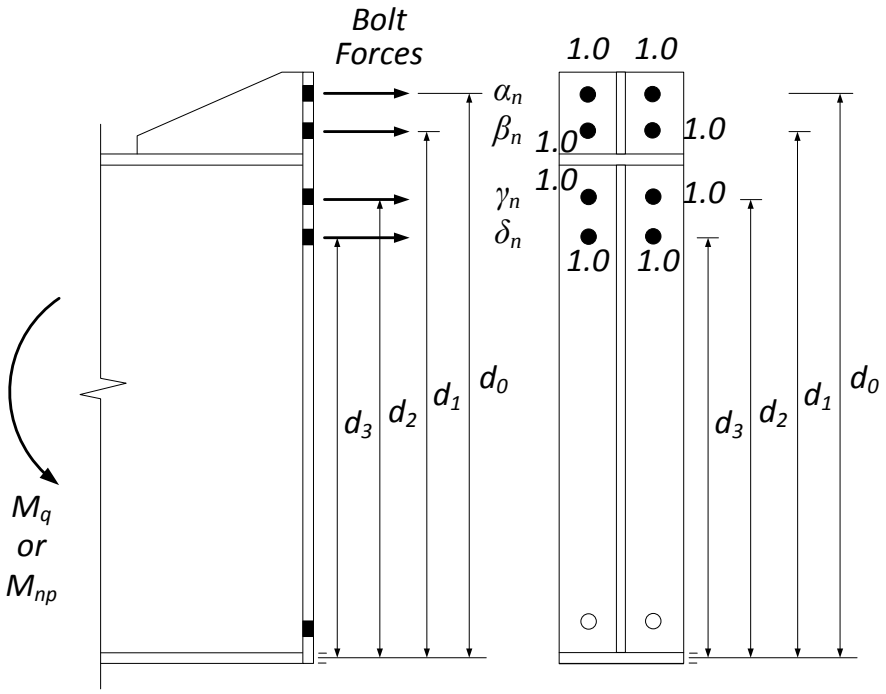

Figure 3-4 Bolt force model for 8ES configuration

Table 3-6 presents a summary of the design procedures discussed for the 8ES end-plate moment connection configuration.

Table 3-6 Summary of Design Procedures for Eight Bolt Extended Stiffened

	Yield Line Mechanism	Bolt Force Model
End-Plate Yield	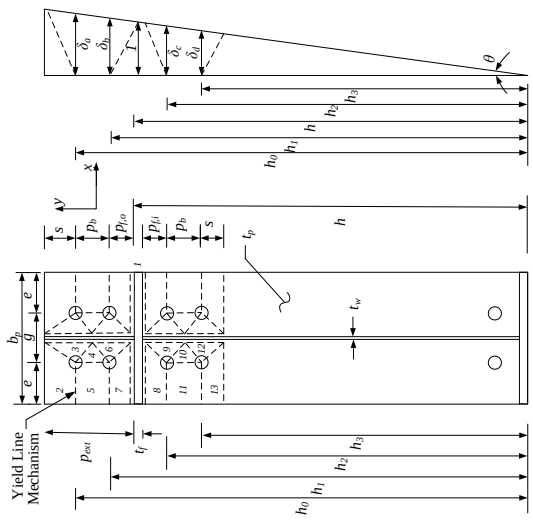	$\phi M_n = \phi M_{pl} = \phi F_{py} t_p^2 Y \qquad \phi = 0.9$ $Y = \frac{b_p}{2}\left[\frac{h_0}{s} + \frac{h_1}{p_{f,o}} + \frac{h_2}{p_{f,i}} + \frac{h_3}{s}\right] + \frac{2}{g}\left[h_0\left(s + \frac{3p_b}{4}\right) + h_1\left(p_{f,o} + \frac{p_b}{4}\right) + h_2\left(p_{f,i} + \frac{3p_b}{4}\right) + h_3(s + \frac{p_b}{4})\right] + g\,, \qquad s = \frac{1}{2}\sqrt{b_p g}$	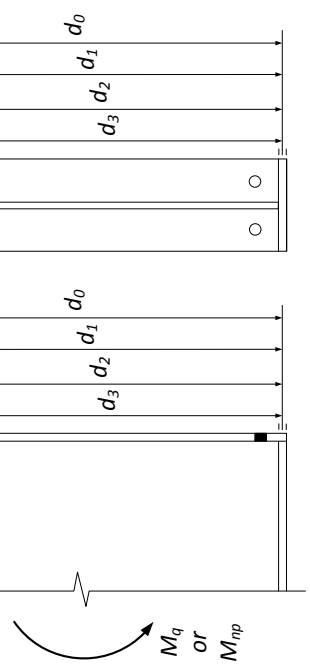
Bolt Rupture with Prying Action		$\phi M_q = max \begin{cases} \phi\begin{bmatrix} 2\alpha_1(P_t - Q_{max,\alpha,1})d_0 + 2\beta_1(P_t - Q_{max,\beta,1})d_1 \\ +2\gamma_1(P_t - Q_{max,\gamma,1})d_2 + 2\delta_1(P_t - Q_{max,\delta,1})d_3 \end{bmatrix} \\ \phi[2\alpha_1 T_b d_0 + 2\beta_1(P_t - Q_{max,\beta,1})d_1 + 2\gamma_1(P_t - Q_{max,\gamma,1})d_2 + 2\delta_1 T_b d_3] \\ \phi[2\alpha_1 T_b d_0 + 2\beta_1(P_t - Q_{max,\beta,1})d_1 + 2\gamma_1 T_b d_2 + 2\delta_1 T_b d_3] \\ \phi[2\alpha_1 T_b d_0 + 2\beta_1 T_b d_1 + 2\gamma_1(P_t - Q_{max,\gamma,1})d_2 + 2\delta_1 T_b d_3] \\ \phi[2T_b(\alpha_1 d_0 + \beta_1 d_1 + \gamma_1 d_2 + \delta_1 d_3)] \end{cases}$ $\phi = 0.75,\ \alpha_1 = 1.0,\ \beta_1 = 1.0,\ \gamma_1 = 1.0,\ \delta_1 = 1.0$	
Bolt Rupture without Prying Action		$\phi M_{np} = \phi[2P_t(d_0 + d_1 + d_2 + d_3)]\,, \qquad \phi = 0.75$	

3.3.Six Bolt Flush Four Wide/Two Wide Unstiffened (6B-4W/2W)

Yield Line Analysis

The yield line mechanism considered for the configuration is shown in Figure 3-5. The end-plate has been divided into thirteen panels (numbered in the figure), formed due to yield lines. The rotation of each panel is given in Table 3-7 and the energy stored in each yield line is presented in Table 3-8.

The yield line mechanism may not be valid if the edge distance is especially large $e > (p_f,\ p_b\ or\ s)$, in which case an alternate yield line mechanism may control. Also, for the shown yield line mechanism to control, the rafter depth should be large compared to the bolt distances away from the flange $h \gg (2t_f + p_f + p_b + s)$, otherwise the yield lines may overlap with the row of bolts on the compression side.

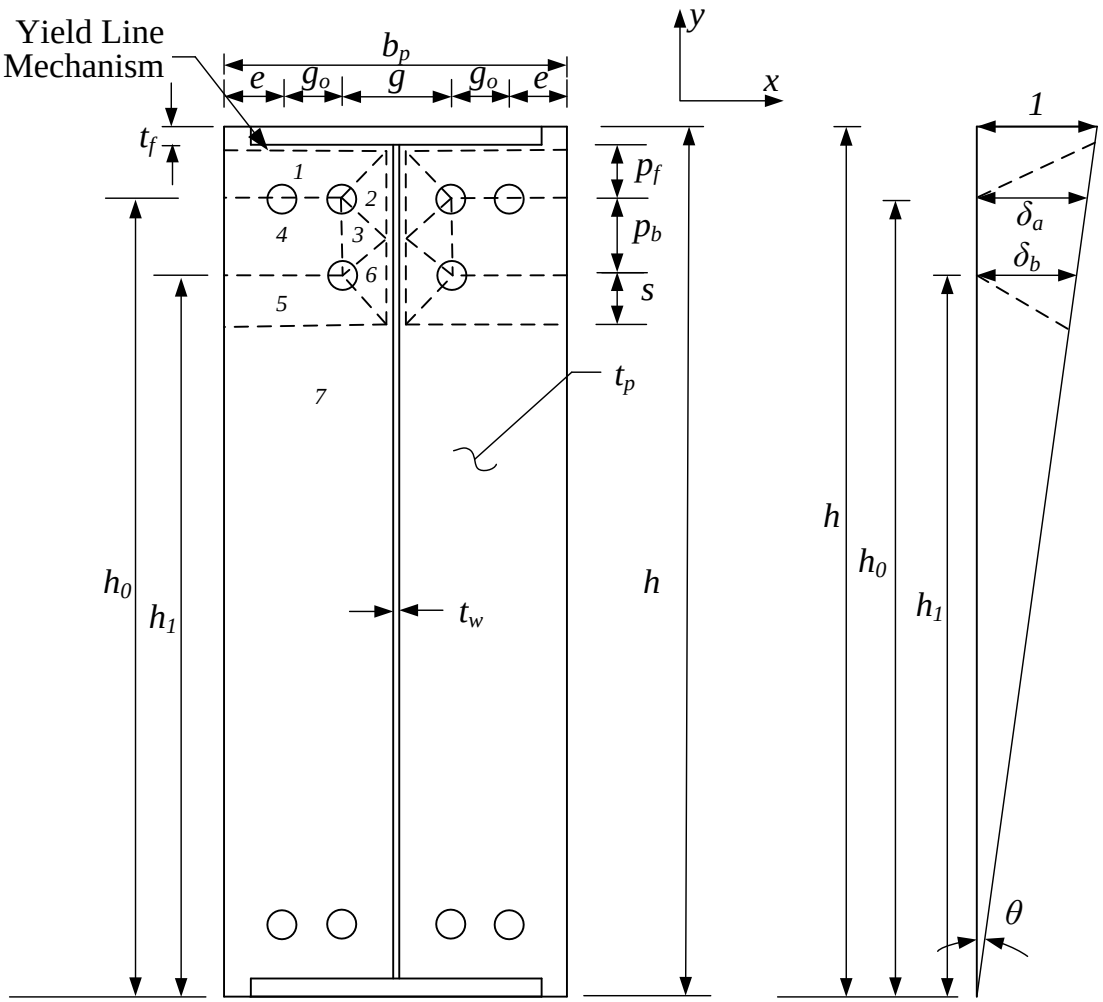

Figure 3-5 Yield Line Mechanism for 6B-4W/2W Configuration

Table 3-7 Rotation of each Panel for 6B-4W/2W Configuration

Panel	$\boldsymbol{\theta_{nx}}$	$\boldsymbol{\theta_{ny}}$
1	$\frac{(\delta_a - p_f\theta)}{p_f}$	0
2	θ	$\frac{2\delta_a}{g}$
3	0	$\frac{\delta_a + \delta_b}{g}$
4	0	0
5	$-\frac{(\delta_b - s\theta)}{s}$	0
6	θ	$\frac{2\delta_b}{g}$
7	θ	0

Table 3-8 Energy Stored in Each Yield Line for 6B-4W/2W Configuration

Yield Line	Energy Stored
$W_{i\text{-}7/1}$	$\frac{m_p b_p}{2}\left(\frac{\delta_a}{p_f}\right)$
$W_{i\text{-}1/2}$	$\frac{m_p g}{2}\left(\frac{\delta_a}{p_f}\right) + m_p p_f\left(\frac{2\delta_a}{g}\right)$
$W_{i\text{-}1/4}$	$m_p\left(\frac{b_p - g}{2}\right)\left(\frac{\delta_a + p_f\theta}{p_f}\right)$
$W_{i\text{-}2/7}$	$m_p\left(p_f + \frac{p_b}{2}\right)\left(\frac{2\delta_a}{g}\right)$
$W_{i\text{-}2/3}$	$\frac{m_p g}{2}(\theta) + \frac{m_p p_b}{2}\left(\frac{\delta_a - \delta_b}{g}\right)$
$W_{i\text{-}3/4}$	$m_p p_b\left(\frac{\delta_a + \delta_b}{g}\right)$
$W_{i\text{-}3/6}$	$\frac{m_p g}{2}(\theta) + \frac{m_p p_b}{2}\left(\frac{\delta_a - \delta_b}{g}\right)$
$W_{i\text{-}4/5}$	$m_p p_b\left(\frac{b_p - g}{2}\right)\left(\frac{\delta_b - s\theta}{s}\right)$
$W_{i\text{-}5/6}$	$\frac{m_p g}{2}\left(\frac{\delta_b}{s}\right) + m_p s\left(\frac{2\delta_b}{g}\right)$
$W_{i\text{-}5/7}$	$\frac{m_p b_p}{2}\left(\frac{\delta_b}{s}\right)$
$W_{i\text{-}6/7}$	$m_p\left(\frac{p_b}{2} + s\right)\left(\frac{2\delta_b}{g}\right)$

Virtual work was used to solve for the moment that causes plastic hinging along every yield line. The internal work was calculated as the plastic moment, m_p, multiplied by the rotation through which the yield line rotates (see Table 3-8). The sum of the internal work, $\sum W_i$, is calculated as the sum of these values and is given by Equation 3-14:

$$\sum W_i = 2m_p\theta\left[b_p\left(\frac{h_0}{p_f} + \frac{h_1}{s}\right) + \frac{1}{g}\left(4p_f h_0 + 3p_b h_0 + 4sh_1 + p_b h_1\right) + g\right] \quad \textbf{(3-14)}$$

To determine the dimension from the interior bolt line to the yield line, *s*, the internal work, $\sum W_i$ is minimized by setting its derivative equal to zero and solving for the related value of *s*. The resulting value of *s* is given by Equation 3-15.

$$\Rightarrow \frac{d(\sum W_i)}{ds} = 0$$

$$\therefore s = \frac{1}{2}\sqrt{b_p g} \qquad \textbf{(3-15)}$$

The moment capacity of the end-plate yielding is found by setting the external work equal to the internal work. The external work, W_e, is given by:

$$W_e = M_{pl}\theta$$

Plugging in the value for end-plate plastic hinge moment capacity, $m_p = F_y \frac{t_p^2}{4}$, and setting external work equal to internal work results in the following:

$$M_{pl} = F_{py} t_p^2 \left[\frac{b_p}{2}\left[\frac{h_0}{p_f} + \frac{h_1}{s}\right] + \frac{2}{g}\left[h_0\left(p_f + \frac{3p_b}{4}\right) + h_1\left(s + \frac{p_b}{4}\right)\right] + \frac{g}{2}\right]$$

For design, this is simplified into the following:

$$\phi M_{pl} = \phi F_{py} t_p^2 Y, \ \phi = 0.9 \qquad \textbf{(3-16)}$$

$$Y = \frac{b_p}{2}\left[\frac{h_0}{p_f} + \frac{h_1}{s}\right] + \frac{2}{g}\left[h_0\left(p_f + \frac{3p_b}{4}\right) + h_1\left(s + \frac{p_b}{4}\right)\right] + \frac{g}{2} \qquad \textbf{(3-17)}$$

Bolt Force Model

Thick Plate Model

The moment capacity for thick plate behavior (bolt rupture without prying action) is the sum of the nominal tensile strengths of the bolts multiplied by their respective lever arms as given in Equation 3-18. The distances, d_1 and d_2 are shown in Figure 3-6 and the nominal tensile strength of the bolt, P_t, is given in Chapter 2.

$$\phi M_{np} = \phi[2P_t(2d_1 + d_2)]\ ,\ \ \phi = 0.75 \qquad \textbf{(3-18)}$$

Thin Plate Model

The thin end-plate bolt model considers a combination of prying forces at the different bolt row levels and since there are two bolt rows which may or not go undergo prying action, four prying action scenarios are possible as given in Equation 3-19. Since it has been experimentally observed that the outer bolts in a row experience less force and thus contribute less to the moment capacity as compared to the inner bolts, bolt distribution factors are used to reduce the contribution of the outer bolts. Similarly, the bolts in the innermost row contribute less as compared to the bolts in the row closest to the flange. These effects have been taken into account by using bolt distribution factors, $\beta\ and\ \gamma$, which have been calibrated based on experimental results and the resulting values are given below and shown in Figure 3-6.

$$\phi M_q = max \begin{vmatrix} \phi\begin{bmatrix}\{2\beta_1(P_t - Q_{max,\beta,1}) + 2\beta_2(P_t - Q_{max,\beta,2})\}d_1 \\ +\{2\gamma_1(P_t - Q_{max,\gamma,1})\}d_2\end{bmatrix} \\ \phi[\{2\beta_1(P_t - Q_{max,\beta,1}) + 2\beta_2(P_t - Q_{max,\beta,2})\}d_1 + (2\gamma_1 T_b)d_2] \\ \phi[(2\beta_1 T_b)d_1 + (2\beta_2 T_b)d_1 + \{2\gamma_1(P_t - Q_{max,\gamma,1})\}d_2] \\ \phi[(2\beta_1 T_b)d_1 + (2\beta_2 T_b)d_1 + (2\gamma_1 T_b)d_2] \end{vmatrix}$$

(3-19)

where,

$\phi = 0.75$

T_b = specified bolt pretension load

$\beta_1 = 1.0$ (first inside row, inner columns), $\beta_2 = 0.75$ (first inside row, outer columns)

$\gamma_1 = 0.75$ (second inside row, inner columns)

P_t = nominal bolt strength, see Chapter 2

$Q_{max,\beta,1}$, $Q_{max,\beta,2}$, $Q_{max,\gamma,1}$ = prying force, see Chapter 2. Note that $Q_{max,\beta,1}$ and $Q_{max,\beta,2}$ are different because the value of w' is different, but that $Q_{max,\beta,1} = Q_{max,\gamma,1}$.

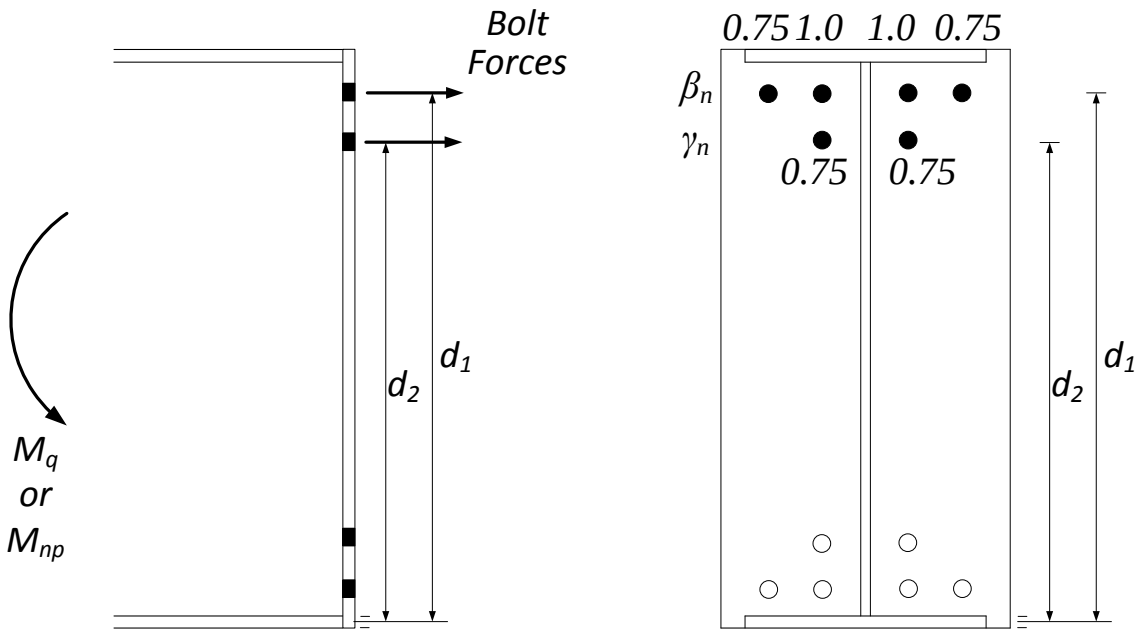

Figure 3-6 Bolt force model and contribution of each bolt for 6B-4W/2W configuration

Table 3-9 presents a summary of the design procedures discussed for this configuration.

Table 3-9 Summary of Design Procedures for Six Bolt Flush Four Wide/Two Wide Unstiffened

	Yield Line Mechanism	Bolt Force Model	
End-Plate Yield			$\phi M_n = \phi M_{pl} = \phi F_{py} t_p^2 Y \qquad \phi = 0.9$ $Y = \frac{b_p}{2}\left[\frac{h_0}{p_f} + \frac{h_1}{s}\right] + \frac{2}{g}\left[h_0\left(p_f + \frac{3p_b}{4}\right) + h_1\left(s + \frac{p_b}{4}\right)\right] + \frac{g}{2}$ $s = \frac{1}{2}\sqrt{b_p g}$
Bolt Rupture with Prying Action			$\phi M_q = max \begin{vmatrix} \phi\begin{bmatrix}\{2\beta_1(P_t - Q_{max,\beta,1}) + 2\beta_2(P_t - Q_{max,\beta,2})\}d_1 \\ +\{2\gamma_1(P_t - Q_{max,\gamma,1})\}d_2\end{bmatrix} \\ \phi[\{2\beta_1(P_t - Q_{max,\beta,1}) + 2\beta_2(P_t - Q_{max,\beta,2})\}d_1 + (2\gamma_1 T_b)d_2] \\ \phi[(2\beta_1 T_b)d_1 + (2\beta_2 T_b)d_1 + \{2\gamma_1(P_t - Q_{max,\gamma,1})\}d_2] \\ \phi[(2\beta_1 T_b)d_1 + (2\beta_2 T_b)d_1 + (2\gamma_1 T_b)d_2] \end{vmatrix}$ $\phi = 0.75,\ \beta_1 = 1.0,\ \beta_2 = 0.75,\ \gamma_1 = 0.75$
Bolt Rupture without Prying Action			$\phi M_{np} = \phi[2P_t(2d_1 + d_2)], \qquad \phi = 0.75$

3.4. Twelve Bolt Multiple Row Extended Four Wide/Two Wide Unstiffened (12B-MRE 1/3-4W/2W)

Yield Line Analysis

The yield line mechanism considered for the configuration is shown in Figure 3-7. The end-plate has been divided into ten panels, formed due to yield lines. The yield line mechanism shown may not be valid if the edge distance is especially large $e > (p_{f,i}, p_{f,o}, p_b \; or \; s)$, in which case an alternate yield line mechanism may control. Similarly, if the rafter if very shallow, the yield lines may overlap with the row of bolts on the compression side, and thus for the yield line mechanism to control it is suggested that, $h \gg (2t_f + p_{f,i} + 2p_b + s)$.

The rotation of each panel has been shown in Table 3-10 and the energy stored in each line has been shown in Table 3-11.

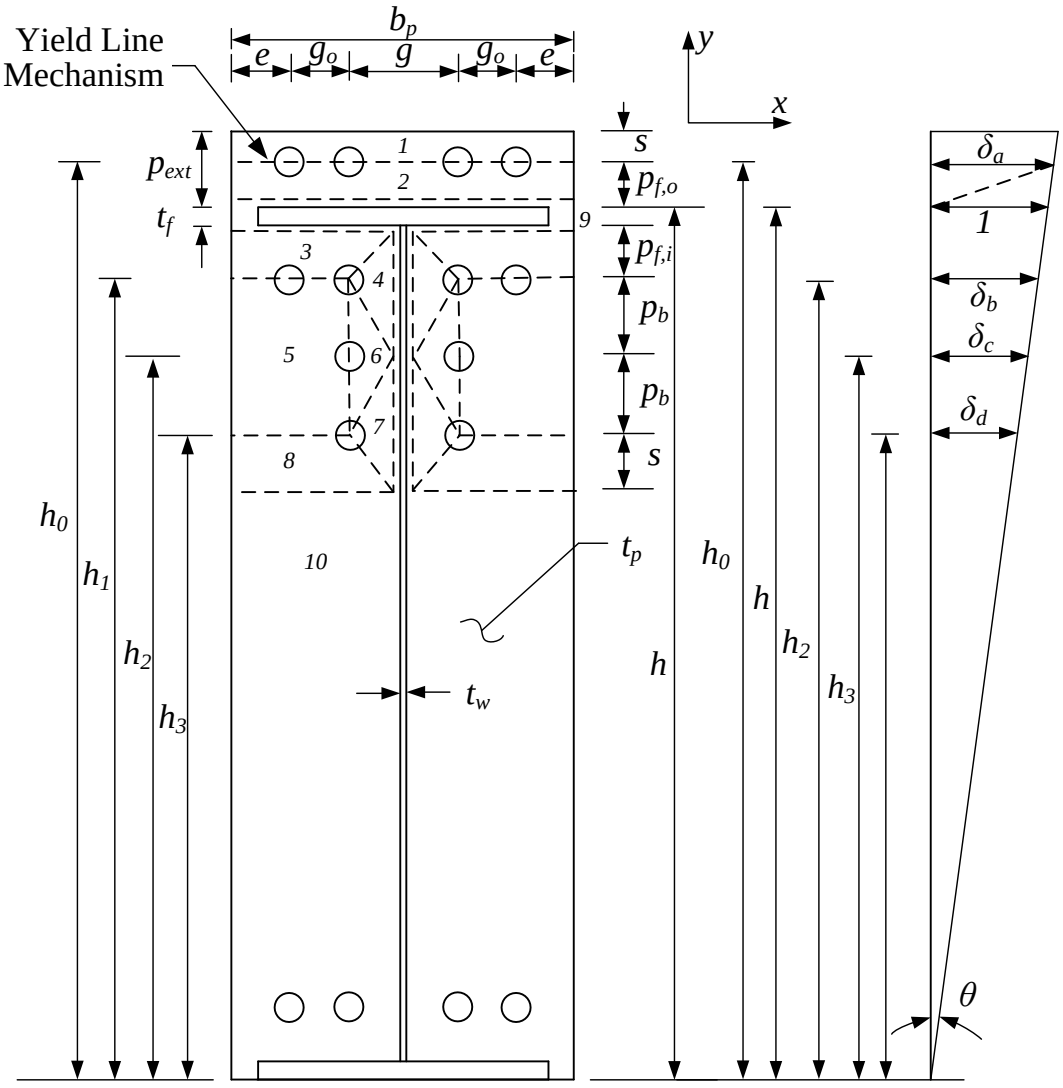

Figure 3-7 Yield Line Mechanism for 12B-MRE 1/3-4W/2W Configuration

Table 3-10 Rotation of each Panel for 12B-MRE 1/3-4W/2W Configuration

Panel	$\boldsymbol{\theta_{nx}}$	$\boldsymbol{\theta_{ny}}$
1	0	0
2	$-\frac{(\delta_a - p_{f,o}\theta)}{p_{f,o}}$	0
3	$\frac{(\delta_b + p_{f,i}\theta)}{p_{f,i}}$	0
4	θ	$\frac{2\delta_b}{g}$
5	0	0
6	0	$\frac{2\delta_c}{g}$
7	θ	$\frac{2\delta_d}{g}$
8	$-\frac{(\delta_c - s\theta)}{s}$	0
9	θ	0
10	0	0

Table 3-11 Energy Stored in Each Yield Line for 12B-MRE 1/3-4W/2W Configuration

Yield Line	Energy Stored
$W_{i\text{-}1/2}$	$\frac{m_p b_p}{2}\left(\frac{\delta_a - p_{f,o}\theta}{p_{f,o}}\right)$
$W_{i\text{-}2/9}$	$\frac{m_p b_p}{2}\left(\frac{\delta_a}{p_{f,o}}\right)$
$W_{i\text{-}9/3}$	$\frac{m_p p_b}{2}\left(\frac{\delta_b}{p_{f,i}}\right)$
$W_{i\text{-}3/4}$	$\frac{m_p g}{2}\left(\frac{\delta_b + p_{f,i}\theta}{p_{f,i}}\right) + m_p p_{f,i}\left(\frac{2\delta_b}{g}\right)$
$W_{i\text{-}3/5}$	$m_p\left(\frac{b_p - g}{2}\right)\left(\frac{\delta_a + p_{f,i}\theta}{p_{f,i}}\right)$
$W_{i\text{-}4/9}$	$m_p\left(\frac{2\delta_b}{g}\right)(p_{f,i} + p_b)$
$W_{i\text{-}4/6}$	$\frac{m_p g}{2}\theta + m_p p_b\left(\frac{2\delta_b - 2\delta_c}{g}\right)$
$W_{i\text{-}6/5}$	$2m_p p_b\left(\frac{2\delta_c}{g}\right)$
$W_{i\text{-}5/8}$	$\frac{m_p(b_p - g)}{2}\left(\frac{\delta_d - s\theta}{s}\right)$
$W_{i\text{-}6/7}$	$\frac{m_p g}{2}\theta + m_p p_b\left(\frac{2\delta_b - 2\delta_c}{g}\right)$
$W_{i\text{-}7/8}$	$\frac{m_p g}{2}\left(\frac{\delta_d}{s}\right) + m_p s\left(\frac{2\delta_d}{g}\right)$
$W_{i\text{-}7/9}$	$m_p(p_b + s)\left(\frac{2\delta_d}{g}\right)$
$W_{i\text{-}8/10}$	$\frac{m_p b_p}{2}\left(\frac{\delta_d - s\theta}{s}\right)$

Virtual work was used to solve for the moment that causes plastic hinging along every yield line. The internal work was calculated as the plastic moment, m_p, multiplied by the rotation through which the yield line rotates (see Table 3-11). The sum of the internal work, $\sum W_i$, is calculated as the sum of these values and is given by Equation 3-20:

$$\sum W_i = 2m_p\theta\left[b_p\left(\frac{h_0}{p_{f,o}}+\frac{h_1}{p_{f,i}}+\frac{h_3}{s}-1\right)+\frac{1}{g}\left(4p_{f,i}h_1+4p_bh_1+4p_bh_2+4sh_3\right)+g\right] \quad \textbf{(3-20)}$$

To determine the dimension from the interior bolt line to the yield line, *s*, the internal work, $\sum W_i$ is minimized by setting its derivative equal to zero and solving for the related value of *s*. The resulting value of *s* is given by Equation 3-21.

$$\Rightarrow \frac{d(\sum W_i)}{ds} = 0$$
$$\therefore s = \frac{1}{2}\sqrt{b_p g} \quad \textbf{(3-21)}$$

The moment capacity of the end-plate yielding is found by setting the external work equal to the internal work. The external work, W_e, is given by:

$$W_e = M_{pl}\theta$$

Plugging in the value for end-plate plastic hinge moment capacity, $m_p = F_y\frac{t_p^2}{4}$, and setting external work equal to internal work results in the following:

$$M_{pl} = F_{py}t_p^2\left[\frac{b_p}{2}\left[\frac{h_0}{p_{f,o}}+\frac{h_1}{p_{f,i}}+\frac{h_3}{s}-1\right]+\frac{2}{g}\left[h_1\left(p_{f,i}+p_b\right)+h_2p_b+h_3s\right]+\frac{g}{2}\right]$$

For design, this is simplified into the following:

$$\phi M_{pl} = \phi F_{py}t_p^2Y,\ \phi = 0.9 \quad \textbf{(3-22)}$$

$$Y = \frac{b_p}{2}\left[\frac{h_0}{p_{f,o}} + \frac{h_1}{p_{f,i}} + \frac{h_3}{s} - 1\right] + \frac{2}{g}\left[h_1\left(p_{f,i} + p_b\right) + h_2 p_b + h_3 s\right] + \frac{g}{2} \quad \textbf{(3-23)}$$

It is noted that the above equation is derived assuming that the vertex of the triangular plane identified as (6) in Figure 3-7 occurs at the same height as the interior row of bolts (i.e. at a distance h_2 from the point of rotation). If it is instead assumed that the vertex is equidistant between the two bolts at distance h_1 and h_3, then the panel is an isosceles triangle, the term (h_2 p_b) becomes p_b (h_1+h_3) / 2 and the yield line parameter becomes:

$$Y = \frac{b_p}{2}\left[\frac{h_0}{p_{f,o}} + \frac{h_1}{p_{f,i}} + \frac{h_3}{s} - 1\right] + \frac{2}{g}\left[h_1\left(p_{f,i} + 1.5p_b\right) + 0.5h_3 p_b + h_3 s\right] + \frac{g}{2} \quad \textbf{(3-24)}$$

Bolt Force Model

Thick Plate Model

The moment capacity for thick plate behavior (bolt rupture without prying action) is the sum of the nominal tensile strengths of the bolts multiplied by their respective moment arms. The moment arm distances, d_0, d_1, d_2, and d_3 are shown in Figure 3-8 and the nominal tensile strength of the bolt, P_t, is given in Chapter 2. The resulting equation for moment capacity is given by Equation 3-25.

$$\phi M_{np} = \phi[2P_t(2d_0 + 2d_1 + d_2 + d_3)]\,, \qquad \phi = 0.75 \quad \textbf{(3-25)}$$

Thin Plate Model

The thin plate bolt model considers a combination of prying forces at the bolt row levels and there are four bolt rows which may or may not undergo prying action. It has been experimentally observed that the "γ row" (see Figure 3-8) does not undergo prying. Also, it has been experimentally observed that the outer bolts in a row experience less force and therefore contribute less to the moment capacity of the connection than the inner bolts.

This is taken into account by using bolt distribution factors, α and β, which have been calibrated based on experimental results with values given below and shown in Figure 3-8. Similarly, the bolts in rows further away from the flange contribute less to the moment capacity of the connection as compared to the bolts in rows closest to the flange. This is taken into account by using the bolt distribution factors γ and δ for the two most interior bolt rows.

$$\phi M_q = max \begin{vmatrix} \phi \begin{bmatrix} 2\alpha_1(P_t - Q_{max,\alpha,1})d_0 + 2\alpha_2(P_t - Q_{max,\alpha,2})d_0 \\ +2\beta_1(P_t - Q_{max,\beta,1})d_1 + 2\beta_2(P_t - Q_{max,\beta,2})d_1 \\ +2\gamma_1(T_b)d_2 + 2\delta_1(P_t - Q_{max,\delta,1})d_3 \end{bmatrix} \\ \phi \begin{bmatrix} 2\alpha_1(T_b)d_0 + 2\alpha_2(T_b)d_0 + 2\beta_1(P_t - Q_{max,\beta,1})d_1 + \\ 2\beta_2(P_t - Q_{max,\beta,2})d_1 + 2\gamma_1(T_b)d_2 + 2\delta_1(P_t - Q_{max,\delta,1})d_3 \end{bmatrix} \\ \phi \begin{bmatrix} 2\alpha_1(P_t - Q_{max,\alpha,1})d_0 + 2\alpha_2(P_t - Q_{max,\alpha,2})d_0 + 2\beta_1(T_b)d_1 + \\ 2\beta_2(T_b)d_1 + 2\gamma_1(T_b)d_2 + 2\delta_1(T_b)d_3 \end{bmatrix} \\ \phi[2T_b\{(\alpha_1 + \alpha_2)d_0 + (\beta_1 + \beta_2)d_1 + (\gamma)d_2 + (\delta)d_3\}] \end{vmatrix}$$

(3-26)

where,

$\phi = 0.75$

T_b = specified bolt pretension load

$\alpha_1 = 1.0$ (outside row, inner columns), $\alpha_2 = 0.5$ (outside row, outer columns)

$\beta_1 = 1.0$ (first inside row, inner columns),

$\beta_2 = 0.75$ (first inside row, outer columns)

$\gamma_1 = 0.75$ (second inside row, inner columns)

$\delta_1 = 0.5$ (third inside row, inner columns)

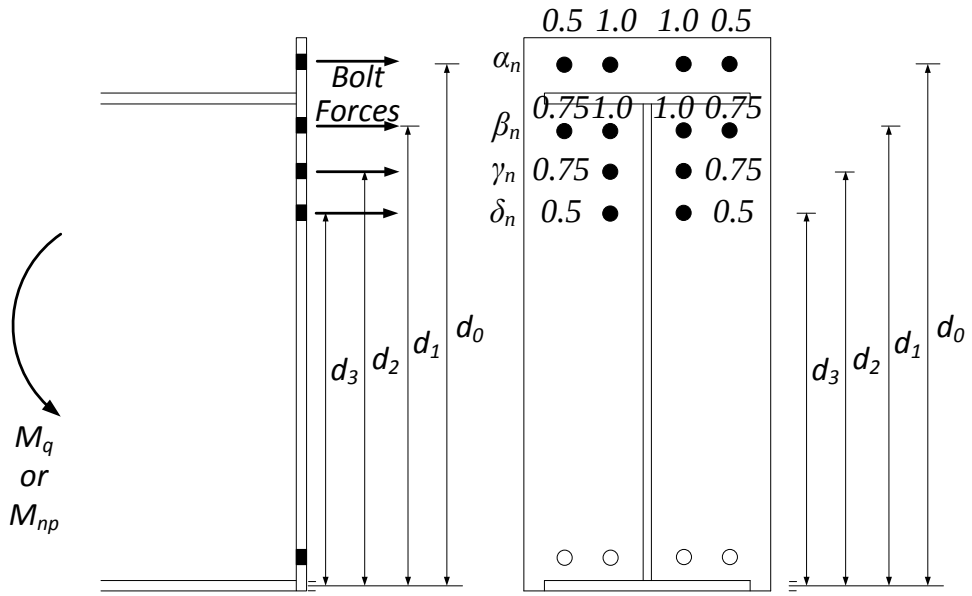

Figure 3-8 Bolt force model and contribution of each bolt for 12B-MRE 1/3-4W/2Wconfiguration

Table 3-12 presents a summary of the design procedures discussed for this configuration.

Table 3-12 Summary of Design Procedures for Twelve Bolt Multiple Row Extended Four Wide/Two Wide Unstiffened

	Yield Line Mechanism	Bolt Force Model
End-Plate Yield		$\phi M_n = \phi M_{pl} = \phi F_{py} t_p^2 Y \qquad \phi = 0.9$ $Y = \frac{b_p}{2}\left[\frac{h_0}{p_{f,o}} + \frac{h_1}{p_{f,i}} + \frac{h_3}{s} - 1\right] + \frac{2}{g}\left[h_1\left(p_{f,i} + 1.5p_b\right) + h_3\left(s + \frac{p_b}{2}\right)\right] + \frac{g}{2}$ $s = \frac{1}{2}\sqrt{b_p g}$
Bolt Rupture with Prying Action		$\phi M_q = max \begin{cases} \phi\left[\begin{matrix} 2\alpha_1(P_t - Q_{max,\alpha,1})d_0 + 2\alpha_2(P_t - Q_{max,\alpha,2})d_0 \\ +2\beta_1(P_t - Q_{max,\beta,1})d_1 + 2\beta_2(P_t - Q_{max,\beta,2})d_1 \\ +2\gamma_1(T_b)d_2 + 2\delta_1(P_t - Q_{max,\delta,1})d_3 \end{matrix}\right] \\ \phi\left[\begin{matrix} 2\alpha_1(T_b)d_0 + 2\alpha_2(T_b)d_0 + 2\beta_1(P_t - Q_{max,\beta,1})d_1 + \\ 2\beta_2(P_t - Q_{max,\beta,2})d_1 + 2\gamma_1(T_b)d_2 + 2\delta_1(P_t - Q_{max,\delta,1})d_3 \end{matrix}\right] \\ \phi\left[\begin{matrix} 2\alpha_1(P_t - Q_{max,\alpha,1})d_0 + 2\alpha_2(P_t - Q_{max,\alpha,2})d_0 + 2\beta_1(T_b)d_1 + \\ 2\beta_2(T_b)d_1 + 2\gamma_1(T_b)d_2 + 2\delta_1(T_b)d_3 \end{matrix}\right] \\ \phi[2T_b\{(\alpha_1 + \alpha_2)d_0 + (\beta_1 + \beta_2)d_1 + (\gamma)d_2 + (\delta)d_3\}] \end{cases}$ $\phi = 0.75,\ \alpha_1 = 1.0,\ \alpha_2 = 0.5,\ \beta_1 = 1.0,\ \beta_2 = 0.75,\ \gamma_1 = 0.75,\ \delta_1 = 0.5$
Bolt Rupture without Prying Action		$\phi M_{np} = \phi[2P_t(2d_0 + 2d_1 + d_2 + d_2)], \quad \phi = 0.75$

4. VALIDATION OF CONNECTION CONFIGURATION DESIGN PROCEDURES BASED ON LITERATURE

This chapter examines data from previous tests and uses this data to compare to the predicted moment capacities presented in the previous chapter. The configurations that are reviewed here are the 8E-4W and 8ES configuration.

Since some tests found in the literature were cyclic tests while others (including the experiments conducted as part of this research described in the following two chapters) were monotonic, it is worthwhile to discuss the potential differences between test results from cyclic and monotonic tests. First, it is noted that the design procedures in the AISC Design Guide 16 are not intended for seismic loading and that monotonic testing has been used for the majority of experimental verification of the Design Guide 16 configurations. Though some of tests used for validation in this chapter utilized quasi-static cyclic loading, it is assumed that cyclic tests will produce the same limit states with relatively similar yield and ultimate strength. Some of the potential differences between quasi-static monotonic and quasi-static cyclic test results may include:

- Strain hardening in cyclic tests might cause larger apparent moments at a given level of rotation than monotonic tests. This may lead to a different post-yield stiffness, but it is expected that the yield moment won't change significantly.
- It is also possible that bolt fracture will occur at smaller rotations because of the repeated loading and unloading (low cycle fatigue), but it is expected that bolt force at rupture, and thus the peak moment, would be the same for cyclic and monotonic loading.

4.1. Previous Testing on the Eight-Bolt Extended Four Wide Unstiffened Configuration

Research on the Eight-Bolt Extended Four Wide Unstiffened configuration has been reported by Sumner et al. (2000), Sumner and Murray (2001), and Sumner (2003). Table 4-1 presents a summary of the specimens that have been tested in the past.

Table 4-1 Summary of Experimental Work

Specimen Identification*		Reference	Configuration	Loading	Depth (in)	Behavior
1	8E-4W-1.25-1.125-30	Sumner et al. (2000)	Beam – Column	Cyclic	30	NA
2	8E-4W-1.25-1-30	Sumner et al. (2000)	Beam – Column	Cyclic	30	Thin
3	8E-4W-1.25-1.375-36	Sumner et al. (2000)	Beam – Column	Cyclic	36	Thick
4	8E-4W-1.25-1.25-36	Sumner et al. (2000)	Beam – Column	Cyclic	36	Thin
5	8E-4W-1-1/2-62	Sumner & Murray (2001)	Splice	Mono.	62	Thin
6	8E-4W-3/4-3/4-62	Sumner & Murray (2001)	Splice	Mono.	62	Thick
7	8E-4W-3/4-3/4-62 (A490)	Sumner & Murray (2001)	Splice	Mono.	62	Thick

*Specimen Identification: “Connection type - Bolt diameter - End-plate thickness - Beam depth”

Test data from four of the seven specimens is used here for verification of the design procedure. The specimens were chosen such that the design procedures could be verified for shallower and deeper specimens with both thick and thin end-plate behavior. The selected specimens are boxed in with heavy lines in Table 4-1. The tests used for verification are as follows: 8E-4W-1.25-1-30, 8E-4W-1.25-1.375-36, 8E-4W-1-1/2-62, and 8E-4W-3/4-3/4-62. Specimens 8E-4W-1.25-1-30 and 8E-4W-1.25-1.375-36 were both subjected to cyclic loading, while 8E-4W-1-1/2-62 and 8E-4W-3/4-3/4-62 were both conducted with monotonic loading. The following sections demonstrate that previous

experimental test results are in reasonable agreement with the limit states and values predicted by the design procedure proposed in Chapter 3.

4.1.1 Shallow Section - Thin Plate Behavior

Specimen 8E-4W-1.25-1-30 (cyclic) from Sumner et al. (2000) had a depth of 30 in. which may be considered relatively shallow for the amount of moment capacity that this configuration can generate. The end-plate geometry is shown in Figure 4-1.

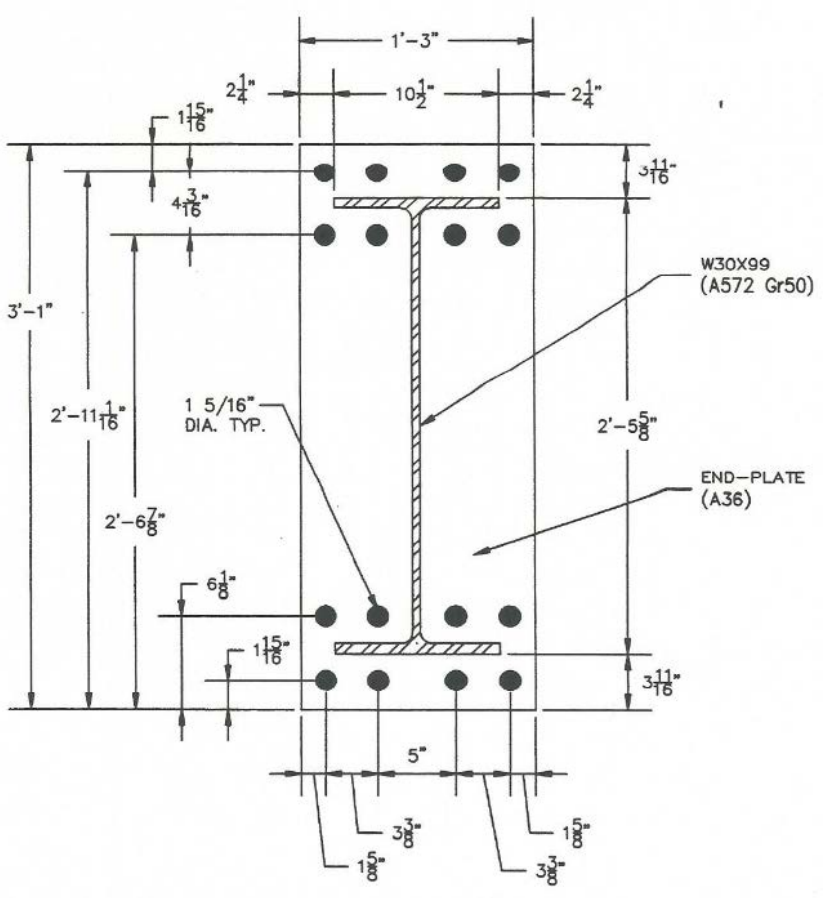

Figure 4-1 End-Plate Layout for Specimen 8E-4W-1.25-1-30 [from (Sumner et al. 2000)]

Using the equations presented in Chapter 3, the moment capacities for end-plate yielding, M_{pl}, bolt rupture with prying action, M_q, and bolt rupture without prying action, M_{np}, were calculated and are given in Table 4-2. The design equations for M_{np} and M_{pl} presented in Chapter 3 for this connection configuration are the same as those from Sumner

and Murray (2001) and calculated values for those limit states match values in Sumner and Murray (2001).

Table 4-2 Predicted and Experimentally Obtained Moment Capacities for Specimen 8E-4W-1.25-1-30

Stage	Predicted (k-in)	Experimental (k-in)	Ratio
Yield	M_{pl} =15,120	M_y =14,570	M_{pl}/M_y =1.04
Ultimate	M_q =18,840	M_u =17,980	M_q/M_u =1.05
Doesn't Control	M_{np} =25,640		

Based on the calculated moment capacities, it is expected that first the end-plate will yield, then the bolts will rupture with prying action. Sumner and Murray (2001) report that this was indeed the progression of behavior. The test was terminated after rupture of the two inner column bolts inside the bottom flange of the test specimen. The moment vs. rotation behavior shown in Figure 4-2 demonstrates that the predicted values for end-plate yielding and bolt rupture are similar to experimentally obtained moments associated with softening, M_y, and peak moment at bolt rupture, M_u. The values for experimental yield moment, M_y, and peak moment, M_u are reported in Sumner and Murray (2001). The ratio of predicted value to experimental value (wherein a number less than unity is conservative), were found to be 1.04 and 1.05 for yield and ultimate moments, respectively. Both predictions are within 5% of the experimentally obtained behavior.

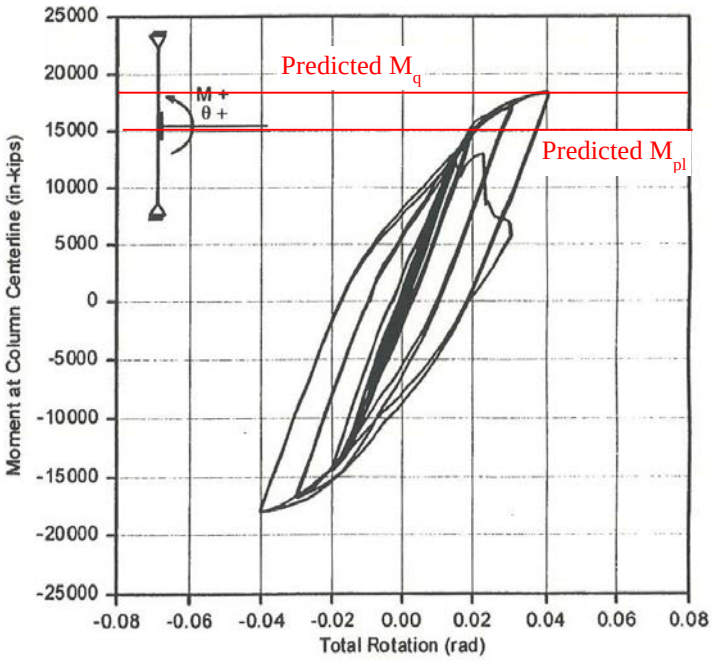

Figure 4-2 Load-deformation behavior for Specimen 8E-4W-1.25-1-30 [from Sumner et al. (2000)]

Instrumented calipers (the same type of calipers used in the experimental program described in the following chapter) were used to measure end-plate separation. Figure 4-3a gives an example of end-plate separation. The plot shows relatively large separations once the yield moment of the end-plate was achieved which is consistent with thin end-plate behavior. Similarly, bolt strains in Bolt 2 (see inset to Figure 4-3b) drastically increased starting at the moment associated with end-plate yielding. This suggests prying forces and is consistent with thin end-plate behavior. This relationship between strain and moment was typical for all bolts in the test so only one bolt strain plot is shown here.

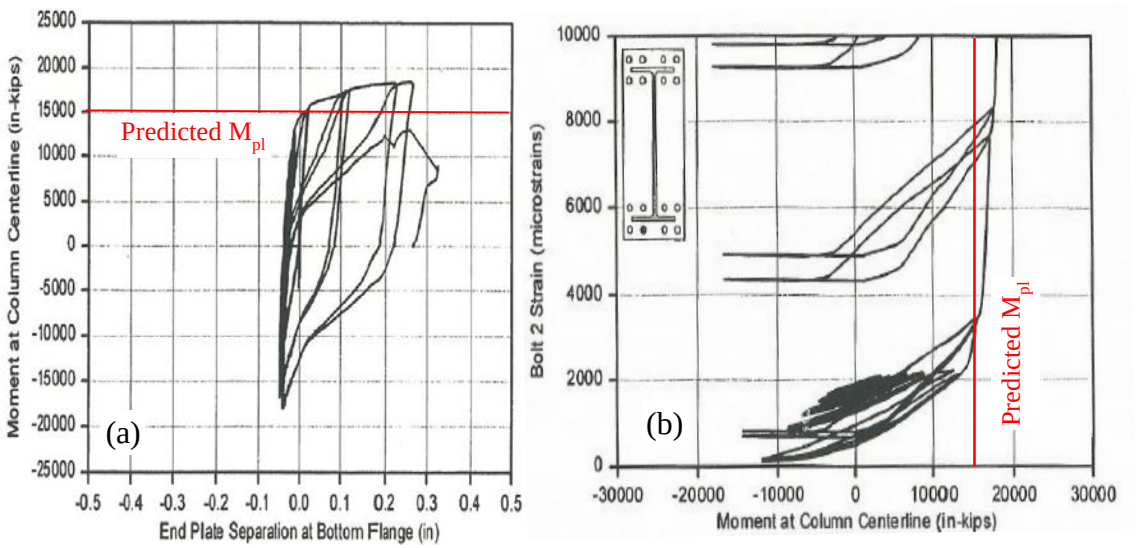

Figure 4-3 (a) End-plate separation and (b) Bolt Strain for Specimen 8E-4W-1.25-1-30 [from Sumner et al. (2000)]

4.1.2 Shallow Section - Thick Plate Behavior

Similar to the previous section, Specimen 8E-4W-1.25-1.375-36 from Sumner et al. (2000) with a rafter depth of 36 in. may be considered shallow in relation to the moment capacity that this configuration can sustain. The specimen end-plate geometry is shown in Figure 4-4. The specimen was subjected to a quasi-static cyclic displacement history.

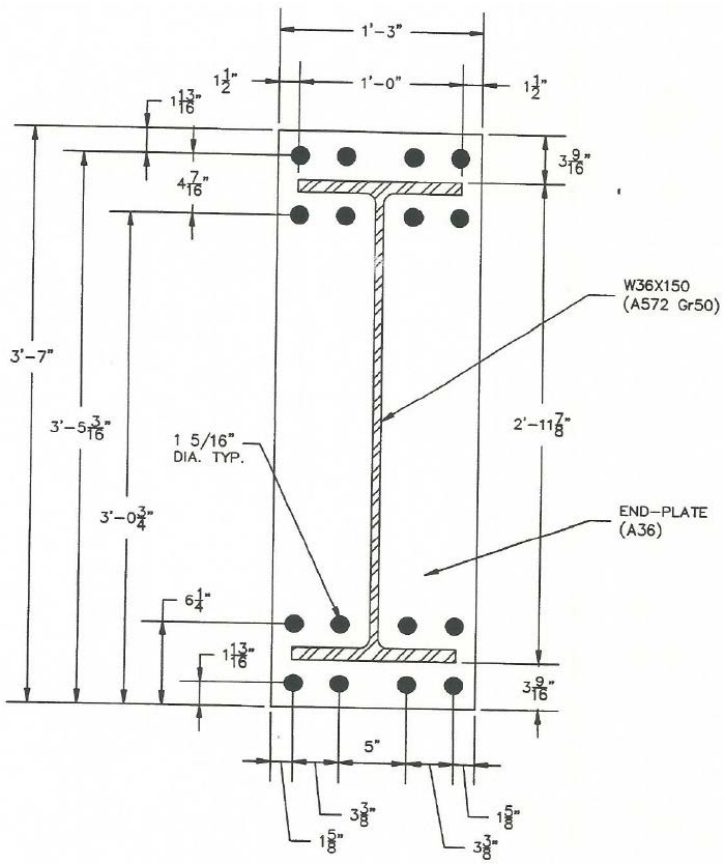

Figure 4-4 End-Plate Layout for Specimen 8E-4W-1.25-1.375-36 [from Sumner et al. (2000)]

The predicted moment capacity, M_{np}, along with the end-plate yield moment, M_{pl}, are given in Table 4-3. Since these values were calculated using the equations presented in Chapter 3 that are the same as those proposed in Sumner and Murray (2001), the values presented here, match those from Sumner and Murray (2001).

Table 4-3 Predicted and Experimentally Obtained Moment Capacities for Specimen 8E-4W-1.25-1.375-36

	Predicted (k-in)	Experimental (k-in)	Ratio
Ultimate	M_{np} =30,900	M_u =32,800	M_{np}/M_u =0.94
Doesn't Control	M_{pl} =35,100		

The peak moment achieved during the test, M_u, is also reported in Table 4-3. The specimen experienced bolt rupture without apparent yielding of the end-plate after

achieving this moment. This limit state is consistent with thick end-plate behavior. The ratio of predicted moment capacity to peak moment during the test was M_{np}/M_u=0.94 which means that the predicted capacity was conservative by 6%. This ratio is also demonstrated graphically as the difference between the peak moment and the predicted moment line in Figure 4-5.

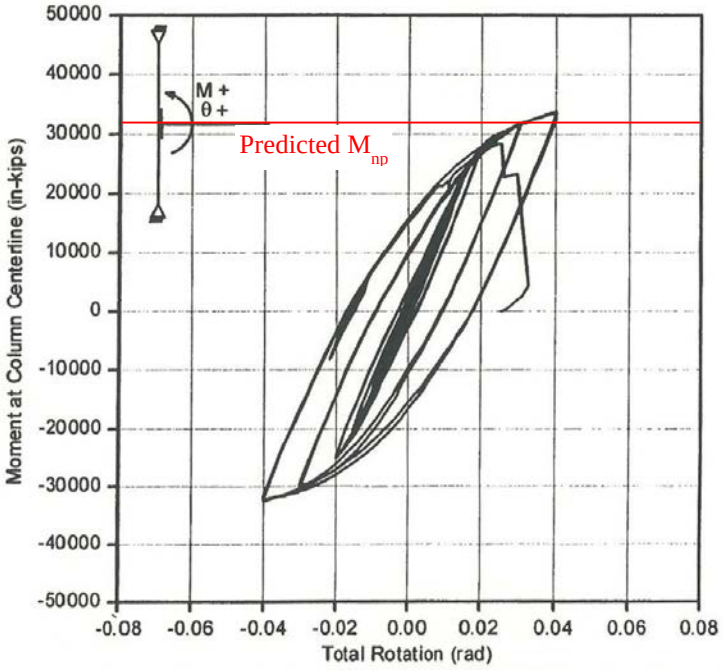

Figure 4-5 Load-deformation behavior for Specimen 8E-4W-1.25-1.375-36 [from Sumner et al. (2000)]

Figure 4-6a shows that the end-plate separation was relatively small (approximately 0.13" at bolt rupture) which suggests minimal end-plate yielding and thus thick end-plate behavior. The bolt strains in Bolt 2 (see inset in Figure 4-6a for bolt location), exhibit a bilinear behavior wherein the bolt strains are constant until the moment overcomes the initial bolt pretension and then linearly increase with additional moment. This suggests minimal prying action.

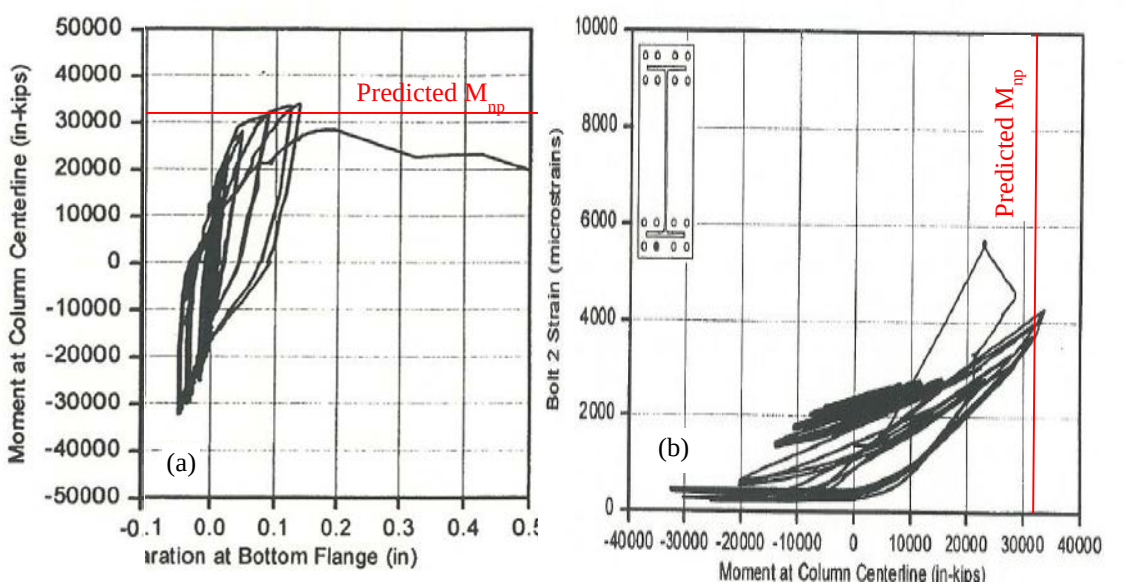

Figure 4-6 (a) End-plate separation and (b) Bolt Strain
Specimen 8E-4W-1.25-1.375-36 [from Sumner et al. (2000)]

4.1.3 Deep Section - Thin Plate Behavior

Specimen 8E-4W-1-1/2-62 from Sumner and Murray (2001) was 62 in. deep with end-plate geometry shown in Figure 4-7. The specimen was subjected to quasi-static monotonic loading.

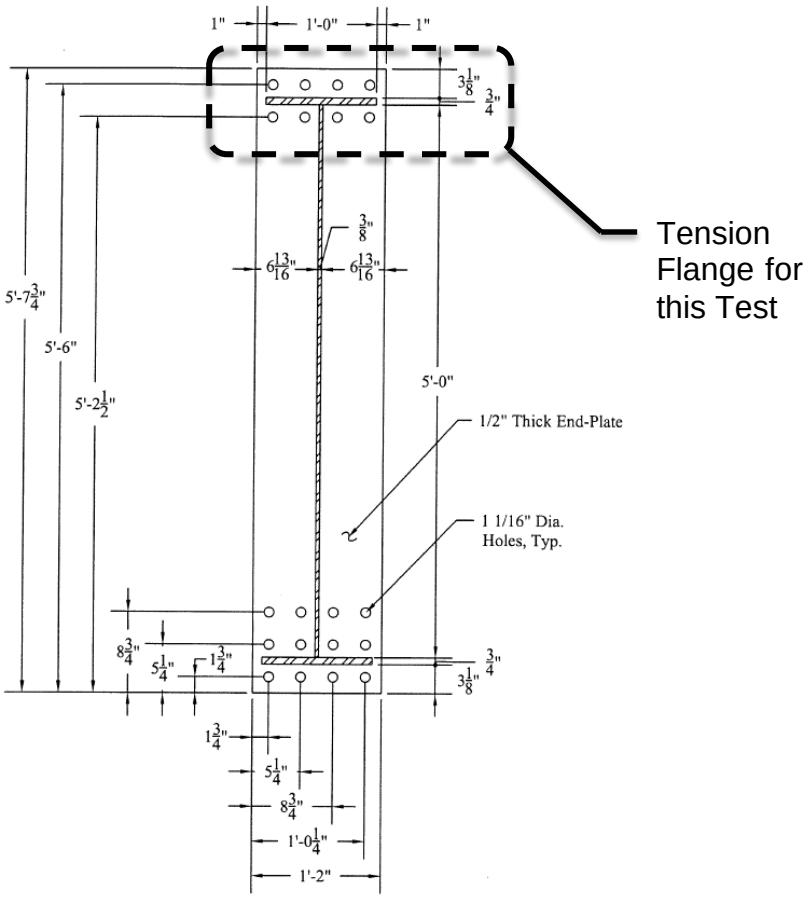

Figure 4-7 End-Plate Layout for Specimen 8E-4W-1-1/2-62 [from Sumner and Murray (2001)]

Predicted moment capacities are given in Table 4-4. The predicted moment capacities were calculated using the equations presented in Chapter 3 which were the same as those in Sumner and Murray (2001). The resulting values were the same as well. Specimen 8E-4W-1-1/2-62 is reported to have experienced end-plate yielding, but the test was stopped prior to bolt rupture. The values for experimental yield moment, M_y, and peak moment experienced during the test, M_u, were reported in Sumner and Murray (2001) and are given in Table 4-4.

The ratios of predicted moment capacity to experimental capacity are also given in Table 4-4. The end-plate yielding moment capacity was conservatively predicted to be 4% smaller than the actual capacity. The predicted moment capacity associated with bolt rupture was 111% of the peak moment experienced during the test, but the test was stopped

prior to bolt rupture. If the test had been conducted up to bolt rupture, the ultimate moment might have been closer to the predicted value.

Table 4-4 Predicted and Experimentally Obtained Moment Capacities for Specimen 8E-4W-1-1/2-62

Stage	Predicted (k-ft)	Experimental (k-ft)	Ratio
Yield	M_{pl} =1034	M_y =1075	M_{pl}/M_y =0.96
Ultimate	M_q =1707	M_u^*=1540	M_q/M_u^* =1.11
Doesn't Control	M_{np} =2863		

* The test was stopped prior to bolt rupture

Figure 4-8 shows the moment versus mid-span deflection response of Specimen 8E-4W-1-1/2-62 and Figures 4-9 and 4-10 show the end-plate separation and bolt forces, respectively. Although the global moment vs. deflection response (Figure 4-8) doesn't show significant softening, the end-plate separations show an increase after achieving the predicted moment associated with end-plate yielding (see Figure 4-9). At the end of the test, the bolt strains (as indicated by the reported bolt forces in Figure 4-10) started to show a sharp increase with a small increase in applied moment. This increasing strain without increasing load implies yielding, which may be related to prying forces after end-plate yielding. The total end-plate separations were relatively small for a thin end-plate test, but that may be related to the fact that the test was stopped prior to bolt rupture.

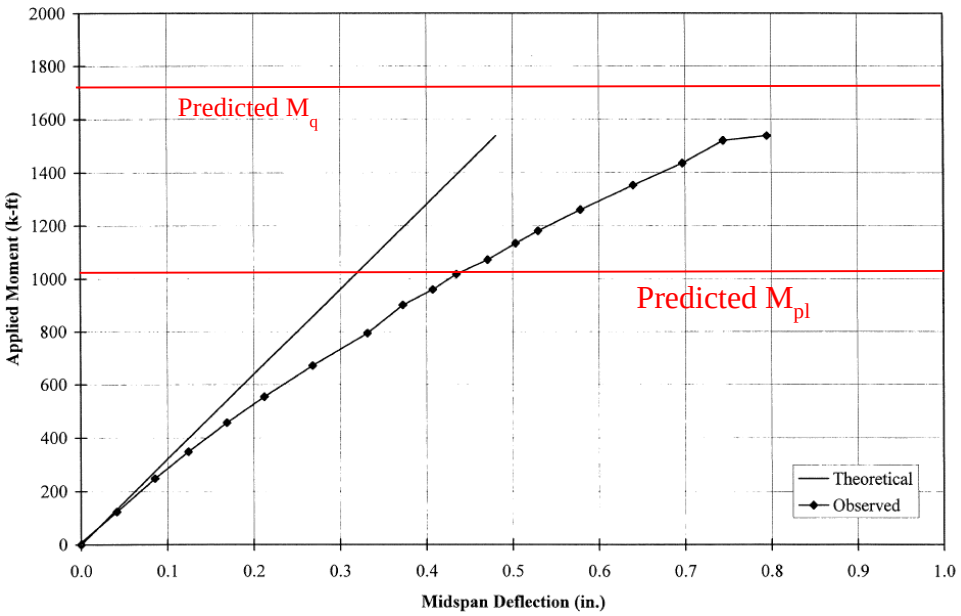

Figure 4-8 Load-deformation behavior for Specimen 8E-4W-1-1/2-62 [from Sumner and Murray (2001)]

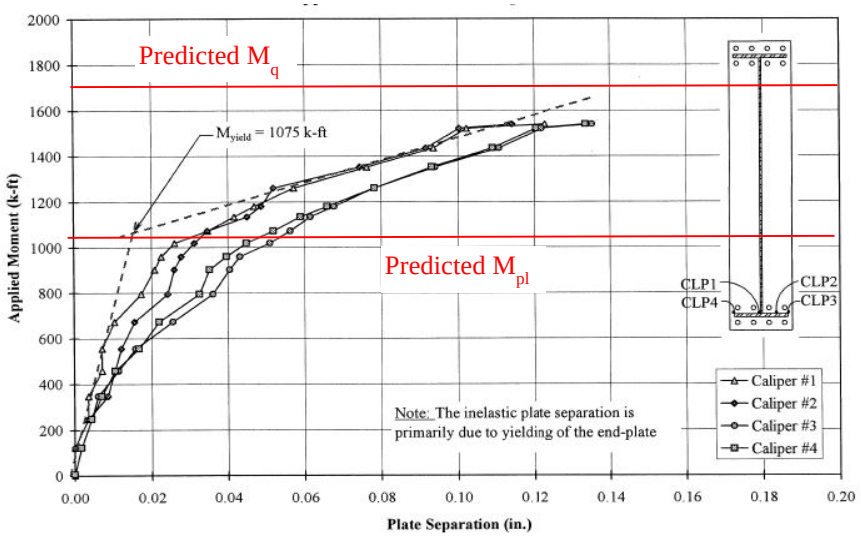

Figure 4-9 End-Plate Separation for Specimen 8E-4W-1-1/2-62 [from Sumner and Murray (2001)]

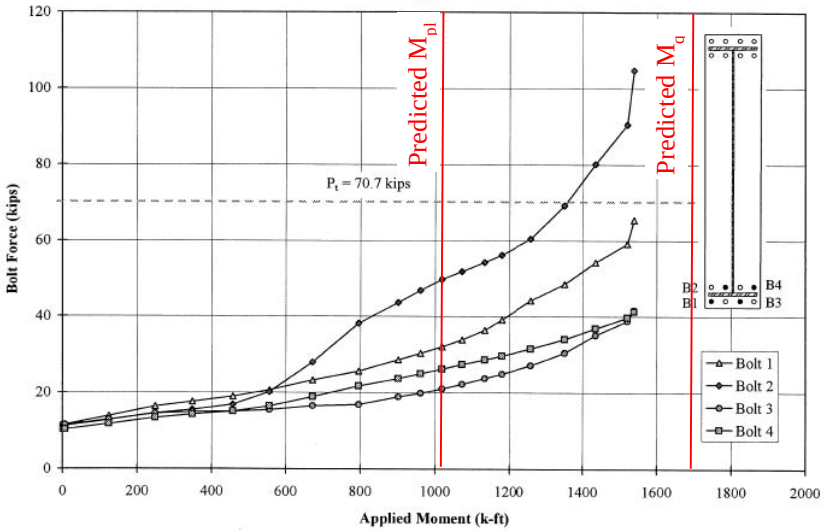

Figure 4-10 Bolt forces for Specimen 8E-4W-1-1/2-62 [from Sumner and Murray (2001)]

4.1.4 Deep Section – Thick End-Plate Behavior

Specimen 8E-4W-3/4-3/4-62 from Sumner and Murray (2001) used a 62 in. deep rafter. Figure 4-11 shows the geometry of the end-plate.

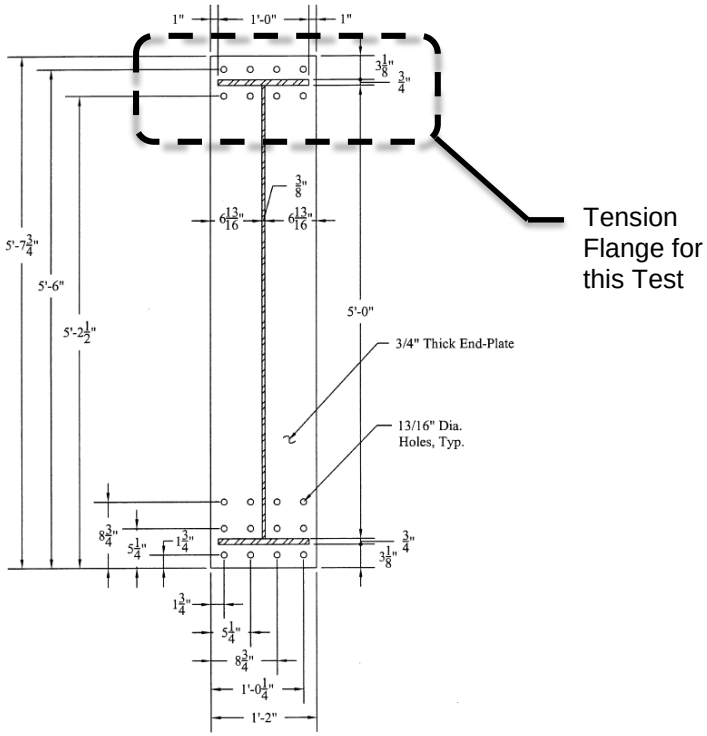

Figure 4-11 End-Plate Layout for Specimen 8E-4W-3/4-3/4-62 [from Sumner and Murray (2001)]

The moment capacities associated with bolt rupture (without prying action) and end-plate yielding are given in Table 4-5 along with the moment at which the bolts ruptured in the test as reported in Sumner and Murray (2001). The design equations and resulting predicted moment capacities were similar to those presented in Sumner and Murray (2001). The ratio of predicted capacity, M_{np}, to achieved moment capacity, M_u, was 0.88 which means the prediction was conservative by 12%.

Table 4-5 Predicted and Experimentally Obtained Moment Capacities for Specimen 8E-4W-3/4-3/4-62

	Predicted (k-ft)	Experimental (k-ft)	Ratio
Ultimate	M_{np} =1612	M_u =1825	M_{np}/M_u =0.88
Doesn't Control	M_{pl} =2602		

The global response, plate separation, and bolt forces are shown in Figure 4-12, 4-13, and 4-14, respectively. The end-plate separation was relatively small suggesting that the end-plate did not undergo significant yielding prior to bolt rupture. A redistribution of bolt forces occurred at large moment (see Figure 4-14) where the exterior bolts experienced an increase of force while the interior bolts unloaded. This redistribution may suggest some inelastic deformations in the end-plate. The exterior bolt forces approached their strength as the applied moment reached the predicted bolt rupture moment, M_{np}.

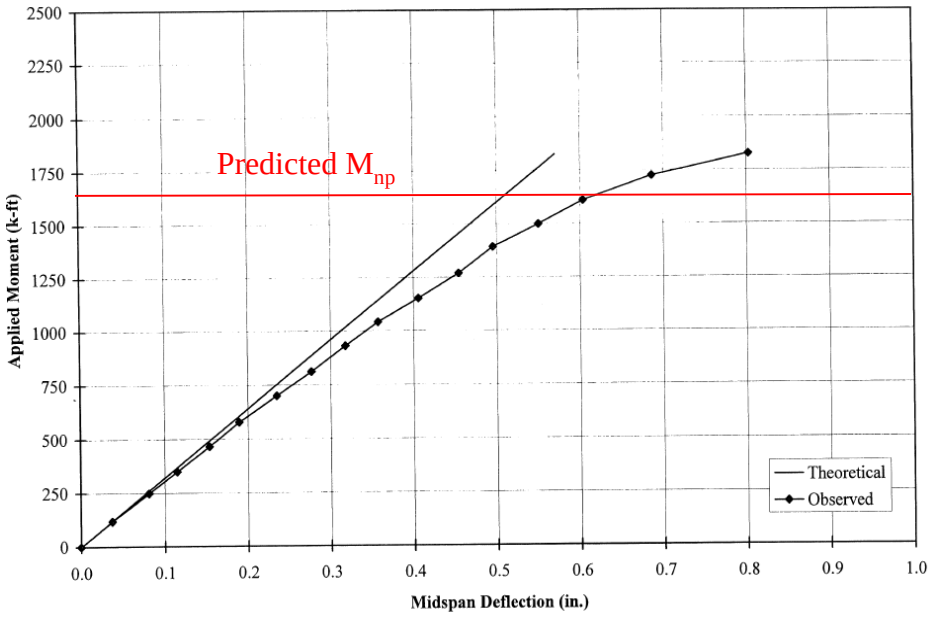

Figure 4-12 Load-deformation behavior for Specimen 8E-4W-3/4-3/4-62 [from Sumner and Murray (2001)]

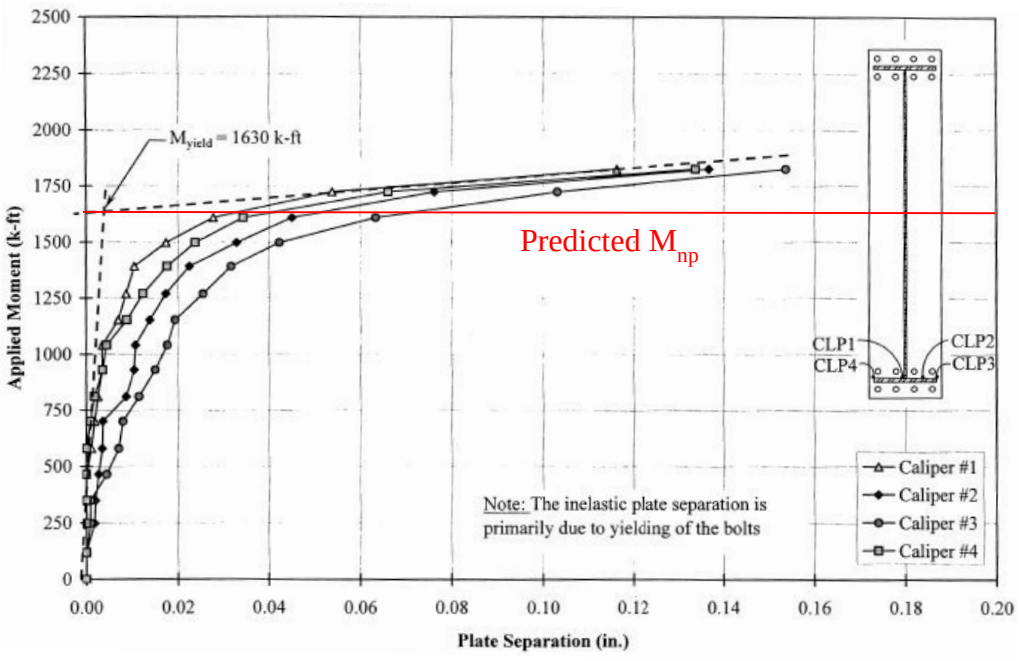

Figure 4-13 End-Plate Separation for Specimen 8E-4W-3/4-3/4-62 [from Sumner and Murray (2001)]

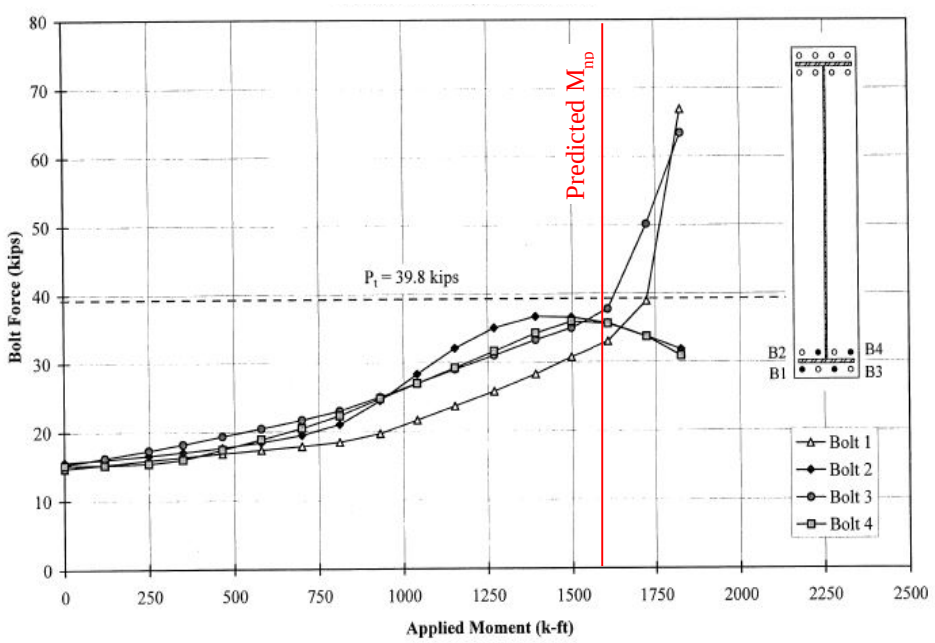

Figure 4-14 Bolt forces for Specimen 8E-4W-3/4-3/4-62 [from Sumner and Murray (2001)]

4.1.5 Summary of Eight Bolt Extended Four Wide Configuration

For the two thin plate specimens, the predicted end-plate moment capacity, M_{pl}, was either 4% less or 4% more than the experimentally observed yield moment, M_y. Also, the moment capacity associated with bolt rupture, M_q, was 5% more than the experimental ultimate moment for one test and was 11% more than the peak moment at the time of stopping the test for the other. End-plate yielding was observed for both the thin plate specimens and the experimentally observed magnitude of end-plate separation was consistent with thin end-plate behavior.

For the two thick plate specimens, 8E-4W-1.25-1.375-36 and 8E-4W-3/4-3/4-62, the predicted moment capacity, M_{np}, was conservative by 6% and 12% respectively. The conservative nature of the prediction was likely related to additional bolt strength above nominal values. The ultimate limit state was bolt rupture without observable end-plate yielding and relatively small end-plate separation which is consistent with thick end-plate behavior.

Based on these observations, it is concluded that the design procedures presented in Chapter 3 for the eight-bolt four wide extended end-plate connection provided a

reasonably accurate prediction of moment capacity and behavior (i.e. progression of expected limit states).

4.2. Previous Testing on the Eight-Bolt Extended Stiffened Configuration

The eight bolt extended, stiffened end-plate connection is included in AISC 358-10 (AISC 2010) as a prequalified moment connection for special moment resisting frames. There have been several tests on the connection configuration, but many have focused on developing a plastic hinge in the beam prior to experiencing end-plate yielding or bolt rupture. The references reviewed in this section focus on tests that may be used to validate design procedures for either thin end-plate or thick end-plate behavior.

Experimental programs on the Eight-Bolt Extended Stiffened configuration have been reported by Ghassemieh et al. (1983), Adey et al. (1997, 2000), Sumner et al. (2000), Sumner and Murray (2002), Sumner (2003) and Seek and Murray (2008). A summary of previous tests on this connection configuration is given in Table 4-6.

Since many of the tests were intended for the development of seismic resisting moment connections, they consisted of beam-column test configurations subjected to cyclic loading. In this section, test specimens 8ES-0.875-0.75-24, 8ES-0.875-1-24, 8ES-1.25-1-30, and 8ES-1.25-1.25-36, which are boxed in thicker lines in Table 4-6, will be examined.

Table 4-6 Summary of Experiments on the Eight Bolt Extended Stiffened Configuration

Test Identification[1]		Reference	Configuration	Loading	Depth	Behavior[2]
1	8ES-0.875-0.75-24 (EP1)	Ghassemieh (1983)	Splice	Mono.	24	Thin
2	8ES-0.875-1-24 (EP2)	Ghassemieh (1983)	Splice	Mono.	24	Thick
3	8ES-1.125-0.75-18 (M5)	Adey et al. (1997)	Beam - Column	Cyclic	18	P.H. / Thin
4	8ES-1.125-0.75-18 (M7)	Adey et al. (1997)	Beam - Column	Cyclic	18	P.H. / Thin
5	8ES-1.125-0.75-18 (B5)	Adey et al. (1997)	Beam - Column	Cyclic	18	P.H. / Thin
6	8ES-1.25-1.75-30	Sumner et al. (2000)	Beam - Column	Cyclic	30	P.H.
7	8ES-1.25-1-30	Sumner et al. (2000)	Beam - Column	Cyclic	30	P.H. / Thin
8	8ES-1.25-2.5-36	Sumner et al. (2000)	Beam - Column	Cyclic	36	P.H.
9	8ES-1.25-1.25-36	Sumner et al. (2000)	Beam - Column	Cyclic	36	Thick
10	8ES-1.125-1.25-27	Seek and Murray (2008)	Beam - Column	Cyclic	27	P.H.

[1]Test Identification: "Connection type - Bolt diameter - End-plate thickness - Beam depth". Identification in parentheses was used in the reference.

[2]P.H. means plastic hinging of the beam.

4.2.1 Shallow Section - Thin Plate Behavior (8ES-1.25-1-30)

The Specimen 8ES-1.25-1-30 end-plate layout is shown in Figure 4-15. The beam was a W30x99 connected to a W14x193 column.

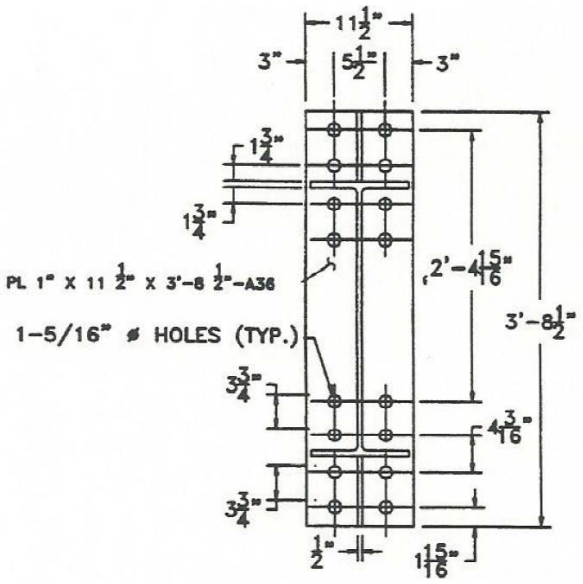

Figure 4-15 End-Plate Layout for Specimen 8ES-1.25-1-30 [from Sumner et al. (2000)]

Predicted moment capacities were calculated based on the equations presented in Chapter 3 and are reported in Table 4-7. The beam plastic moment capacity, M_p of 16400 k-in (calculated as measured yield stress multiplied by the plastic section modulus) was slightly less than the end-plate yield moment capacity, M_{pl} of 17700 k-in (also calculated using measured yield stress).

Table 4-7 Predicted and Experimentally Obtained Moment Capacities for Specimen 8ES-1.25-1-30

Stage	Predicted (k-in)	Experimental (k-in)	Ratio
End-Plate Yield	M_{pl} =17,700	M_y =16,900	M_{pl}/M_y =1.05
Beam Yield	M_p =16,400		
Ultimate	M_q =19,100	M_u *=20,900	M_q/M_u *=0.91
Doesn't Control	M_{np} =25,700		

* Due to beam yielding and local buckling, moments reduced and the end-plate bolts did not rupture

Sumner et al. (2000) reported that the specimen first experienced yielding in the flanges of the beam at the base of the stiffeners, followed by yielding in the column web doubler plate and the end-plate. During subsequent cycles, full yield of the beam flanges

led to local flange buckling while inelasticity spread to many parts of the specimen: end-plate, beam web, column web, end-plate stiffeners. The test was stopped after cycles up to 0.055 rad after severe lateral displacements of the beam.

Yielding of the beam was likely the reason that the observed yield moment was 5% less than the predicted end-plate yield moment. Also, because of beam flange local buckling, the moment degraded before bolt rupture was obtained. However, the specimen sustained a moment that was approximately 10% larger than the predicted bolt rupture moment meaning that the prediction was conservative.

Figure 4-16 shows the moment rotation behavior for the specimen. The moment-rotation plot is difficult to interpret (in terms of validating the end-plate moment capacity) because several limit states were occurring including plastic hinging of the beam.

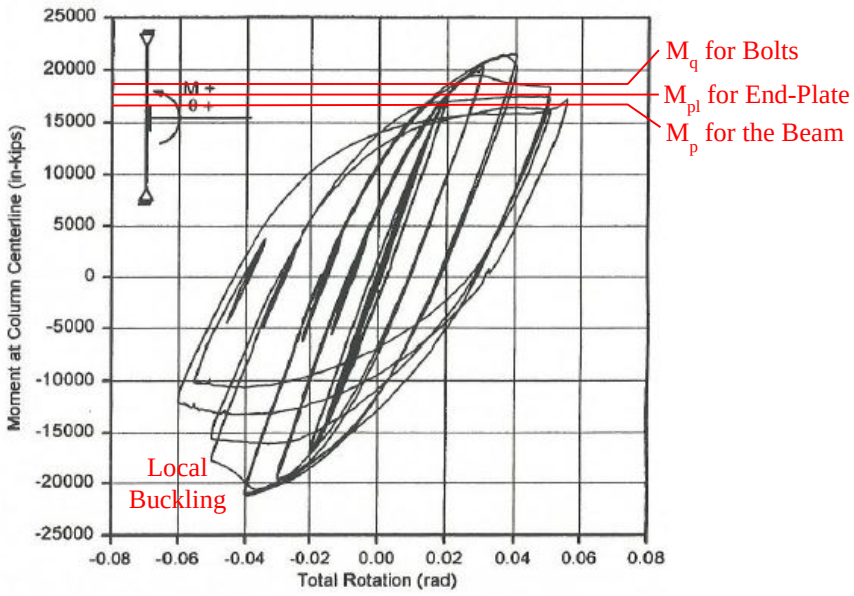

Figure 4-16 Moment vs. Rotation Behavior for Specimen 8ES-1.25-1-30 [from Sumner et al. (2000)]

Figure 4-17a displays end-plate separation. The nonlinearity in the end-plate separation shown in Figure 4-17a may be related to end-plate yielding although the magnitude of end-plate separation is smaller than expected if end-plate yielding were the only controlling limit state. Figure 4-17b shows the strain from Bolt 11 (see inset). A steep increase in the strains with little increase in moment is exhibited at the peak moment. This suggests prying action in the connection associated with end-plate yielding.

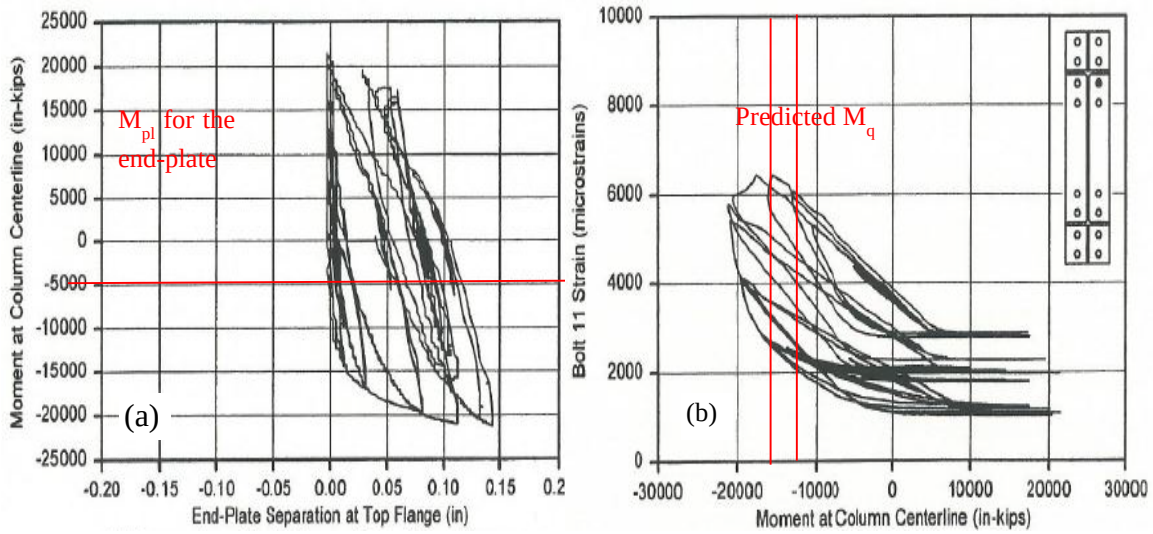

Figure 4-17 (a) End-plate separation and (b) Bolt Strain for Specimen 8ES-1.25-1-30 [from Sumner et al. (2000)]

4.2.2 Shallow Section - Thin Plate Behavior (8ES-0.875-0.75-24)

See Figure 4-18 for end-plate layout for Specimen 8ES-0.875-0.75-24 reported in Ghassemieh et al. (1983).

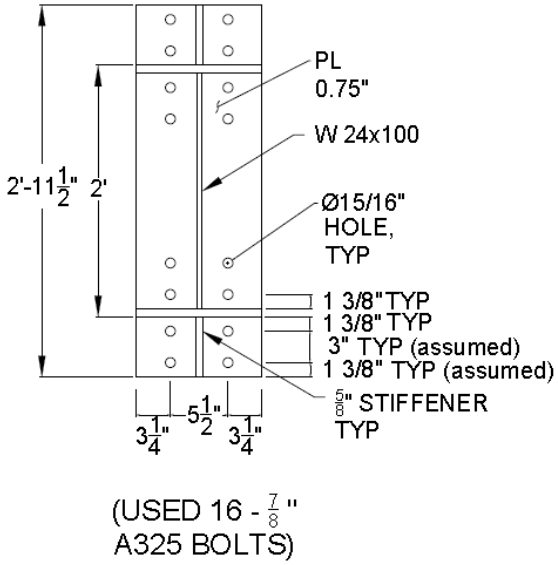

Figure 4-18 End-Plate Layout for Specimen 8ES-0.875-0.75-24 [redrawn from Ghassemieh et al. (1983)]

Predicted moment capacities were calculated according the equations presented in Chapter 3 and are given in Table 4-8. It is noted that the predicted moment capacity for bolt rupture with prying action, M_q, was calculated to be smaller than the moment capacity associated with end-plate yielding, M_{pl} (based on measured yield stress). It is not typical to design the bolts to rupture with prying action before end-plate yielding in the thin end-plate design approach. Ghassemieh et al. (1983) reported nonlinearity starting at 350 k-ft, a yield moment of approximately 500 k-ft, and ultimate moment equal to 680 k-ft. It was also stated that end-plate yielding was observed at the ultimate moment.

Table 4-8 Predicted and Experimentally Obtained Moment Capacities 8ES-0.875-0.75-24

Stage	Predicted (k-ft)	Experimental (k-ft)	Ratio
End-Plate Yield	M_{pl} =788	M_y =500	M_{pl}/M_y =1.58
Ultimate	M_q =648	M_u *=680	M_q/M_u * =0.95
Doesn't Control	M_{np} =853		
	M_p =840		

* Test stopped prior to bolt rupture

Figure 4-19 shows the moment-deflection behavior whereas Figure 4-20 shows both the plate separation and bolt forces. It is hypothesized that as soon as the bolt pretension force was overcome, end-plate separation began which led to prying forces. As the prying forces increased, the bolts yielded (going off the plot in Figure 20b). It is likely that the end-plates didn't experience much yielding because bolt inelasticity was responsible for the softening of the connection.

It is stated in Ghassemieh et al. (1983) that end-plate yielding was observed at 680 k-ft of moment (at the ultimate moment). This further supports the previous hypothesis. Although it appears from Ghassemieh et al. (1983) that the test was stopped prior to bolt fracture, based on the nonlinearity and excessive bolt forces, the predicted moment capacity for bolt rupture with prying action appears reasonable even if it wasn't possible to evaluate end-plate yielding predictions.

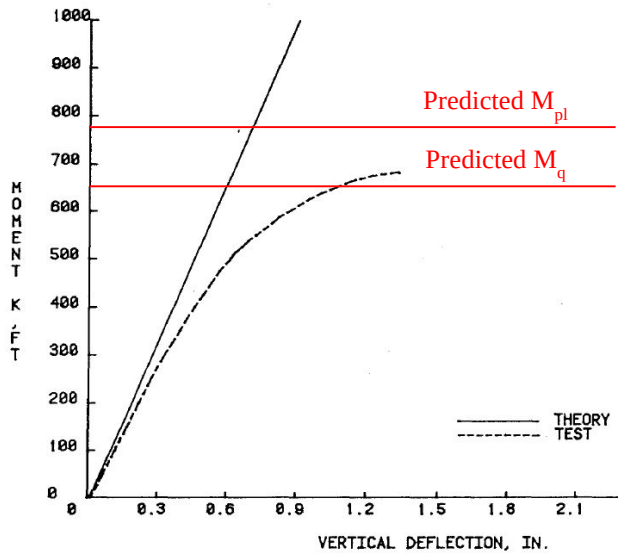

Figure 4-19 Moment-Deflection behavior for Specimen 8ES-0.875-0.75-24 [from (Ghassemieh et al. 1983)]

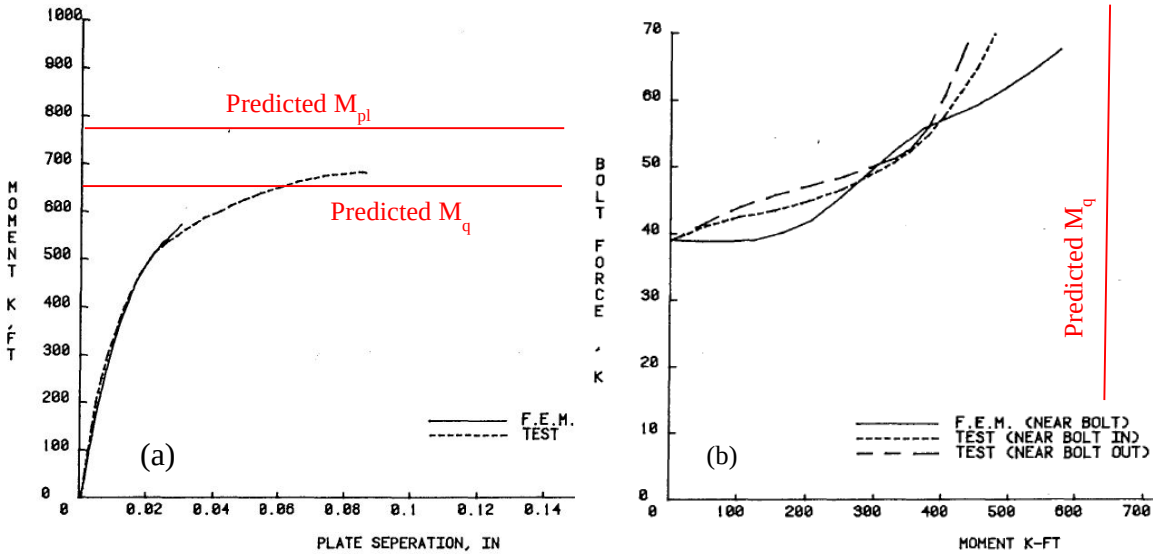

Figure 4-20 (a) Plate Separation and (b) Bolt forces for 8ES-0.875-0.75-24 [Ghassemieh et al. (1983)]

4.2.3 Shallow Section - Thick Plate Behavior (Specimen 8ES-1.25-1.25-36)

Specimen 8ES-1.25-1.25-36 consisted of a W36x150 beam connected to a W14x257 column. The specimen was subjected to quasi-static cyclic loading. Figure 4-21 shows the end-plate layout for the specimen.

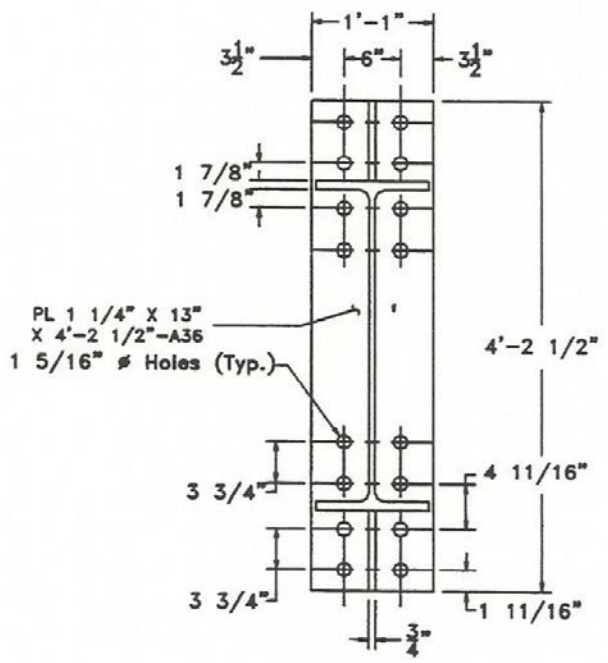

Figure 4-21 End-plate Layout for Specimen 8ES-1.25-1.25-36 [from Sumner et al. 2000]

Equation in Chapter 3 were used to calculate the predicted moment capacities given in Table 4-9.

Table 4-9 Predicted and Experimentally Obtained Moment Capacities for Specimen 8ES-1.25-1.25-36

	Predicted (k-in)	Experimental (k-in)	Ratio
Ultimate	M_{np} =30,800	M_u =32,700	M_{np}/M_u =0.94
Doesn't Control	M_{pl} =36,800		
	M_p =32,500		

The global response of the specimen is shown in Figure 4-22 whereas the plate separation and bolts strains are demonstrated in Figure 4-23. Yielding in both the beam flanges and the end-plate were reported starting at 0.010 rad story drift and continuing until bolt rupture at 0.04 rad story drift. The moment associated with bolt rupture without prying action, M_{np} =30800 k-in, was 94% of the experimentally obtained moment at bolt rupture of 32700 k-in.

The large end-plate separation (Figure 4-23a) suggests that some end-plate yielding occurred (corroborating the reported observation of end-plate yielding). However, the large bolts strains (Figure 4-23b) suggest that some of the end-plate separation may have been related to yielding of the bolts.

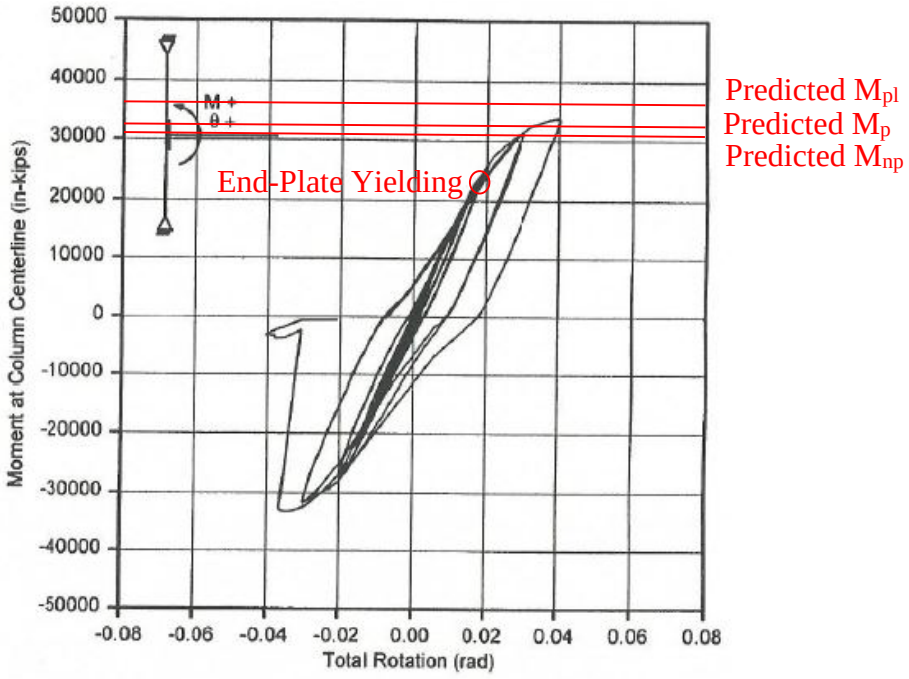

Figure 4-22 Load-deformation behavior for Specimen 8ES-1.25-1.25-36 [from Sumner et al. (2000)]

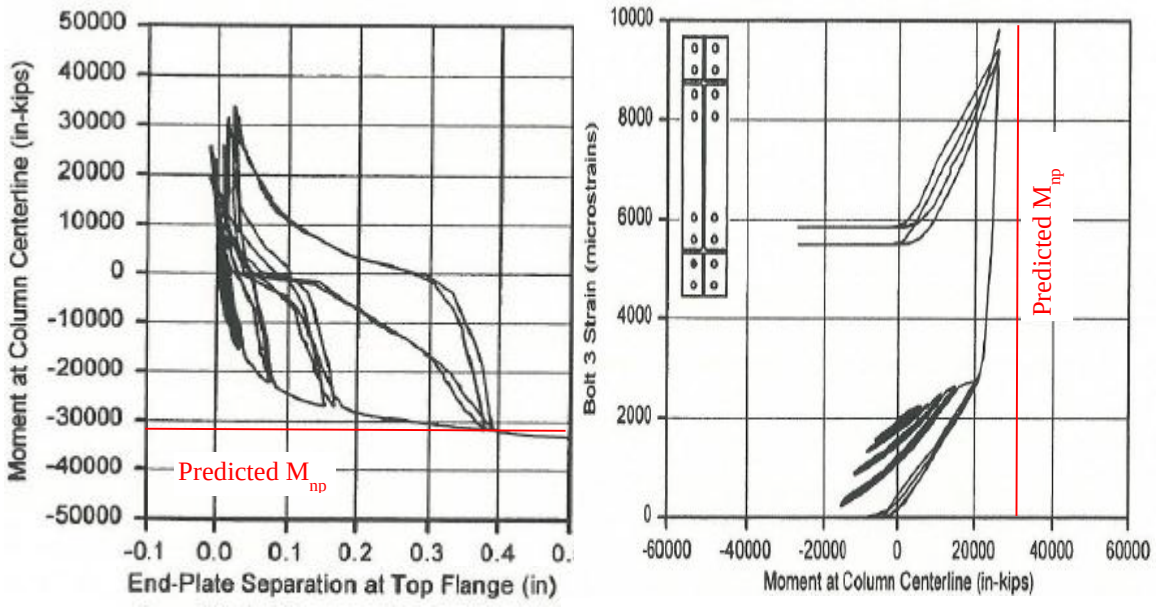

Figure 4-23 (a) End-plate separation and (b) Bolt Strain for Specimen 8ES-1.25-1.25-36 [from Sumner et al. (2000)]

4.2.4 Shallow Section - Thick Plate Behavior (Specimen 8ES-0.875-1-24)

Specimen 8ES-0.875-1-24 from Ghassemieh et al. (1983) was very similar to Specimen 8ES-0.875-0.75-24 examined in Section 4.2.2. but with a 1 in. thick end-plate. The end-plate geometry is shown in Figure 4-24.

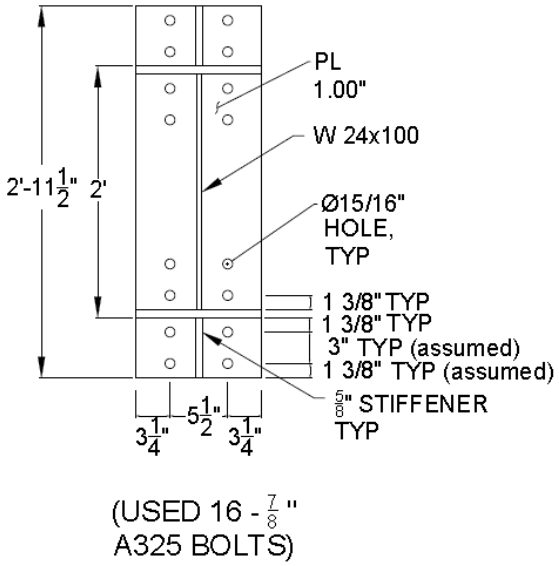

Figure 4-24 End-Plate Layout for Specimen 8ES-0.875-1-24 [redrawn from Ghassemieh et al. (1983)

As given in Table 4-10, the beam plastic moment capacity, M_p, was calculated to be 840 k-ft (using measured yield stress) which was close to the calculated moment capacity associated with bolt rupture without prying action, M_{np}, (853 k-ft). Based on the predicted moment capacities, it is expected that beam inelasticity and bolt rupture would occur. Ghassemieh et al. (1983) does not describe the limit states actually observed. Because bolt rupture is not mentioned, it is assumed that the test was stopped prior to bolt rupture.

Table 4-10 Predicted and Experimentally Obtained Moment Capacities for Specimen 8ES-0.875-1-24

	Predicted (k-ft)	Experimental (k-ft)	Ratio
Ultimate	M_{np} =853	M_u^* =750	M_{np}/M_u^* =1.13
Doesn't Control	M_{pl} =1460		
	M_p =840		

* Test stopped prior to bolt rupture

Ghassemieh et al. (1983) reported a yield moment, M_y, of 637 k-ft and an ultimate moment, M_u, of 750 k-ft. Figure 4-25 shows the moment-deflection behavior. The moment reported when the test was stopped was 750 k-ft. This is 88% of the predicted moment capacity for bolt rupture without prying action. Based on Figure 4-25, it is deemed unlikely that the specimen would have reached the predicted moment capacity even if the test was continued.

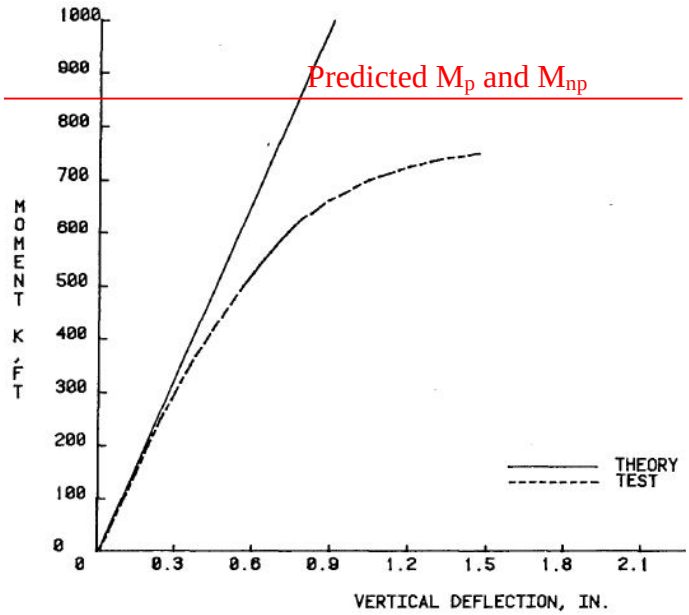

Figure 4-25 Load-deformation behavior for Specimen 8ES-0.875-1-24 [from (Ghassemieh et al. 1983)]

Figure 4-26a shows that the end-plate separation was quite small which may imply that the end-plate exhibited thick plate behavior and that nonlinearity in the global moment vs. deflection plot was not related to end-plate yielding.

Figure 4-26b shows typical bolt forces during the test. The bolt forces shown in the figure increase to the nominal tensile strength of the 7/8" A325 bolt (54 kips) by 300 k-ft to 400 k-ft for the bolts nearest the flange. The predicted end moment capacity without prying is 850 k-ft assuming all bolts are resisting their nominal tensile strength. It is possible that the top and bottom rows of bolts are not resisting as much load (supported by data in Sumner et al. (2000)) leading to a reduced moment capacity when the bolts start to yield.

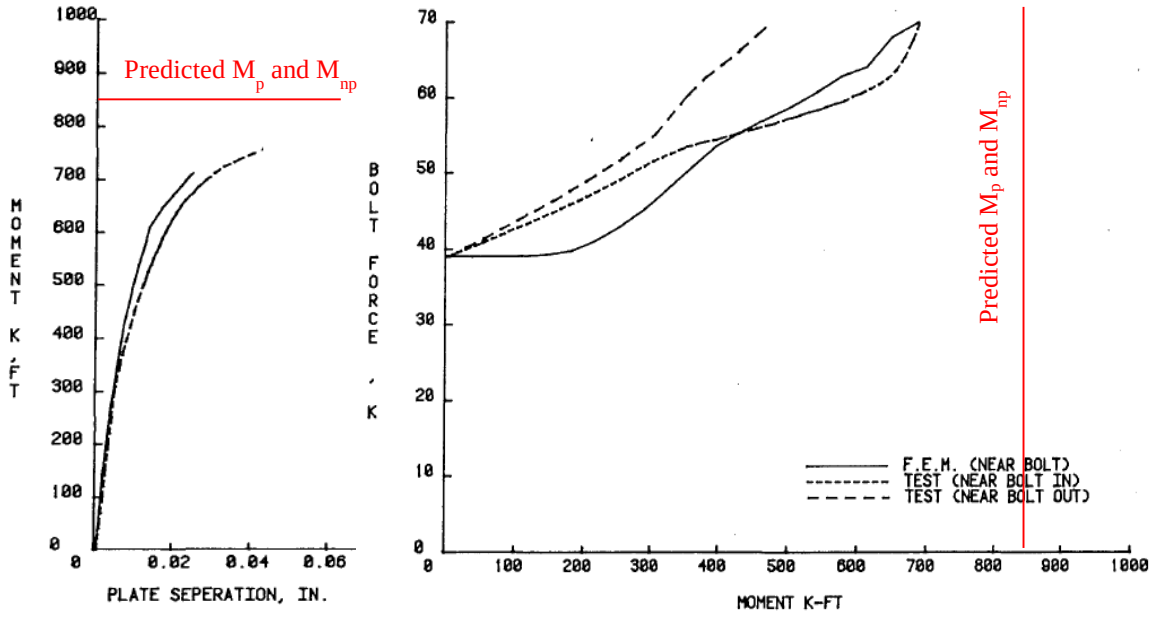

Figure 4-26 (a) End-plate separation and (b) Bolt Forces for Specimen 8ES-0.875-1-24 [Ghassemieh et al. (1983)]

4.2.5 Summary of the Eight Bolt Extended Stiffened Configuration

Ten tests on eight-bolt extended, stiffened end-plates were included in four separate experimental programs. Most specimens were designed with strong end-plates and bolts to develop plastic hinging in the beam since the connection configuration was originally intended for large ductility seismic connections. This section investigated four of these specimens identified as potentially having the most useful data for validating design procedures for thick and thin end-plate behavior.

The behavior of the four specimens were all quite different and the relationship between experimentally obtained end-plate yield moment and predicted values varied considerably. Although the predicted end-plate yield moment capacity, M_{pl}, was within 5% of the experimental yield moment for Specimen 8ES-1.25-1-30, significant nonlinearity in the response of Specimen 8ES-0.875-0.75-24 was observed at only 63% of the predicted moment, M_{pl}. However, it was hypothesized that the discrepancy for Specimen 8ES-0.875-0.75-24 was related to bolt capacity being too small to develop end-plate yielding.

The equation predicting moment capacity associated with prying action, M_q, appeared effective or conservative as Specimen 8ES-0.875-0.75-24 from Ghassemieh et al.

(1983) produced a moment at the end of the test similar to the predicted M_q value, and Specimen 8ES-1.25-1-30 reached 110% of M_q before the test was stopped without bolt fracture.

There were mixed results as to the effectiveness of the equation predicting moment capacity without prying action, M_{np}. Specimen 8ES-1.25-1.25-36 experienced bolt rupture at a moment that was within 6% of the predicted value, M_{np}. On the other hand, it is unlikely that Specimen 8ES-0.875-1-24 would have reached the predicted M_{np} as the test was stopped at 88% of M_{np} after significant softening.

Because some of the previous testing had multiple limit states occurring simultaneously and the resulting comparisons between predicted and actual moment capacities were not as clean as hoped, additional testing was deemed necessary. The additional testing reported in the next two chapters included two additional specimens. Since the previous testing was conducted with hot-rolled beam shapes with a maximum nominal depth of 36 in., the new tests were seen as an opportunity to not only test specimens with well separated limit states, but also evaluate whether the design procedures are appropriate for deeper (56 in. deep) built-up rafters.

5. EXPERIMENTAL TESTING

5.1. Test Specimens

A total of ten end-plate moment connection tests were performed. These include four tests each on 6B-4W/2W configuration and 12B-MRE 1/3-4W/2W configuration, and two tests on deep 8ES configuration.

Each test specimen consisted of two built-up beam sections spliced together at mid-span using A325 bolts. Each built-up beam had an end-plate at each end so that it could be used for two tests. This was done by rotating the built-up beam by 180 degrees, such that the unused end came in the center and flipping it over, such that the bottom flange came on the top. The shallower built-up beam sections (shown in Figure 5-1a) were 36 in. deep with 3/4 in. by 12 in. flanges and a 1/4 in. thick web. Four such built-up beams were fabricated, two each for the 6B-4W/2W and 12B-MRE 1/3-4W/2W configurations.

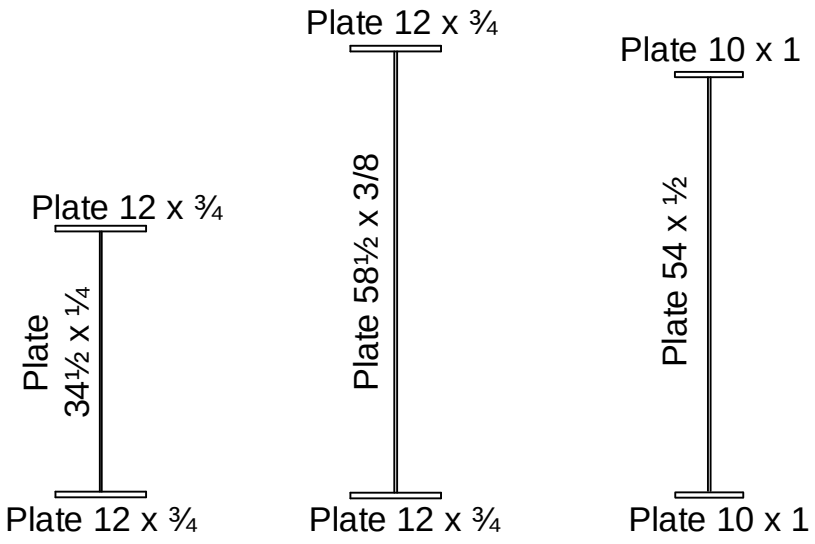

(a) 36 in. deep rafter (b) 60 in. deep rafter (c) 56 in. deep rafter

Figure 5-1 Built-Up Rafter Sections Used for Testing

The deep built-up rafters were of two types. Firstly, for the 6B-4W/2W and 12B-MRE 1/3-4W/2W configuration beam section (shown in Figure 5-1b) was 60 in. deep. Four of the deep built-up beams were fabricated, two of the 6B-4W/2W configuration and two

of the 12B-MRE 1/3-4W/2W configuration. For the 8ES connection, the beam section (shown in Figure 5-1c) was 56 in. deep. Refer to Appendix D for the drawings of the specimens.

An end-plate width of 14 in. was used for 12B-MRE 1/3-4W/2W and 6B-4W/2W connection configurations while a 10 in. width was used for the 8ES configuration. The thickness of end-plate was either 1 in. or 3/4 in. depending on whether it was a thick end-plate or a thin end-plate respectively. The geometry of the end-plates including bolt gage, and pitches are shown in Figures 5-2, 5-3, and 5-4.

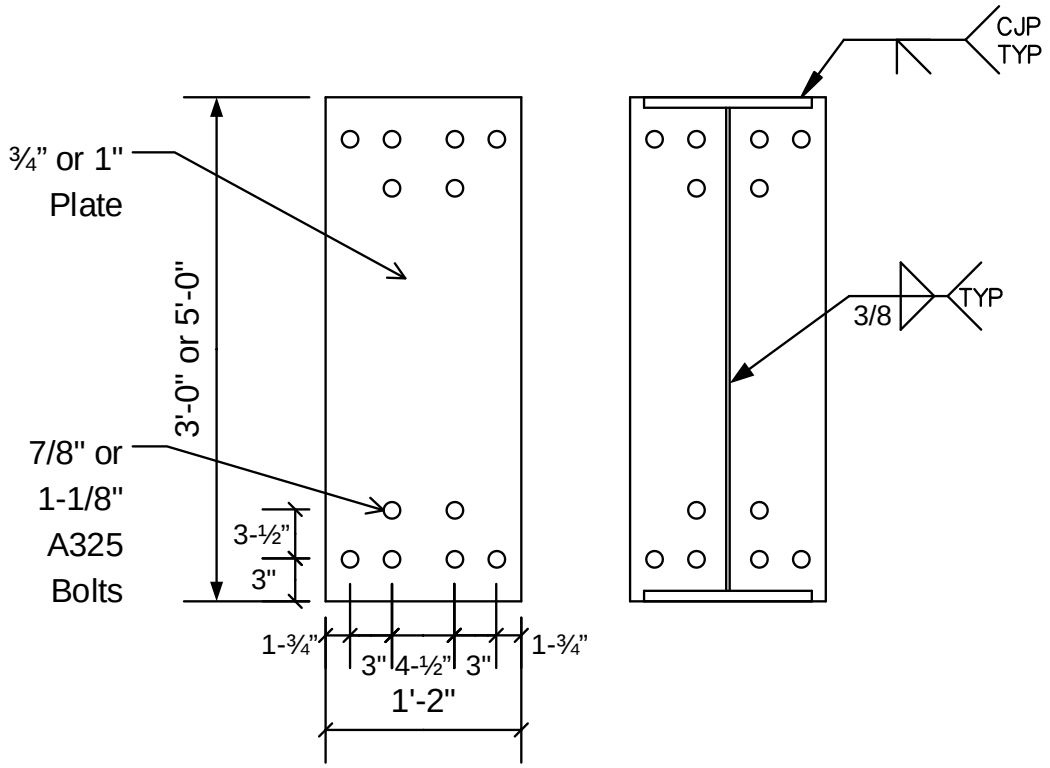

Figure 5-2 End-Plate Parameters for 6B-4W/2W Configuration

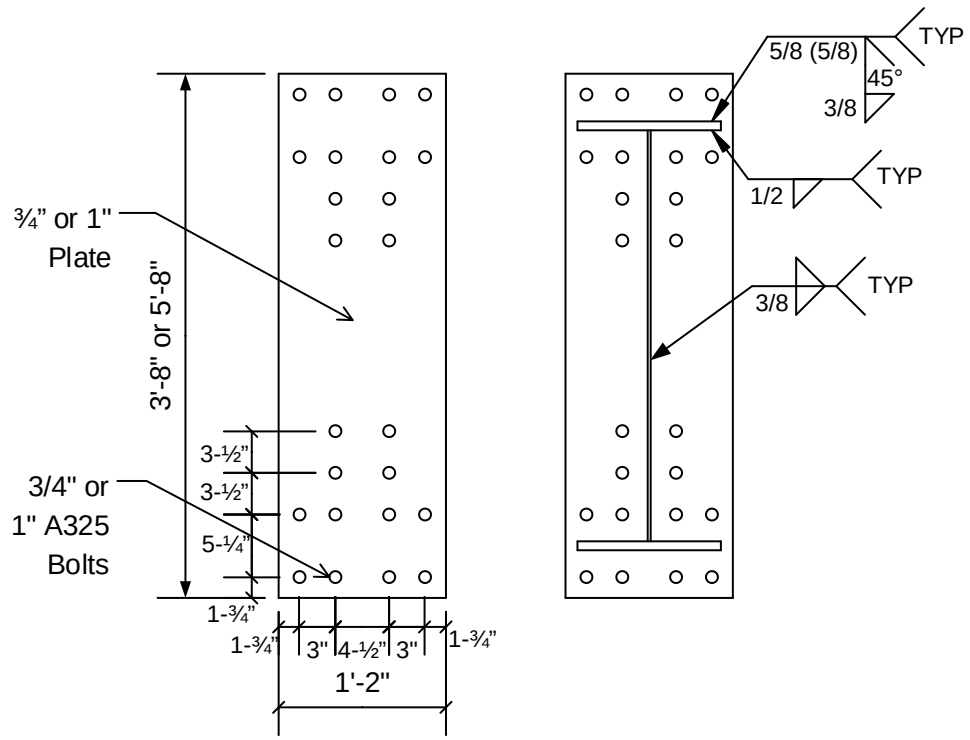

Figure 5-3 End-Plate Parameters for 12B-MRE 1/3-4W/2W Configuration

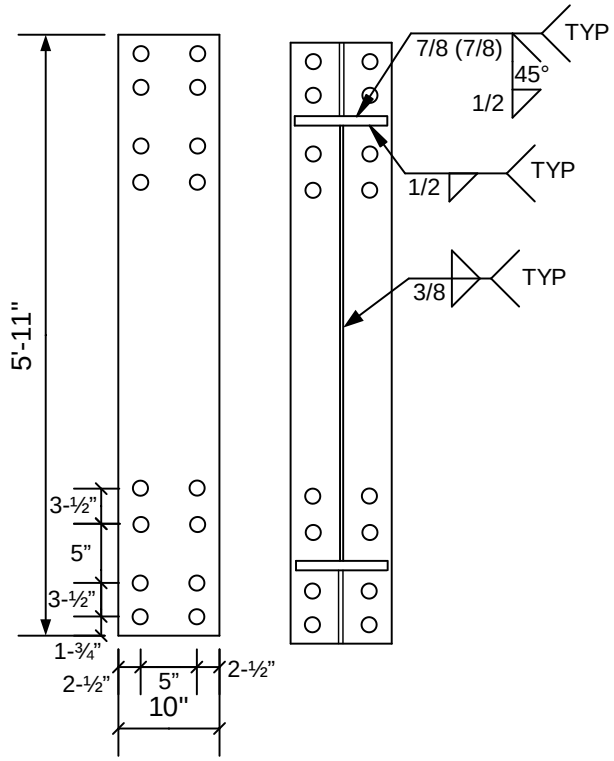

Figure 5-4 End-Plate Dimensions for 8ES Configuration

Refer to Appendix A for the mill test reports of the material used in the fabrication of the specimens. Additional information about end-plate tension coupon tests and bolt strengths reported in the mill test reports is presented later in this chapter.

Fully pretensioned ASTM A325 bolts were used with ASTM A563 nuts. No washers were used with the exception of washers being used for Specimen 8ES-1.25-0.75-56 end-plate connection. This was done because the grip (thickness of the two end-plates combined) was too small for the length of bolts for that particular specimen.

The test matrix shown in Table 5-1 gives dimensions related to the built-up beam section and the bolted connections. Table 5-2 provides the predicted moment capacities for the limit states of end-plate yielding, M_{pl}, bolt rupture without prying action, M_{np}, and beam plastic hinging, M_p, as calculated using the equations presented in Chapter 3. Refer to Appendix D for detailed drawings of the specimens. The specimens were designed without using any ϕ factors.

Table 5-1 Test Matrix With Geometry

Specimen Identification[1]	Bolt Dia., d_b (in.)	Bolt Grade	No. of Tension Bolts	End-Plate Thickness (in.)	Pitch, p_b (in.)	Gage, g, g_o (in.)	End-Plate Width, b_p (in.)	Flange Width, b_f (in.)	Beam Depth, d (in.)
6B-4W/2W-0.875-1.00-36	7/8	A325	6	1	3 1/2	4 1/2, 3	14	12	36
6B-4W/2W-1.125-0.75-36	1 1/8	A325	6	3/4	3 1/2	4 1/2, 3	14	12	36
6B-4W/2W-0.875-1.00-60	7/8	A325	12	1	3 1/2	4 1/2, 3	14	12	60
6B-4W/2W-1.125-0.75-60	1 1/8	A325	12	3/4	3 1/2	4 1/2, 3	14	12	60
12B- MRE 1/3 - 4W/2W-0.75-1.00-36	3/4	A325	6	1	3 1/2	4 1/2, 3	14	12	36
12B- MRE 1/3 - 4W/2W-1.00-0.75-36	1	A325	6	3/4	3 1/2	4 1/2, 3	14	12	36
12B- MRE 1/3 - 4W/2W-0.75-1.00-60	3/4	A325	12	1	3 1/2	4 1/2, 3	14	12	60
12B- MRE 1/3 - 4W/2W-1.00-0.75-60	1	A325	12	3/4	3 1/2	4 1/2, 3	14	12	60
8ES-1.00-1.00-56	1	A325	8	1	3 1/2	5	10	10	56
8ES-1.25-0.75-56	1 1/4	A325	8	3/4	3 1/2	5	10	10	56

[1] Test Identification: “Conn. type - Bolt dia. - End-plate thickness - Beam depth”

Table 5-2 Specimen Predicted Moment Capacities

Specimen Identification		M_{pl} (k-ft)	M_{np} (k-ft)	M_p (k-ft)
1	6B4W/2W-1.125-0.75-36	684	1410	1795
2	6B4W/2W-0.875-1-36	1217	851	1795
3	6B4W/2W-1.125-0.75-60	1202	2481	3915
4	6B4W/2W-0.875-1-60	2136	1501	3915
5	MRE13/4W2W-1-0.75-36	1037	2306	1795
6	MRE13/4W2W-0.75-1-36	1843	1298	1795
7	MRE13/4W2W-1-0.75-60	1817	4003	3915
8	MRE13/4W2W-0.75-1-60	3229	2252	3915
9	8ES-1.25-0.75-56	2268	4087	4191
10	8ES-1-1-56	4031	2615	4191

5.2. Test Setup

Figure 5-5 shows the test setup for the deep rafter specimens and Figure 5-6 shows the test setup for shallow rafter specimens. The spliced built-up beams were simply supported by rollers at each end. The rollers in turn were supported on a stiffened steel beam connected to the reaction floor. The specimen was held down at the support using a ratchet and chain mechanism. Two MTS 201.80 actuators, supported by vertical reaction frames, were used to load the specimen symmetrically. The top flange of the specimen was connected to the actuators by four 1 1/4 dia bolts so that when the bolts ruptured, the specimen never hit the floor. Each actuator is capable of applying 445 kip compressive (downward) force and a 300 kip tensile (upward) force. A picture of the deep rafter test setup and the shallow rafter test setup are shown in Figures 5-7 and 5-8 respectively.

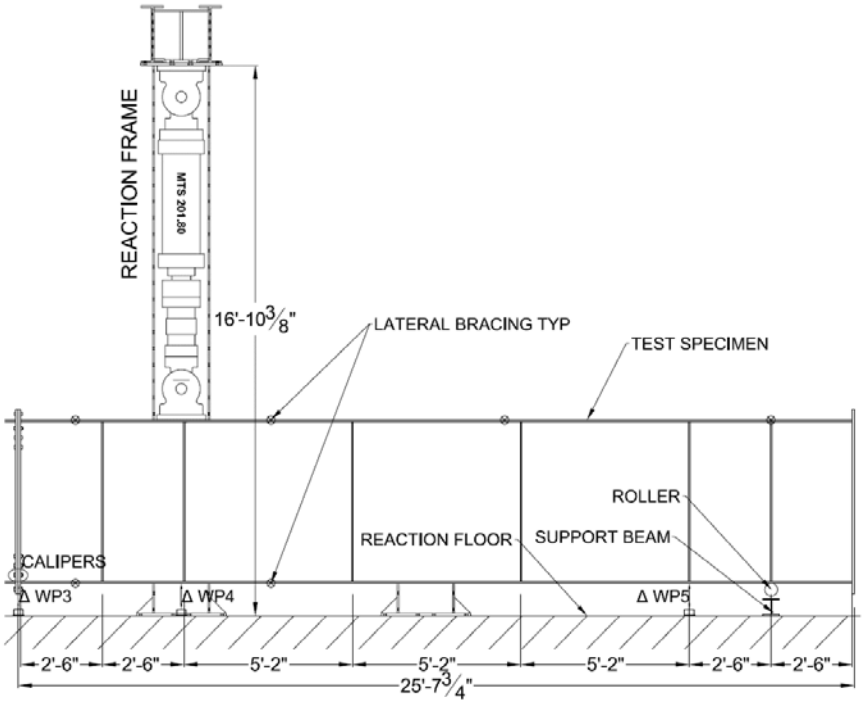

Figure 5-5 Half Diagram of Deep Beam Test Setup

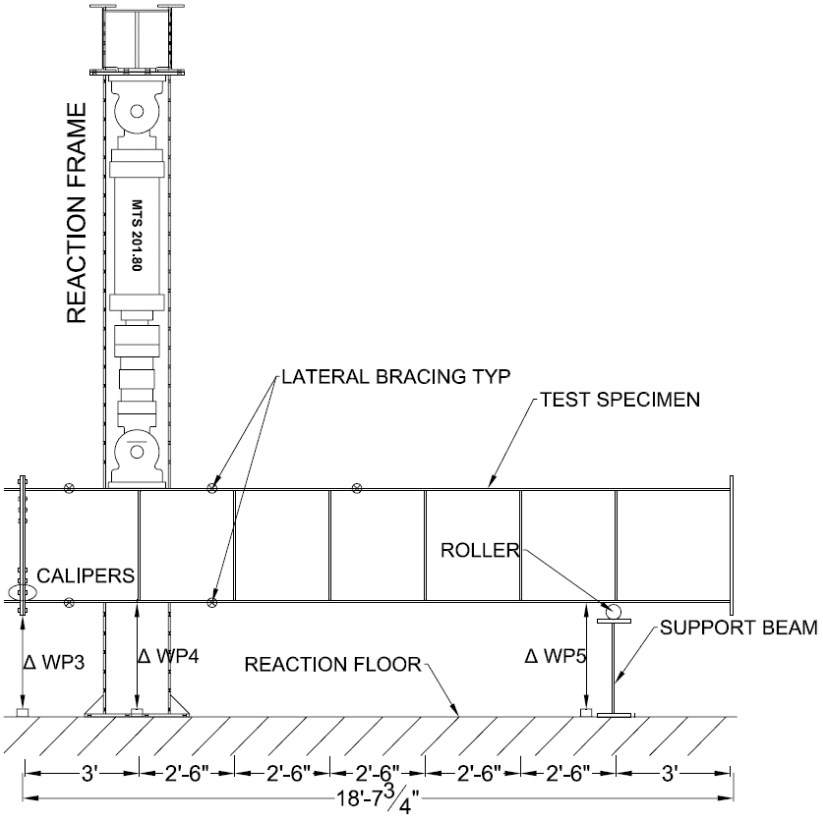

Figure 5-6 Half Diagram of Shallow Beam Test Setup

Figure 5-7 Picture of a Typical Deep Beam Test Setup

Figure 5-8 Picture of a Typical Shallow Beam Test Setup

The lateral braces allowed motion in the longitudinal and vertical directions while restraining motion in the lateral direction. Each lateral brace consisted of a hinged link in the center and an adjustable length rod on each side of the link. The center of the link was bolted onto a stud which was in turn welded on a plate that was bolted onto the flange of the specimen. A picture of the lateral bracing is shown in Figure 5-9.

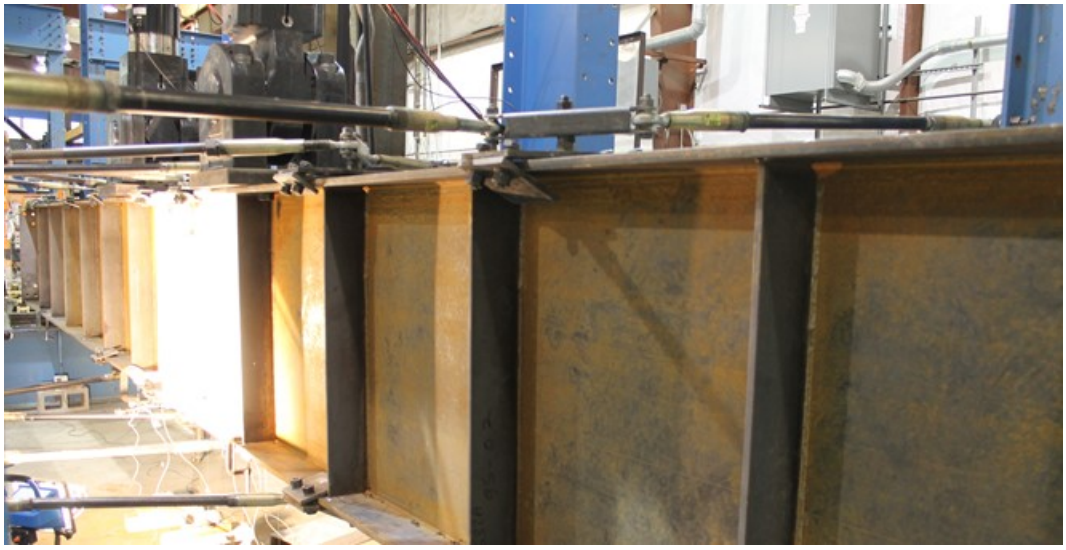

Figure 5-9 Picture of Lateral Bracing

The specimens were laterally braced at ten points, with six brace points on the top flange and four brace points on the bottom flange. Lateral bracing locations are shown in Figure 5-5 and 5-6. The bracing locations were kept as close as possible to the load point, near midspan and at about 7 ft from the support. Lateral bracing locations are shown on Figure 5-10.

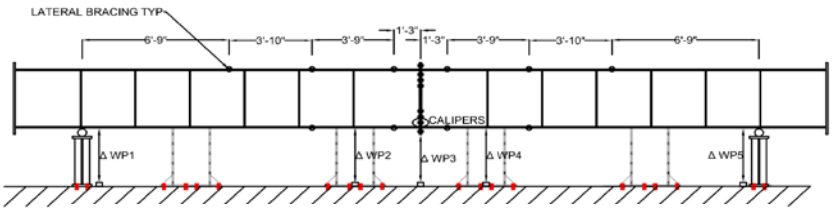

(a) Shallow Rafter Setup Lateral Bracing Locations

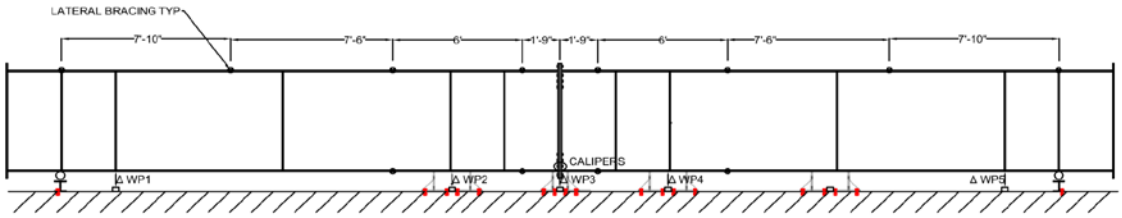

(b) Deep Rafter Setup Lateral Bracing Locations

Figure 5-10 Lateral Bracing Locations

5.3. Instrumentation

Three types of instrumentation were used to measure the specimen deflection, bolt forces and end-plate separation for each test. Also, the actuators had an in-built load cell and LVDT, the data from which was also recorded by the data acquisition system. Calibrated string potentiometers (wirepots) measured the deflection of the specimen at five points: midspan, the two load points, and near the two supports. The string potentiometer locations are shown graphically on Figures 5-5, 5-6, and 5-10.

Bolt forces were measured using calibrated strain gaged bolts. Calibration of the bolts was conducted using a 300 kip SATEC universal testing machine to determine the elastic load-strain relationship. 120 ohm bolt strain gages (BTM-6C) were inserted in a 2 mm diameter hole drilled in the shank of the bolt and glued using bolt adhesive (A-2). Half of the bolts on the tension side were instrumented (strain gaged) bolts. They were placed in such a way that each bolt could also represent another non-instrumented bolt mirrored about the centerline of the web. The locations of the strain gaged bolts are shown in Figure 5-11.

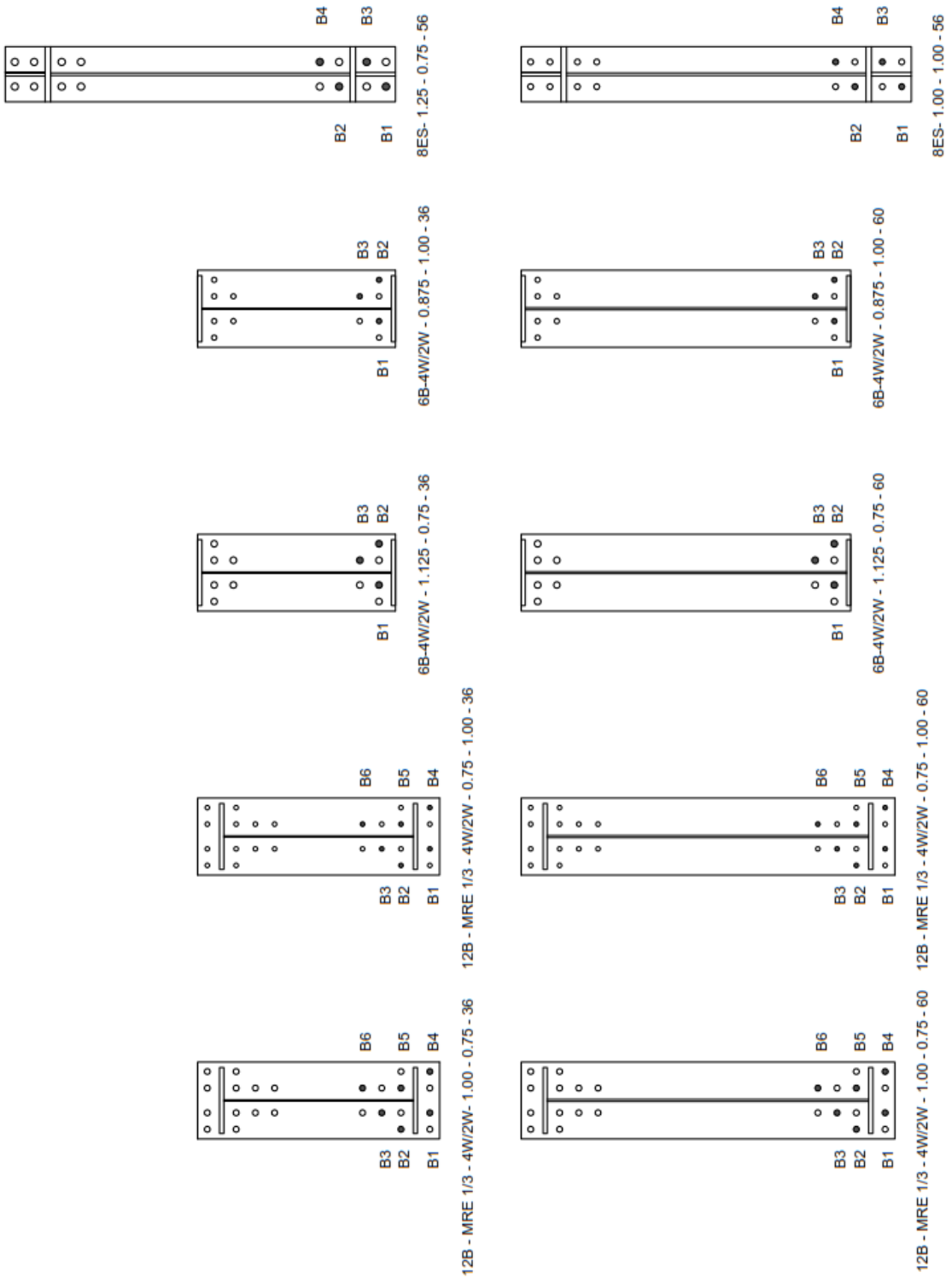

Figure 5-11 Location of Strain Gaged Bolts

Four calipers were used to measure end-plate separation. An instrumented caliper (shown in Figure 5-12) uses strain gages calibrated to read displacement. It has two pointed ends which are spring-loaded to close and are capable of gripping an end-plate. The calipers were calibrated using high precision machinist parallel blocks. Two calipers were placed inside of the bottom flange at the flange to end plate weld near each edge. Another caliper was placed at the same horizontal level but as close to the web, as possible. The fourth caliper was placed midway between the first inside bolt hole (near the web) and the second inside bolt hole (near the web). The location of calipers is shown in Figure 5-13.

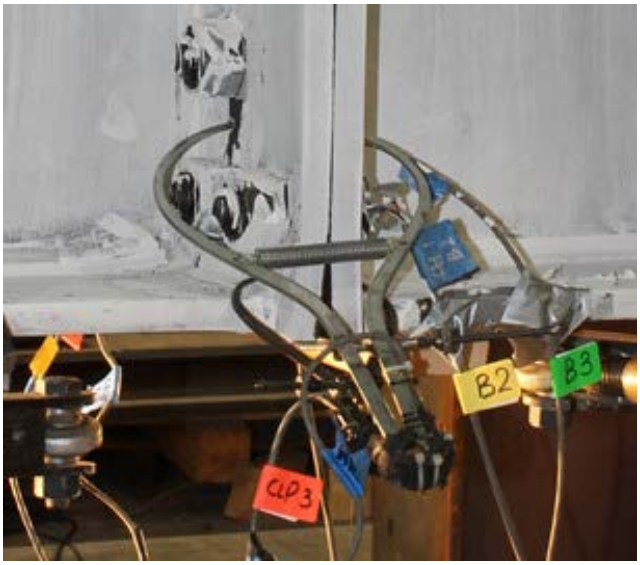

Figure 5-12 Instrumented Calipers Measuring End-Plate Separation

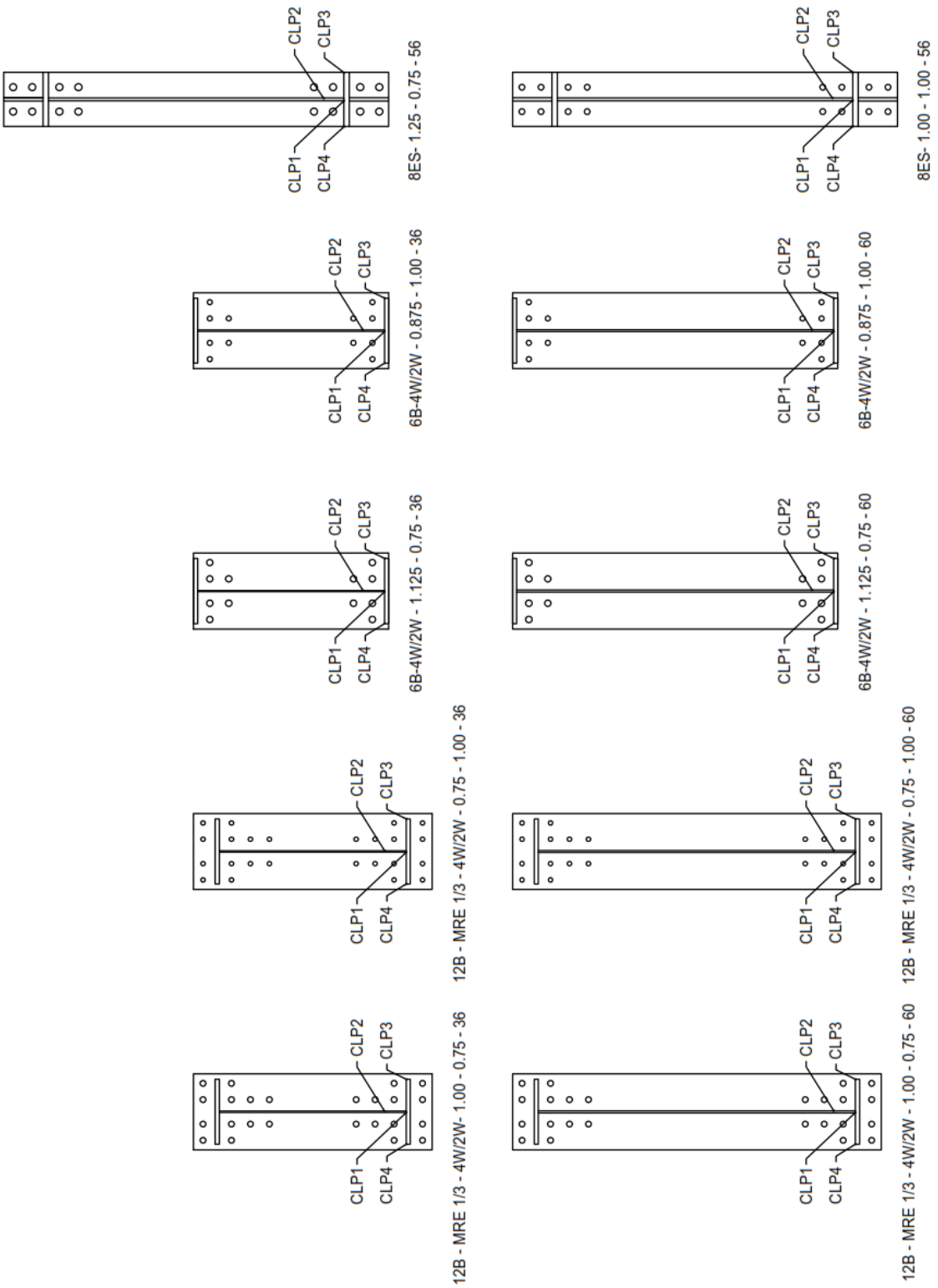

Figure 5-13 Location of Calipers

5.4. Testing Procedure

The procedure for installing a specimen is as follows. Each test specimen was placed between the reaction frames and set on blocks. Since some of the built-up sections were not exactly square, the best possible vertical plumbness of the end-plate on each end of the built-up beam was achieved by shimming thin plates under the roller supports. Also, the specimen was horizontally leveled throughout its span by adjusting the height of intermediate blocks. All the bolts including the instrumented bolts in the connection were inserted. The instrumented bolts were connected to the data acquisition system and then all the bolts were tightened to a snug tight level. The tightening sequence started from the stiffest part of the connection and then moved towards the least stiff part of the connection. Multiple rounds of the tightening sequence were followed until all the bolts were snug tight. After this, each bolt end and the nut was match-marked and pretensioned using the turn of the nut method as described in the RCSC (2009). The force in the instrumented bolts was checked and additional turn of the nut was applied to get the full minimum pretension. Similar additional turn was applied to all bolts, even those that were not instrumented.

The lateral bracings were then installed. The section of the specimen between the actuators was whitewashed to observe yielding in the connection and beam ends. Finally, the remaining instrumentation (i.e. calipers and string potentiometers), was installed. Three cameras were set up, each of which captured a picture every two seconds through every test. Test pictures from two shallow specimen tests were combined together at 24 frames per second into a time-lapse video. Typical time-lapse camera views are shown in Figure 5-14.

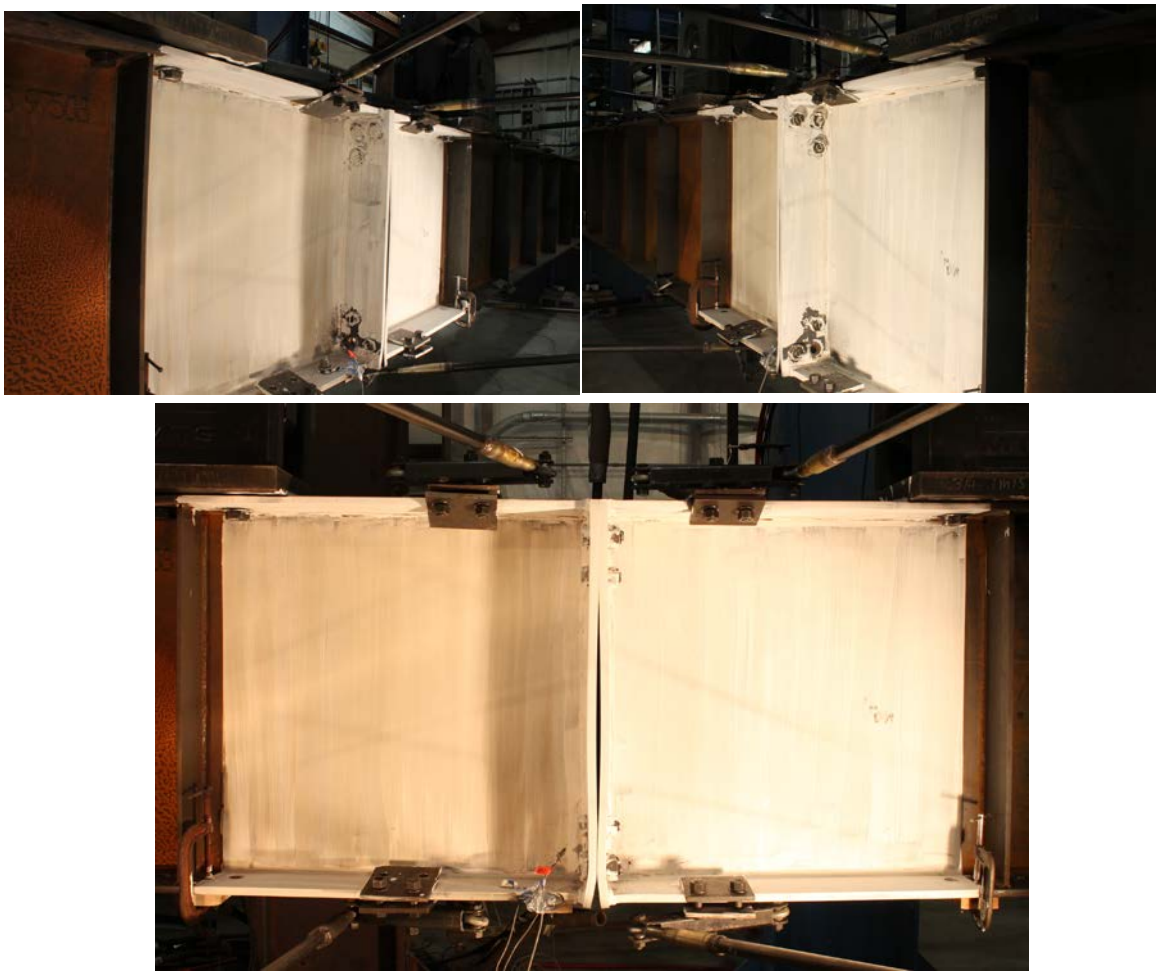

Figure 5-14 Typical Time-lapse Camera Views

The actuator displacements were zeroed before initiating the displacement ramp whereby the specimens were displaced monotonically in the downward direction. Both the actuators used displacement control at a quasistatic rate of 0.10 in. /min. LabVIEW SignalExpress was used to record data points every 0.2 seconds. Since the actuators were displacement controlled, when the difference in the load between each actuator exceeded 5 kips, the displacement of one or both actuators was manually controlled until the loads were within approximately 1 kips. The specimen was loaded until failure or until it stopped taking more load.

5.5. Tensile Coupon Tests

Coupons from the same heat of material as used in the end-plates were cut into standard dogbone shapes and subjected to monotonically increasing displacement in a 300 kip SATEC Universal Testing Machine. The 12B-MRE 1/3-4W/2W and 6B-4W/2W built-up beams were fabricated in such a way that the end-plates of the same thickness used the material from the same heat. Since, there were only two thicknesses of end-plates being used viz. 3/4 in. and 1 in., three coupons of each thickness were taken from each heat of the material. Also, for the 56 in. deep specimens, two coupons of each thickness (3/4 in. and 1 in.) were tested. In total, ten tensile coupon tests were performed. The test coupons and testing procedure conformed to ASTM E8 - “Standard Test Methods for Tension Testing of Metallic Materials”. Refer to Table 5-3 for a summary of tensile coupon tests and, Figure 5-15 to Figure 5-18 for the results from all the coupons.

Table 5-3 Summary of Tensile Coupon Tests

Specimens using this end-plate material	Coupon Number	Thickness (in.)	Yield Stress (ksi)	Tensile Stress (ksi)	Elongation, 8 in. Gage (%)	Average Yield Stress (ksi)
6B-4W/2W-0.875-1.00-36 6B-4W/2W-0.875-1.00-60 12B- MRE 1/3 -4W/2W-0.75-1.00-36 12B- MRE 1/3 -4W/2W-0.75-1.00-60	1	1.004	59.3	83.7	24	59.3
	2	1.004	59.5	83.6	23	
	3	1.003	59.0	83.2	26	
6B-4W/2W-1.125-0.75-36 6B-4W/2W-1.125-0.75-60 12B- MRE 1/3 -4W/2W-1.00-0.75-36 12B- MRE 1/3 -4W/2W-1.00-0.75-60	4	0.750	54.4	76.7	24	54.6
	5	0.748	54.7	76.5	24	
	6	0.750	54.6	76.5	24	
8ES-1.25-0.75-56	7	0.754	57.5	81.3	23	57.2
	8	0.754	56.9	80.0	25	
8ES-1.00-1.00-56	9	1.009	58.9	83.8	24	58.2
	10	1.004	57.5	85.2	23	

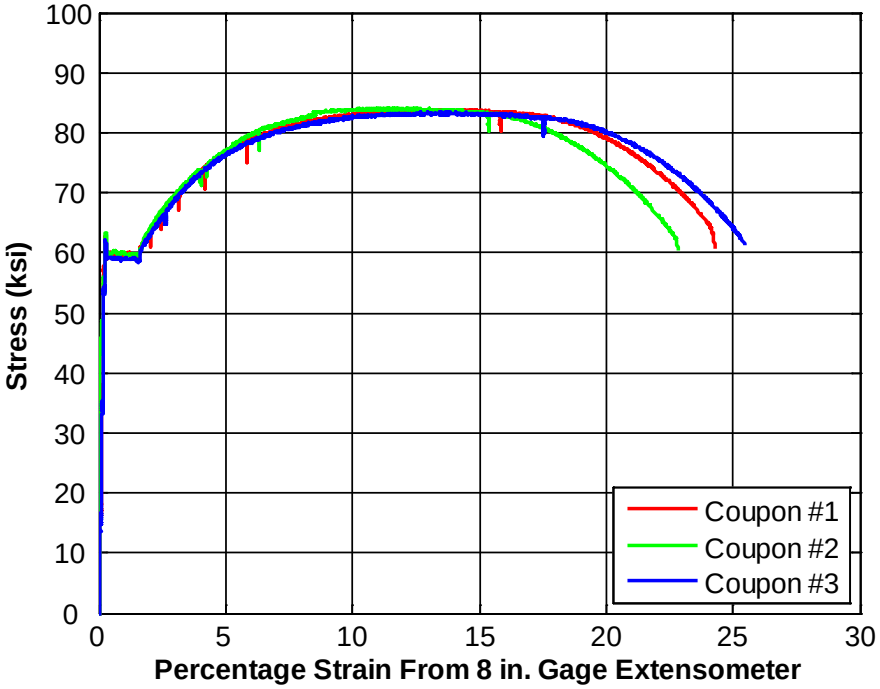

Figure 5-15 Results of Tensile Coupon Testing for 1 in. thick end-plate

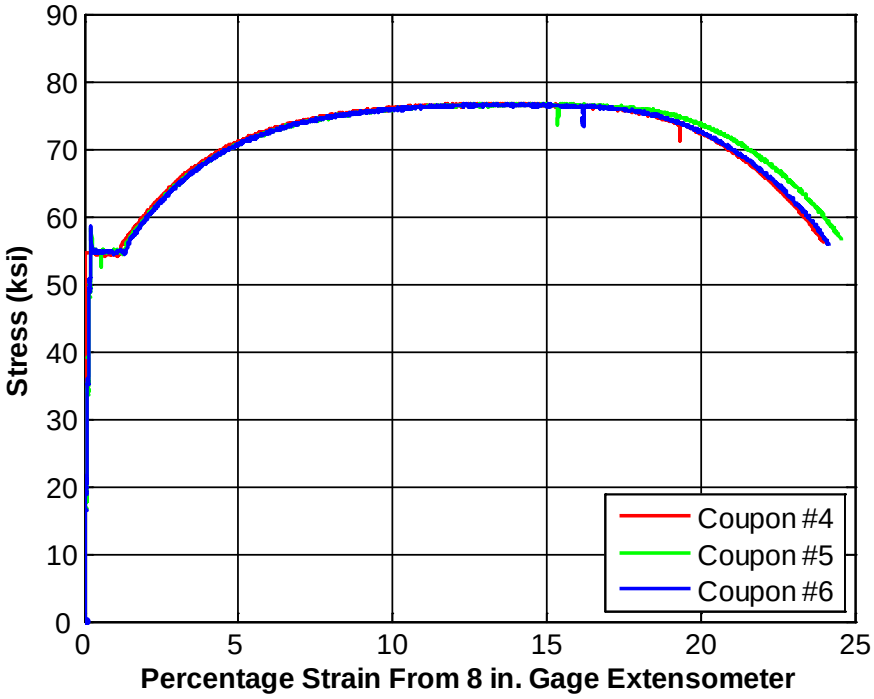

Figure 5-16 Results of Tensile Coupon Testing for 0.75 in. thick end-plate

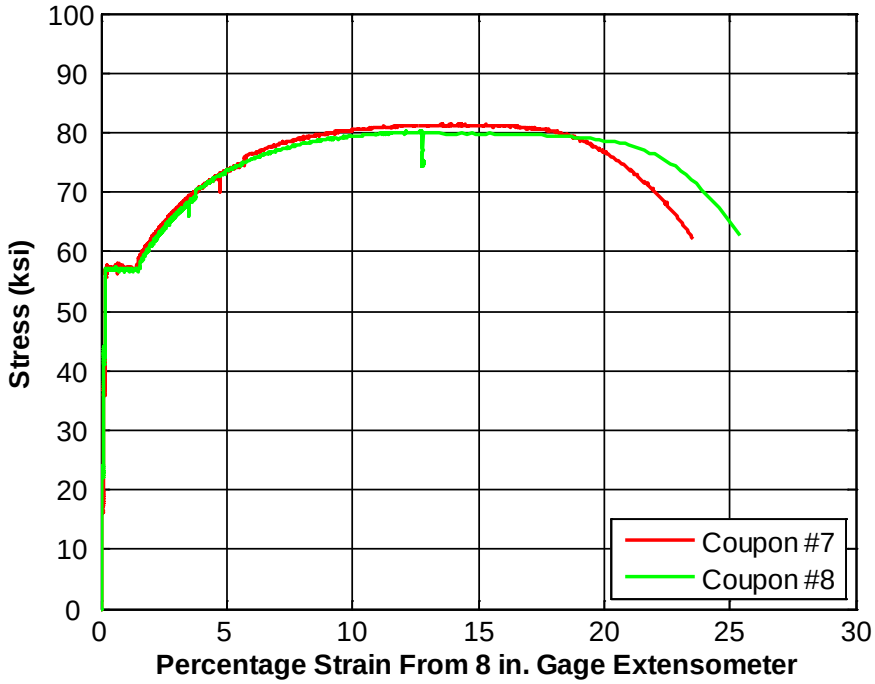

Figure 5-17 Results of Tensile Coupon Testing for 0.75 in. thick end-plate

Figure 5-18 Results of Tensile Coupon Testing for 1.00 in. thick end-plate

5.6. Bolt Rupture Reports

Mill test reports for the mechanical properties were obtained for the bolts used in the six bolt and twelve bolt configurations. No reports could be obtained for the bolts used for the 8ES configuration. The results from the material test reports are summarized in the Table 5-4 and the detailed reports are attached in Appendix B.

Table 5-4 Summary of A325 Bolt Material Testing Reports

Specimens using these bolts	Bolt Dia (in.)	Average Tensile Rupture Stress According to Mill Test Report (ksi)	No. of Samples	Specified Minimum Tensile Stress (ksi)
12B-MRE 1/3-4W/2W-**0.75**-1.00-36 12B-MRE 1/3-4W/2W-**0.75**-1.00-60	3/4	149	3	120
6B-4W/2W-**0.875**-1.00-36 6B-4W/2W-**0.875**-1.00-60	7/8	150	3	120
12B-MRE 1/3-4W/2W-**1.00**-0.75-36 12B-MRE 1/3-4W/2W-**1.00**-0.75-60	1	152	4	120
6B-4W/2W-**1.125**-0.75-36 6B-4W/2W-**1.125**-0.75-60	1 1/8	Too short to test	-	105
8ES-**1.00**-1.00-56	1	No report Provided	-	120
8ES-**1.25**-0.75-56	1 1/4	No report Provided	-	105

6. EXPERIMENTAL RESULTS

The results of ten full-scale tests are reported in this chapter. For the sake of the plots shown below, the data was down-sampled at the rate of one data point for every five hundred data points (except for the specimen 12B-MRE 1/3-4W/2W-1.00-0.75-60). This was done for the clarity of plots.

The moment capacity for end-plate yielding, M_{pl}, was calculated based on the average tensile stress found from the tensile coupon tests reported in the previous chapter. The moment capacity at bolt rupture with prying action, M_q, and moment capacity at bolt rupture without prying action, M_{np}, were calculated based on the nominal values (M_q , M_{np}) and expected strength (M_q^{exp} and M_{np}^{exp}). The calculations for nominal capacity is the nominal tensile stress of the bolt (for A325 bolt F_n = 90 ksi) multiplied by the nominal unthreaded area of bolt.

The actual tensile strength of the bolts, however, is often larger than the nominal strength. The mill test reports (Table 5-4 and Appendix B) for the rupture stress of bolts predict about a 25% higher value than the specified minimum tensile stress of bolts. The parameters, M_q^{exp} and M_{np}^{exp}, are introduced to represent the moment capacities based on expected bolt strength. A typical overstrength in the bolts was determined using the bolt test reports (Table 5-4). For bolt diameters between ¾ in. and 1 in., the test reports indicated an ultimate stress of approximately 150 ksi which is 25% more than the specified minimum tensile stress of 120 ksi. Measured ultimate stress was not available for some bolts, viz. 1 1/8 in., 1 1/4 in. and 1 in. (used for specimen 8ES-1.00-1.00-56). For the purpose of calculation of expected moment capacities involving these bolts, an average value of 125% of nominal tensile stress was assumed (150 ksi for 1 in. diameter bolt and 131 ksi for 1 1/8 in. and 1 1/4in. diameter bolt). M_q^{exp} and M_{np}^{exp} were calculated based on the expected bolt tensile stress (either from bolt test reports or the assumed 125% of nominal) and the net tensile area of the bolt (Table 7-17 of AISC Steel Construction Manual, 2011).

The green theoretical line in the applied moment vs midspan deflection plots shown in this chapter has been calculated based on the stiffness of a simply supported beam with

the same cross sectional properties as the specimen but assuming that the specimen is continuous at midspan without any connection.

The experimental end-plate yield moment (M_y) was found using the applied moment vs. end-plate separation plots. The curve was approximated as a bilinear curve, drawing two lines matching the initial and final slope of the curve. The point on the plot where these two lines meet is assumed to be the yield moment

.

6.1. Testing on the Six Bolt, Four-Wide/Two-Wide, Flush, Unstiffened (6B-4W/2W) Configuration

6.1.1 Shallow Section - Thin Plate Behavior

Specimen 6B-4W/2W-1.125-0.75-36 had a depth of 36 in. and can be considered shallow in relation to the moment capacity of this configuration. It was designed to exhibit thin plate behavior.

Limit States – Predictions and Progression

Equations presented in Chapter 3 were used to calculate the moment capacities given in Table 6-1. The specimen behaved as expected. End-plate yielding occurred followed by bolt rupture with prying action. The test was terminated after the rupture of the bottom inside bolt on one side (shown in Figure 6-5) and both the inside bolts on the other side.

Table 6-1 Predicted and Experimentally Obtained Moment Capacities for Specimen 6B-4W/2W-1.125-0.75-36

Stage	Nominal Predicted (k-ft)	Expected Predicted (k-ft)	Experimental Capacity (k-ft)	Ratio Compared to Nominal	Ratio Compared to Expected
Yield		M_{pl}=748	M_y=730		M_{pl}/M_y=1.02
Ultimate	M_q=957	M_q^{exp} =1100	M_u=1110	M_q/M_u=0.86	M_q^{exp}/M_u =0.99
Doesn't Control	M_{np}=1410				
	M_p =1795				

A yield moment, M_y (from Figure 6-2) of 730 k-ft and an ultimate moment, M_u of 1110 k-ft were experimentally obtained. They are demonstrated graphically and compared

with the predicted values in the Figure 6-1. Though the ratio of M_{pl}/M_y in Table 6-1 is slightly non-conservative (greater than 1.0), the prediction is within 2% of the experimental yield moment. Also, the ratio M_q/M_u in Table 6-1 is quite conservative (bolt rupture prediction based on nominal bolt tension capacity). The predicted bolt rupture strength considering expected bolt strength, M_q^{exp}, on the other hand, is within 1% of the ultimate moment observed.

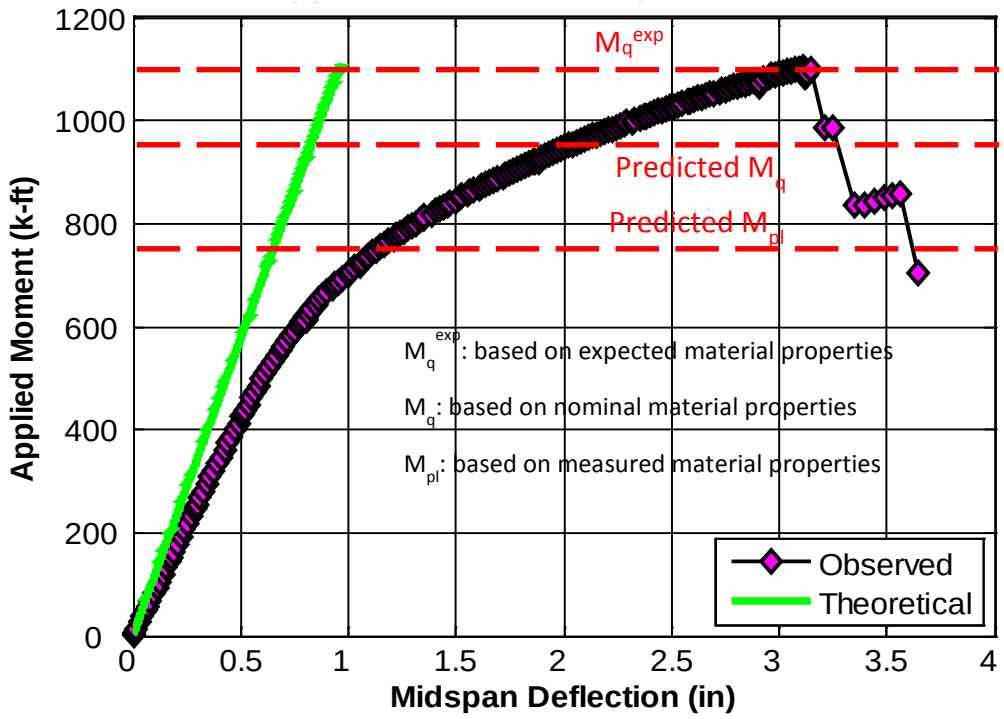

Figure 6-1 Applied Moment vs Midspan deflection for Specimen 6B-4W/2W-1.125-0.75-36

Experimental Results - End-Plate Separation and Bolt Forces

Instrumented calipers were used to measure end-plate separation. Figure 6-2 displays the end-plate separation in relation to the moment at the mid-span of the specimen. The plot verifies that thin plate behavior was achieved because of large separations after achieving the predicted end-plate yield moment.

Strain gages were installed in the shank of the bolts used in the experiment in order to determine bolt forces throughout the duration of the test. As shown in Figure 6-3, the bolt forces increased exponentially past the point of end-plate yielding.

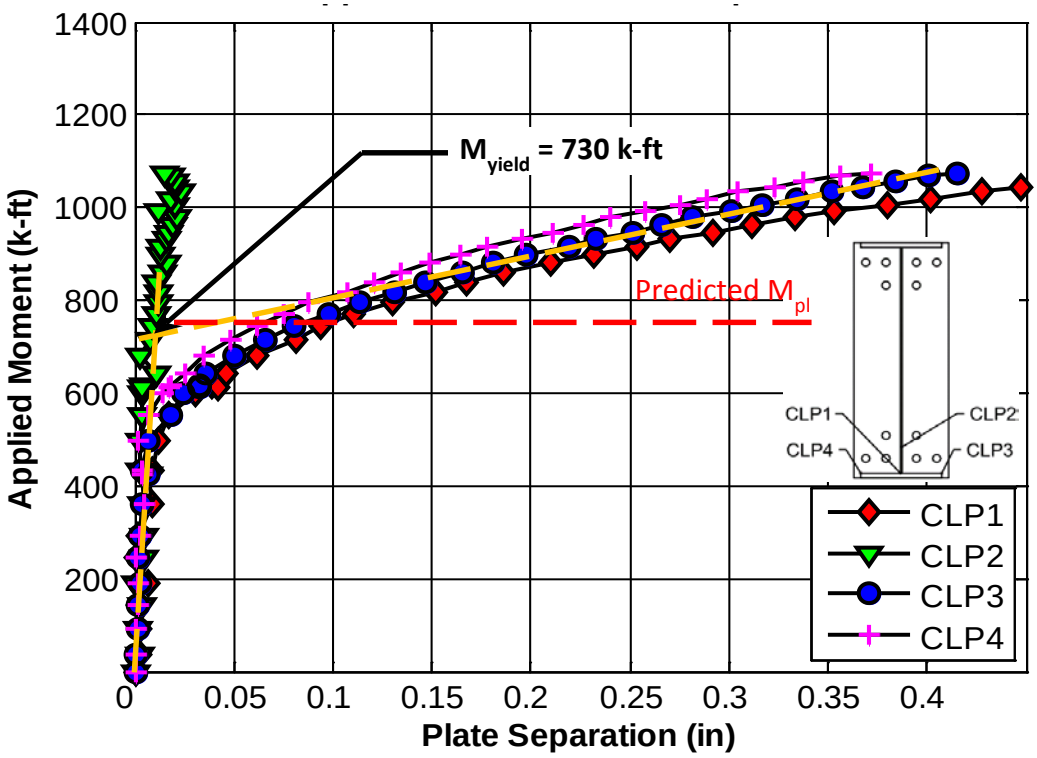

Figure 6-2 End-plate separation for Specimen 6B-4W/2W-1.125-0.75-36.

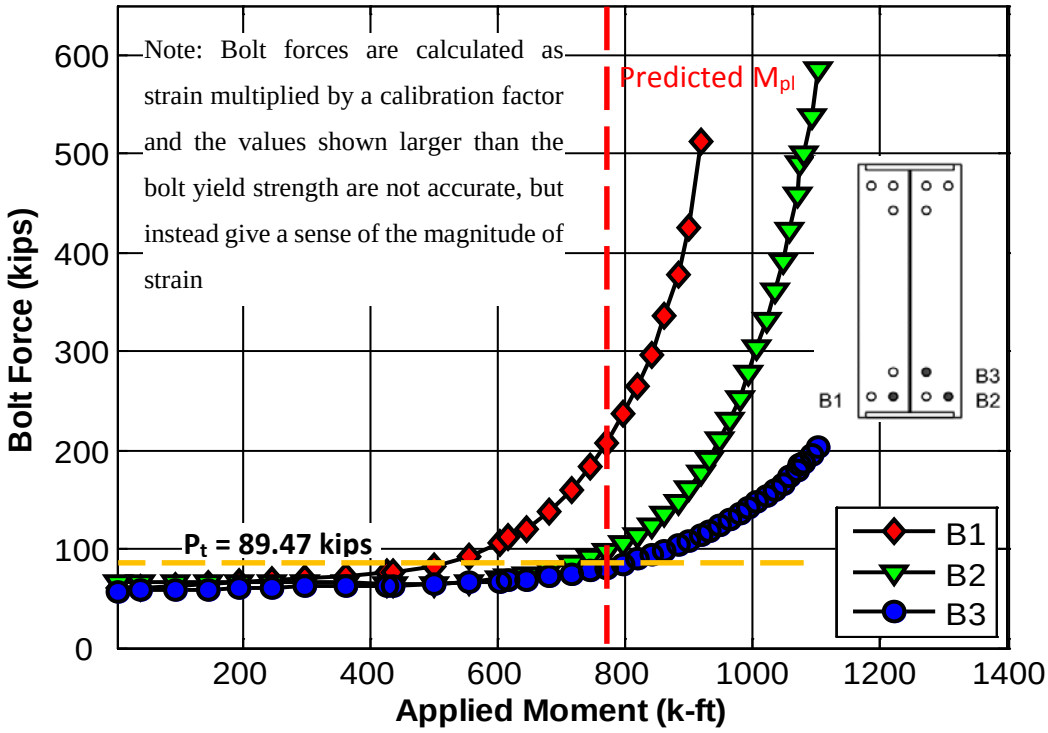

Figure 6-3 Bolt Forces for Specimen 6B-4W/2W-1.125-0.75-36

Experimental Results - Pictures of Specimen

Figure 6-4 and Figure 6-5 show the difference in the specimen at the start and the end of the test. From the pictures it is clear that there was end-plate yielding. Three yield lines: horizontal, vertical and diagonal, were observed on the end-plate. The first yield line to develop was the horizontal yield line at the bottom and then the vertical yield line started developing. The diagonal yield line started developing only after the bottom inside bolt had ruptured. Technically, the connection could be considered to have failed after the rupture of the bottom inside bolt and that is why the diagonal yield line is not a part of the actual yield line mechanism considered in Chapter 3.

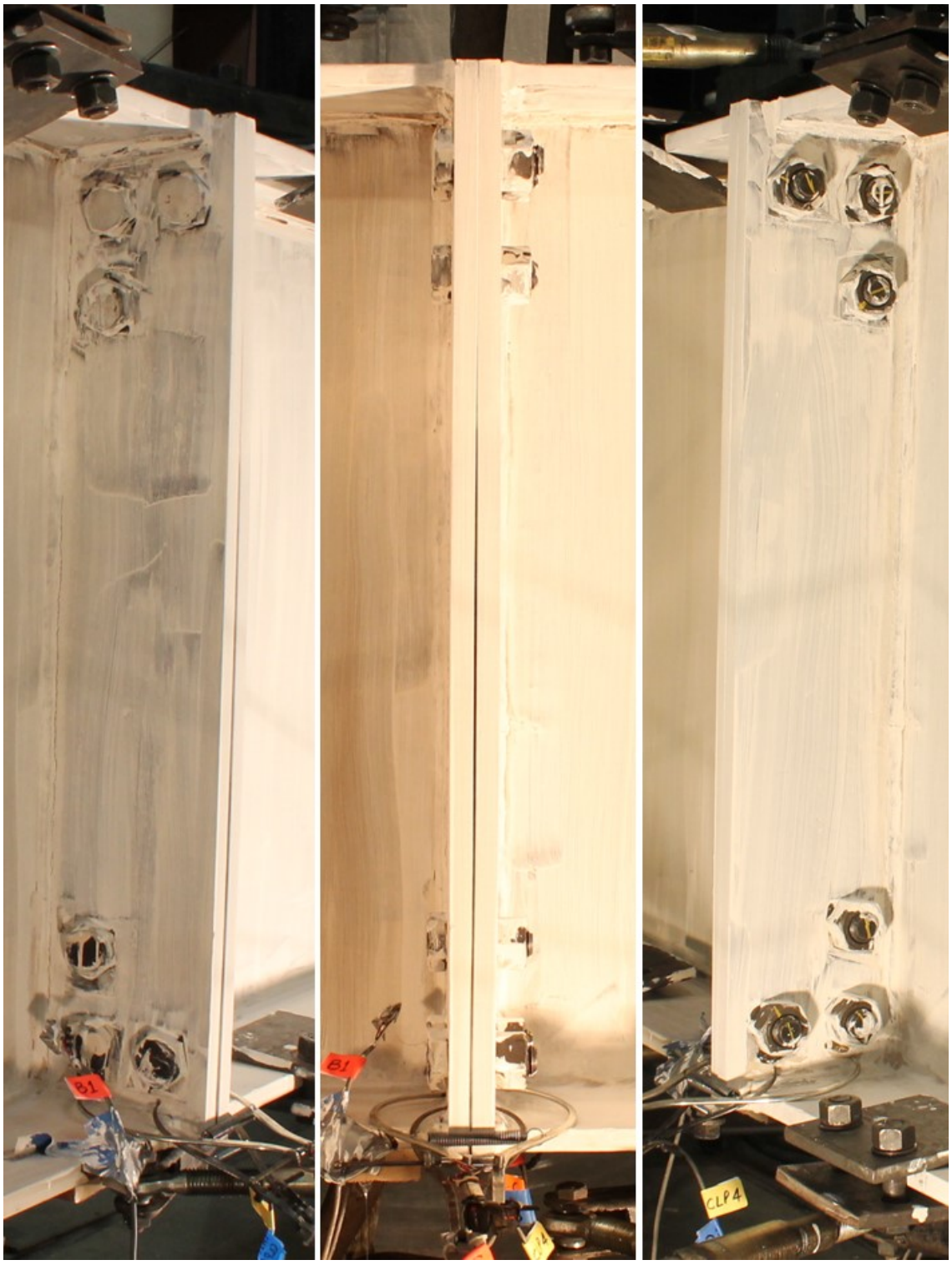

Figure 6-4 Three views of the Specimen 6B-4W/2W-1.125-0.75-36 at the start of the test

Figure 6-5 Three views of the specimen 6B-4W/2W-1.125-0.75-36 at the end of the test

6.1.2 Shallow Section - Thick Plate Behavior

Specimen 6B-4W/2W-0.875-1.00-36 had a depth of 36 in. and can be assumed to be shallow in relation to the moment capacity of this configuration. It was designed to exhibit thick end-plate behavior.

Limit State – Predictions and Progression

The predictions for bolt rupture without prying action, M_{np}, and moment capacity for end-plate yielding, M_{pl}, were calculated according to equations given in Chapter 3 and are given in Table 6-2.

Table 6-2 Predicted and Experimentally Obtained Moment Capacities for Specimen 6B-4W/2W-0.875-1.00-36

Stage	Nominal Predicted (k-ft)	Expected Predicted (k-ft)	Experimental Capacity (k-ft)	Ratio Compared to Nominal	Ratio Compared to Expected
Yield			M_y =770		
Ultimate	M_{np} =851	M_{np}^{exp} =1090	M_u =1030	M_{np}/M_u =0.83	M_{np}^{exp}/M_u =1.06
Doesn't Control	M_{pl} =1440				
	M_p =1795				

The specimen behaved largely as expected with some minor end-plate yielding that was not expected. Bolt rupture without significant end-plate yielding controlled the strength of the connection. The six bolts on the tension side of the connection ruptured at once and no end-plate yielding was observed (shown in Figure 6-10). A yield moment, M_y (shown in Figure 6-7) of 730 k-ft and an ultimate moment, M_u of 1030 k-ft were experimentally obtained. They are demonstrated graphically and compared with the predicted value, M_{np}, in the Figure 6-6. The ratio M_{np}/M_u in Table 6-2 is conservative (less than 1.0), but the related moment capacity based on expected bolt strength, M_{np}^{exp}, was found to be within 6% of the experimentally obtained moment capacity.

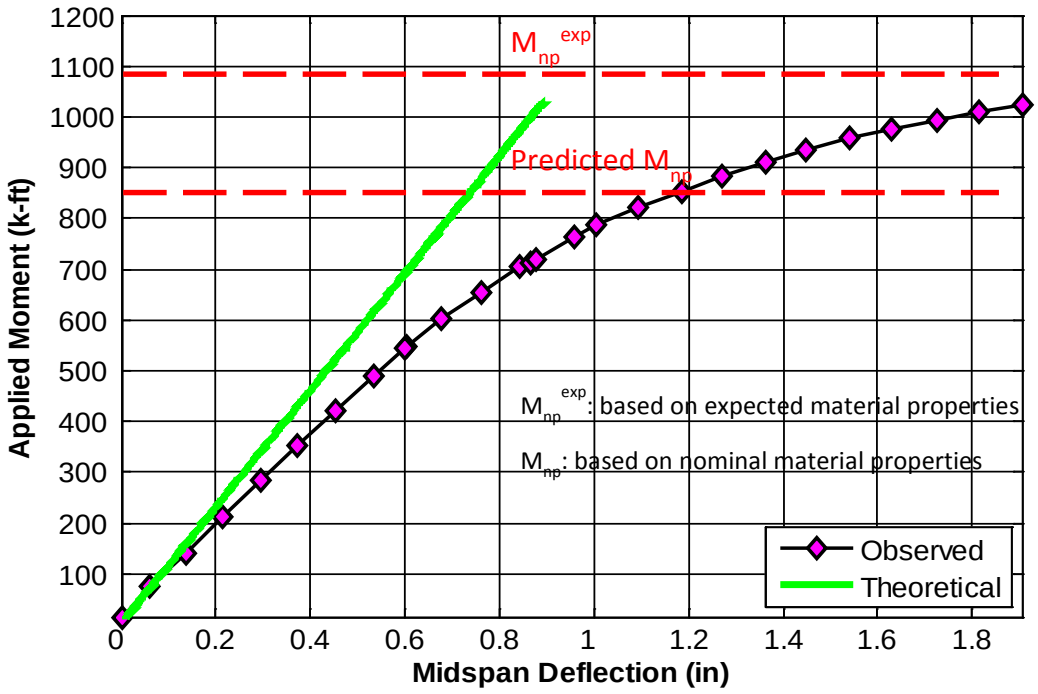

Figure 6-6 Applied Moment vs Midspan deflection for Specimen 6B-4W/2W-0.875-1.00-36

Experimental Results - End-Plate Separation and Bolt Forces

Figure 6-7 displays the end-plate separation in relation to the moment at the mid-span of the specimen. The plot suggests that there may have been some yielding of the end-plate because of the magnitude of end-plate separation. The pictures shown in Figure 6-10, corroborate this hypothesis as some minor yielding was noted in the plates. However, the degree of yielding was not significant and the response was still considered to be mostly thick end-plate behavior (i.e. moment capacity is controlled by bolt rupture without prying action). As is shown in Figure 6-8, the bolt strains (as indicated by plotted bolt forces) did not exhibit an exponential growth and thus prying forces were likely small.

Experimental Results - Pictures of Specimen

Figure 6-9 and Figure 6-10 show the difference in the specimen at the start and the end of the test. From the pictures it is clear that a horizontal yield line had just started to develop though it is evident that this was an incomplete yield line.

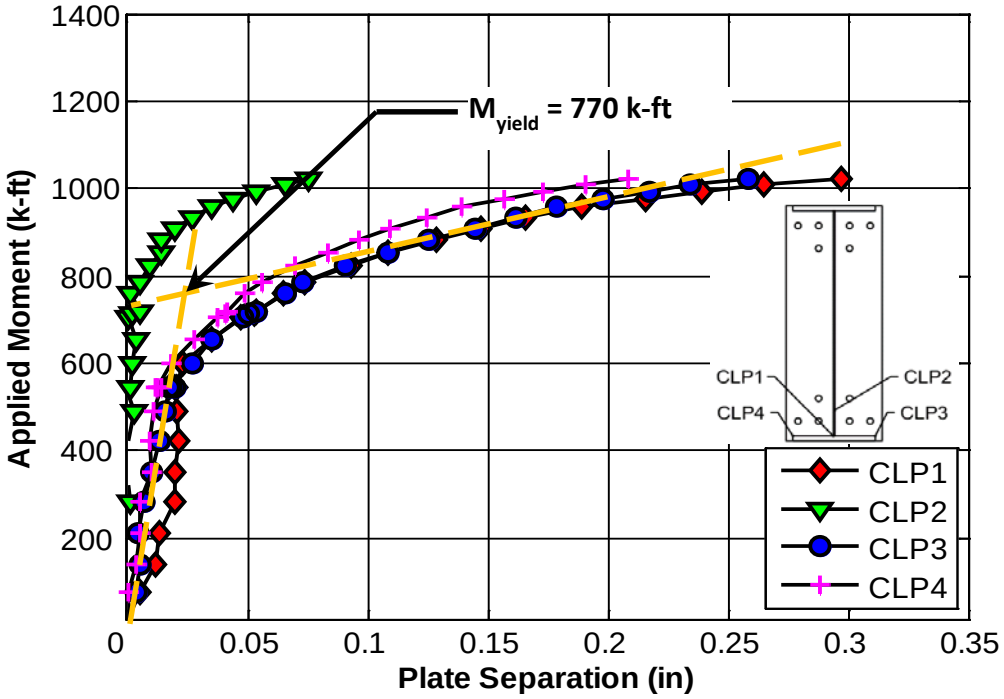

Figure 6-7 End-plate separation for Specimen 6B-4W/2W-0.875-1.00-36.

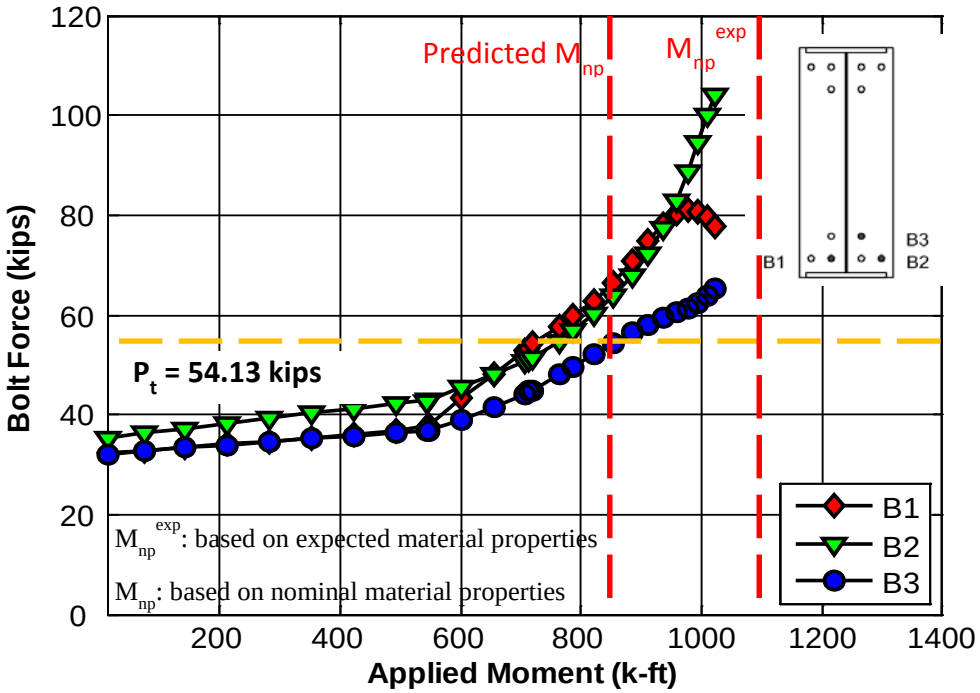

Note: Bolt forces are calculated as strain multiplied by a calibration factor and the values shown larger than the bolt yield strength are not accurate, but instead give a sense of the magnitude of strain

Figure 6-8 Bolt Forces for specimen 6B-4W/2W-0.875-1.00-36

Figure 6-9 Three views of the Specimen 6B-4W/2W-0.875-1.00-36 at the start of the test

Figure 6-10 Three views of the specimen 6B-4W/2W-0.875-1.00-36 at the end of the test

6.1.3 Deep Section - Thin Plate Behavior

Specimen 6B-4W/2W-1.125-0.75-60 was a 60 in. deep section designed to exhibit thin end-plate behavior.

Limit State – Predictions and Progression

From the equations presented in Chapter 3, moment capacity at bolt rupture without prying action (M_{np}), moment capacity for end-plate yielding (M_{pl}), and moment capacity at bolt rupture with prying action (M_q) were calculated and are given in Table 6-3.

Table 6-3 Predicted and Experimentally Obtained Moment Capacities for Specimen 6B-4W/2W-1.125-0.75-60

Stage	Nominal Predicted (k-ft)	Expected Predicted (k-ft)	Experimental Capacity (k-ft)	Ratio Compared to Nominal	Ratio Compared to Expected
Yield		M_{pl} =1310	M_y =1400		M_{pl}/M_y =0.94
Ultimate	M_q =1680	M_q^{exp} =1930	M_u =1980	M_q/M_u =0.85	M_q^{exp}/M_u =0.97
Doesn't Control	M_{np} =2480				
	M_p =3915				

The specimen behaved as expected. End-plate yielding occurred followed by bolt rupture with prying action. The test was terminated after the rupture of the all the inside bolts on both sides of the web. The outer bolt on each side of the web didn't rupture (shown in Figure 6-15). A yield moment, M_y (shown in Figure 6-12) of 1400 k-ft and an ultimate moment, M_u of 1980 k-ft were experimentally obtained. They are demonstrated graphically and compared with the predicted values in the Figure 6-11.

The ratio M_{pl}/M_y in Table 6-3 is conservative (less than 1.0) and shows that the predicted, M_{pl}, is within 6% of the observed, M_y. Also, the ratio M_q/M_u in Table 6-3 is fairly conservative, but the expected moment capacity, M_q^{exp}, was within 3% of the ultimate moment, M_u.

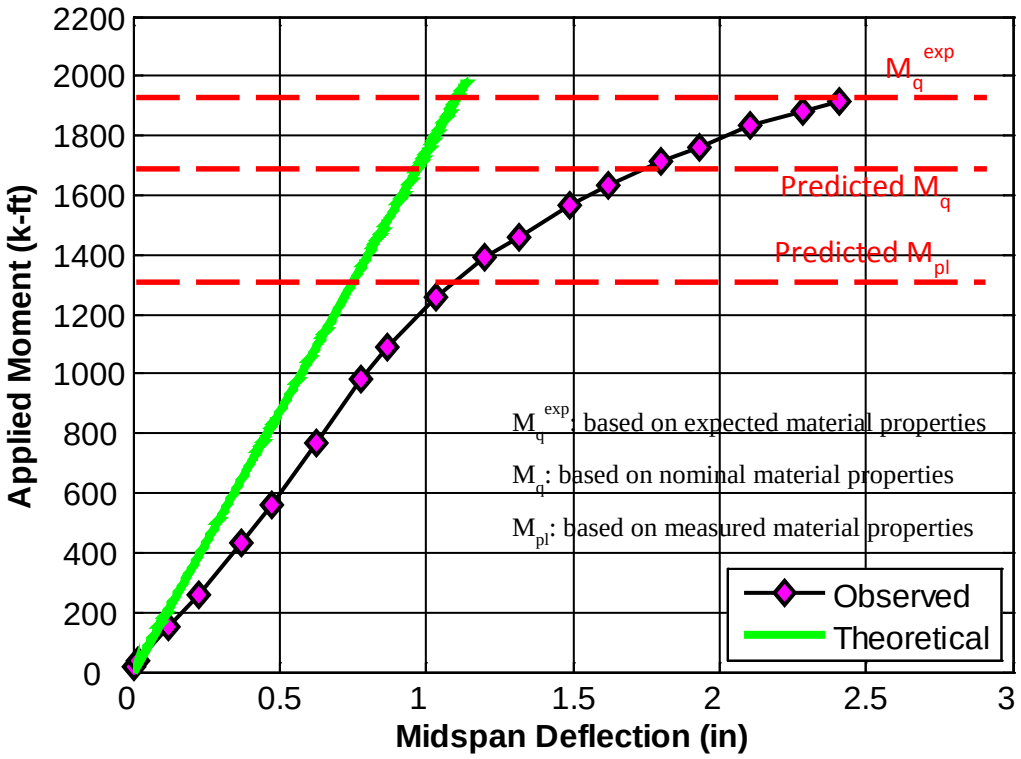

Figure 6-11 Applied Moment vs Midspan deflection for Specimen 6B-4W/2W-1.125-0.75-60

Experimental Results - End-Plate Separation and Bolt Forces

Figure 6-12 displays the end-plate separation in relation to the moment at the mid-span of the specimen. The plot verifies that thin plate behavior was achieved. This is evident from the occurrence of large end-plate separations after sustaining the predicted end-plate yield moment.

As shown in Figure 6-13, the bolt forces, especially in B1 and B3, increased drastically after the predicted end-plate yielding moment. This indicates substantial prying forces as a result of thin end-plate behavior.

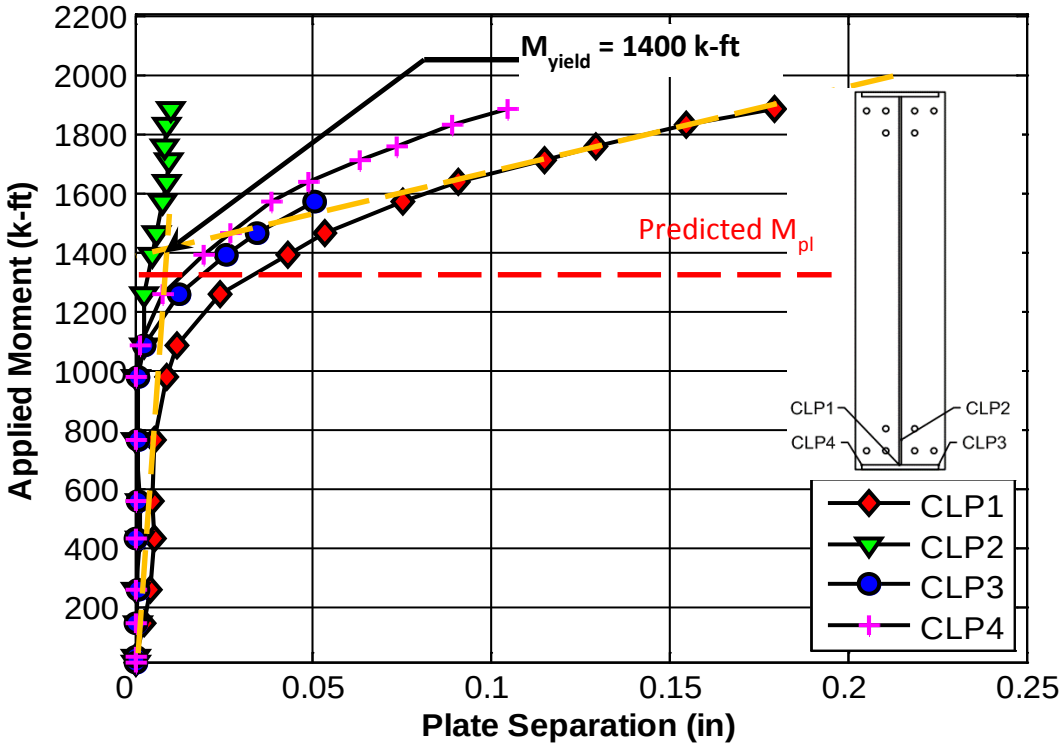

Figure 6-12 End-plate separation for Specimen 6B-4W/2W-1.125-0.75-60.

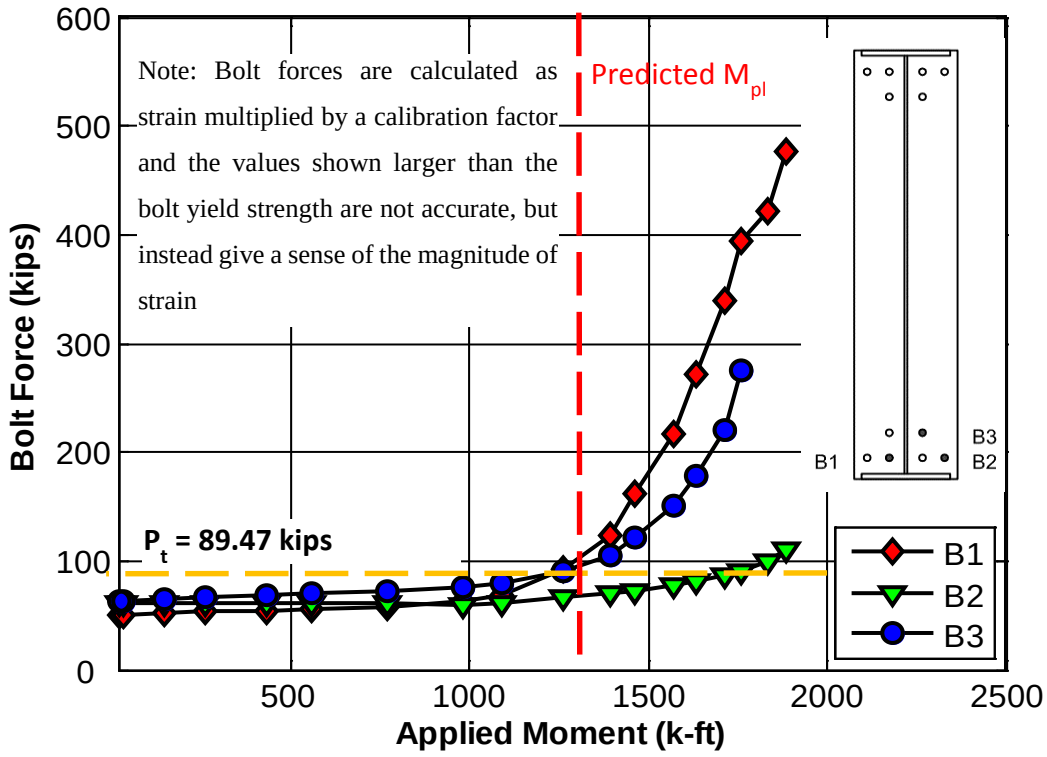

Figure 6-13 Bolt Forces for specimen 6B-4W/2W-1.125-0.75-60

Experimental Results - Pictures of Specimen

Figure 6-14 and Figure 6-15 show the difference in the specimen at the start and the end of the test. From the pictures it is clear that there was end-plate yielding. Three yield lines, horizontal, vertical and diagonal, were seen on the end-plate on each side of the web. The first yield line to develop was the horizontal yield line at the bottom and then the vertical yield line started developing. The diagonal yield line started developing only after the bottom inside bolt had ruptured. Technically, the connection could be considered to have failed after the rupture of the bottom inside bolt and therefore, the diagonal yield line is not a part of the actual yield line mechanism considered in Chapter 3. Also the profile of the end-plates as viewed from the side (middle picture in Figure 6-15) clearly shows that there was distortion in the end-plate.

Figure 6-14 Three views of the Specimen 6B-4W/2W-1.125-0.75-60 at the start of the test

Figure 6-15 Three views of the specimen 6B-4W/2W-1.125-0.75-60 at the end of the test

6.1.4 Deep Section - Thick Plate Behavior

Specimen 6B-4W/2W-0.875-1.00-60 was a 60 in. deep section designed to exhibit thick end-plate behavior.

Limit State – Predictions and Progression

Equations presented in Chapter 3 were used to calculate the moment capacity at bolt rupture without prying action (M_{np}, and M_{np}^{exp}) and moment capacity for end-plate yielding (M_{pl}) as given in Table 6-4.

Table 6-4 Predicted and Experimentally Obtained Moment Capacities for Specimen 6B-4W/2W-0.875-1.00-60

Stage	Nominal Predicted (k-ft)	Expected Predicted (k-ft)	Experimental Capacity (k-ft)	Ratio Compared to Nominal	Ratio Compared to Expected
Yield			M_y =1390		
Ultimate	M_{np} =1500	M_{np}^{exp} =1920	M_u =1730	M_{np}/M_u =0.87	M_{np}^{exp}/M_u =1.11
Doesn't Control	M_{pl} =2530				
	M_p =3915				

The specimen behaved as expected. Bolt rupture without prying action, M_{np}, controlled the strength of the connection. The six bolts on the tension side of the connection ruptured at once and no end-plate yielding was observed (shown in Figure 6-20).

A yield moment, M_y (shown in Figure 6-17) of 1390 k-ft and an ultimate moment, M_u of 1730 k-ft were experimentally obtained. They are demonstrated graphically and compared with the predicted value, M_{np}, in the Figure 6-16.

The ratio M_{np}/M_u = 0.87 in Table 6-4 is conservative (less than 1.0) and the ratio of expected moment capacity to ultimate was, M_{np}^{exp}/M_u = 1.11. The expected moment capacity was within 11% of the ultimate moment strength. This implies that, for this specimen, the equation predicting bolt rupture without prying action was 11% unconservative, but because the bolts have substantial overstrength, the moment capacity calculated using nominal bolt strength was 13% conservative.

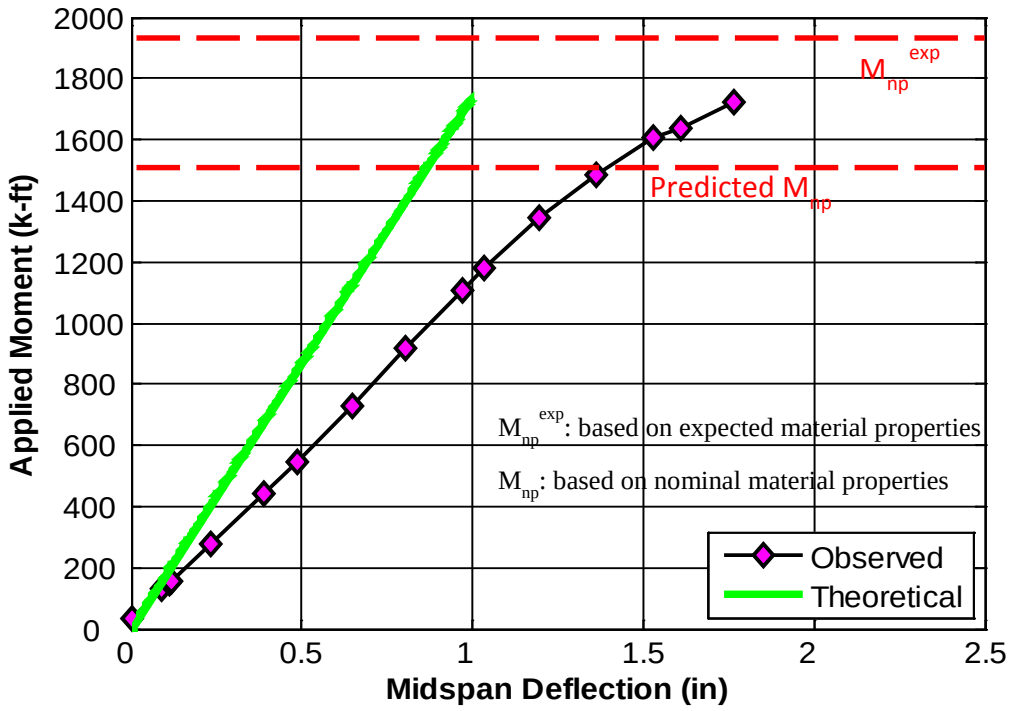

Figure 6-16 Applied Moment vs Midspan deflection for Specimen 6B-4W/2W-0.875-1.00-60

Experimental Results - End-Plate Separation and Bolt Forces

Figure 6-17 displays the end-plate separation in relation to the moment at the mid-span of the specimen. Since the magnitude of end-plate separation was relatively small, there was likely negligible end-plate yielding. This is corroborated by the pictures shown in Figure 6-20, which don't show any visually observable yielding in the end-plates.

As shown in Figure 6-18, the bolt forces did not increase in an exponential way. Bolt, B2 showed an increase towards the end of the test, but not as much increase as might be expected in a thin end-plate with prying action.

Experimental Results - Pictures of Specimen

Figure 6-19 and Figure 6-20 show the difference in the specimen at the start and the end of the test. From the pictures it is clear that no end-plate yielding was seen. This validates that the specimen had the behavior of a thick plate.

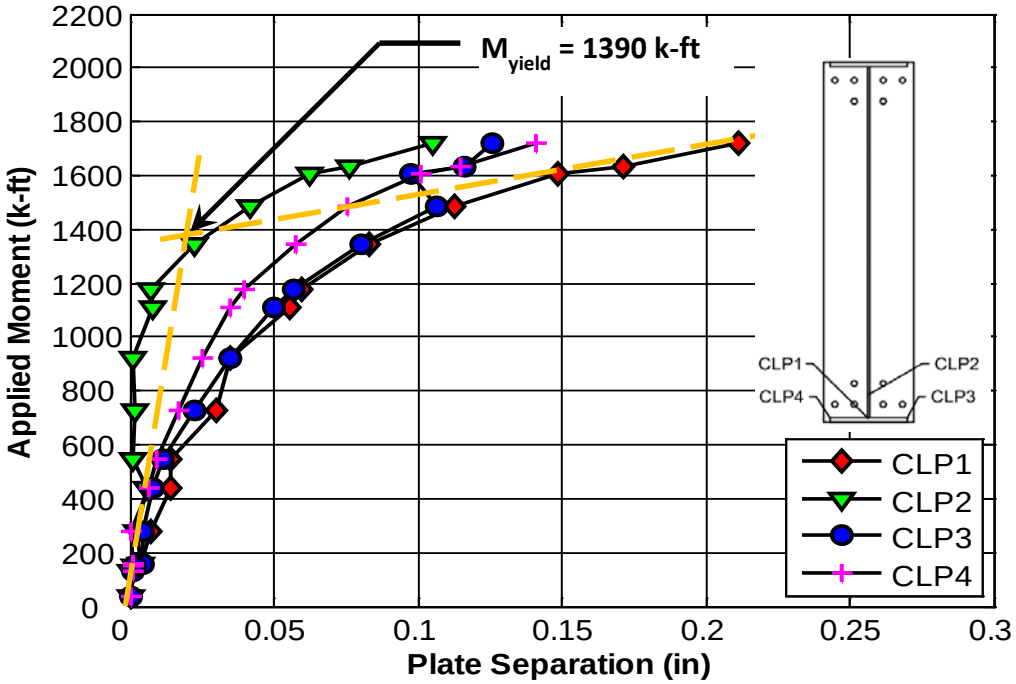

Figure 6-17 End-plate separation for Specimen 6B-4W/2W-0.875-1.00-60.

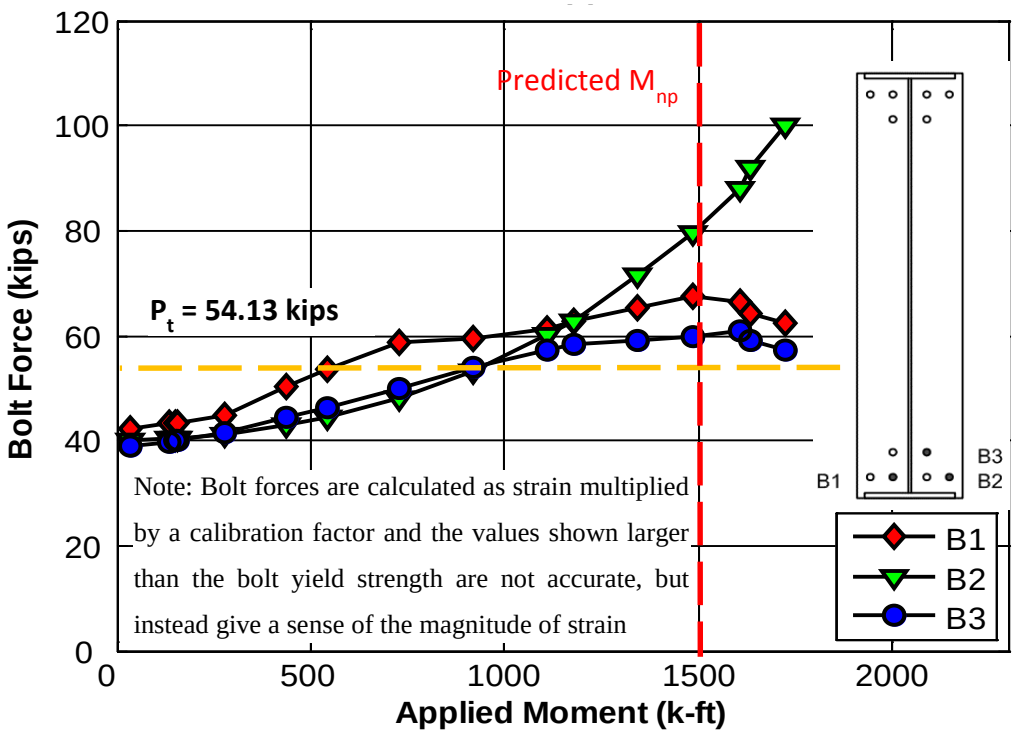

Figure 6-18 Bolt Forces for specimen 6B-4W/2W-0.875-1.00-60

Figure 6-19 Three views of the Specimen 6B-4W/2W-0.875-1.00-60 at the start of the test

Figure 6-20 Three views of the specimen 6B-4W/2W-0.875-1.00-60 at the end of the test

6.1.5 Summary of the Six Bolt Flush Configuration and Recommendations

A total of four tests were conducted for the 6B-4W/2W configuration and all of them were tested until bolt rupture. Table 6-5 summarizes the four specimens investigated herein.

Table 6-5 Summary of the Four Test Specimens of the Six Bolt Flush Unstiffened Configuration

Specimen Identification[1]	Depth (in.)	Behavior	Remarks[2]
6B-4W/2W-1.125-0.75-36	36	Thin	M_{pl} +2% of yield moment. M_q was -14% of the observed M_u. M_q^{exp} was -1% of the observed M_u. End-plate yielding observed.
6B-4W/2W-0.875-1.00-36	36	Thick	M_{np} was -17% of the observed M_u. M_{np}^{exp} was +6% of the observed M_u. Minor end-plate yielding observed.
6B-4W/2W-1.125-0.75-60	60	Thin	Predicted M_{pl} -6% of the observed yield moment, M_y. Predicted M_q was -13% of the observed M_u. M_q^{exp} was -3% of the observed M_u. End-plate yielding observed.
6B-4W/2W-0.875-1.00-60	60	Thick	M_{np} was -13% of the observed M_u. M_{np}^{exp} was +11% of the observed M_u. No end-plate yielding observed.

[1]Specimen Identification: "No. of bolts in the connection – No. of bolts in a row - Bolt diameter - End-plate thickness - Beam depth".

[2]Remarks: A postive percentage means an unconservative calculation, whereas a negative percentage means a safe prediction.

For the two thin plate tests, the moment capacity associated with end-plate yielding, M_{pl}, was either 2% more (unconservative) than the experimental yield moment (for shallow beam) or 6% less (conservative) than the experimental yield moment (for deep beam).

Furthermore, experimentally measured end-plate separation was found to be consistent with thin end-plate behavior wherein end-plate yielding allows end-plate separation prior to bolt fracture. The equation for moment capacity and associated yield line mechanism presented in Chapter 3 is therefore considered to be fairly accurate for the range of parameters tested.

The nominal moment capacity for bolt rupture with prying action, M_q, was 14% and 15% less (conservative) than the observed M_u for shallow and deep beam, respectively. The moment capacity for bolt rupture using expected bolt strength, M_q^{exp}, was 1% and 3% less (conservative) than the observed M_u for shallow and deep beam, respectively. Thus, the equation for predicting moment capacity for bolt rupture with prying action was considered to be fairly accurate for the parameters tested. It is noted that typical overstrength of structural bolts like ASTM A325 will lead to reserve capacity, not considered in the predicted bolt rupture moment.

For thick end-plate specimens, the behavior was also similar to predicted response. Specimen 6B-4W/2W-0.875-1.00-36 exhibited some minor end-plate yielding, but was still considered to exhibit thick end-plate behavior. The calculated nominal moment capacities for bolt rupture without prying action, M_{np}, were 17% and 13% less (conservative) than the observed ultimate moment, M_u. The moment capacities calculated using expected bolt strength, M_{np}^{exp}, were 6% and 11% more (unconservative) than the observed M_u for shallow and deep beam, respectively. The experimental moment capacity of the connection for both specimens was found to lie between the predicted moment capacity based on nominal material properties and the moment capacity of the connection based on expected material properties. Considering the former as the lower bound and the latter as the upper bound, it appears that the bolt force model for thick plate behavior appears to be reasonable.

6.2. Testing on the Twelve Bolt, Multiple Row Extended, Four-Wide/Two-Wide (12B-MRE 1/3-4W/2W), Unstiffened Configuration

6.2.1 Shallow Section - Thin Plate Behavior

Specimen 12B-MRE 1/3-4W/2W-1.00-0.75-36 could be considered to be a shallow section (depth = 36 in.) considering the moment capacity of this configuration. It was designed to exhibit thin end-plate behavior.

Limit State – Predictions and Progression

Equations presented in Chapter 3 were used to calculate the moment capacity at bolt rupture without prying action (M_{np}), moment capacity for end-plate yielding (M_{pl}) and moment capacity at bolt rupture with prying action (M_q) as given in Table 6-6.

Table 6-6 Predicted and Experimentally Obtained Moment Capacities for Specimen 12B-MRE 1/3-4W/2W-1.00-0.75-36

Stage	Nominal Predicted (k-ft)	Expected Predicted (k-ft)	Experimental Capacity (k-ft)	Ratio Compared to Nominal	Ratio Compared to Expected
Yield		M_{pl} =1130	M_y =1230		M_{pl}/M_y =0.92
Ultimate	M_q =1420	M_q^{exp} =1870	M_u =1640*	M_q/M_u =0.87*	M_q^{exp}/M_u =1.14*
Doesn't Control	M_{np} =2310				
	M_p =1795				

* Test was stopped prior to bolt rupture due to local buckling of the rafter

The test specimen experienced end-plate yielding, but the test had to be stopped prior to bolt rupture. This was due to the flange and web local buckling of the section. The plastic capacity of the section was calculated to be 1795 k-ft and the nominal moment capacity to be 1630 k-ft (calculated using AISC 360-10 and a yield stress of 55 ksi). As the flange and web local buckling occurred, the specimen was unable to resist any additional load and the specimen load started to reduce with increasing displacement as shown in Figure 6-21.

A yield moment, M_y (shown in Figure 6-22) of 1230 k-ft and an ultimate moment, M_u of 1640 k-ft (none of the bolts were ruptured) were experimentally obtained. They are demonstrated graphically and compared with the predicted values in the Figure 6-21.

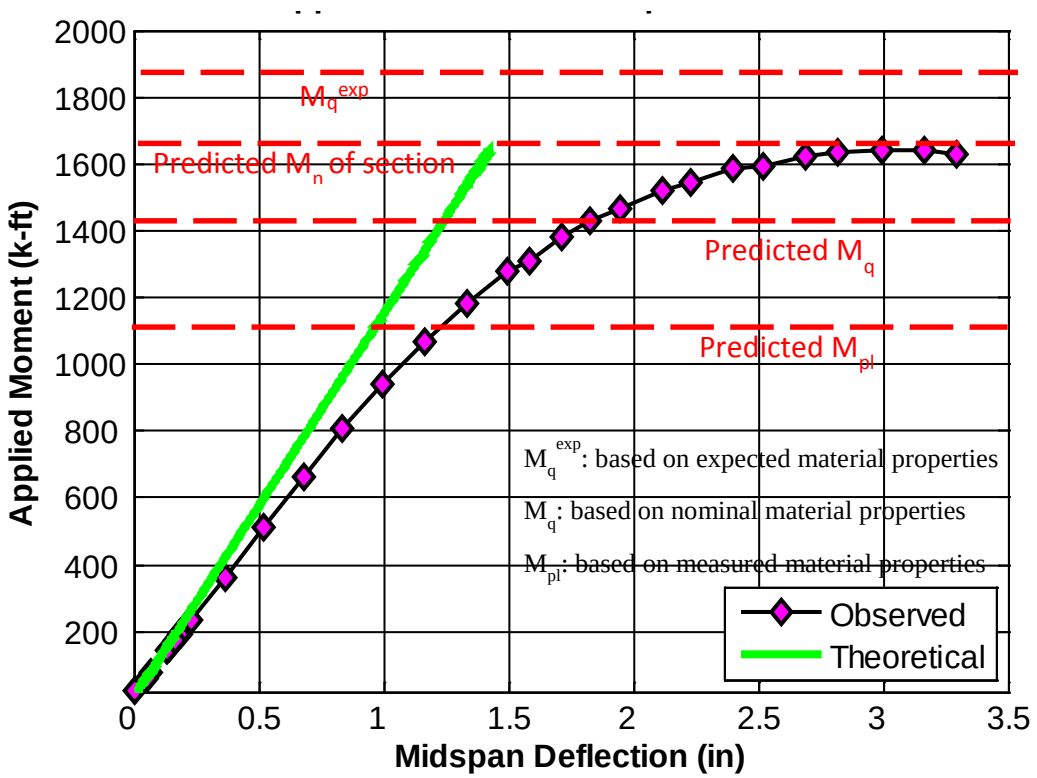

Figure 6-21 Applied Moment vs Midspan deflection for Specimen 12B-MRE 1/3-4W/2W-1.00-0.75-36

The ratio M_{pl}/M_y in Table 6-6 is conservative (less than 1.0) and it is within 8% of the predicted value. Also, the nominal moment capacity for bolt rupture is shown to be conservative in Table 6-6 (as demonstrated by M_q/M_u). The specimen did not achieve the expected moment capacity associated with bolt rupture, M_q^{exp}, but that is because the test was stopped prior to bolt rupture.

Experimental Results - End-Plate Separation and Bolt Forces

Figure 6-22 displays the end-plate separation in relation to the moment at the mid-span of the specimen. The plot verifies that thin plate behavior was achieved. This is evident from the occurrence of large separations once the end-plate began to yield.

As shown in Figure 6-23, the bolt forces increased drastically, especially in bolts B1, B2, B4 and B5, past the point of end-plate yielding, which is approximately 1230 k-ft. This indicates substantial prying forces in the rows containing the above mentioned four bolts. Another important thing to be observed in the plot is that there was no exponential

increase in the forces for bolt B3. This could be attributed to the absence of prying in this row of bolts.

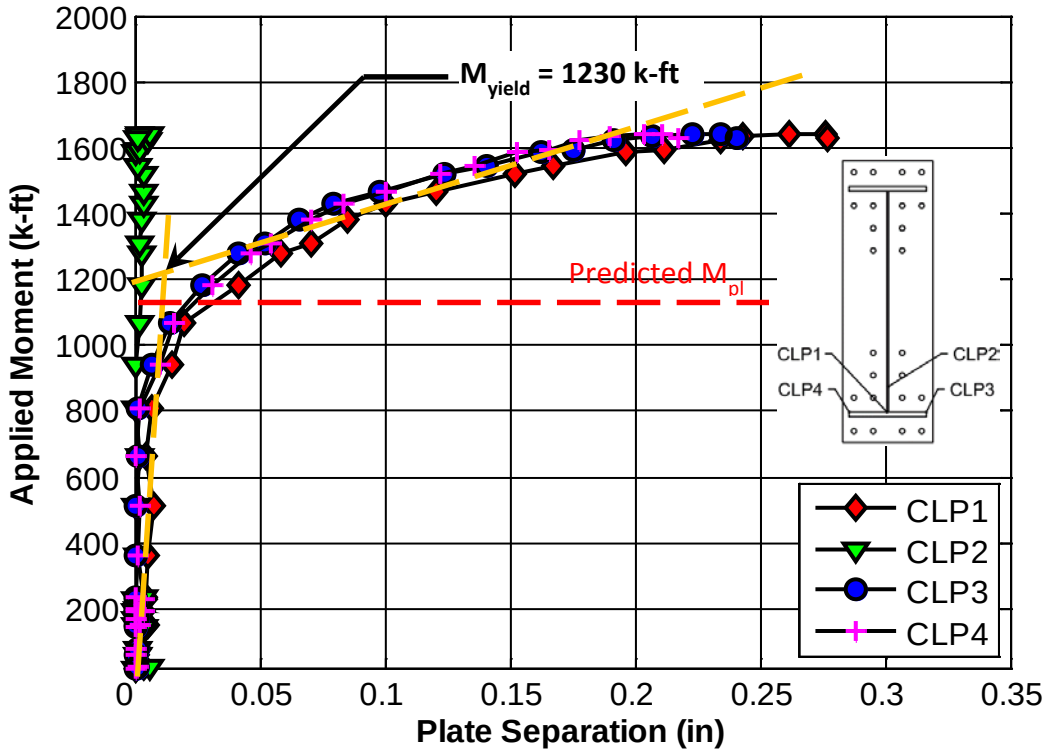

Figure 6-22 End-plate separation for Specimen 12B-MRE 1/3-4W/2W-1.00-0.75-36.

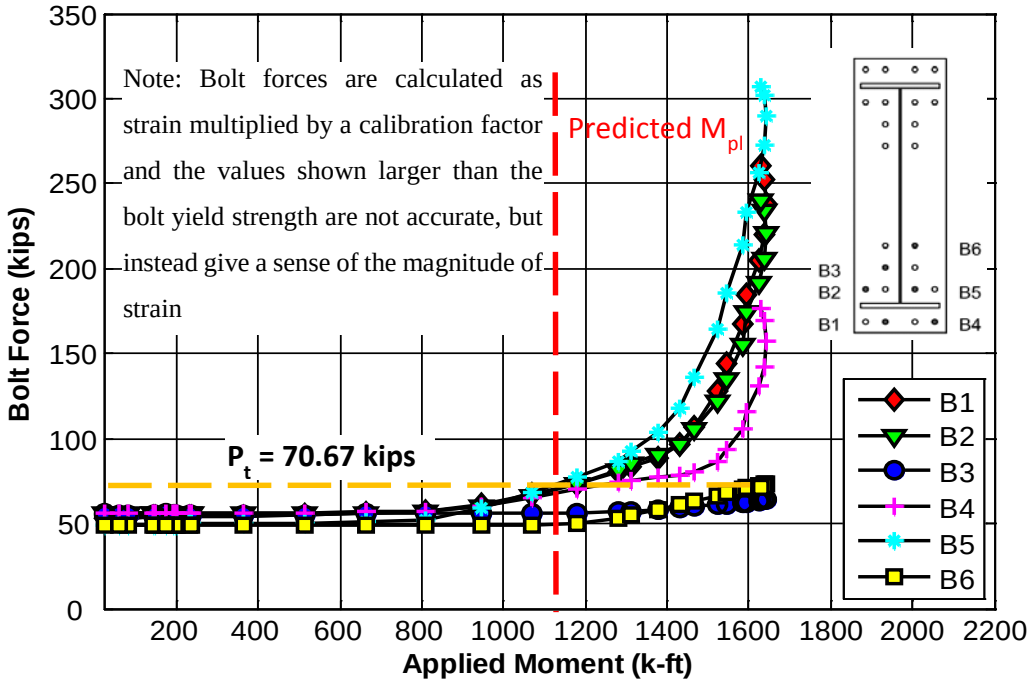

Figure 6-23 Bolt Forces for specimen 12B-MRE 1/3-4W/2W-1.00-0.75-36

Experimental Results - Pictures of Specimen

Figure 6-24 and Figure 6-25 show the difference in the specimen at the start and the end of the test. The pictures show end-plate yielding. Two horizontal yield lines were visually observed: one in the line of bolts outside the flange and the other in the line of bolts just inside of the flange.

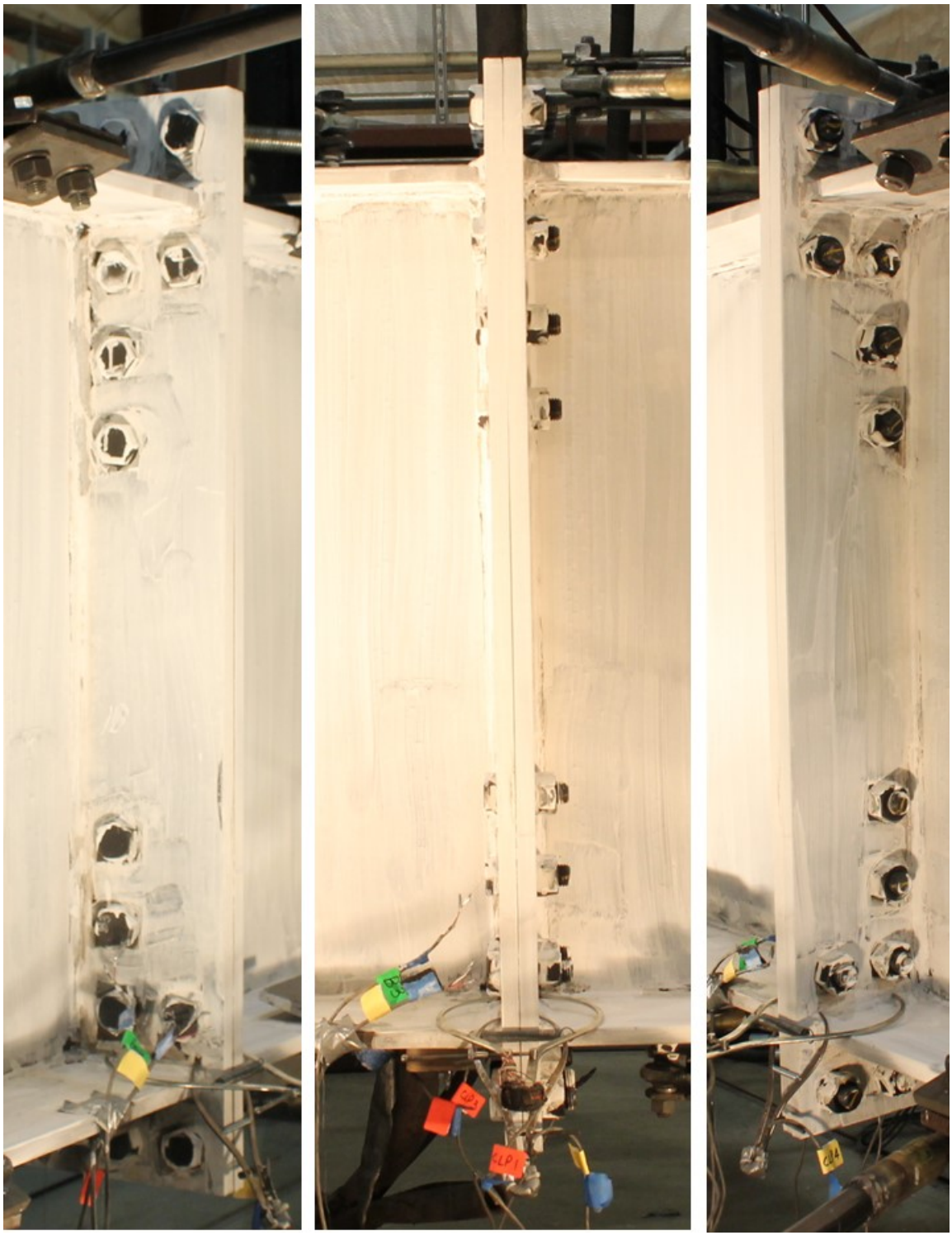

Figure 6-24 Three views of the Specimen 12B-MRE 1/3-4W/2W-1.00-0.75-36 at the start of the test

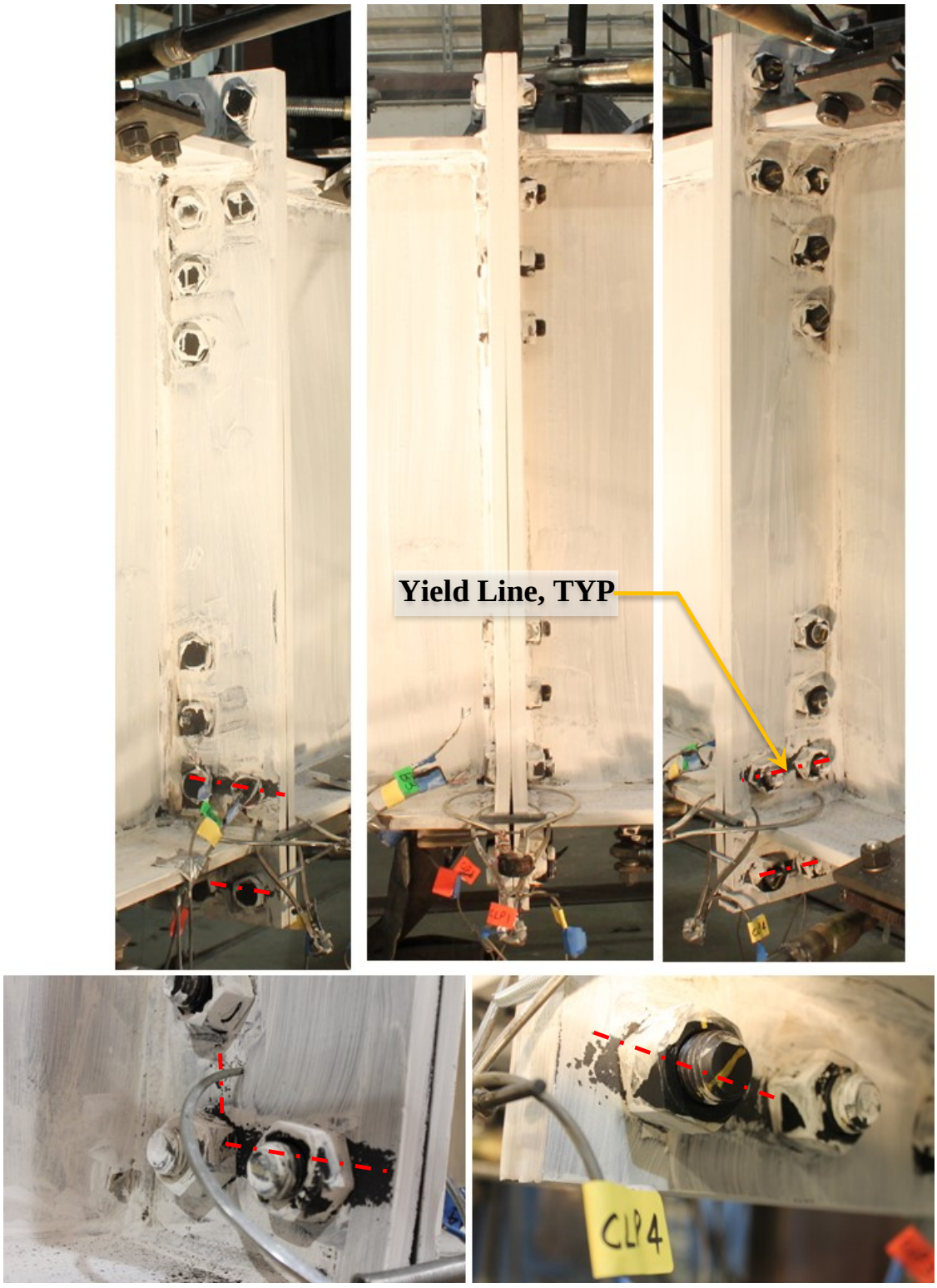

Figure 6-25 Three views of the specimen 12B-MRE 1/3-4W/2W-1.00-0.75-36 and the yield lines seen, at the end of the test

6.2.2 Shallow Section - Thick Plate Behavior

Since this end-plate configuration can sustain a relatively large moment, the 36 in. beam section could be considered to be a shallow section. It was designed to exhibit thick end-plate behavior.

Limit State – Predictions and Progression

Equations presented in Chapter 3 were used to calculate a moment capacity at bolt rupture without prying action (M_{np}) and moment capacity for end-plate yielding (M_{pl}) of as given in Table 6-7.

Table 6-7 Predicted and Experimentally Obtained Moment Capacities for Specimen 12B-MRE 1/3-4W/2W-0.75-1.00-36

Stage	Nominal Predicted (k-ft)	Expected Predicted (k-ft)	Experimental Capacity (k-ft)	Ratio Compared to Nominal	Ratio Compared to Expected
Yield			M_y =960		
Ultimate	M_{np} =1300	M_{np}^{exp} =1630	M_u =1490	M_{np}/M_u =0.87	M_{np}^{exp}/M_u =1.09
Doesn't Control	M_{pl} =2190				
	M_p =1795				

The specimen behaved as expected. During the actual test, bolt rupture without prying action, M_{np}, controlled the strength of the connection. The six bolts on the tension side of the connection ruptured at once and no end-plate yielding was observed (see Figure 6-30).

A yield moment, M_y (Figure 6-27) of 960 k-ft and an ultimate moment, M_u of 1490 k-ft were experimentally obtained. They are demonstrated graphically and compared with the predicted value, M_{np}, in the Figure 6-26.

The ratio M_{np}/M_u in Table 6-7 is conservative (less than 1.0) as based on nominal bolt strength, but the moment capacity calculated using expected bolt strength, M_{np}^{exp}, was found to be 9% more (unconservative) than the experimentally observed ultimate moment.

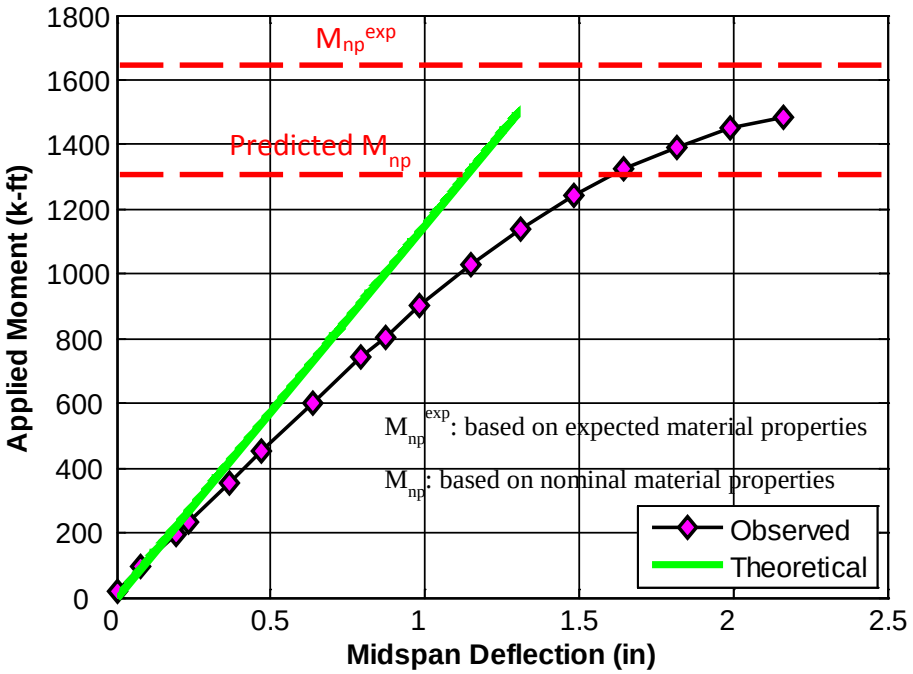

Figure 6-26 Applied Moment vs Midspan deflection for Specimen 12B-MRE 1/3-4W/2W-0.75-1.00-36

Experimental Results - End-Plate Separation

Figure 6-27 displays the end-plate separation in relation to the moment at the mid-span of the specimen. The plot shows that there was not much end-plate separation before the bolts ruptured, which is typical of a thick plate behavior. Also, the pictures shown in Figure 6-30, prove that there was no white wash flaking off the plates and hence, the end-plates didn't yield.

Experimental Results - Bolt Forces

As shown in Figure 6-28, the bolt forces did not increase significantly until they reached their nominal tensile strength (force values plotted past this point are considered invalid due to unaccounted for nonlinearity in the relationship between stress and strain). The lack of exponential bolt strain increase indicates that prying forces were negligible.

Experimental Results - Pictures of Specimen

Figure 6-29 and Figure 6-30 show the difference in the specimen at the start and the end of the test. From the pictures it is clear that no yielding was observed. Also, the end-plate separation throughout the depth, was like a simple wedge with no distortions seen from the side view (middle picture in Figure 6-30), which is typical of thick plate behavior.

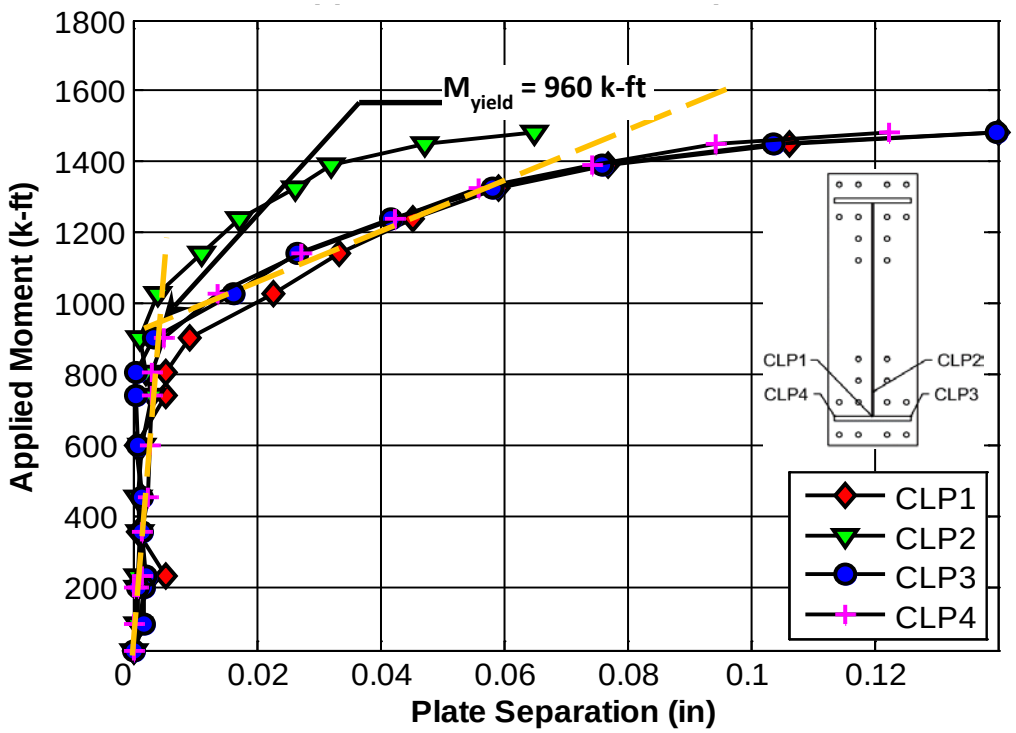

Figure 6-27 End-plate separation for Specimen 12B-MRE 1/3-4W/2W-0.75-1.00-36.

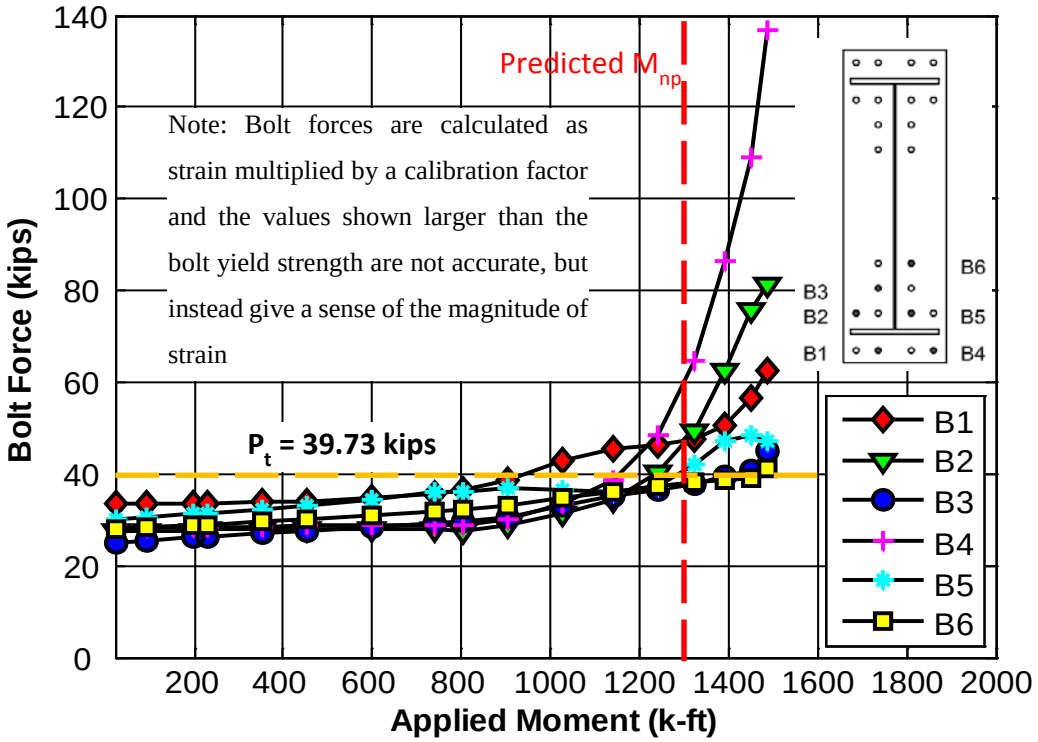

Figure 6-28 Bolt Forces for specimen 12B-MRE 1/3-4W/2W-0.75-1.00-36

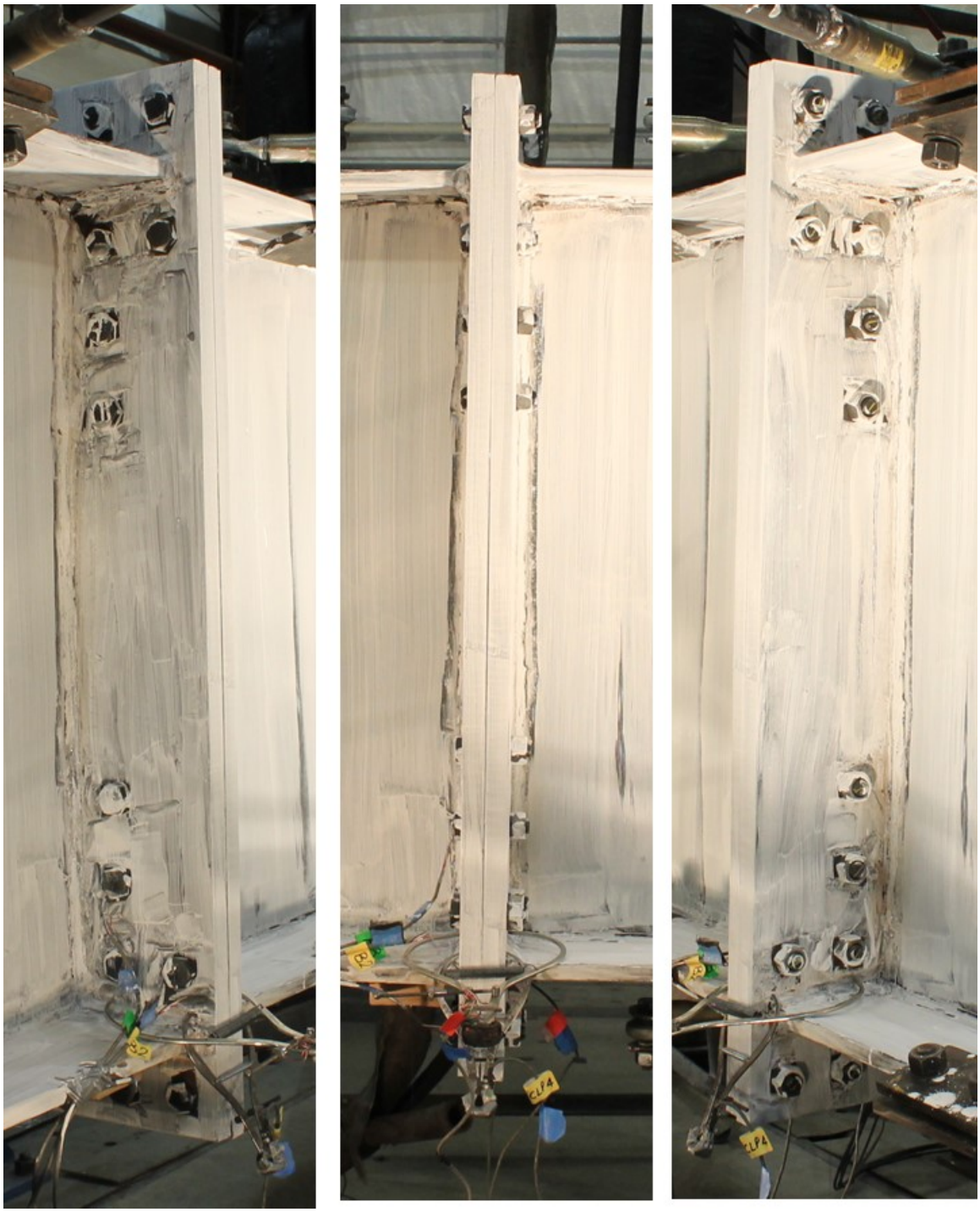

Figure 6-29 Three views of the Specimen 12B-MRE 1/3-4W/2W-0.75-1.00-36 at the start of the test

Figure 6-30 Three views of the specimen 12B-MRE 1/3-4W/2W-0.75-1.00-36 at the end of the test

6.2.3 Deep Section - Thin Plate Behavior

Specimen 12B-MRE 1/3-4W/2W-1.00-0.75-60 was 60 in. deep and designed to exhibit thin end-plate behavior.

Limit State – Predictions and Progression

Equations presented in Chapter 3 were used to calculate a moment capacity at bolt rupture without prying action (M_{np}), moment capacity for end-plate yielding (M_{pl}) and moment capacity at bolt rupture with prying action (M_q) as given in Table 6-8.

Table 6-8 Predicted and Experimentally Obtained Moment Capacities for Specimen 12B-MRE 1/3-4W/2W-1.00-0.75-60

Stage	Nominal Predicted (k-ft)	Expected Predicted (k-ft)	Experimental Capacity (k-ft)	Ratio Compared to Nominal	Ratio Compared to Expected
Yield		M_{pl} =1980	M_y =2230		M_{pl}/M_y =0.89
Ultimate	M_q =2450	M_q^{exp} =3220	M_u =2760*	M_q/M_u =0.89*	M_q^{exp}/M_u =1.17*
Doesn't Control	M_{np} =4000				
	M_p =3915				

* Test stopped prior to bolt rupture because lateral torsional buckling of specimen.

The specimen exhibited some end-plate yielding, but the test had to be stopped prior to bolt rupture. This was due to lateral torsional buckling for which the lateral bracing was insufficient to restrain, and this is shown in Figure 6-31. As shown in the moment vs. deflection plot of Figure 6-32, the specimen was loaded up to up to a moment of approximately 2500 k-ft and then unloaded. An additional lateral brace was installed. After reloading to a slightly larger moment, lateral torsional buckling deformations again got large and the specimen could not sustain any additional load. This is shown in the Figure 6-32. End-plate yielding was observed and is shown in Figure 6-38.

Experimental Results - Yield and Ultimate Moments

A yield moment, M_y (Figure 6-33 and Figure 6-34) of 2230 k-ft was experimentally obtained and the maximum applied moment was 2760 k-ft. They are demonstrated graphically and compared with the predicted values in the Figure 6-32.

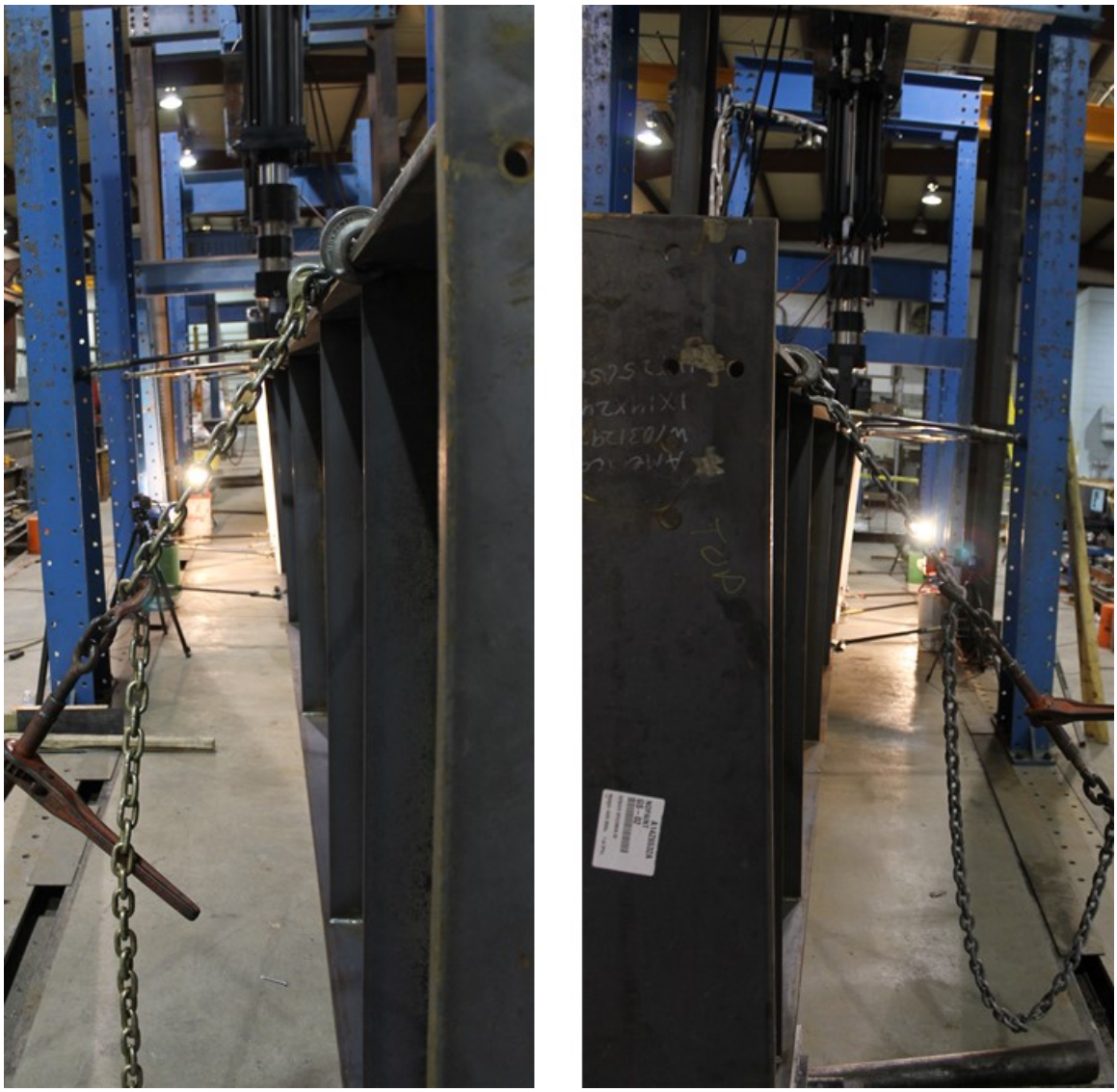

Figure 6-31 Twisting of the Specimen Viewed from the two ends of the specimen

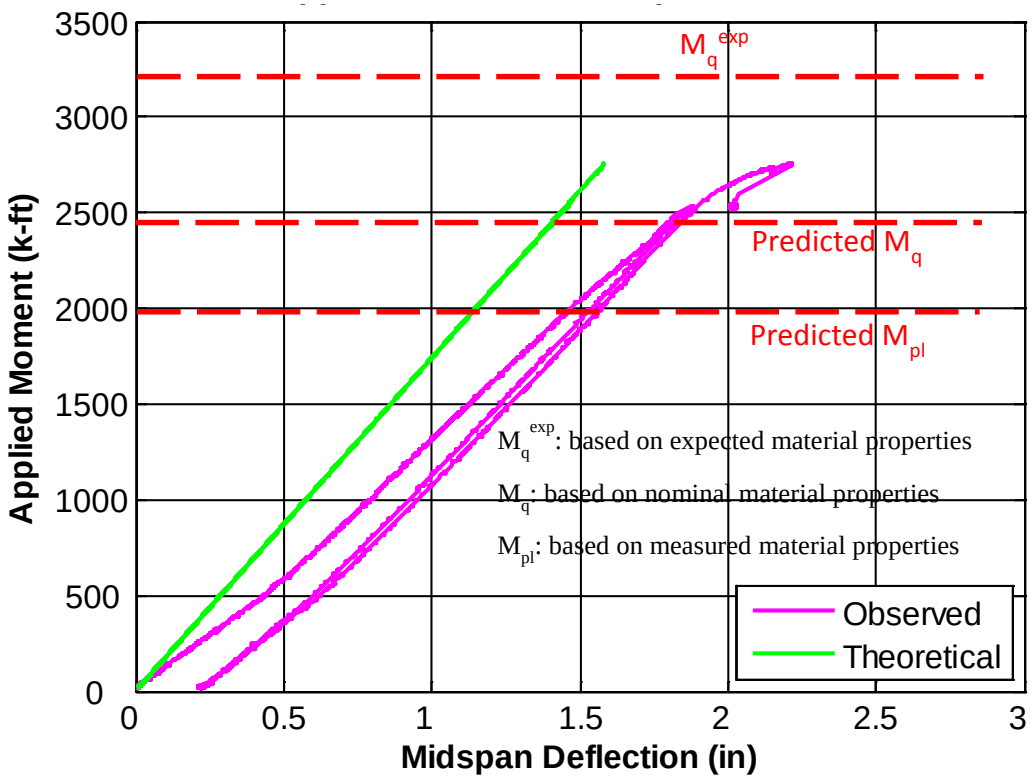

Figure 6-32 Applied Moment vs Midspan deflection for Specimen 12B-MRE 1/3-4W/2W-1.00-0.75-60

The ratio M_{pl}/M_y = 0.89 in Table 6-8 is conservative (less than 1.0) and the predicted, M_{pl}, is within 11% of the observed, M_y. Also, the ratio M_q/M_u in Table 6-8 is conservative. The bolt rupture moment based on expected bolt strength, M_q^{exp}, was calculated to be 17% more (unconservative) than the observed maximum moment. However, this discrepancy would have been smaller if the test had been conducted to bolt rupture.

Experimental Results - End-Plate Separation and Bolt Forces

Figure 6-33 and Figure 6-34 display the end-plate separation in relation to the moment at the mid-span of the specimen. Since the end-plate separations are small, it is not clear that the end-plate yielding was significant. Some end-plate yielding was observed, however, and is shown in Figure 6-38.

As shown in Figure 6-35 and Figure 6-36, the bolt forces, especially B1 and B5, increased drastically past the observed end-plate yielding moment, which is 2230 k-ft. This

indicates the presence of prying forces in these rows of the bolts, as a result of thin end-plate behavior.

Experimental Results - Pictures of Specimen

Figure 6-37 and Figure 6-38 show the difference in the specimen at the start and the end of the test. From the pictures it is clear that there was some end-plate yielding. Since the specimen couldn't be taken to bolt rupture, therefore not all the yield lines were observed. Only a horizontal yield line was seen in the row just inside of the flange, which is generally the first yield line to develop.

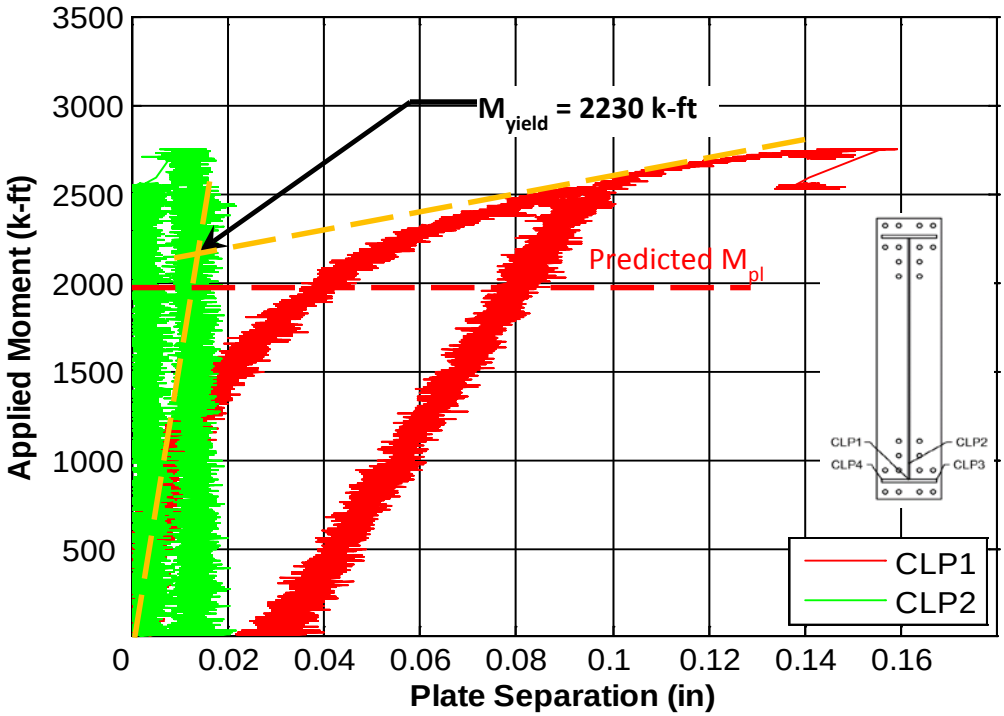

Figure 6-33 End-plate separation for Specimen 12B-MRE 1/3-4W/2W-1.00-0.75-60 (Caliper 1 and 2)

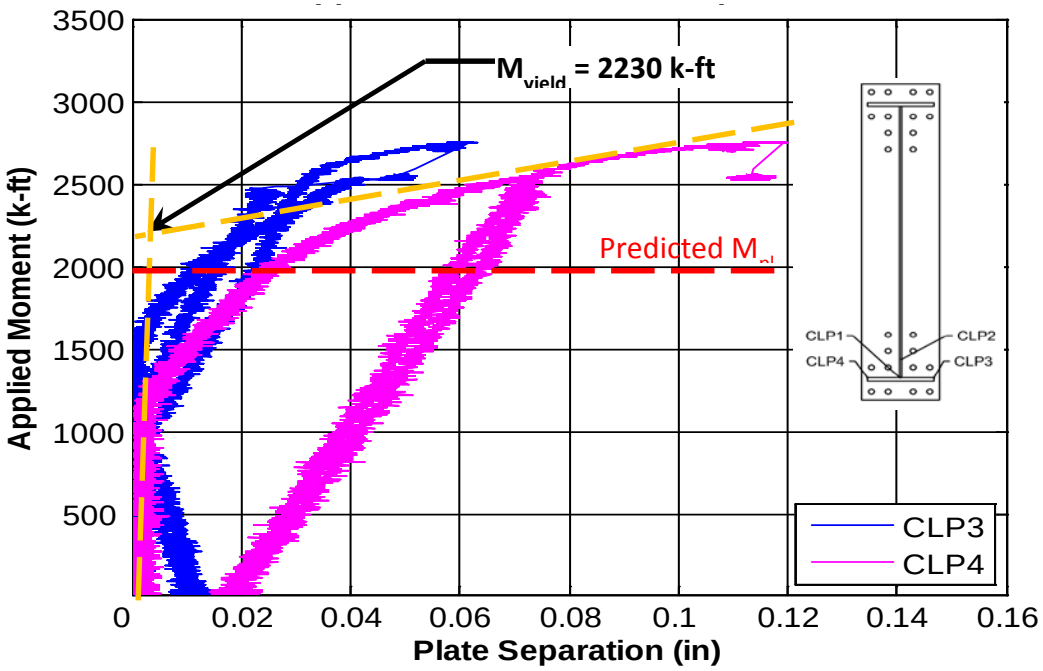

Figure 6-34 End-plate separation for Specimen 12B-MRE 1/3-4W/2W-1.00-0.75-60 (Caliper 3 and 4)

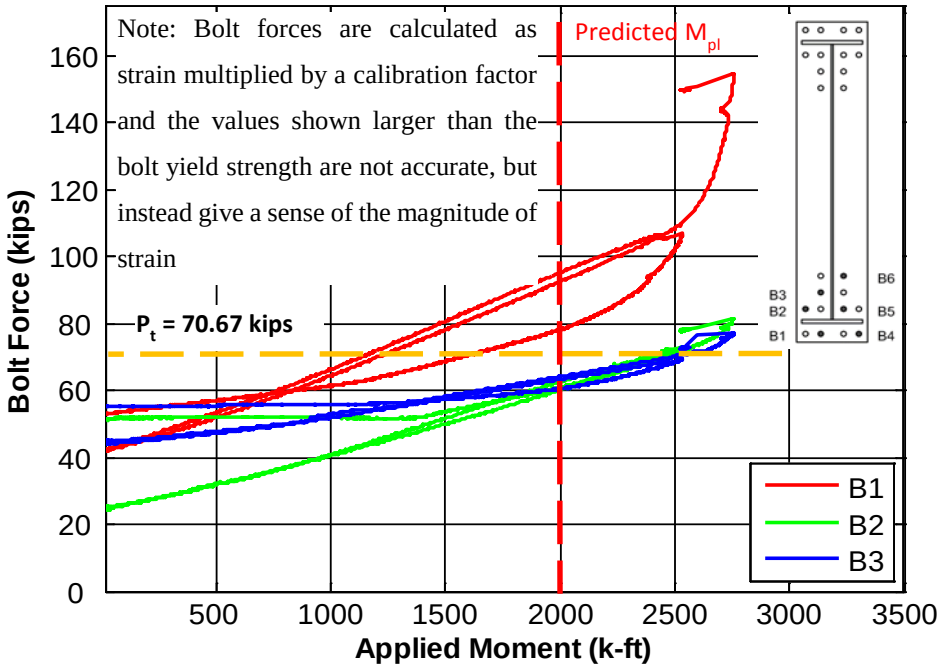

Figure 6-35 Bolt Forces for specimen 12B-MRE 1/3-4W/2W-1.00-0.75-60 (Bolt 1, 2 and 3)

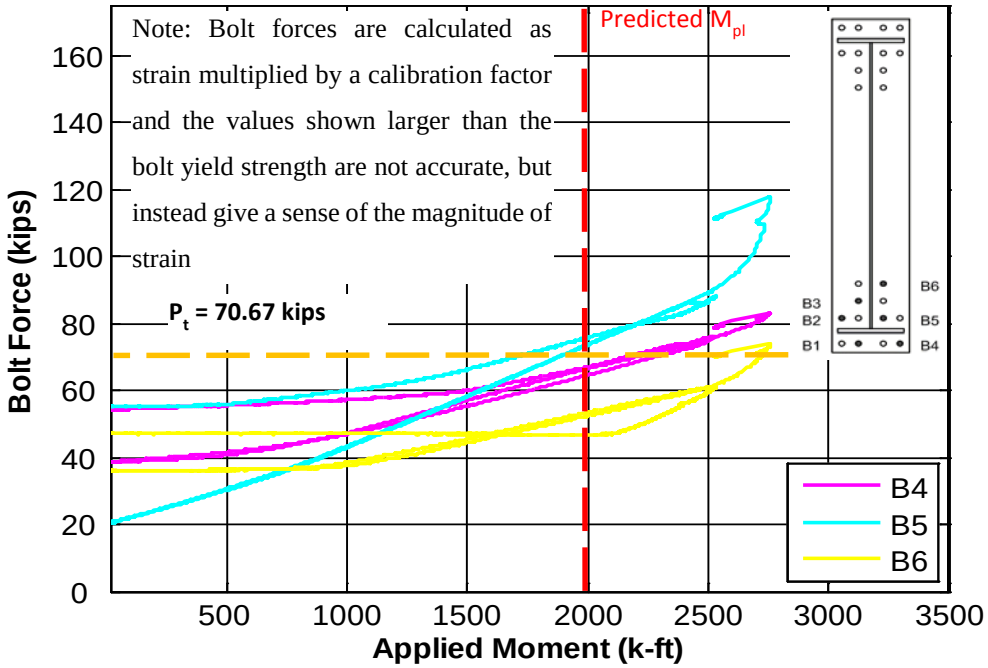

Figure 6-36 Bolt Forces for specimen 12B-MRE 1/3-4W/2W-1.00-0.75-60 (Bolt 4, 5 and 6)

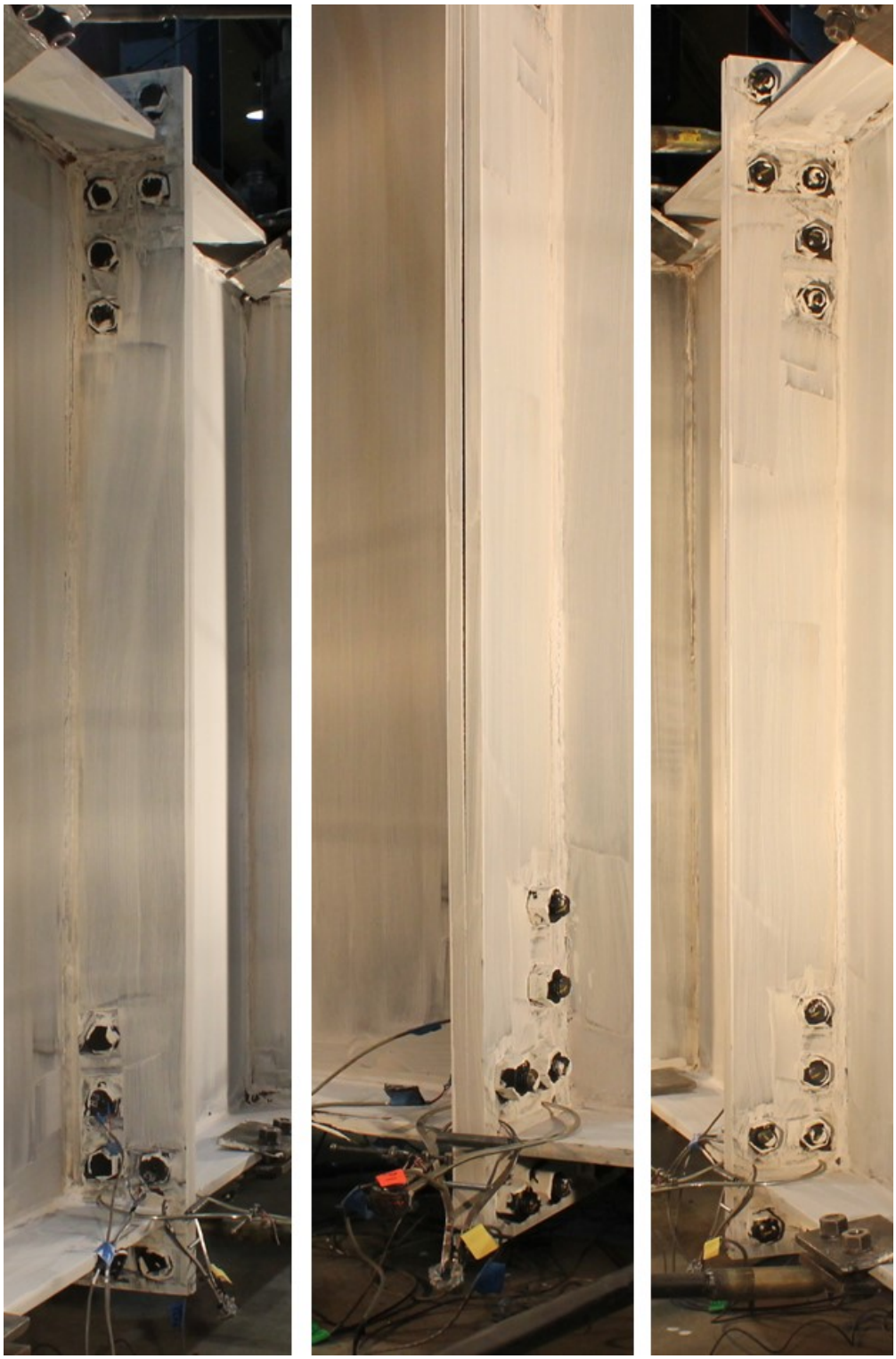

Figure 6-37 Three views of the Specimen 12B-MRE 1/3-4W/2W-1.00-0.75-60 at the start of the test

Figure 6-38 Three views of the specimen 12B-MRE 1/3-4W/2W-1.00-0.75-60 and zoomed in views of the connection to show any yield lines, at the end of the test

6.2.4 Deep Section - Thick Plate Behavior

Specimen 12B-MRE 1/3-4W/2W-0.75-1.00-60 was a 60 in. deep section designed to exhibit thick end-plate behavior.

Limit State – Predictions and Progression

The predictions for moment capacity at bolt rupture without prying action (M_{np}) and moment capacity for end-plate yielding (M_{pl}) were calculated according to equations in Chapter 3 and are presented in Table 6-9.

Table 6-9 Predicted and Experimentally Obtained Moment Capacities for Specimen 12B-MRE 1/3-4W/2W-0.75-1.00-60

Stage	Nominal Predicted (k-ft)	Expected Predicted (k-ft)	Experimental Capacity (k-ft)	Ratio Compared to Nominal	Ratio Compared to Expected
Yield			M_y =2100		
Ultimate	M_{np} =2250	M_{np}^{exp} =2820	M_u =2490	M_{np}/M_u =0.90	M_{np}^{exp}/M_u =1.13
Doesn't Control	M_{pl} =3830				
	M_p =3915				

The specimen behaved as expected. Bolt rupture without prying action, M_{np}, controlled the strength of the connection. Twelve bolts on the tension side and two bottom bolts on the compression side of the connection, ruptured at once and no end-plate yielding was observed (shown in Figure 6-43).

A yield moment, M_y (Figure 6-40) of 2100 k-ft and an ultimate moment, M_u of 2490 k-ft were experimentally obtained. They are demonstrated graphically and compared with the predicted value, M_{np}, in the Figure 6-39. The ratio M_{np}/M_u in Table 6-9 is conservative (less than 1.0). but M_{np}^{exp} was 13% more (unconservative) than the observed ultimate moment.

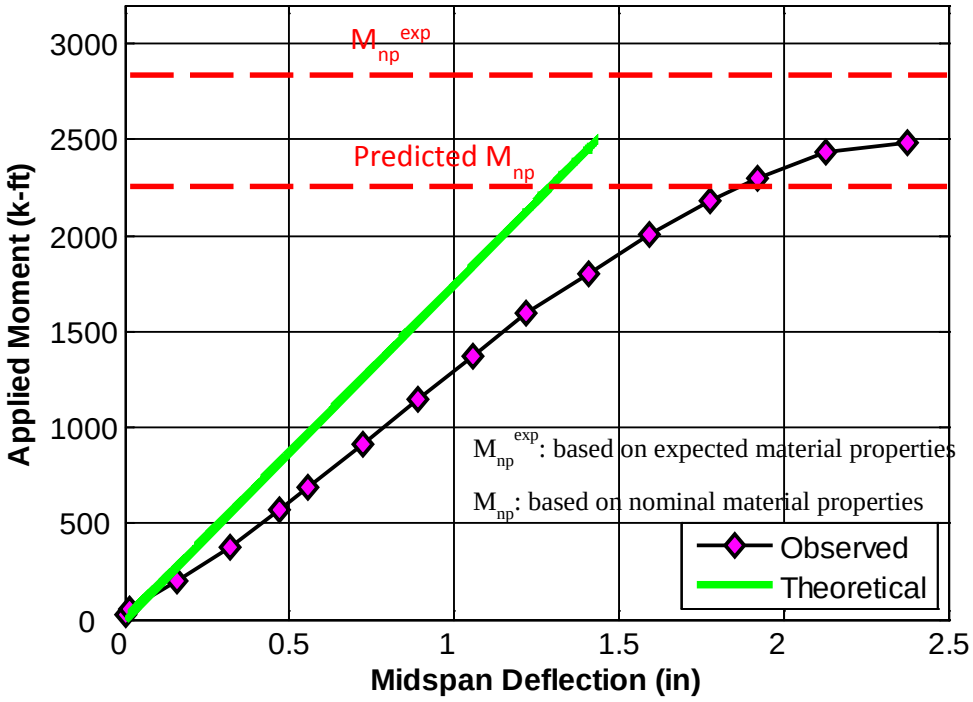

Figure 6-39 Applied Moment vs Midspan deflection for Specimen 12B-MRE 1/3-4W/2W-0.75-1.00-60

Experimental Results - End-Plate Separation and Bolt Forces

Figure 6-40 displays the end-plate separation in relation to the moment at the mid-span of the specimen. Since the end-plate separations in Figure 6-40 are small, it can be deduced that the there was no yielding of the end-plate. Also, the pictures shown in Figure 6-43, do not show any yielding in the end-plates. Hence, the behavior conforms to a thick end-plate.

As shown in Figure 6-41, the bolt forces, except for B1, remained linear well until the nominal tensile strength of the bolt. Even after that, except for B4, all the other bolts were fairly linear for most of the time. This is in line with thick plate behavior.

Experimental Results - Pictures of Specimen

Figure 6-42 and Figure 6-43 show the difference in the specimen at the start and the end of the test. From the pictures it is demonstrated that no yield lines were observed. Also, no distortion was seen in the profile of the end-plates when seen from the side (center picture in Figure 6-43). This validates that the specimen had the behavior of a thick plate.

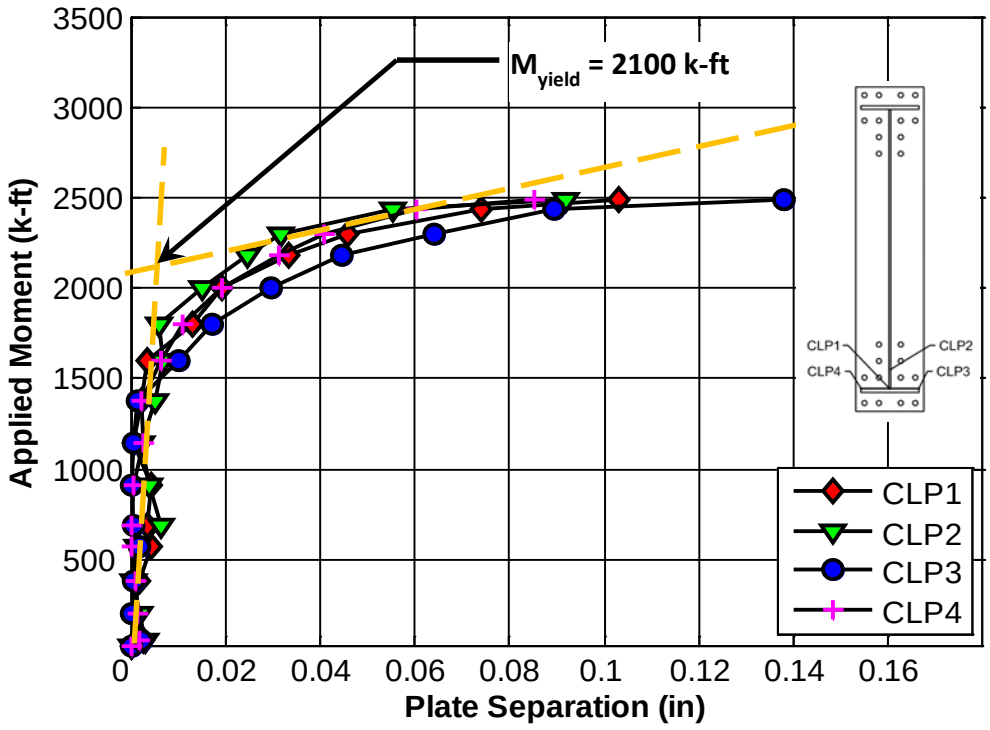

Figure 6-40 End-plate separation for Specimen 12B-MRE 1/3-4W/2W-0.75-1.00-60.

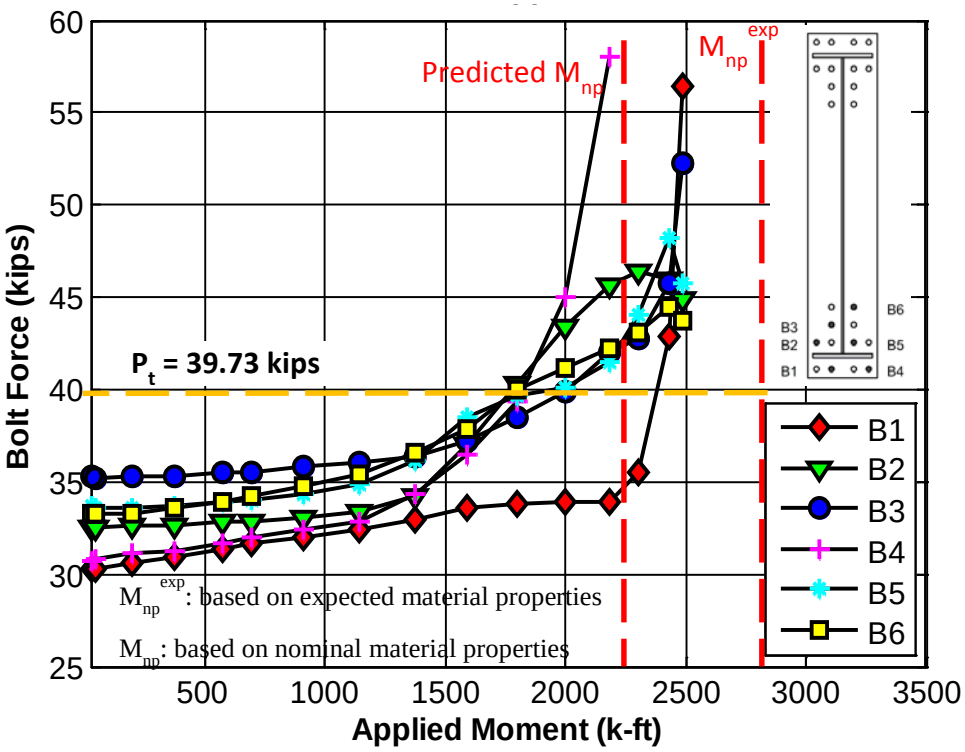

Note: Bolt forces are calculated as strain multiplied by a calibration factor and the values shown larger than the bolt yield strength are not accurate, but instead give a sense of the magnitude of strain

Figure 6-41 Bolt Forces for specimen 12B-MRE 1/3-4W/2W-0.75-1.00-60

Figure 6-42 Three views of the Specimen 12B-MRE 1/3-4W/2W-0.75-1.00-60 at the start of the test

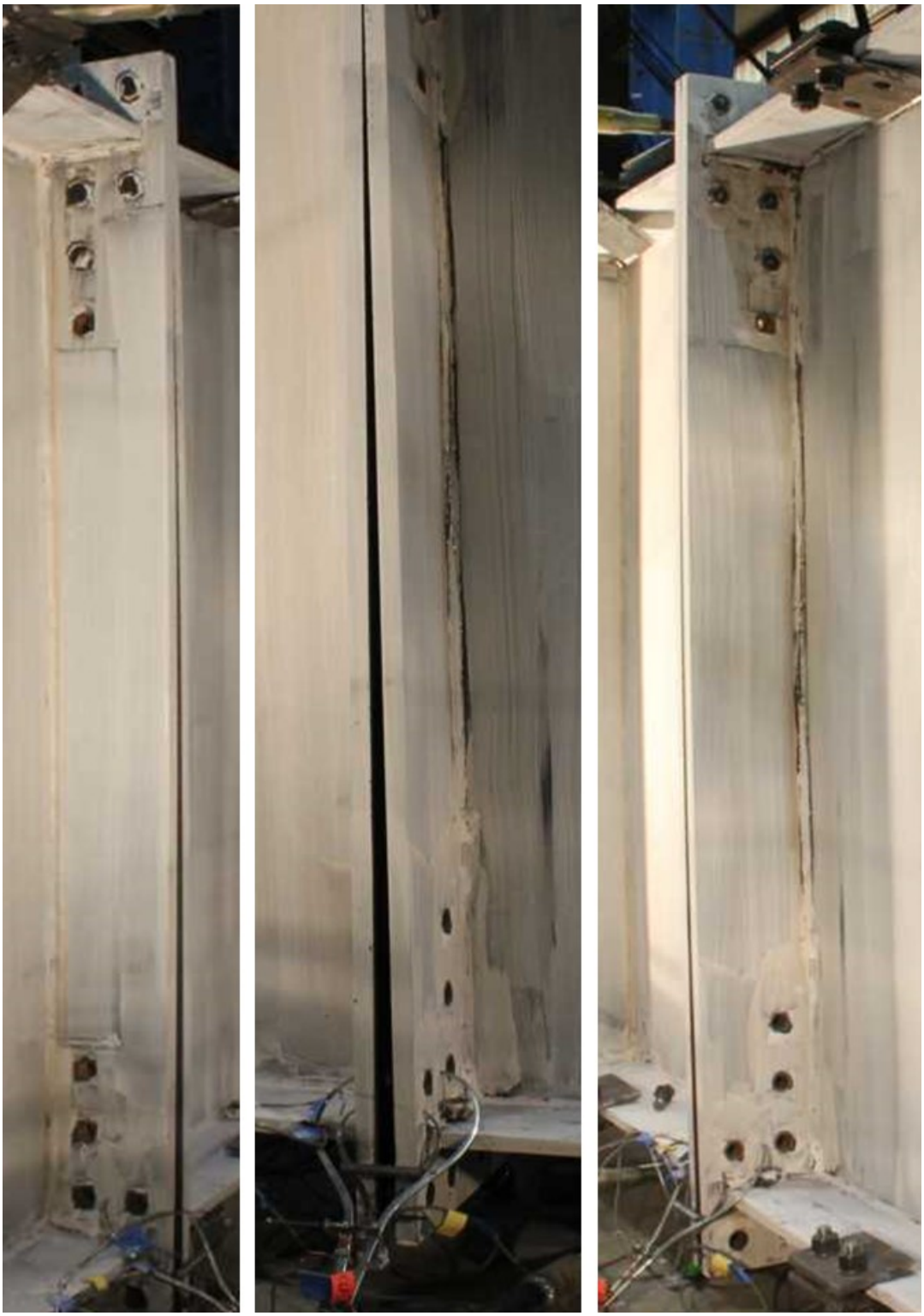

Figure 6-43 Three views of the specimen 12B-MRE 1/3-4W/2W-0.75-1.00-60 at the end of the test

6.2.5 Summary of the Twelve Bolt Extended Unstiffened Configuration

Table 6-10 summarizes the four specimens investigated herein. Both the thin plate specimens could not be taken to bolt rupture (due to local buckling or lateral torsional buckling of the rafter), but the thick end-plate were tested to failure of the connection. Because the thin end-plate specimens were stopped prior to bolt rupture, the level of end-plate yielding and separation was not large. However, yielding of the end-plates for both thin end-plate specimens was achieved.

Table 6-10 Summary of the Four Test Specimens of the Twelve Bolt Extended Unstiffened Configuration

Specimen Identification[1]	Depth (in.)	Behavior	Remarks[2]
12B-MRE 1/3-4W/2W-1.00-0.75-36	36	Thin	M_{pl} was -8% of yield moment. Predicted M_q -13% of the maximum applied moment. M_q^{exp} was +14% of the maximum applied moment. End-plate yielding observed. None of the bolts ruptured.
12B-MRE 1/3-4W/2W-0.75-1.00-36	36	Thick	M_{np} was -13% of the observed M_u. M_{np}^{exp} was +9% of M_u. No end-plate yielding seen
12B-MRE 1/3-4W/2W-1.00-0.75-60	60	Thin	Predicted M_{pl} -11% of the experimental yield moment, M_y. Predicted M_q was -11% of the observed M_u. M_q^{exp} was +17% of M_u. Some End-plate yielding observed. No bolts were ruptured.
12B-MRE 1/3-4W/2W-0.75-1.00-60	60	Thick	M_{np} -10% of the observed M_u. M_{np}^{exp} was +9% of M_u. No end-plate yielding observed.

[1]Specimen Identification: "No. of bolts in the connection - Multiple Row Extended with one bolt row outside the flange and three bolt rows inside the flange – No. of bolts in a row - Bolt diameter - End-plate thickness - Beam depth".

[2]Remarks: A postive percentage means an unconservative calculation, whereas a negative percentage means a safe prediction.

For the two thin plate tests, M_{pl} was 8% to 11% less (conservative) than the experimental yield moment. Furthermore, for the shallow specimen, experimentally measured end-plate separation was found to be consistent with thin end-plate behavior wherein end-plate yielding allows end-plate separation prior to bolt fracture. It is concluded, therefore, that the equations and associated yield line mechanism presented in Chapter 3 for end-plate yielding moment capacity were slightly conservative for the range of parameters tested.

The nominal moment capacity for bolt rupture with prying action, M_q, was 11% to 13% less (conservative) than the observed M_u. The moment capacity for bolt rupture using expected bolt strengths, M_q^{exp}, was 14% to 17% unconservative compared to the peak moment experienced during the test. If the tests had been conducted to bolt rupture there would have been less error between the predicted and actual ultimate capacity. Based on the nominal moment capacity, it is concluded that the proposed bolt model and M_q moment capacity equations will produce conservative results for connections similar to those tested with typical structural bolts (e.g. A325 and A490), in part because of the inherent bolt overstrength.

For thick end-plate specimens, the behavior of the two specimens was quite as expected. No end-plate yielding was visually observed. M_{np} was between 10% and 13% less (conservative) than the observed M_u. The calculated moment capacity using expected bolt strength, M_{np}^{exp}, was 9% and 13% more (unconservative) than the observed ultimate moment, M_u. Similar to the above discussion for bolt rupture with prying action, the prediction equations for bolt rupture without prying action are expected to produce conservative results for connections similar to those tested with typical structural bolts (e.g. A325 and A490), because of the inherent bolt overstrength.

6.3. Testing on the Eight Bolt Extended Stiffened (8ES) Configuration

6.3.1 Deep Section - Thin Plate Behavior

Specimen 8ES-1.25-0.75-56 was a 56 in. deep section designed to exhibit thin end-plate behavior. It is to be noted that for each bolt, one ASTM Grade F436 washer was used

on the nut side. This was done because the shank length of the bolt was about 0.1 in. longer than the combined thickness (1.5 in) of the two end-plates being connected.

Limit State – Predictions and Progression

The predictions for moment capacity at bolt rupture without prying action (M_{np}), moment capacity for end-plate yielding (M_{pl}) and moment capacity at bolt rupture with prying action (M_q) were calculated using equations in Chapter 3 and are given in Table 6-11. The specimen experienced end-plate yielding, but was stopped prior to bolt rupture because of lateral torsional buckling for which the lateral bracing was insufficient to restrain. The lateral torsional buckling is shown in Figure 6-44.

Table 6-11 Predicted and Experimentally Obtained Moment Capacities for Specimen 8ES-1.25-0.75-56

Stage	Nominal Predicted (k-ft)	Expected Predicted (k-ft)	Experimental Capacity (k-ft)	Ratio Compared to Nominal	Ratio Compared to Expected
Yield		M_{pl} =2300	M_y =2400		M_{pl}/M_y =0.96
Ultimate	M_q =2650	M_q^{exp} =2960	M_u =2920*	M_q/M_u =0.91*	M_q^{exp}/M_u =1.01*
Doesn't Control	M_{np} =4110				
	M_p =4191				

* Test was stopped prior to bolt rupture due to lateral torsional buckling

A yield moment, M_y, (Figure 6-46) of 2400 k-ft was experimentally obtained and the maximum applied moment was 2920 k-ft. They are demonstrated graphically and compared with the predicted values in the Figure 6-45.

The ratio M_{pl}/M_y in Table 6-11 is conservative and the predicted, M_{pl}, is within 4% of the observed, M_y. Also, the ratio M_q/M_u given in Table 6-11 shows that the specimen achieved a moment capacity 9% greater than the predicted capacity before the test was stopped. The moment capacity calculated based on expected bolt strength, M_q^{exp}, was found to be within 1% of the maximum applied moment when the test was stopped.

Figure 6-44 Twisting of the Specimen Viewed from one end of the specimen

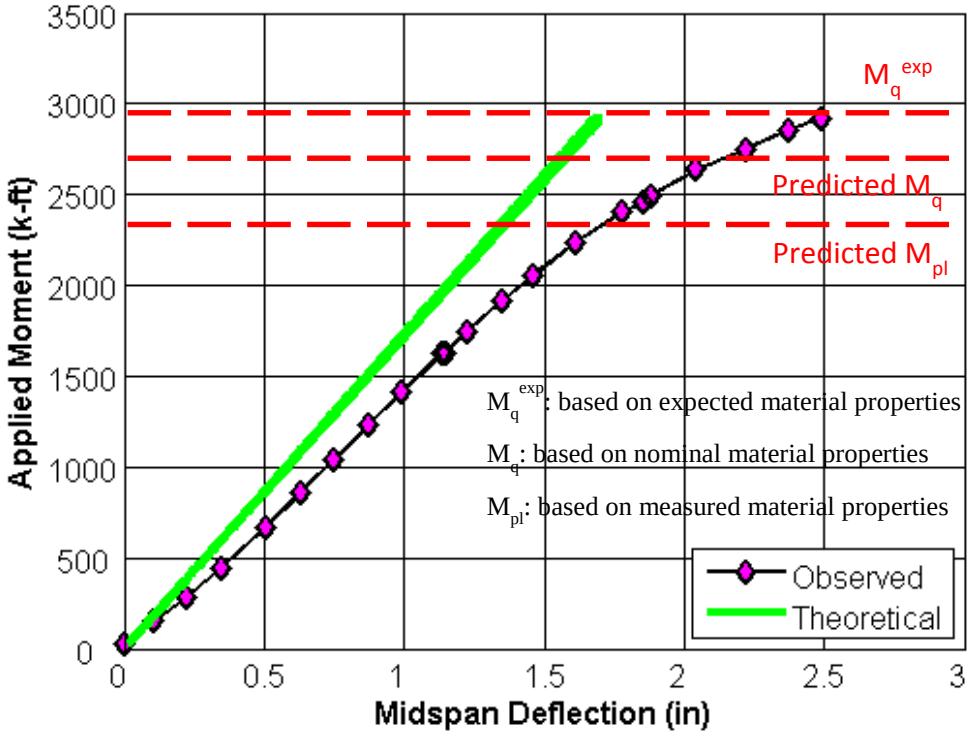

Figure 6-45 Applied Moment vs Midspan deflection for Specimen 8ES-1.25-0.75-56

Experimental Results - End-Plate Separation and Bolt Forces

Figure 6-46 displays the end-plate separation in relation to the moment at the mid-span of the specimen. Significant end-plate separation was seen before the test was stopped. Hence, it can be said from the plots that the behavior was of a thin end-plate.

As is shown in Figure 6-47, the bolt forces increased exponentially past the observed end-plate yielding moment, which is 2400 k-ft. This indicates the presence of prying forces in these rows of the bolts, as a result of thin end-plate behavior.

Experimental Results - Pictures of Specimen

Figure 6-48 and Figure 6-49 show the difference in the specimen at the start and the end of the test. From the pictures it is clear that there was end-plate yielding. White wash spalling was seen in in the top three horizontal bolt rows and also along the vertical direction on both sides of the web. When viewed from the side, end-plate distortion was observed, which further corroborates the yielding of end-plate.

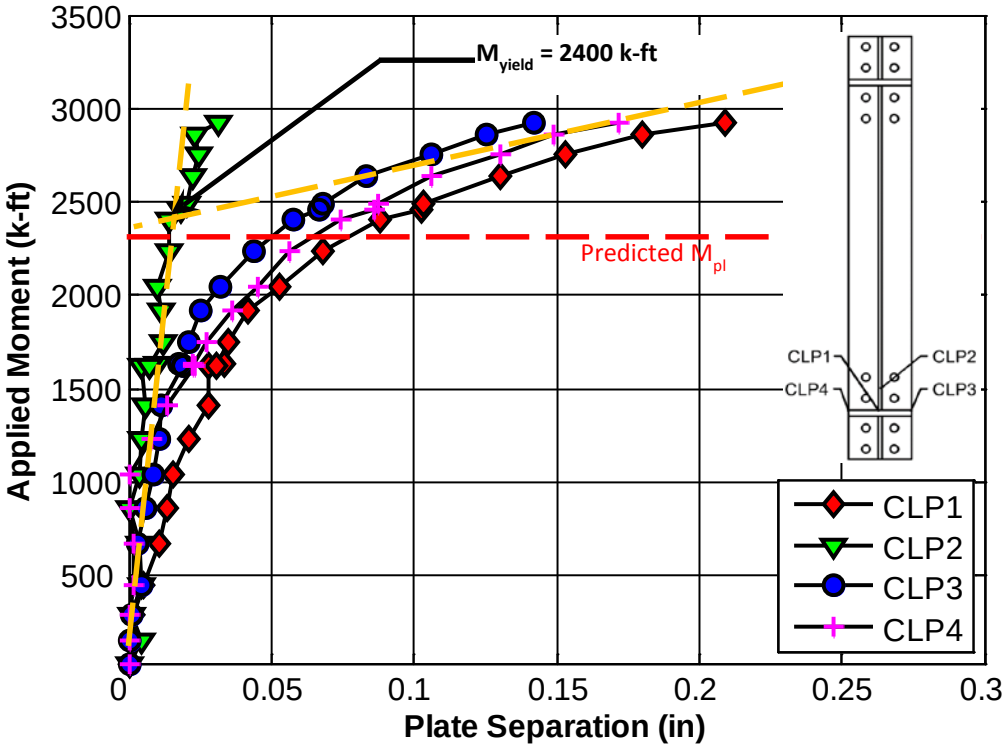

Figure 6-46 End-plate separation for Specimen 8ES-1.25-0.75-56

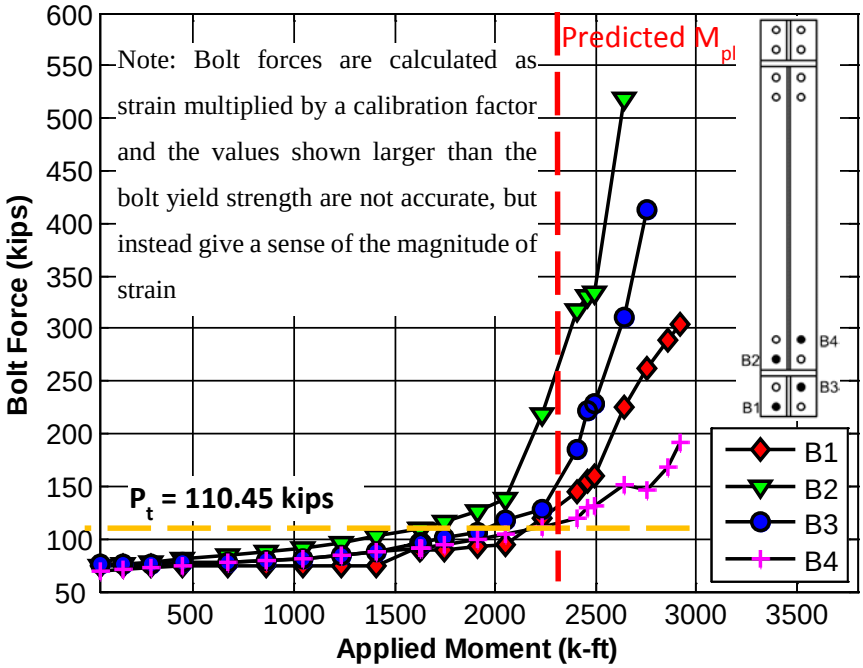

Figure 6-47 Bolt Forces for specimen 8ES-1.25-0.75-56

Figure 6-48 Three views of the Specimen 8ES-1.25-0.75-56 at the start of the test

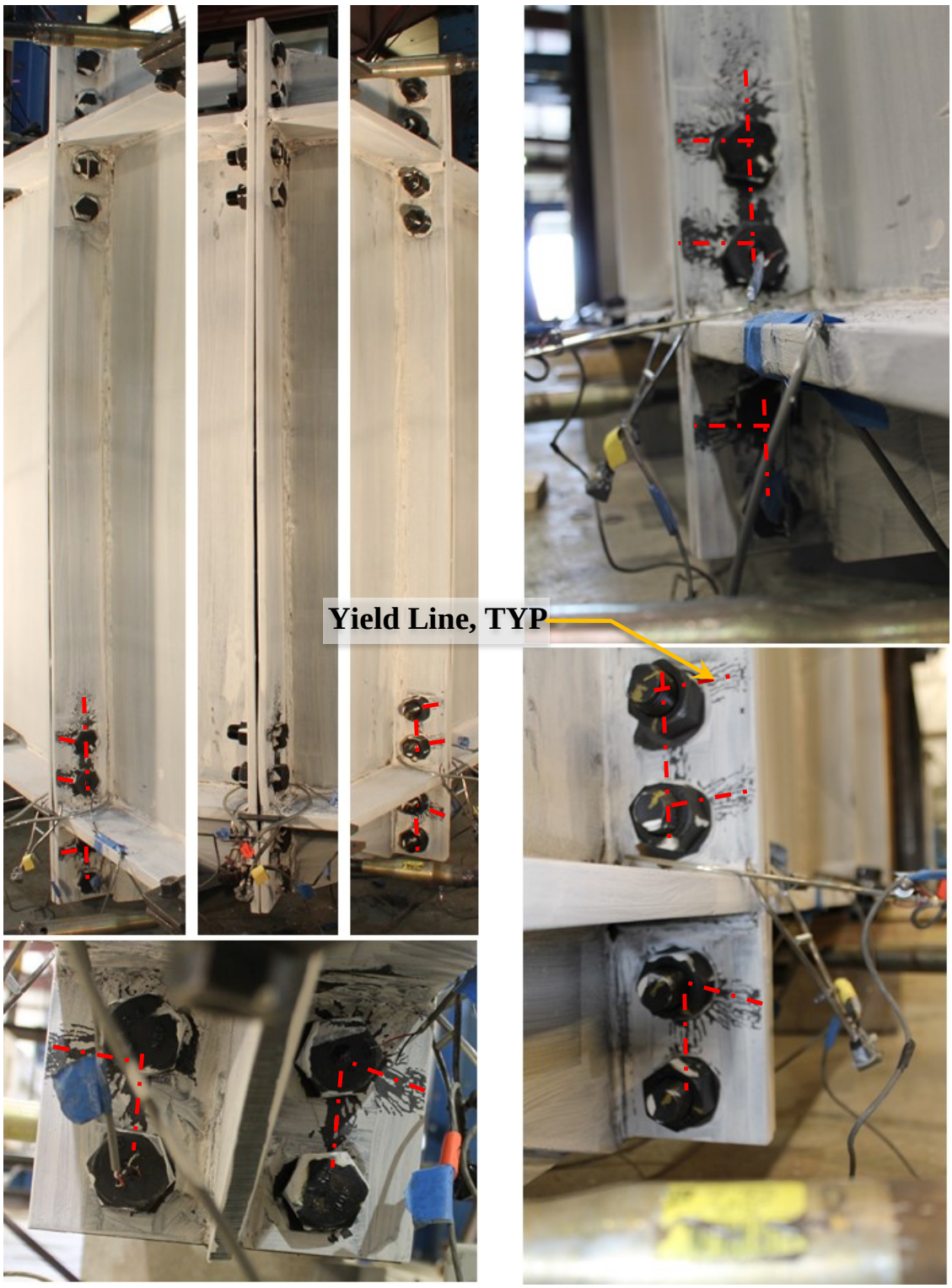

Figure 6-49 Three views of the specimen 8ES-1.25-0.75-56 and zoomed in views of the connection to show any yield lines, at the end of the test

6.3.2. Deep Section - Thick Plate Behavior

Specimen 8ES-1.00-1.00-56 was a 56 in. deep section designed to exhibit thick end-plate behavior.

Limit State – Predictions and Progression

Equations presented in Chapter 3 calculate a moment capacity at bolt rupture without prying action (M_{np}) and moment capacity for end-plate yielding (M_{pl}) as given in Table 6-12.

The specimen behaved as expected for a thick end-plate connection. Bolt rupture without prying action, M_{np}, controlled the strength of the connection. All eight bolts on the tension side, ruptured at once and marginal spalling of white wash was seen around the bolts (shown in Figure 6-54).

Table 6-12 Predicted and Experimentally Obtained Moment Capacities for Specimen 8ES-1.00-1.00-56

Stage	Nominal Predicted (k-ft)	Expected Predicted (k-ft)	Experimental Capacity (k-ft)	Ratio Compared to Nominal	Ratio Compared to Expected
Yield			M_y =2520		
Ultimate	M_{np} =2630	M_{np}^{exp} =3420	M_u =3050	M_{np}/M_u =0.86	M_{np}^{exp}/M_u =1.12
Doesn't Control	M_{pl} =4160				
	M_p =4191				

A yield moment, M_y (Figure 6-51) of 2520 k-ft and an ultimate moment, M_u of 3050 k-ft were experimentally obtained. They are demonstrated graphically and compared with the predicted value, M_{np}, in the Figure 6-50. The ratio of predicted to actual moment capacity, M_{np}/M_u in Table 6-12 is conservative (less than 1.0) by 14% whereas M_{np}^{exp} was shown to be unconservative by 12%.

Experimental Results - End-Plate Separation and Bolt Forces

Figure 6-51 displays the end-plate separation in relation to the moment at the mid-span of the specimen. Since the end-plate separation in Figure 6-51 is about 0.14 in., it can be deduced that the there was no yielding of the end-plate. Also, the pictures shown in

Figure 6-54, show that there was no visually observable yielding in the plates and hence, the behavior was of a thick plate.

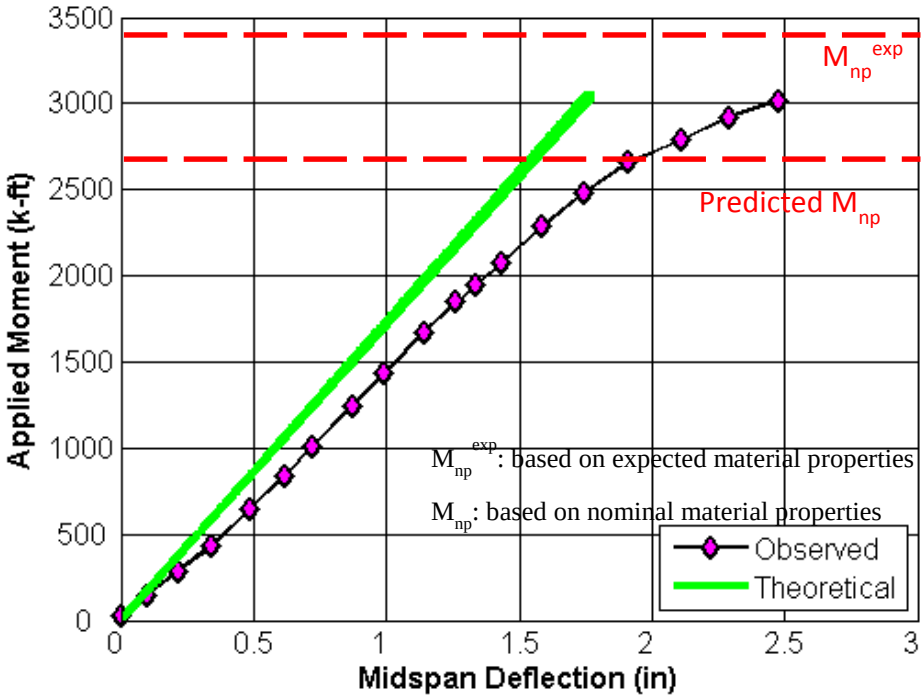

Figure 6-50 Applied Moment vs Midspan deflection for Specimen 8ES-1.00-1.00-56

As shown in Figure 6-52, the bolt forces were fairly linear with increasing moment with the bolt forces increasing more sharply towards the end of the test. However, there was no exponential increase in bolt strains implying prying forces were likely negligible.

Experimental Results - Pictures of Specimen

Figure 6-53 and Figure 6-54 show the difference in the specimen at the start and the end of the test. Some local yielding was observed around the bolt holes, but overall there was minimal yielding. Also, no distortion was seen in the profile of the end-plates when seen from the side (top center picture in Figure 6-54). This validates that the specimen had the behavior of a thick plate.

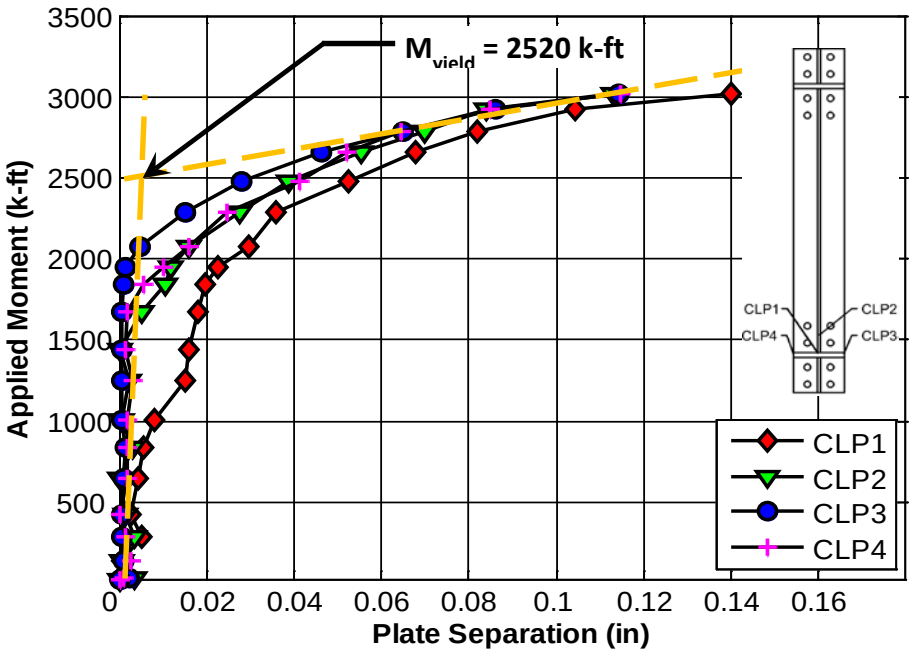

Figure 6-51 End-plate separation for Specimen 8ES-1.00-1.00-56.

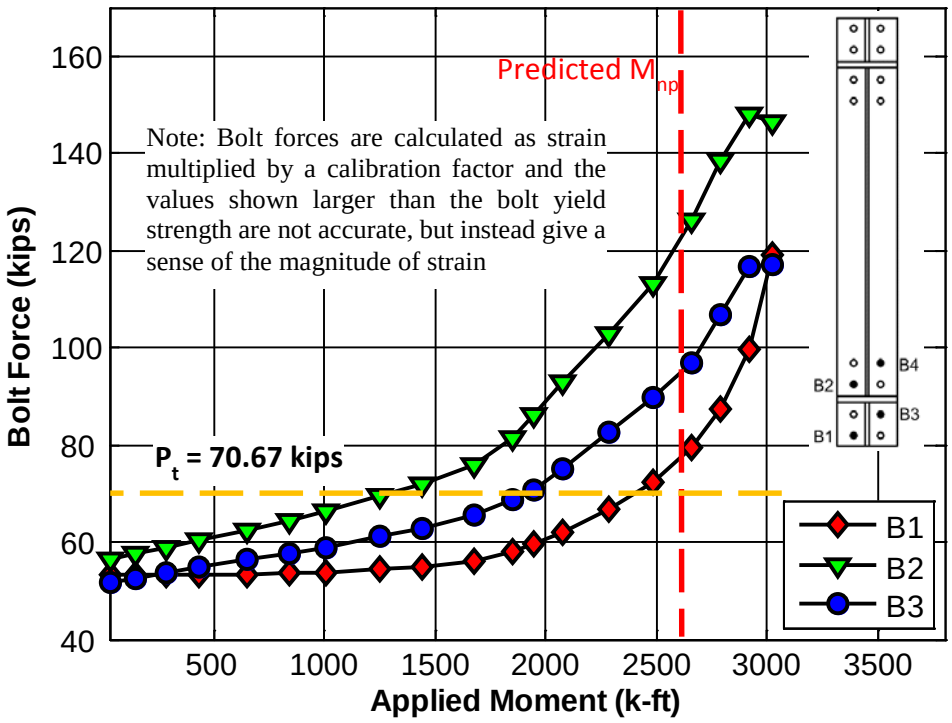

Figure 6-52 Bolt Forces for specimen 8ES-1.00-1.00-56

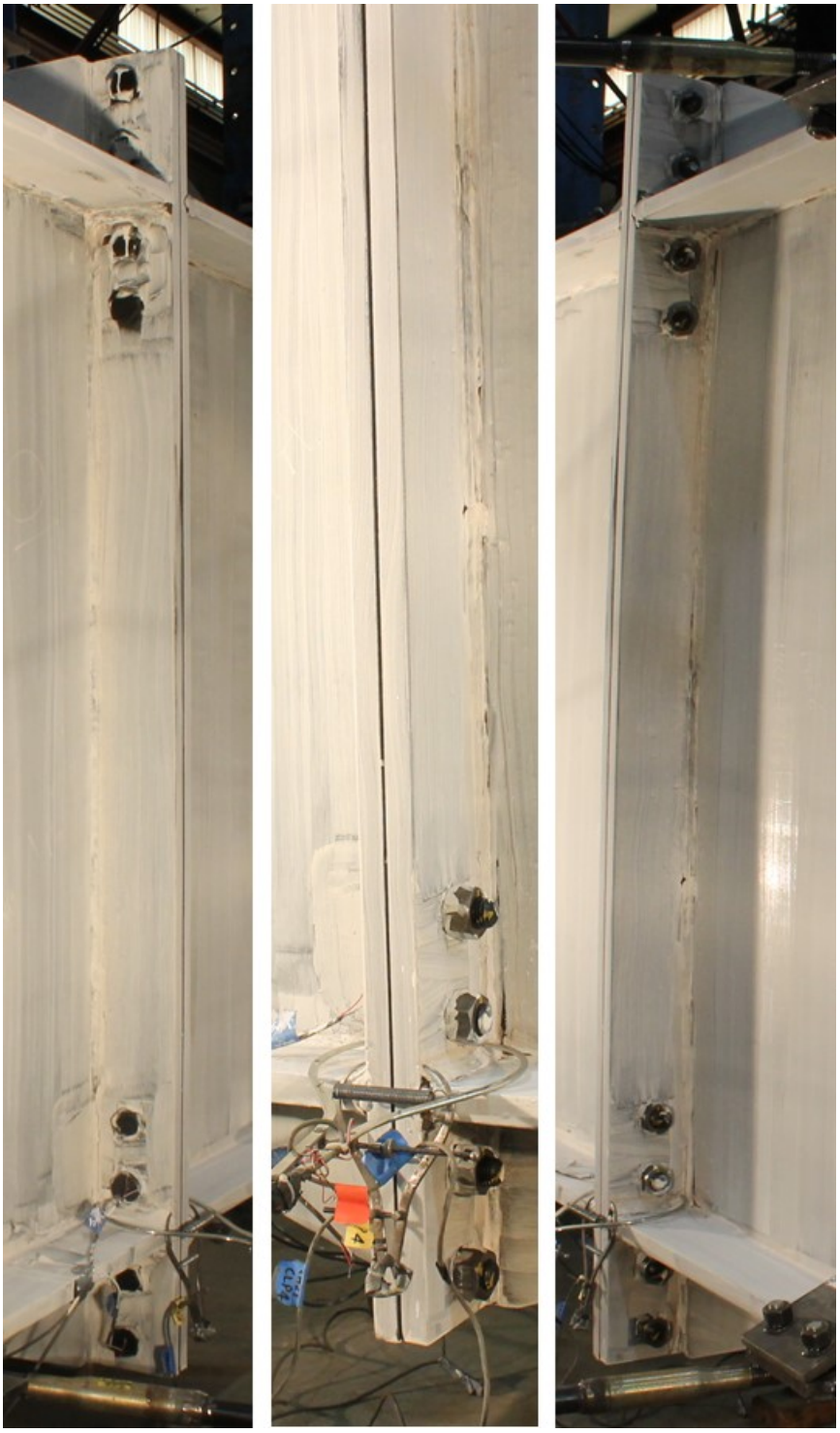

Figure 6-53 Three views of the Specimen 8ES-1.00-1.00-56 at the start of the test

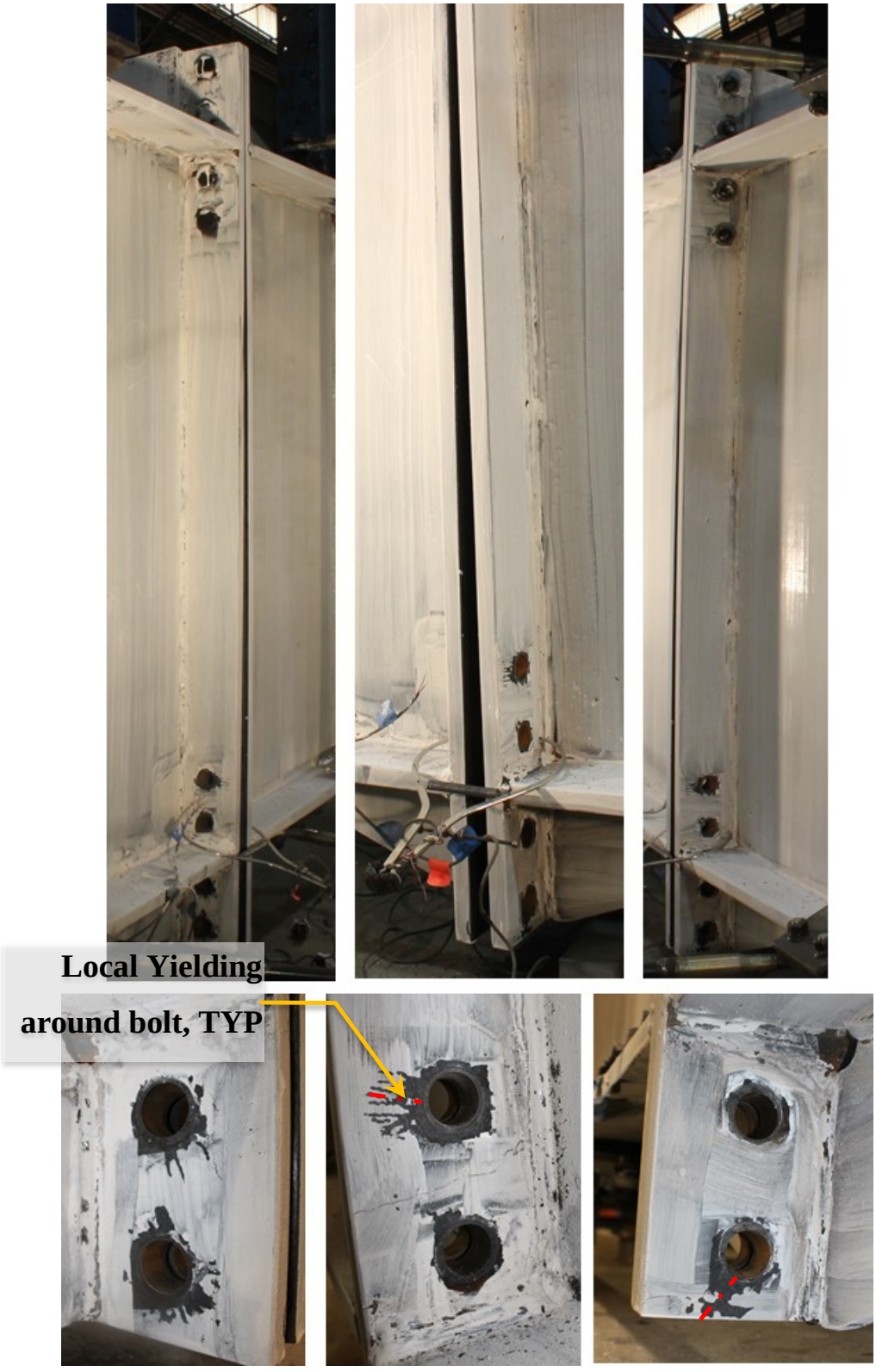

Figure 6-54 Three views of the specimen 8ES-1.00-1.00-56 and zoomed in views to show local yielding around the bolts, at the end of the test

6.3.3. Summary of the Eight Bolt Extended Configuration

Table 6-13 summarizes the two specimens investigated herein. The thin plate test was stopped prior to bolt rupture, but the thick end-plate was tested to connection failure. End-plate yielding was clearly observed in the thin plate specimen.

The predicted moment capacity associated with end-plate yielding was within 4% of the observed yield moment. This implies that the yield line mechanism and prediction equation presented in Chapter 3 are accurate for the tested parameters.

The predicted bolt rupture moments (with or without prying), M_{np} and M_q, was always lower than the maximum applied moment, M_u, implying they are conservative. Predicted M_{np} was within 14% of the observed ultimate moment, M_u and predicted M_q was within 9% of the observed maximum moment, even though the bolts were not ruptured. The expected moment capacity associated with bolt rupture calculated using expected bolt strength, M_{np}^{exp} and M_q^{exp} were found out to be 12% more and 1% more (unconservative) than the maximum applied moment, respectively. Thus, it was concluded that the bolt model and equations for predicting moment capacity associated with bolt rupture will likely produce conservative results for connections similar to those tested with typical structural bolts (e.g. A325 and A490), in part because of the inherent overstrength in the bolts.

Table 6-13 Summary of the Two Test Specimens of the Eight Bolt Extended Unstiffened Configuration

Specimen Identification[1]	Depth (in.)	Behavior	Remarks[2]
8ES-1.25-0.75-56	56	Thin	Predicted M_{pl} -4% of the observed yield moment, M_y. Predicted M_q was -9% of the maximum applied moment. M_q^{exp} was +1% of the maximum applied moment. End-plate yielding observed. No bolts were ruptured.
8ES-1.00-1.00-56	56	Thick	M_{np} -14% of the observed M_u. M_{np}^{exp} was +12% of M_u. Minimal end-plate yielding observed.

[1]Specimen Identification: "No. of bolts in the connection - Bolt diameter - End-plate thickness - Beam depth".

[2]Remarks: A postive percentage means an unconservative calculation, whereas a negative percentage means a safe prediction.

7. SUMMARY AND CONCLUSIONS

7.1. Overview

This report examines the design procedures for four end-plate moment connections. Selected configurations were the: eight-bolt extended four wide unstiffened configuration (8E-4W), eight bolt extended stiffened configuration (8ES), six bolt flush four wide / two wide unstiffened configuration (6B-4W/2W), and twelve bolt multiple row extended four wide / two wide unstiffened configuration (12B-MRE 1/3-4W/2W). Design procedures were presented for each of these end-plate configurations. In particular, equations were provided that predict the moment capacity associated with three limit states including bolt rupture with prying action (M_q), bolt rupture without prying action (M_{np}), and end-plate yielding (M_{pl}).

Experimental data found in the literature was used to evaluate the effectiveness of design procedures for both the 8E-4W and 8ES configurations. In addition, ten full-scale experiments were conducted to provide data used in evaluating the effectiveness of design equations for the 8ES (two specimens), 6B-4W/2W (four specimens), and the 12B-MRE 1/3-4W/2W (four specimens) configurations. It was found that the predicted moment capacities were typically within 10% of the experimentally obtained moment capacities. It was therefore concluded that the proposed yield line mechanisms, bolt models, and design equations were reasonably accurate for the range of parameters tested. A summary of the details for each connection configuration are provided in the following sections.

7.2. 8E-4W Configuration

Four tests from the literature (Sumner et. al 2000, Sumner and Murray 2001) were examined for this configuration (Section 4.1). These were chosen in such a way that the design procedures could be evaluated for shallower and deeper specimens with both thick and thin end-plate behavior for a range of different design parameters. Rolled sections (30 in. and 36 in. deep) were used for the shallow specimens whereas built-up sections (both 61.5 in. deep) were used for deep specimens. For the two thick end-plate tests, the ratio M_{np}/M_u was conservative (less than 1.0) having values of 0.94 and 0.88 for the shallow and

deep beam respectively. For the two thin plate tests, M_{pl}/M_y was within 4% of unity (1.04 for shallow and 0.96 for deep). M_q/M_u was 1.05 for the shallow-thin specimen whereas the deep-thin specimen couldn't be taken to bolt rupture. The end-plate separation for all the tests was found to be consistent with their expected behavior. It was concluded that the proposed design equations were relatively accurate for the range of parameters tested.

7.3. 8ES Configuration

A total of six tests, four from the literature (Ghassemieh 1983, Sumner et. al 2000) and two new tests, were examined for this configuration (Sections 4.2 and 6.3). The behavior of the four specimens from the literature were all quite different and the relationship between experimentally obtained end-plate yield moment and predicted values varied considerably. Although the predicted end-plate yield moment capacity, M_{pl}, was within 5% of the experimental yield moment for Specimen 8ES-1.25-1-30 from Sumner et al. (2000), end-plate yielding was observed in Specimen 8ES-1.25-1.25-36 at only 63% of the predicted moment, M_{pl}. Specimen 8ES-0.875-0.75-24 from Ghassemieh et al. (1983) produced a moment at the end of the test similar to the predicted M_q value, but Specimen 8ES-1.25-1-30 reached 110% of M_q before the test was stopped without bolt fracture. Specimen 8ES-1.25-1.25-36 experienced bolt rupture at a moment that was within 6% of the predicted value, M_{np}, but it is unlikely that Specimen 8ES-0.875-1-24 would have reached the predicted M_{np} and was stopped at 88% of M_{np} after significant softening.

One of the challenges associated with the previous test data was that many of the specimens were experiencing multiple limit states at the same time. Since this connection configuration was intended for seismic applications, several specimens had beam plastic moment capacity that was near the connection moment capacity. Yielding and local buckling of the beam confused the results from some of these tests.

Two new specimens were designed with larger separation between the moment capacities associated with the desired limit state and all other limit states. End-plate yielding was clearly observed in the new thin end-plate specimen and the predicted moment capacity associated with end-plate yielding was within 4% of the experimental yield

moment. The test was stopped prior to bolt rupture, but the peak moment achieve during the test was 9% larger than the predicted bolt rupture moment capacity.

The calculated moment capacity for bolt rupture with prying, M_{np} was smaller than the maximum applied moment, M_u by 14%. The conservative nature of the moment capacities associated with bolt rupture was concluded to be related to the use of nominal bolt strengths in the calculation. Bolt testing reports showed that the bolts had approximately 25% over-strength compared to nominal values.

It was concluded that the proposed design equations were relatively accurate for the range of parameters tested.

7.4. 6B-4W/2W Configuration

A total of four new tests were done for this configuration (Section 6.1). The specimens had either a thin end-plate or a thick end-plate with either a deeper (60 in. deep) or shallower (36 in. deep) rafter. This was done so that the procedures could be validated for a range of end-plate depths. The four specimens behaved as expected.

For the two thin end-plate specimens, the calculated moment capacity for end-plate yielding was either 6% lower (deep beam) or 2 % higher (shallow beam) than actual yield moment. The calculated moment at bolt rupture with prying action, M_q, was approximately 14% lower than the maximum applied moment, M_u. As with the other connection configurations, the conservativeness of this prediction is related to overstrength in the bolts. Experimentally measured end-plate separation (0.22 in to 0.45 in.) was found to be consistent with thin end-plate behavior wherein end-plate yielding allows end-plate separation prior to bolt fracture. Also, end-plate yielding and some yield lines were observed on the specimens.

The thick end-plate Specimen 6B-4W/2W-0.875-1.00-36, exhibited minor end-plate yielding, but there was no observable distortion of the end-plate when viewed from side. The calculated moment capacity for bolt rupture without prying, M_{np}, was lower (by 13% to 17%) than the maximum applied moment, M_u, for both specimens due to overstrength in the bolts.

It was concluded that the proposed design equations were relatively accurate for the range of parameters tested.

7.5. 12B-MRE 1/3-4W/2W Configuration

A total of four new tests were done for this configuration (Section 6.2). The specimens were either a thin end-plate or a thick end-plate with either a deeper (60 in. deep) or shallower (36 in. deep) beam. This was done so that the procedures could be validated for a range of end-plate depths.

For thin end-plate specimens, the predicted end-plate yield moment capacity was conservative by 8% to 11% as compared to the yield moment observed from test data. The end-plate yielding and end-plate separation was small because the tests were stopped prior to bolt rupture. However, the calculated moment capacity at bolt rupture with prying, M_q, was between 11% and 14% lower (conservative) than the maximum applied moment, M_u.

Both the thick end-plate specimens behaved as expected. The moment capacity for bolt rupture without prying action, M_{np}, was lower than the peak moment, M_u, by at least 10% for both thick end-plate specimens. Similar to the other specimens, one of the reasons the moment capacities predicted were conservative for limit states related to bolt rupture was that the bolts had considerable overstrength (approximately 25% from bolt test reports).

It was concluded that the proposed design equations were relatively accurate for the range of parameters tested.

References

Adey, B.T., Grondin, G.Y., and Cheng, J.J.R. (1997) *Extended End Plate Moment Connections Under Cyclic Loading*, Structural Engineering Report No. 216, University of Alberta Department of Civil and Environmental Engineering.

Adey, B.T., Adey, B.T., Grondin, G.Y., and Cheng, J.J.R. (2000) "Cyclic Loading of End Plate Moment Connections", *Canadian Journal of Civil Engineering*, Vol. 27, pp. 683-701.

Borgsmiller, J. T., & Murray, T. M. (1995). *Simplified Method for the Design of Moment End-Plate Connections.* Blacksburg, VA: Department of Civil Engineering, Virginia Polytechnic Institute and State University.

Ghassemieh, M., Kukreti, A., and Murray, T.M. (1983) *Inelastic Finite Element Analysis of Stiffened End-Plate Moment Connections*, Report No. FSEL/AISC 83-02, School of Civil Engineering and Environmental Science, University of Oklahoma, Norman, OK.

Kennedy, N. A., Vinnakota, S., & Sherbourne, A. N. (1981). The Split-Tee Anlogy in Bolted Splices and Beam-Column Connections. *Proceedings of the International Conference on Joints in Structural Steelwork*, (pp. 2.138-2.157).

Kulak, G.L., Fisher, J.W., Struik, J.H.A., (2001) "Guide to Design Criteria for Bolted and Riveted Joints", *American Institute of Steel Construction*, Chicago, IL

Murray, T. M. (1988). Recent Developments for the Design of Moment End-Plate Connections. *Journal of Constructional Steel Research*, 133-162.

Murray, T. M., & Shoemaker, W. L. (2002). Flush and Extended Multiple-Row Moment End-Plate Connections. *AISC.*

Seek, M.W., and Murray, T.M., (2008) "Seismic Strength of Moment End-Plate Connections with Attached Concrete Slab", *Proceedings of the Connections in Steel Structures VI Workshop*, Chicago, Il. June 23-25.

Specification for Structural Joints Using High-Strength Bolts. (2009). *Research Council on Structural Connections (RCSC).*

Sumner, E. A. (2003). *Unified Design of Extended End-Plate Moment Connections Subject to Cyclic Loading.* Blacksburg, VA: Department of Civil Engineering, Viriginia Polytechnic Institute and State University.

Sumner, E. A., & Murray, T. M. (2001). *Experimental Investigation of Four Bolt Wide Extended End-Plate Moment Connections.* Blacksburg, VA: Department of Civil Engineering, Virginia Polytechnic Institute and State University.

Sumner, E. A., Mays, T. W., & Murray, T. M. (2000). *Cyclic Testing of Bolted Moment End-Plate Connections.* Blacksburg, VA: Virginia Polytechnic Institute and State University.

Appendix A Mill Test Report for Beam Material

6B-4W/2W-0.875-1.00-36
6B-4W/2W-0.875-1.00-60
12B- MRE 1/3 -4W/2W-0.75-1.00-36
12B- MRE 1/3 -4W/2W-0.75-1.00-60

NUCOR
PLATE MILL
P.O.Box 279
Winton, NC 27986
(252) 356-3700

Mill Test Report

NUCOR It's our Nature!

Issuing Date : 08/18/2012 B/L No. : 334335 Load No. : 336264 Our Order No. : 103114/2 Cust. Order No. : PPC516
Vehicle No: TTPX 804776
Specification : 1.0000" x 120.000" x 480.000"
ASTM A572 Grade 50-12/ASTM A709 Grade 50-11/AASHTO M270-50
Type 2

Sold To : METALS USA PLATES AND SHAPES NORTHEAST LP
2025 GREENTREE RD
PITTSBURGH,PA 15220

Ship To : METALS USA C/O HARTWELL WAREHOUSE
5 N WILSON AVE
BRISTOL,PA 19007

Marking :

Heat No	C	Mn	P	S	Si	Cu	Ni	Cr	Mo	Al(tot)	V	Nb	Ti	N	Ca	B	Sn	CEQ	PCM
2505623	0.20	1.20	0.023	0.004	0.18	0.13	0.05	0.10	0.01	0.036	0.043	0.002	0.002		0.0009	0.0002	0.007	0.44	0.28

	Tensile Test							Charpy Impacts											
Plate Serial No	Pieces	Tons	Dir.	(psi) Yield	(psi) Tensile	Elongation % in 2"	Elongation % in 8"	Dir.	(ft-lbs) 1	(%) shear	(ft-lbs) 2	(%) shear	(ft-lbs) 3	(%) shear	(ft-lbs) Avg.	(%) shear	Size	Temp (°F)	Min Ave.
2505623-05	2	16.33	T	56,800	83,200		21.1	H-L	34.8		46.6		20.6		34.0		10mm	-22	15
			T	51,400	81,200		22.5	H-L	67.1		63.0		41.8		57.3		10mm	-22	15

NFCM, T1 and T2, 15ft-lbs @ +40 F (20J @ +4 C), H frequency. Temperature reduced by 15 F for each 10 ksi over 65 ksi;

Manufactured to fully killed fine grain practice by Electric Arc Furnace. Welding or weld repair was not performed on this material. Mercury has not been used in the direct manufacturing of this material. Produced as continuous cast discrete plate as-rolled, unless otherwise noted in Specification.

Yield by 0.5EUL method unless otherwise specified. Ceq = C+(Mn/6)+((Cr+Mo+V)/5)+((Cu+Ni)/15)

Pcm = C+(Si/30)+(Mn/20)+(Cu/20)+(Ni/60)+(Cr/20)+(Mo/15)+(V/10)+5B

Melted and manufactured in the USA. ISO 9001:2008 certified (#008063) by SRI Quality System Registrar (#0985-09). PED 97/23/EC 7/2 Annex 1, Para. 4.3 Compliant. DIN 50049 3.1.B/EN 10204 3.1B(2004), DIN EN 10204 3.1(2005) compliant. For ABS grades only, Quality Assurance certificate 14-MMPOA-723

We hereby certify that the contents of this report are accurate and correct. All test results and operations performed by the material manufacturer are in compliance with the applicable specifications, including customer specifications.

T. A. Depretis

T. A. Depretis, Metallurgist

08/20/2012 8:54:04 AM

14" x 3/4" SPLICE PLATES

6B-4W/2W-1.125-0.75-36
6B-4W/2W-1.125-0.75-60
12B- MRE 1/3 -4W/2W-1.00-0.75-36
12B- MRE 1/3 -4W/2W-1.00-0.75-60

NUCOR
PLATE MILL
P.O.Box 279
Winton, NC 27986
(252) 356-3700

Mill Test Report

NUCOR It's our Nature!

Issuing Date : 06/30/2011 B/L No. : 297636 Load No. : 299124 Our Order No. : 91906/3 Cust. Order No. : VA-35442

Vehicle No: 7312

Specification : 0.7500" x 96.000" x 480.000"
ASTM A572 Grade 50/345-07/A709 Grade 50-10/ AASHTO M270 50 97
Type 2

Sold To : INFRAMETALS CO PETERSBURG
580 MIDDLETON BLVD STE D100
LANGHORNE,PA 19047

Ship To : INFRA - METALS
1900 BESSEMER RD
PH 8049575900
PETERSBURG,VA 23805

Marking :

Heat No	C	Mn	P	S	Si	Cu	Ni	Cr	Mo	Al(tot)	V	Nb	Ti	N	Ca	B	Sn	CEQ	PCM
1504480	0.17	1.17	0.010	0.002	0.17	0.21	0.08	0.10	0.02	0.034	0.043	0.001	0.002		0.0000	0.0002	0.008	0.41	0.26

Tensile Test

Plate Serial No	Pieces	Tons	Dir.	(psi) Yield	(psi) Tensile	Elongation % in 2"	Elongation % in 8"
1504480-07	2	9.80	T	52,700	80,900		19.2
			T	63,100	86,700		20.0

Charpy Impacts

Dir.	1	(%) shear	2	(%) shear	3	(%) shear	Ave.	(%) shear	Size	Temp	Min Ave.

Manufactured to fully killed fine grain practice by Electric Arc Furnace. Welding or weld repair was not performed on this material. Mercury has not been used in the direct manufacturing of this material. Produced as continuous cast discrete plate as-rolled, unless otherwise noted in Specification.

Yield by 0.5EUL method unless otherwise specified. Ceq = C+(Mn/6)+((Cr+Mo+V)/5)+((Cu+Ni)/15)

Pcm = C+(Si/30)+(Mn/20)+(Cu/20)+(Ni/60)+(Cr/20)+(Mo/15)+(V/10)+5B

Melted and manufactured in the USA. ISO 9001:2008 certified (#008063) by SRI Quality System Registrar (#0985-09). PED 97/23/EC 7/2 Annex 1, Para. 4.3 Compliant. DIN 50049 3.1.B/EN 10204 3.1B(2004), DIN EN 10204 3.1(2005) compliant. For ABS grades only, Quality Assurance certificate 14-MMPQA-723

We hereby certify that the contents of this report are accurate and correct. All test results and operations performed by the material manufacturer are in compliance with the applicable specifications, including customer specifications.

T. A. Depretis, Metallurgist

06/30/2011 1:27:19 PM

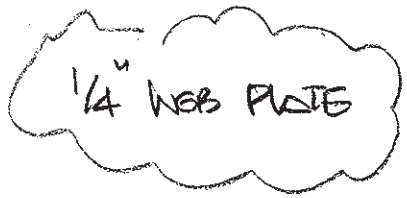

6B-4W/2W-1.125-0.75-36
6B-4W/2W-1.125-0.75-60
6B-4W/2W-0.875-1.00-36
6B-4W/2W-0.875-1.00-60

Report - Of - Information

FERALLOY CORPORATION

OWNER:

SHIP TO:
AMERICAN BUILDINGS CO
GOLDEN EAGLE DRIVE
LA CROSSE , VA 23950

DATE: 6/12/14

BILL OF LADING: 607 - 131481 - 10
HEAT/MILL COIL: 2404585 2404585-3
SKID NO: 256763
TAG NUMBER: 97508 - 01
PROCESSED AS: ASTM A529 HR C-Mn Steel Plate, Gr 55
REFERENCING: ASTM A-529 High Strength C-Mn Structural Steel

PART NO: 1/4X60X241 - *
SIZE: .2400 X 60.000 X 241.000
PRODUCT: HR PL55 A529
CUSTOMER PO NUMBER: 1-20198 051414

Element	C	Mn	P	S	Si	Cu	Ni	Cr	Mo	Sn
Weight %	.2600	1.1300	.0110	.0020	.2100	.0700	.0300	.0300	.0100	.0050
Element	Al	B	Nb	V	Ti	N	CA	H	O	
Weight %	.0270	.0000	.0010	.0060	.0010	.0060	.0020			

Location	Yield (PSI)	Tensile (PSI)	Elongation(% in 2")
HEAD	67600	91100	25.0
CENTER	69500	93000	25.0

Bend Test	n Value	Hardness	r Value	
	.000	88RB	.00	

NOTICE: FERALLOY MAKES NO REPRESENTATION OR WARRANTY AS TO THE INFORMATION CONTAINED IN THIS REPORT. The values published on this 'report-of-information' are transcribed from information provided by the owner and the owner's suppliers including mills, testing laboratories, etc. This is NOT a certificate of specification, inspection, or grade.

This material processed at & shipped from:
FERALLOY CHARLESTON
CHARLESTON DIVISION
1020 NORTH STEEL CIRCLE
HUGER , SC 29450

12B- MRE 1/3 -4W/2W-0.75-1.00-36
12B- MRE 1/3 -4W/2W-0.75-1.00-60
12B- MRE 1/3 -4W/2W-1.00-0.75-36
12B- MRE 1/3 -4W/2W-1.00-0.75-60

Report - Of - Information

FERALLOY CORPORATION

OWNER:

SHIP TO:
AMERICAN BUILDINGS CO
GOLDEN EAGLE DRIVE
LA CROSSE , VA 23950

DATE: 6/16/14

BILL OF LADING: 607 - 131547 - 10
HEAT/MILL COIL: 2404762 2404762-3
SKID NO: 257429
TAG NUMBER: 97552 - 01
PROCESSED AS: ASTM A529 HR C-Mn Steel Plate, Gr 55
REFERENCING: ASTM A-572 HSLA Cb-V Structural Steel

PART NO: 3/8X60X241 - *
SIZE: .3650 X 60.000 X 241.000
PRODUCT: HR PL55 A572
CUSTOMER PO NUMBER: 1-20200 051514

Element	C	Mn	P	S	Si	Cu	Ni	Cr	Mo	Sn
Weight %	.0500	1.4100	.0130	.0050	.3300	.0900	.0300	.0300	.0100	.0070
Element	Al	B	Nb	V	Ti	N	CA	H	O	
Weight %	.0380	.0000	.0400	.0060	.0020	.0080	.0020			

Location	Yield (PSI)	Tensile (PSI)	Elongation(% in 2")
HEAD	69900	82000	37.0
CENTER	69800	81600	39.0

Bend Test	n Value	Hardness	r Value	
	.000		.00	

NOTICE: FERALLOY MAKES NO REPRESENTATION OR WARRANTY AS TO THE INFORMATION CONTAINED IN THIS REPORT. The values published on this 'report-of-information' are transcribed from information provided by the owner and the owner's suppliers including mills, testing laboratories, etc. This in NOT a certificate of specification, inspection, or grade.

This material processed at & shipped from:
FERALLOY CHARLESTON
CHARLESTON DIVISION
1020 NORTH STEEL CIRCLE
HUGER , SC 29450

NUCOR
NUCOR CORPORATION
NUCOR STEEL TEXAS

Mill Certification
4/15/2014

MTR #: 0000020634
8812 Hwy 79 W
Jewett, TX 75846
(903) 626-4461
Fax: (903) 626-6290

Sold To: AMERICAN BUILDINGS CO
PO BOX 800
EUFAULA, AL 36027-0000
(334) 688-2276
Fax: (334) 687-9733

Ship To: AMERICAN BUILDINGS CO
501 GOLDEN EAGLE DR
LA CROSSE, VA 23950-0000
(000) 000-0000

Customer P.O.	1-20145	Sales Order	200741.3
Product Group	Merchant Bar Quality	Part Number	53750C004805300
Grade	ASTM A529/A529M-05 GR 55	Lot #	JW1410158251
Size	3/4x12" Flat	Heat #	JW14101582
Product	3/4x12" Flat 40' A529 Gr55	B.L. Number	J1-668160
Description	A529 Gr55	Load Number	J1-272301
Customer Spec		Customer Part #	

I hereby certify that the material described herein has been manufactured in accordance with the specifications and standards listed above and that it satisfies those requirements.

Roll Date: 2/22/2014 **Melt Date: 2/20/2014** **Qty Shipped LBS: 19,600** **Qty Shipped Pcs: 16**

C	Mn	P	S	Si	Cu	Ni	Cr	Mo	V	Cb	CEA529
0.14%	1.12%	0.009%	0.024%	0.24%	0.25%	0.16%	0.11%	0.050%	0.0830%	0.001%	0.44%
CBV	MN/C										
0.080%	08.00%										

CEA529: A529 CARBON EQUIVALENT
CBV: CB+V
MN/C: MN / C

Yield 1: 61,300psi (423MPa) Tensile 1: 78,900psi (544MPa) Elongation: 19% in 8"(% in 203.3mm)
Yield 2: 61,600psi (425MPa) Tensile 2: 80,900psi (558MPa) Elongation 18% in 8"(% in 203.3mm)

Specification Comments:

Comments: E-mail: websales@nstexas.com

ALL MANUFACTURING PROCESSES OF THE STEEL MATERIALS IN THIS PRODUCT, INCLUDING MELTING, HAVE OCCURRED WITHIN THE UNITED STATES. ALL PRODUCTS PRODUCED ARE WELD FREE. MERCURY, IN ANY FORM, HAS NOT BEEN USED IN THE PRODUCTION OR TESTING OF THIS MATERIAL.

12" x 3/4" FLANGES

6B-4W/2W-1.125-0.75-36
6B-4W/2W-1.125-0.75-60
6B-4W/2W-0.875-1.00-36
6B-4W/2W-0.875-1.00-60
12B- MRE 1/3 -4W/2W-0.75-1.00-36
12B- MRE 1/3 -4W/2W-0.75-1.00-60
12B- MRE 1/3 -4W/2W-1.00-0.75-36
12B- MRE 1/3 -4W/2W-1.00-0.75-60

Kim Pritchard
Division Metallurgist

NUCOR

NUCOR CORPORATION
NUCOR STEEL SOUTH CAROLINA

Mill Certification

1/9/2014

MTR #: 0000001200
300 Steel Mill Road
DARLINGTON, SC 29540
(843) 393-5641
Fax: (843) 395-8701

Sold To: AMERICAN BUILDINGS CO
PO BOX 800
EUFAULA, AL 36027-0000
(888) 307-4338
Fax: (334) 688-2275

Ship To: AMERICAN BUILDINGS CO
501 GOLDEN EAGLE DR
LA CROSSE, VA 23950-0000
(434) 757-2220
Fax: (334) 688-2275

Customer P.O.	1-20122	Sales Order	195339.2
Product Group	Merchant Bar Quality	Part Number	535005004805300
Grade	ASTM A529/A529M-05 GR 55	Lot #	DL1310508901
Size	1/2x5" Flat	Heat #	DL13105089
Product	1/2x5" Flat 40' A529 Gr55	B.L. Number	C1-622195
Description	A529 Gr55	Load Number	C1-302384
Customer Spec		Customer Part #	

I hereby certify that the material described herein has been manufactured in accordance with the specifications and standards listed above and that it satisfies those requirements.

Roll Date: 9/7/2013 Melt Date: 8/25/2013 Qty Shipped LBS: 8,847 Qty Shipped Pcs: 26

C	Mn	P	S	Si	Cu	Ni	Cr	Mo	V	Cb
0.24%	1.22%	0.009%	0.035%	0.14%	0.37%	0.10%	0.13%	0.020%	0.0130%	0.003%

Yield 1: 57,000psi (393MPa) Tensile 1: 85,000psi (586MPa) Elongation: 26% in 8"(% in 203.3mm)
Yield 2: 58,000psi (400MPa) Tensile 2: 85,000psi (586MPa) Elongation 26% in 8"(% in 203.3mm)

Specification Comments:

1. WELDING OR WELD REPAIR WAS NOT PERFORMED ON THIS MATERIAL
2. MELTED AND MANUFACTURED IN THE USA
3. MERCURY, RADIUM, OR ALPHA SOURCE MATERIALS IN ANY FORM HAVE NOT BEEN USED IN THE PRODUCTION OF THIS MATERIAL

5" x 1/2" STIFFENERS

6B-4W/2W-1.125-0.75-36
6B-4W/2W-1.125-0.75-60
6B-4W/2W-0.875-1.00-36
6B-4W/2W-0.875-1.00-60
12B- MRE 1/3 -4W/2W-0.75-1.00-36
12B- MRE 1/3 -4W/2W-0.75-1.00-60
12B- MRE 1/3 -4W/2W-1.00-0.75-36
12B- MRE 1/3 -4W/2W-1.00-0.75-60

James H. Blew
Division Metallurgist

CERTIFIED MATERIAL TEST REPORT

GERDAU

US-ML-CARTERSVILLE
384 OLD GRASSDALE ROAD NE
CARTERSVILLE, GA 30121
USA

CUSTOMER SHIP TO	CUSTOMER BILL TO
BLUESCOPE BUILDINGS NORTH AMER 1274 CHURCH AVE RAINSVILLE,AL 35986-6230 USA	BLUESCOPE BUILDINGS N AMERICA KANSAS CITY,MO 64141-6917 USA

GRADE	SHAPE / SIZE	LENGTH	WEIGHT	HEAT / BATCH
A529-55M	Flat / 1 X 8	40'00"	8,704 LB	55036396/04

SALES ORDER	CUSTOMER MATERIAL Nº
1477282/000040	092040

SPECIFICATION / DATE or REVISION
1-ASTM A529 GR55-05
2-BUTLER SPEC 10004.20 GR 55

CUSTOMER PURCHASE ORDER NUMBER	BILL OF LADING	DATE
252990	1323-0000037378	11/03/2014

CHEMICAL COMPOSITION

C %	Mn %	P %	S %	Si %	Cu %	Ni %	Cr %	Mo %	V %	Nb %	N %	Pb %
0.18	0.95	0.011	0.027	0.19	0.31	0.09	0.09	0.077	0.030	0.000	0.0110	0.0010

CHEMICAL COMPOSITION

Sn %
0.011

MECHANICAL PROPERTIES

Elong. %	G/L Inch	UTS PSI	UTS MPa	YS 0.2% PSI	YS MPa
18.60	8.000	83200	574	61900	427
18.10	8.000	85000	586	60300	416

COMMENTS / NOTES

MB
11/7/14

The above figures are certified chemical and physical test records as contained in the permanent records of company. We certify that these data are correct and in compliance with specified requirements. This material, including the billets, was melted and manufactured in the USA. CMTR complies with EN 10204 3.1.

BHASKAR YALAMANCHILI
QUALITY DIRECTOR

YAN WANG
QUALITY ASSURANCE MGR.

CERTIFIED MATERIAL TEST REPORT

GERDAU

US-ML-CARTERSVILLE
384 OLD GRASSDALE ROAD NE
CARTERSVILLE, GA 30121
USA

CUSTOMER SHIP TO	CUSTOMER BILL TO
BLUESCOPE BUILDINGS NORTH AMER 1274 CHURCH AVE RAINSVILLE,AL 35986-6230 USA	BLUESCOPE BUILDINGS N AMERICA KANSAS CITY,MO 64141-6917 USA

GRADE	SHAPE / SIZE	LENGTH	WEIGHT	HEAT / BATCH
A529-55M	Flat / 1 X 8	40'00"	8,704 LB	**55036396**/04

SALES ORDER	CUSTOMER MATERIAL Nº
1477282/000040	092040

SPECIFICATION / DATE or REVISION
1-ASTM A529 GR55-05
2-BUTLER SPEC 10004.20 GR 55

CUSTOMER PURCHASE ORDER NUMBER	BILL OF LADING	DATE
252990	1323-0000037378	11/03/2014

CHEMICAL COMPOSITION

C %	Mn %	P %	S %	Si %	Cu %	Ni %	Cr %	Mo %	V %	Nb %	N %	Pb %
0.18	0.95	0.011	0.027	0.19	0.31	0.09	0.09	0.077	0.030	0.000	0.0110	0.0010

CHEMICAL COMPOSITION

Sn %
0.011

MECHANICAL PROPERTIES

Elong. %	G/L Inch	UTS PSI	UTS MPa	YS 0.2% PSI	YS MPa
18.60	8.000	83200	574	61900	427
18.10	8.000	85000	586	60300	416

COMMENTS / NOTES

KB
11/7/14

The above figures are certified chemical and physical test records as contained in the permanent records of company. We certify that these data are correct and in compliance with specified requirements. This material, including the billets, was melted and manufactured in the USA. CMTR complies with EN 10204 3.1.

BHASKAR YALAMANCHILI
QUALITY DIRECTOR

YAN WANG
QUALITY ASSURANCE MGR.

CERTIFIED MATERIAL TEST REPORT

GERDAU

US-ML-CARTERSVILLE
384 OLD GRASSDALE ROAD NE
CARTERSVILLE, GA 30121
USA

CUSTOMER SHIP TO	CUSTOMER BILL TO
BLUESCOPE BUILDINGS NORTH AMER 1274 CHURCH AVE RAINSVILLE,AL 35986-6230 USA	BLUESCOPE BUILDINGS N AMERICA KANSAS CITY,MO 64141-6917 USA

GRADE	SHAPE / SIZE
A529-55M	Flat / 1 X 10

LENGTH	WEIGHT	HEAT / BATCH
40'00"	8,160 LB	**55033984**/04

SALES ORDER	CUSTOMER MATERIAL Nº
1477282/000030	092042

SPECIFICATION / DATE or REVISION
1-ASTM A529 GR55-05
2-BUTLER SPEC 10004.20 GR 55

CUSTOMER PURCHASE ORDER NUMBER	BILL OF LADING	DATE
252990	1323-0000037378	11/03/2014

CHEMICAL COMPOSITION

C %	Mn %	P %	S %	Si %	Cu %	Ni %	Cr %	Mo %	V %	Nb %	N %	Pb %
0.20	0.97	0.013	0.031	0.17	0.30	0.09	0.07	0.025	0.030	0.002	0.0110	0.0060

CHEMICAL COMPOSITION

Sn %
0.017

MECHANICAL PROPERTIES

Elong. %	G/L Inch	UTS PSI	UTS MPa	YS 0.2% PSI	YS MPa
20.00	8.000	84500	583	62700	432
18.20	8.000	84700	584	61900	427

COMMENTS / NOTES

MB
11/7/14

The above figures are certified chemical and physical test records as contained in the permanent records of company. We certify that these data are correct and in compliance with specified requirements. This material, including the billets, was melted and manufactured in the USA. CMTR complies with EN 10204 3.1.

Bhaskar — BHASKAR YALAMANCHILI, QUALITY DIRECTOR

YAN WANG, QUALITY ASSURANCE MGR.

CERTIFIED MATERIAL TEST REPORT

GERDAU

US-ML-CARTERSVILLE
384 OLD GRASSDALE ROAD NE
CARTERSVILLE, GA 30121
USA

CUSTOMER SHIP TO	CUSTOMER BILL TO
BLUESCOPE BUILDINGS NORTH AMER 1274 CHURCH AVE RAINSVILLE,AL 35986-6230 USA	BLUESCOPE BUILDINGS N AMERICA KANSAS CITY,MO 64141-6917 USA

GRADE	SHAPE / SIZE
A529-55M	Flat / 1 X 10

LENGTH	WEIGHT	HEAT / BATCH
40'00"	16,320 LB	**55035144**/04

SALES ORDER	CUSTOMER MATERIAL Nº
1477282/000030	092042

SPECIFICATION / DATE or REVISION
1-ASTM A529 GR55-05
2-BUTLER SPEC 10004.20 GR 55

CUSTOMER PURCHASE ORDER NUMBER	BILL OF LADING	DATE
252990	1323-0000037378	11/03/2014

CHEMICAL COMPOSITION

C %	Mn %	P %	S %	Si %	Cu %	Ni %	Cr %	Mo %	V %	Nb %	N %	Pb %
0.21	1.00	0.013	0.031	0.19	0.40	0.09	0.07	0.034	0.033	0.002	0.0110	0.0030

CHEMICAL COMPOSITION

Sn %
0.013

MECHANICAL PROPERTIES

Elong. %	G/L Inch	UTS PSI	UTS MPa	YS 0.2% PSI	YS MPa
20.30	8.000	85100	587	61800	426
20.40	8.000	84800	585	61300	423

COMMENTS / NOTES

MB
11/7/14

The above figures are certified chemical and physical test records as contained in the permanent records of company. We certify that these data are correct and in compliance with specified requirements. This material, including the billets, was melted and manufactured in the USA. CMTR complies with EN 10204 3.1.

BHASKAR YALAMANCHILI
QUALITY DIRECTOR

YAN WANG
QUALITY ASSURANCE MGR.

OLYMPIC STEEL
5080 RICHMOND ROAD
BEDFORD HEIGHTS, OH 44146 USA
PHONE: 216-292-3800

METALLURGICAL TEST REPORT

>>>>>> CERTIFICATE OF ANALYSIS AND TESTS <<<<<<

Sold To: OLYMPIC STEEL - SOUTHERN
587 BARROW PARK DRIVE
WINDER, GA 30680

Ship To: BLUESCOPE BUILDINGS
1274 CHURCHILL AVE.
RAINSVILLE, AL 35986

Sales Order:	316975 - 01	B/L No: 519304	Release:	3	Date: 25-Aug-2014
Reference:	KATZ, NEIL (11473)	2nd B/L:	Cus Ord #:	282960	
			Cus Name:	OLYMPIC STEEL - SOUTHERN	

Description of Material and Specification

DOMESTIC PO 243135/ASTM A572 GR. 55
.5" x 60" x 241"

93393 REV O

TAG#: 23166906,23166907,23166909,23166910,23166911

HEAT#: 178933/NORTH STAR BLUESCOPE STEEL LLC

MC # 22923073

Chem Elem Symbol / Elem Content Value:

<C : .05> <MN : .81> <P : .013> <S : .004> <SI : .02> <AL : .02> <V : .057> <CU : .11> <NI : .04> <CR : .06>
<MO : .01> <N : .01> <TI : .001> <B : 0> <CA : .002> <SN : .01> <NB : 0>

Melted and manufactured in the USA

YIELD STRENGTH	MIN:	62790 PSI	MAX	62790 PSI
TENSILE STRENGTH	MIN:	72920 PSI	MAX	72920 PSI
ELONGATION 2"	MIN:	31.6 %	MAX	31.6 %

We hereby certify the above is correct as contained in the records of the corporation

8/29/14

Branch Certification Manager

USER: REPORTS@SEMSPRD
REPORT: ST_MSR_OSI

25-Aug-2014 12:37
Page 1 of 1

Certified Test Report

NORTH STAR BLUESCOPE STEEL LLC
6767 County Road 9
Delta, Ohio 43515
Telephone: (888) 822-2112

Customer:
Olympic Steel Inc.
5080 Richmond Road
Cleveland, OH 44146

Customer P.O.: 644796

Cust. Ref/Part # A1018 / HSLAS55

Order Number	306169	**Ordered Width (mm/in)**	1524.000 / 60.000
Line Item Number	1	**Ordered Gauge (mm/in)**	12.446 / 0.490
Heat Number	178933	**Material Description**	ASTM A1018-55-1-10, For Conversion to ASTM A572-55-12
Coil Number	1412240	**Production Date/Time**	May 6 2014 9:51PM

Heat Chemical Analysis (wt%)

Type	C	Mn	P	S	Si	Al	Cu	Cr	Ni	Mo	Sn	N	B	V	Nb	Ti	Ca
Heat	0.05	0.81	0.013	0.004	0.02	0.02	0.11	0.06	0.04	0.01	0.01	0.010	0.0000	0.057	0.000	0.001	0.002

Mechanical Test Report

All mechanical tests are performed on a sample from the tail of a coil.

Yield Strength	Tensile Strength	% Elongation in 2 inches
62,790 psi	72,920 psi	31.6%

This material has been produced to conform to EN 10204:2005. This material has been produced and tested in accordance with each of the following applicable standards: ASTM E 1806-96, ASTM E 415-99a, ASTM A 751-01, ASTM A 370-03a, JIS Z2201:1998, JIS Z 2241:1998. This report certifies that the above test results are representative of those contained in the records of North Star BlueScope Steel LLC for the material identified in this test report and is intended to comply with the requirements of the material description. North Star BlueScope Steel LLC is not responsible for the inability of this material to meet specific applications. Any modifications to this certification as provided negates the validity of this test report. All reproductions must have the written approval of North Star BlueScope Steel. This product was manufactured, melted, cast, and hot-rolled (min. 3:1 reduction ratio), entirely within the U.S.A at North Star BlueScope Steel LLC, Delta, Ohio. This material was not exposed to Mercury or any alloy which is liquid at ambient temperature during processing or while in North Star BlueScope Steel LLC possession. Test equipment calibration certificates are available upon request. NIST traceability is established through test equipment calibration certificates which are available upon request. Uncertainty calculations are calculated in accordance with NIST standards and are maintained at a 4:1 ratio in accordance with NIST standards. Uncertainty data is available upon request.

Tim Mitchell **Manager Quality Assurance and Technology**

Date Issued: May 15, 2014 16:00:10
Revision#: 01

8/29/14

OLYMPIC STEEL
5080 RICHMOND ROAD
BEDFORD HEIGHTS, OH 44146 USA
PHONE: 216-292-3800

METALLURGICAL TEST REPORT

>>>>>> CERTIFICATE OF ANALYSIS AND TESTS <<<<<<

Sold To: OLYMPIC STEEL - SOUTHERN
587 BARROW PARK DRIVE
WINDER, GA 30680

Ship To: BLUESCOPE BUILDINGS
1274 CHURCHILL AVE.
RAINSVILLE, AL 35986

Sales Order:	316975 - 01	B/L No: 519304	Release:	3	Date: 25-Aug-2014
Reference:	KATZ, NEIL (11473)	2nd B/L:	Cus Ord #:	282960	
			Cus Name:	OLYMPIC STEEL - SOUTHERN	

Description of Material and Specification

DOMESTIC PO 243135/ASTM A572 GR. 55
.5" x 60" x 241"

93393 REV O

TAG#: 23166906,23166907,23166909,23166910,23166911

HEAT#: 178933/NORTH STAR BLUESCOPE STEEL LLC

MC # 22923073

Chem Elem Symbol / Elem Content Value:

<C : .05> <MN : .81> <P : .013> <S : .004> <SI : .02> <AL : .02> <V : .057> <CU : .11> <NI : .04> <CR : .06> <MO : .01> <N : .01> <TI : .001> <B : 0> <CA : .002> <SN : .01> <NB : 0>

Melted and manufactured in the USA

YIELD STRENGTH	MIN:	62790 PSI	MAX	64000 PSI
TENSILE STRENGTH	MIN:	71700 PSI	MAX	72920 PSI
ELONGATION 2"	MIN:	25.0 %	MAX	31.6 %
CARBON EQUIV	MIN:	.24	MAX	.24

We hereby certify the above is correct as contained in the records of the corporation

8/29/14

Branch Certification Manager

USER: REPORTS@SEMSPRD
REPORT: ST_MSR_OSI

26-Aug-2014 3:42 PM
Page 1 of 1

Appendix B Mill Test Report for Bolts

NUCOR
FASTENER DIVISION

LOT NO.
335852A

12B- MRE 1/3 -4W/2W-0.75-1.00-36
12B- MRE 1/3 -4W/2W-0.75-1.00-60

Post Office Box 6100
Saint Joe, Indiana 46785
Telephone 260/337-1600

CUSTOMER NO/NAME
9000 BIRMINGHAM-CONS/SHIPPING

NUCOR ORDER # 857190
CUST PART # 75C300A32P/NND
CUSTOMER P.O. # 6044932

TEST REPORT SERIAL# FB420998
TEST REPORT ISSUE DATE 12/11/13
DATE SHIPPED 1/23/14
NAME OF LAB SAMPLER: RYAN UNGER, LAB TECHNICIAN

A325 n

**********CERTIFIED MATERIAL TEST REPORT**********

NUCOR PART NO	QUANTITY	LOT NO.	DESCRIPTION
160600	3600	335852A	3/4-10 X 3 A325 HVY HX

MANUFACTURE DATE 11/22/13 STRUC SCREW PLAIN

--CHEMISTRY MATERIAL GRADE -1039ML1

MATERIAL NUMBER	HEAT NUMBER	**CHEMISTRY COMPOSITION (WT% HEAT ANALYSIS) BY MATERIAL SUPPLIER C	MN	P	S	SI	NUCOR STEEL - NEBRASKA
RM028677	NF13204672	.41	.89	.009	.009	.24	

--MECHANICAL PROPERTIES IN ACCORDANCE WITH ASTM A325-10

SURFACE HARDNESS (R30N)	CORE HARDNESS (RC)	PROOF LOAD 28400 LBS	TENSILE STRENGTH 10 DEG-WEDGE (LBS)	STRESS (PSI)
N/A	31.2	PASS	49580	148443
N/A	31.0	PASS	49790	149072
N/A	29.9	PASS	50190	150269
N/A	30.0			
N/A	30.9			
AVERAGE VALUES FROM TESTS		PRODUCTION LOT SIZE 38100 PCS		
	30.6		49853	149261

--VISUAL INSPECTION IN ACCORDANCE WITH ASTM A325-10 5 PCS. SAMPLED LOT PASSED
HEAT TREATMENT - AUSTENITIZED, OIL QUENCHED & TEMPERED (MIN 800 DEG F)

--DIMENSIONS PER ASME B18.2.6-2010

CHARACTERISTIC	#SAMPLES TESTED	MINIMUM	MAXIMUM
Width Across Corners	8	1.3980	1.4070
Grip Length	8	1.4900	1.5500
Head Height	8	0.4740	0.4780
Threads	8	PASS	PASS

ALL TESTS ARE IN ACCORDANCE WITH THE LATEST REVISIONS OF THE METHODS PRESCRIBED IN THE APPLICABLE SAE AND ASTM SPECIFICATIONS. THE SAMPLES TESTED CONFORM TO THE SPECIFICATIONS AS DESCRIBED/LISTED ABOVE AND WERE MANUFACTURED FREE OF MERCURY CONTAMINATION. NO HEATS TO WHICH BISMUTH, SELENIUM, TELLURIUM, OR LEAD WAS INTENTIONALLY ADDED HAVE BEEN USED TO PRODUCE THE BOLTS.
THE STEEL WAS MELTED AND MANUFACTURED IN THE U.S.A. AND THE PRODUCT WAS MANUFACTURED AND TESTED IN THE U.S.A. PRODUCT COMPLIES WITH DFARS 252.225-7014. WE CERTIFY THAT THIS DATA IS A TRUE REPRESENTATION OF INFORMATION PROVIDED BY THE MATERIAL SUPPLIER AND OUR TESTING LABORATORY. THIS CERTIFIED MATERIAL TEST REPORT RELATES ONLY TO THE ITEMS LISTED ON THIS DOCUMENT AND MAY NOT BE REPRODUCED EXCEPT IN FULL.

A2LA ACCREDITED

MECHANICAL FASTENER
CERTIFICATE NO. A2LA 0139.01
EXPIRATION DATE 12/31/13

NUCOR FASTENER
A DIVISION OF NUCOR CORPORATION

John W. Ferguson

JOHN W. FERGUSON
QUALITY ASSURANCE SUPERVISOR

NUCOR
FASTENER DIVISION

LOT NO. 320001A
6B-4W/2W-0.875-1.00-36
6B-4W/2W-0.875-1.00-60

Post Office Box 6100
Saint Joe, Indiana 46785
Telephone 260/337-1600

CUSTOMER NO/NAME
9000 BIRMINGHAM-CONS/SHIPPING

NUCOR ORDER # 848284
CUST PART # 87C325A32P/NND
CUSTOMER P.O. # 6039103

TEST REPORT SERIAL# FB402003
TEST REPORT ISSUE DATE 2/07/13
DATE SHIPPED 11/13/13
NAME OF LAB SAMPLER: LISA EDGAR, LAB TECHNICIAN

**********CERTIFIED MATERIAL TEST REPORT**********

NUCOR PART NO	QUANTITY	LOT NO.	DESCRIPTION
161450	2475	320001A	7/8-9 X 3 1/4 A325 HVY HX STRUC SCREW PLAIN

MANUFACTURE DATE 1/29/13

--CHEMISTRY MATERIAL GRADE -1037ML

MATERIAL NUMBER	HEAT NUMBER	**CHEMISTRY COMPOSITION (WT% HEAT ANALYSIS) BY MATERIAL SUPPLIER C	MN	P	S	SI	CR	
RM027879	NF12103881	.37	.77	.007	.021	.24	.35	NUCOR STEEL - NEBRASKA
	MIN	.30	.60			.15		
	MAX	.52		.040	.050	.30		

--MECHANICAL PROPERTIES IN ACCORDANCE WITH ASTM A325-10

SURFACE HARDNESS (R30N)	CORE HARDNESS (RC)	PROOF LOAD 39300 LBS	TENSILE STRENGTH 10 DEG-WEDGE (LBS)	STRESS (PSI)
N/A	31.0	PASS	69770	151017
N/A	29.5	PASS	70150	151840
N/A	29.9	PASS	68180	147576
N/A	29.7			
AVERAGE VALUES FROM TESTS	30.0	PRODUCTION LOT SIZE	69367	12500 PCS 150144

--VISUAL INSPECTION IN ACCORDANCE WITH ASTM A325-10 4 PCS. SAMPLED LOT PASSED
HEAT TREATMENT - AUSTENITIZED, OIL QUENCHED & TEMPERED (MIN 800 DEG F)

--DIMENSIONS PER ASME B18.2.6-2006

CHARACTERISTIC	#SAMPLES TESTED	MINIMUM	MAXIMUM
Width Across Corners	8	1.6220	1.6280
Grip Length	8	1.6700	1.6900
Head Height	8	0.5470	0.5600
Threads	8	PASS	PASS

ALL TESTS ARE IN ACCORDANCE WITH THE LATEST REVISIONS OF THE METHODS PRESCRIBED IN THE APPLICABLE SAE AND ASTM SPECIFICATIONS. THE SAMPLES TESTED CONFORM TO THE SPECIFICATIONS AS DESCRIBED/LISTED ABOVE AND WERE MANUFACTURED FREE OF MERCURY CONTAMINATION. NO HEATS TO WHICH BISMUTH, SELENIUM, TELLURIUM, OR LEAD WAS INTENTIONALLY ADDED HAVE BEEN USED TO PRODUCE THE BOLTS.
THE STEEL WAS MELTED AND MANUFACTURED IN THE U.S.A. AND THE PRODUCT WAS MANUFACTURED AND TESTED IN THE U.S.A. PRODUCT COMPLIES WITH DFARS 252.225-7014. WE CERTIFY THAT THIS DATA IS A TRUE REPRESENTATION OF INFORMATION PROVIDED BY THE MATERIAL SUPPLIER AND OUR TESTING LABORATORY. THIS CERTIFIED MATERIAL TEST REPORT RELATES ONLY TO THE ITEMS LISTED ON THIS DOCUMENT AND MAY NOT BE REPRODUCED EXCEPT IN FULL.

ACCREDITED

MECHANICAL FASTENER
CERTIFICATE NO. A2LA 0139.01
EXPIRATION DATE 12/31/13

NUCOR FASTENER
A DIVISION OF NUCOR CORPORATION

John W. Ferguson

JOHN W. FERGUSON
QUALITY ASSURANCE SUPERVISOR

12B- MRE 1/3 -4W/2W-1.00-0.75-36
12B- MRE 1/3 -4W/2W-1.00-0.75-60

FONTANA FASTENERS

TEST REPORT

Operations Center
3281 West County Road 0 NS
Frankfort, IN 46041-6966
T. 765.654.0477
F. 765.654.0857

Ship Date	
Certification	374619*3*4
Report Date	10-01-13

Cust PO	6032446
Lot No	718615
Quantity	2025
Mfg Date	09-04-13

Birmingham Fastener, Inc.
Hanceville Dist. Center
1100 Main Street S.E.
Hanceville, AL 35077

PART INFORMATION

Part Number	100C300A32P/NND
Description	1-8 X 3 A325-1 HEAVY HEX STRUCTURAL DOUBLE MADE IN USA
Finish	PLAIN
Head Marking	A325 LE USA

RAW MATERIAL ANALYSIS

Steel Heat No	Steel Supplier	Steel Grade Code	Element		Rpd Min Pct	Rpd Max Pct	Percent
CR10266090	Charter Steel	30MnCrB1	C	Carbon	0.30	0.33	0.32
			Mn	Manganese	0.85	1.00	0.92
			P	Phosphorus	0.000	0.020	0.010
			S	Sulfur	0.000	0.015	0.007
			Si	Silicon	0.150	0.250	0.220
			Ni	Nickel	0.00	0.10	0.04
			Cr	Chromium	0.15	0.25	0.16
			Mo	Molybdenum	0.07	0.12	0.08
			Cu	Copper	0.00	0.15	0.08
			Al	Aluminum	0.020	0.050	0.025
			B	Boron	0.0010	0.0030	0.0030
			Ti	Titanium	0.010	0.050	0.018

Certification test results include those reported by the following laboratories:

Charter Steel, A2LA, 01-31-13

LEP Special Fasteners, Inc, ISO17025-A2LA Cert#0122.02, 05-31-12

MECHANICAL PROPERTIES

Wedge Angle	10
Proof Load	51500/85000 (lbs/Psi)

Test Performed	Required	High	Low	Average	Samples
Tensile, PSI	120000 / 160000	152000	150000	151500	4
Proof Load Elongation	0.0000 / 0.0005	0.0004	0	0.0003	4
Superficial R30N	45 / 54	50	48	49	4
Core Hardness, HRC	25 / 34	30	29	30	4

NUCOR
FASTENER DIVISION

LOT NO.
296893A

6B-4W/2W-1.125-0.75-36
6B-4W/2W-1.125-0.75-60

Post Office Box 6100
Saint Joe, Indiana 46785
Telephone 260/337-1600

CUSTOMER NO/NAME
9000 BIRMINGHAM-CONS/SHIPPING

NUCOR ORDER # 800846
TEST REPORT SERIAL# FB374074
CUST PART #
TEST REPORT ISSUE DATE 10/24/11
DATE SHIPPED 10/04/12
CUSTOMER P.O. # 6005629
NAME OF LAB SAMPLER: JEFFREY HOERING, LAB TECHNICIAN

**********CERTIFIED MATERIAL TEST REPORT**********

NUCOR PART NO	QUANTITY	LOT NO.	DESCRIPTION
163200	680	296893A	1 1/8-7 X 3 A325 HVY HX
MANUFACTURE DATE 10/19/11			STRUC SCREW PLAIN

--CHEMISTRY MATERIAL GRADE -1039ML

MATERIAL NUMBER	HEAT NUMBER	**CHEMISTRY COMPOSITION (WT% HEAT ANALYSIS) BY MATERIAL SUPPLIER						
		C	MN	P	S	SI	CR	NUCOR STEEL - NEBRASKA
RM026821	NF11103101	.38	.79	.011	.020	.24	.43	
	MIN	.30	.60			.10		
	MAX	.52		.040	.050	.30		

--MECHANICAL PROPERTIES IN ACCORDANCE WITH ASTM A325-10

SURFACE HARDNESS (R30N)	CORE HARDNESS (RC)	PROOF LOAD N/A	TENSILE STRENGTH (LBS)	DEG-WEDGE STRESS (PSI)
N/A	28.9	N/A	N/A	N/A
N/A	27.0	N/A	N/A	N/A
N/A	27.6	N/A	N/A	N/A
N/A	26.4	N/A	N/A	N/A
AVERAGE VALUES FROM TESTS		PRODUCTION LOT SIZE		3275 PCS
	27.5		TOO SHORT TO TEST	

--VISUAL INSPECTION IN ACCORDANCE WITH ASTM A325-10 4 PCS. SAMPLED LOT PASSED
HEAT TREATMENT - AUSTENITIZED, OIL QUENCHED & TEMPERED (MIN 800 DEG F)

--DIMENSIONS PER ASME B18.2.6-2006

CHARACTERISTIC	#SAMPLES TESTED	MINIMUM	MAXIMUM
Width Across Corners	4	2.0550	2.0630
Grip Length	4	0.8840	0.9550
Head Height	4	0.6830	0.7090
Threads	4	PASS	PASS

ALL TESTS ARE IN ACCORDANCE WITH THE LATEST REVISIONS OF THE METHODS PRESCRIBED IN THE APPLICABLE SAE AND ASTM SPECIFICATIONS. THE SAMPLES TESTED CONFORM TO THE SPECIFICATIONS AS DESCRIBED/LISTED ABOVE AND WERE MANUFACTURED FREE OF MERCURY CONTAMINATION. NO HEATS TO WHICH BISMUTH, SELENIUM, TELLURIUM, OR LEAD WAS INTENTIONALLY ADDED HAVE BEEN USED TO PRODUCE THE BOLTS.
THE STEEL WAS MELTED AND MANUFACTURED IN THE U.S.A. AND THE PRODUCT WAS MANUFACTURED AND TESTED IN THE U.S.A. PRODUCT COMPLIES WITH DFARS 252.225-7014. WE CERTIFY THAT THIS DATA IS A TRUE REPRESENTATION OF INFORMATION PROVIDED BY THE MATERIAL SUPPLIER AND OUR TESTING LABORATORY. THIS CERTIFIED MATERIAL TEST REPORT RELATES ONLY TO THE ITEMS LISTED ON THIS DOCUMENT AND MAY NOT BE REPRODUCED EXCEPT IN FULL.

ACCREDITED

MECHANICAL FASTENER
CERTIFICATE NO. A2LA 0139.01
EXPIRATION DATE 12/31/11

NUCOR FASTENER
A DIVISION OF NUCOR CORPORATION

BOB HAYWOOD
QUALITY ASSURANCE SUPERVISOR

Appendix C Test Summaries

TEST SUMMARY

TEST NAME: TEST 1: 6B-4W/2W-0.875-1.00-36 (THICK END PLATE BEHAVIOR)
TEST DATE: 5-Dec-14

CONNECTION DESCRIPTION

TYPE	Flush - Unstiffened End-Plate, 4 Bolts Wide	
NUMBER OF TENSION BOLTS	6 (all inside)	
NUMBER OF COMPRESSION BOLTS	6	

BEAM DATA

SECTION TYPE	Built-Up	
DEPTH, h	36	in.
FLANGE WIDTH, b_f	12	in.
FLANGE THICKNESS, t_f	0.75	in.
NOMINAL WEB THICKNESS, t_w	0.25	in.
MOMENT OF INERTIA, I	6445	in^4.
NOMINAL YIELD STRESS, F_y	55	ksi

END PLATE DATA

END PLATE THICKNESS, t_p	1	in.
END PLATE WIDTH, b_p	14	in.
END PLATE LENGTH, L_p	36	in.
END PLATE EXTENSION OUTSIDE FLANGE, p_{ext}	0	in.
OUTER PITCH, BOLT TO FLANGE, p_{fo}	N.A.	in.
INNER PITCH, BOLT TO FLANGE, p_{fi}	2.25	in.
INSIDE PITCH, BOLT TO BOLT, p_b	3.5	in.
INSIDE BOLT GAGE, g	4.5	in.
OUTSIDE BOLT GAGE, g_o	3	in.
MEASURED YIELD STRESS, F_{yp}	59.3	ksi

BOLT DATA

NOMINAL BOLT DIAMETER, d_b	0.875	in.
NOMNAL BOLT LENGTH, L_b	3.25	in.
BOLT TYPE	ASTM A325	
AVERAGE BOLT PRETENSION, T_b	Turn of the Nut Method (34 kips)	
NOMINAL BOLT TENSILE STRESS(AISC J3.6), F_t:	90	ksi
NOMINAL BOLT TENSILE STRENGTH, P_t	54.13	kips

EXPERIMENTAL RESULTS

MAXIMUM APPLIED MOMENT, M_u	1030	k-ft
YIELD MOMENT (based on plate separation), M_y	770	k-ft
FAILURE MODE	Bolt Rupture with negligible end-plate yielding	

PREDICTED STRENGTHS

END PLATE STRENGTH, M_{pl}	1440	k-ft
BOLT TENSION RUPTURE (with prying), M_q	N.A.	k-ft
BOLT TENSION RUPTURE (without prying), M_{np}	851	k-ft
CONTROLLING STRENGTH, M_n	851	k-ft
BOLT TENSION RUPTURE (without prying), M_{np}^{exp}	1090	k-ft

TEST SUMMARY

TEST NAME: TEST 2: 6B-4W/2W-1.125-0.75-36 (THIN END PLATE BEHAVIOR)
TEST DATE: 19-Dec-14

CONNECTION DESCRIPTION

TYPE	Flush - Unstiffened End-Plate, 4 Bolts Wide	
NUMBER OF TENSION BOLTS	6 (all inside)	
NUMBER OF COMPRESSION BOLTS	6	

BEAM DATA

SECTION TYPE	Built-Up	
DEPTH, h	36	in.
FLANGE WIDTH, b_f	11 15/16	in.
FLANGE THICKNESS, t_f	0.755	in.
NOMINAL WEB THICKNESS, t_w	0.25	in.
MOMENT OF INERTIA, I	6447.9	in^4.
NOMINAL YIELD STRESS, F_y	55	ksi

END PLATE DATA

END PLATE THICKNESS, t_p	0.753	in.
END PLATE WIDTH, b_p	14	in.
END PLATE LENGTH, L_p	36	in.
END PLATE EXTENSION OUTSIDE FLANGE, p_{ext}	0	in.
OUTER PITCH, BOLT TO FLANGE, p_{fo}	N.A.	in.
INNER PITCH, BOLT TO FLANGE, p_{fi}	2.25	in.
INSIDE PITCH, BOLT TO BOLT, p_b	3.5	in.
INSIDE BOLT GAGE, g	4.5	in.
OUTSIDE BOLT GAGE, g_o	3	in.
MEASURED YIELD STRESS, F_{yp}	54.6	ksi

BOLT DATA

NOMINAL BOLT DIAMETER, d_b		1.125	in.
NOMNAL BOLT LENGTH, L_b		3	in.
BOLT TYPE		ASTM A325	
AVERAGE BOLT PRETENSION, T_b	(almost 1/2 turn)	58	kips
NOMINAL BOLT TENSILE STRESS(AISC J3.6), F_t:		90	ksi
NOMINAL BOLT TENSILE STRENGTH, P_t		89.47	kips

EXPERIMENTAL RESULTS

MAXIMUM APPLIED MOMENT, M_u	1110	k-ft
YIELD MOMENT (based on plate separation), M_y	730	k-ft
FAILURE MODE	End Plate Yielding followed by Bolt Rupture	

PREDICTED STRENGTHS

END PLATE STRENGTH, M_{pl}	748	k-ft
BOLT TENSION RUPTURE (with prying), M_q	957	k-ft
BOLT TENSION RUPTURE (without prying), M_{np}	1410	k-ft
CONTROLLING STRENGTH, M_n	748	k-ft
BOLT TENSION RUPTURE (with prying), M_q^{exp}	1100	k-ft

TEST SUMMARY

TEST NAME: TEST 3: 12BE-MRE 1/3-4W/2W-1.00-0.75-36 (THIN END PLATE BEHAVIOR)
TEST DATE: 28-Jan-15

CONNECTION DESCRIPTION

TYPE	Multiple Row Extended Unstiffened End-Plate, 4 Bolts Wide
NUMBER OF TENSION BOLTS	12 (4 outside in one row, 8 inside in 3 rows)
NUMBER OF COMPRESSION BOLTS	12 (4 outside in one row, 8 inside in 3 rows)

BEAM DATA

SECTION TYPE		Built-Up	
DEPTH, h		36	in.
FLANGE WIDTH, b_f		12	in.
FLANGE THICKNESS, t_f		0.75	in.
NOMINAL WEB THICKNESS, t_w		0.25	in.
MOMENT OF INERTIA, I		6447.9	in^4.
NOMINAL YIELD STRESS, F_y		55	ksi

END PLATE DATA

END PLATE THICKNESS, t_p		0.753	in.
END PLATE WIDTH, b_p		14	in.
END PLATE LENGTH, L_p		36	in.
END PLATE EXTENSION OUTSIDE FLANGE, p_{ext}		4	in.
OUTER PITCH, BOLT TO FLANGE, p_{fo}		2.25	in.
INNER PITCH, BOLT TO FLANGE, p_{fi}		2.25	in.
INSIDE PITCH, BOLT TO BOLT, p_b		3.5	in.
INSIDE BOLT GAGE, g		4.5	in.
OUTSIDE BOLT GAGE, g_o		3	in.
MEASURED YIELD STRESS, F_{yp}		54.6	ksi

BOLT DATA

NOMINAL BOLT DIAMETER, d_b		1	in.
NOMNAL BOLT LENGTH, L_b		2.75	in.
BOLT TYPE		ASTM A325	
AVERAGE BOLT PRETENSION, T_b	(aprox 150 degree)	53	kips
NOMINAL BOLT TENSILE STRESS(AISC J3.6), F_t:		90	ksi
NOMINAL BOLT TENSILE STRENGTH, P_t		70.67	kips

EXPERIMENTAL RESULTS

MAXIMUM APPLIED MOMENT, M_u	1640	k-ft
YIELD MOMENT (based on plate separation), M_y	1230	k-ft
FAILURE MODE	End Plate Yielding	

(Bolt Rupture couldn't be observed due to insufficient capacity of the section)

PREDICTED STRENGTHS

END PLATE STRENGTH, M_{pl}	1130	k-ft
BOLT TENSION RUPTURE (with prying), M_q	1420	k-ft
BOLT TENSION RUPTURE (without prying), M_{np}	2310	k-ft
CONTROLLING STRENGTH, M_n	1130	k-ft
BOLT TENSION RUPTURE (with prying), M_q^{exp}	1870	k-ft

TEST SUMMARY

TEST NAME: TEST 4: 12B-MRE 1/3-4W/2W-0.75-1.00-36 (THICK END PLATE BEHAVIOR)
TEST DATE: 3-Feb-15

CONNECTION DESCRIPTION

TYPE	Multiple Row Extended Unstiffened End-Plate, 4 Bolts Wide
NUMBER OF TENSION BOLTS	12 (4 outside in one row, 8 inside in 3 rows)
NUMBER OF COMPRESSION BOLTS	12 (4 outside in one row, 8 inside in 3 rows)

BEAM DATA

SECTION TYPE		Built-Up	
DEPTH, h		36	in.
FLANGE WIDTH, b_f		12	in.
FLANGE THICKNESS, t_f		0.75	in.
NOMINAL WEB THICKNESS, t_w		0.25	in.
MOMENT OF INERTIA, I		6447.9	in^4.
NOMINAL YIELD STRESS, F_y		55	ksi

END PLATE DATA

END PLATE THICKNESS, t_p		1	in.
END PLATE WIDTH, b_p		14	in.
END PLATE LENGTH, L_p		36	in.
END PLATE EXTENSION OUTSIDE FLANGE, p_{ext}		4	in.
OUTER PITCH, BOLT TO FLANGE, p_{fo}		2.25	in.
INNER PITCH, BOLT TO FLANGE, p_{fi}		2.25	in.
INSIDE PITCH, BOLT TO BOLT, p_b		3.5	in.
INSIDE BOLT GAGE, g		4.5	in.
OUTSIDE BOLT GAGE, g_o		3	in.
MEASURED YIELD STRESS, F_{yp}		59.3	ksi

BOLT DATA

NOMINAL BOLT DIAMETER, d_b		0.75	in.
NOMNAL BOLT LENGTH, L_b		3	in.
BOLT TYPE		ASTM A325	
AVERAGE BOLT PRETENSION, T_b	(aprox 150 degree)	28.7	kips
NOMINAL BOLT TENSILE STRESS(AISC J3.6), F_t:		90	ksi
NOMINAL BOLT TENSILE STRENGTH, P_t		39.73	kips

EXPERIMENTAL RESULTS

MAXIMUM APPLIED MOMENT, M_u	1490	k-ft
YIELD MOMENT (based on plate separation), M_y	960	k-ft
FAILURE MODE	Bolt Rupture	

PREDICTED STRENGTHS

END PLATE STRENGTH, M_{pl}	2190	k-ft
BOLT TENSION RUPTURE (with prying), M_q	N.A.	k-ft
BOLT TENSION RUPTURE (without prying), M_{np}	1300	k-ft
CONTROLLING STRENGTH, M_n	1300	k-ft
BOLT TENSION RUPTURE (without prying), M_{np}^{exp}	1630	k-ft

TEST SUMMARY

TEST NAME: TEST 5: 6B/4W-0.875-1.00-60 (THICK END PLATE BEHAVIOR)
TEST DATE: 27-Feb-15

CONNECTION DESCRIPTION

TYPE	Flush - Unstiffened End-Plate, 4 Bolts Wide	
NUMBER OF TENSION BOLTS	6 (all inside)	
NUMBER OF COMPRESSION BOLTS	6	

BEAM DATA

SECTION TYPE	Built-Up	
DEPTH, h	60	in.
FLANGE WIDTH, b_f	12	in.
FLANGE THICKNESS, t_f	0.75	in.
NOMINAL WEB THICKNESS, t_w	0.375	in.
MOMENT OF INERTIA, I	22054.7	in^4.
NOMINAL YIELD STRESS, F_y	55	ksi

END PLATE DATA

END PLATE THICKNESS, t_p	1	in.
END PLATE WIDTH, b_p	14	in.
END PLATE LENGTH, L_p	60	in.
END PLATE EXTENSION OUTSIDE FLANGE, p_{ext}	N.A.	in.
OUTER PITCH, BOLT TO FLANGE, p_{fo}	N.A.	in.
INNER PITCH, BOLT TO FLANGE, p_{fi}	2.25	in.
INSIDE PITCH, BOLT TO BOLT, p_b	3.5	in.
INSIDE BOLT GAGE, g	4.5	in.
OUTSIDE BOLT GAGE, g_o	3	in.
MEASURED YIELD STRESS, F_{yp}	59.3	ksi

BOLT DATA

NOMINAL BOLT DIAMETER, d_b		0.875	in.
NOMNAL BOLT LENGTH, L_b		3	in.
BOLT TYPE	ASTM A325		
AVERAGE BOLT PRETENSION, T_b	(aprox 165 degree)	40.0	kips
NOMINAL BOLT TENSILE STRESS(AISC J3.6), F_t:		90	ksi
NOMINAL BOLT TENSILE STRENGTH, P_t		54.13	kips

EXPERIMENTAL RESULTS

MAXIMUM APPLIED MOMENT, M_u	1730	k-ft
YIELD MOMENT (based on plate separation), M_y	1390	k-ft
FAILURE MODE	Bolt Rupture without any end-plate yielding	

PREDICTED STRENGTHS

END PLATE STRENGTH, M_{pl}	2530	k-ft
BOLT TENSION RUPTURE (with prying), M_q	N.A.	k-ft
BOLT TENSION RUPTURE (without prying), M_{np}	1500	k-ft
CONTROLLING STRENGTH, M_n	1500	k-ft
BOLT TENSION RUPTURE (without prying), M_{np}^{exp}	1920	k-ft

TEST SUMMARY

TEST NAME: TEST 6: 6B-4W/2W-1.125-0.75-60 (THIN END PLATE BEHAVIOR)
TEST DATE: 5-Mar-15

CONNECTION DESCRIPTION

TYPE	Flush - Unstiffened End-Plate, 4 Bolts Wide	
NUMBER OF TENSION BOLTS	6 (all inside)	
NUMBER OF COMPRESSION BOLTS	6	

BEAM DATA

SECTION TYPE	Built-Up	
DEPTH, h	60	in.
FLANGE WIDTH, b_f	12	in.
FLANGE THICKNESS, t_f	0.75	in.
NOMINAL WEB THICKNESS, t_w	0.375	in.
MOMENT OF INERTIA, I	22054.7	in^4.
NOMINAL YIELD STRESS, F_y	55	ksi

END PLATE DATA

END PLATE THICKNESS, t_p	0.75	in.
END PLATE WIDTH, b_p	14	in.
END PLATE LENGTH, L_p	60	in.
END PLATE EXTENSION OUTSIDE FLANGE, p_{ext}	N.A.	in.
OUTER PITCH, BOLT TO FLANGE, p_{fo}	N.A.	in.
INNER PITCH, BOLT TO FLANGE, p_{fi}	2.25	in.
INSIDE PITCH, BOLT TO BOLT, p_b	3.5	in.
INSIDE BOLT GAGE, g	4.5	in.
OUTSIDE BOLT GAGE, g_o	3	in.
MEASURED YIELD STRESS, F_{yp}	54.6	ksi

BOLT DATA

NOMINAL BOLT DIAMETER, d_b		1.125	in.
NOMNAL BOLT LENGTH, L_b		3	in.
BOLT TYPE		ASTM A325	
AVERAGE BOLT PRETENSION, T_b	(aprox 165 degree)	59.0	kips
NOMINAL BOLT TENSILE STRESS(AISC J3.6), F_t:		90	ksi
NOMINAL BOLT TENSILE STRENGTH, P_t		89.47	kips

EXPERIMENTAL RESULTS

MAXIMUM APPLIED MOMENT, M_u	1980	k-ft
YIELD MOMENT (based on plate separation), M_y	1400	k-ft
FAILURE MODE	End-Plate Yielding followed by Bolt Rupture	

PREDICTED STRENGTHS

END PLATE STRENGTH, M_{pl}	1310	k-ft
BOLT TENSION RUPTURE (with prying), M_q	1680	k-ft
BOLT TENSION RUPTURE (without prying), M_{np}	2480	k-ft
CONTROLLING STRENGTH, M_n	1310	k-ft
BOLT TENSION RUPTURE (with prying), M_q^{exp}	1930	k-ft

TEST SUMMARY

TEST NAME: TEST 7: 12B-MRE 1/3-4W/2W-1.00-0.75-60 (THIN END PLATE BEHAVIOR)
TEST DATE: 20-Mar-15

CONNECTION DESCRIPTION

TYPE	Extended - Unstiffened End-Plate, 4 Bolts Wide	
NUMBER OF TENSION BOLTS	8 inside + 4 outside	
NUMBER OF COMPRESSION BOLTS	12	

BEAM DATA

SECTION TYPE	Built-Up	
DEPTH, h	60	in.
FLANGE WIDTH, b_f	12	in.
FLANGE THICKNESS, t_f	0.75	in.
NOMINAL WEB THICKNESS, t_w	0.375	in.
MOMENT OF INERTIA, I	22054.7	in^4.
NOMINAL YIELD STRESS, F_y	55	ksi

END PLATE DATA

END PLATE THICKNESS, t_p	0.75	in.
END PLATE WIDTH, b_p	14	in.
END PLATE LENGTH, L_p	60	in.
END PLATE EXTENSION OUTSIDE FLANGE, p_{ext}	4	in.
OUTER PITCH, BOLT TO FLANGE, p_{fo}	2.25	in.
INNER PITCH, BOLT TO FLANGE, p_{fi}	2.25	in.
INSIDE PITCH, BOLT TO BOLT, p_b	3.5	in.
INSIDE BOLT GAGE, g	4.5	in.
OUTSIDE BOLT GAGE, g_o	3	in.
MEASURED YIELD STRESS, F_{yp}	54.5	ksi

BOLT DATA

NOMINAL BOLT DIAMETER, d_b		1	in.
NOMNAL BOLT LENGTH, L_b		2.75	in.
BOLT TYPE	ASTM A325		
AVERAGE BOLT PRETENSION, T_b	(aprox 120 degree)	52.0	kips
NOMINAL BOLT TENSILE STRESS(AISC J3.6), F_t:		90	ksi
NOMINAL BOLT TENSILE STRENGTH, P_t		70.69	kips

EXPERIMENTAL RESULTS

MAXIMUM APPLIED MOMENT, M_u	2760	k-ft
YIELD MOMENT (based on plate separation), M_y	2230	k-ft
FAILURE MODE	No Bolt Rupture but end-plate yielding seen	

PREDICTED STRENGTHS

END PLATE STRENGTH, M_{pl}	1980	k-ft
BOLT TENSION RUPTURE (with prying), M_q	2450	k-ft
BOLT TENSION RUPTURE (without prying), M_{np}	4000	k-ft
CONTROLLING STRENGTH, M_n	1980	k-ft
BOLT TENSION RUPTURE (with prying), M_q^{exp}	3220	k-ft

TEST SUMMARY

TEST NAME: TEST 8: 12B-MRE 1/3-4W/2W-0.75-1.00-60 (THICK END PLATE BEHAVIOR)
TEST DATE: 3-Apr-15

CONNECTION DESCRIPTION

TYPE	Extended - Unstiffened End-Plate, 4 Bolts Wide	
NUMBER OF TENSION BOLTS	8 inside + 4 outside	
NUMBER OF COMPRESSION BOLTS	12	

BEAM DATA

SECTION TYPE	Built-Up	
DEPTH, h	60	in.
FLANGE WIDTH, b_f	12	in.
FLANGE THICKNESS, t_f	0.75	in.
NOMINAL WEB THICKNESS, t_w	0.375	in.
MOMENT OF INERTIA, I	22054.7	in^4.
NOMINAL YIELD STRESS, F_y	55	ksi

END PLATE DATA

END PLATE THICKNESS, t_p	1	in.
END PLATE WIDTH, b_p	14	in.
END PLATE LENGTH, L_p	60	in.
END PLATE EXTENSION OUTSIDE FLANGE, p_{ext}	4	in.
OUTER PITCH, BOLT TO FLANGE, p_{fo}	2.25	in.
INNER PITCH, BOLT TO FLANGE, p_{fi}	2.25	in.
INSIDE PITCH, BOLT TO BOLT, p_b	3.5	in.
INSIDE BOLT GAGE, g	4.5	in.
OUTSIDE BOLT GAGE, g_o	3	in.
MEASURED YIELD STRESS, F_{yp}	59.3	ksi

BOLT DATA

NOMINAL BOLT DIAMETER, d_b		0.75	in.
NOMNAL BOLT LENGTH, L_b		3	in.
BOLT TYPE		ASTM A325	
AVERAGE BOLT PRETENSION, T_b	(aprox 150 degree)	32.0	kips
NOMINAL BOLT TENSILE STRESS(AISC J3.6), F_t:		90	ksi
NOMINAL BOLT TENSILE STRENGTH, P_t		39.76	kips

EXPERIMENTAL RESULTS

MAXIMUM APPLIED MOMENT, M_u	2490	k-ft
YIELD MOMENT (based on plate separation), M_y	2100	k-ft
FAILURE MODE	Bolt Rupture with no end-plate yielding	

PREDICTED STRENGTHS

END PLATE STRENGTH, M_{pl}	3830	k-ft
BOLT TENSION RUPTURE (with prying), M_q	N.A.	k-ft
BOLT TENSION RUPTURE (without prying), M_{np}	2250	k-ft
CONTROLLING STRENGTH, M_n	2250	k-ft
BOLT TENSION RUPTURE (without prying), M_{np}^{exp}	2820	k-ft

TEST SUMMARY

TEST NAME: TEST 9: 8ES-1.00-1.00-56 (THICK END PLATE BEHAVIOR)
TEST DATE: 10-Apr-15

CONNECTION DESCRIPTION

TYPE	Extended - Stiffened End-Plate	
NUMBER OF TENSION BOLTS	4 inside + 4 outside	
NUMBER OF COMPRESSION BOLTS	12	

BEAM DATA

SECTION TYPE	Built-Up	
DEPTH, h	56	in.
FLANGE WIDTH, b_f	10	in.
FLANGE THICKNESS, t_f	1	in.
NOMINAL WEB THICKNESS, t_w	0.5	in.
MOMENT OF INERTIA, I	21688	in^4.
NOMINAL YIELD STRESS, F_y	55	ksi

END PLATE DATA

END PLATE THICKNESS, t_p	1	in.
END PLATE WIDTH, b_p	10	in.
END PLATE LENGTH, L_p	71	in.
END PLATE EXTENSION OUTSIDE FLANGE, p_{ext}	7.5	in.
OUTER PITCH, BOLT TO FLANGE, p_{fo}	2.25	in.
INNER PITCH, BOLT TO FLANGE, p_{fi}	2.25	in.
INSIDE PITCH, BOLT TO BOLT, p_b	3.5	in.
INSIDE BOLT GAGE, g	5	in.
OUTSIDE BOLT GAGE, g_o	N.A	in.
MEASURED YIELD STRESS, F_{yp}	58.2	ksi

BOLT DATA

NOMINAL BOLT DIAMETER, d_b		1	in.
NOMNAL BOLT LENGTH, L_b		3.5	in.
BOLT TYPE	ASTM A325		
AVERAGE BOLT PRETENSION, T_b	(aprox 120 degree)	53.0	kips
NOMINAL BOLT TENSILE STRESS(AISC J3.6), F_t:		90	ksi
NOMINAL BOLT TENSILE STRENGTH, P_t		70.69	kips

EXPERIMENTAL RESULTS

MAXIMUM APPLIED MOMENT, M_u	3050	k-ft
YIELD MOMENT (based on plate separation), M_y	2520	k-ft
FAILURE MODE	Bolt Rupture with minimal end-plate yielding	

PREDICTED STRENGTHS

END PLATE STRENGTH, M_{pl}	4160	k-ft
BOLT TENSION RUPTURE (with prying), M_q	N.A.	k-ft
BOLT TENSION RUPTURE (without prying), M_{np}	2630	k-ft
CONTROLLING STRENGTH, M_n	2630	k-ft
BOLT TENSION RUPTURE (without prying), M_{np}^{exp}	3420	k-ft

TEST SUMMARY

TEST NAME: TEST 10: 8ES-1.25-0.75-56 (THICK END PLATE BEHAVIOR)
TEST DATE: 17-Apr-15

CONNECTION DESCRIPTION

TYPE	Extended - Stiffened End-Plate	
NUMBER OF TENSION BOLTS	4 inside + 4 outside	
NUMBER OF COMPRESSION BOLTS	12	

BEAM DATA

SECTION TYPE	Built-Up	
DEPTH, h	56	in.
FLANGE WIDTH, b_f	10	in.
FLANGE THICKNESS, t_f	1	in.
NOMINAL WEB THICKNESS, t_w	0.5	in.
MOMENT OF INERTIA, I	21688	in^4
NOMINAL YIELD STRESS, F_y	55	ksi

END PLATE DATA

END PLATE THICKNESS, t_p	1	in.
END PLATE WIDTH, b_p	10	in.
END PLATE LENGTH, L_p	71	in.
END PLATE EXTENSION OUTSIDE FLANGE, p_{ext}	7.5	in.
OUTER PITCH, BOLT TO FLANGE, p_{fo}	2.25	in.
INNER PITCH, BOLT TO FLANGE, p_{fi}	2.25	in.
INSIDE PITCH, BOLT TO BOLT, p_b	3.5	in.
INSIDE BOLT GAGE, g	5	in.
OUTSIDE BOLT GAGE, g_o	N.A	in.
MEASURED YIELD STRESS, F_{yp}	57.2	ksi

BOLT DATA

NOMINAL BOLT DIAMETER, d_b		1.25	in.
NOMNAL BOLT LENGTH, L_b		3.5	in.
BOLT TYPE	ASTM A325		
AVERAGE BOLT PRETENSION, T_b	(aprox 120 degree)	72.0	kips
NOMINAL BOLT TENSILE STRESS(AISC J3.6), F_t:		90	ksi
NOMINAL BOLT TENSILE STRENGTH, P_t		110.45	kips

EXPERIMENTAL RESULTS

MAXIMUM APPLIED MOMENT, M_u	2920	k-ft
YIELD MOMENT (based on plate separation), M_y	2400	k-ft
FAILURE MODE	No Bolt Rupture, but end-plate yielding seen	

PREDICTED STRENGTHS

END PLATE STRENGTH, M_{pl}	2300	k-ft
BOLT TENSION RUPTURE (with prying), M_q	2650	k-ft
BOLT TENSION RUPTURE (without prying), M_{np}	4110	k-ft
CONTROLLING STRENGTH, M_n	2300	k-ft
BOLT TENSION RUPTURE (with prying), M_q^{exp}	2960	k-ft

Appendix D Fabrication Drawings

D2

NOTE: SPECIMENS WILL BE REUSED FOR A SECOND TEST BY ROTATING BEAM 180 DEGREES, FLIPPING OVER, AND CONNECTING THE UNTESTED END-PLATES

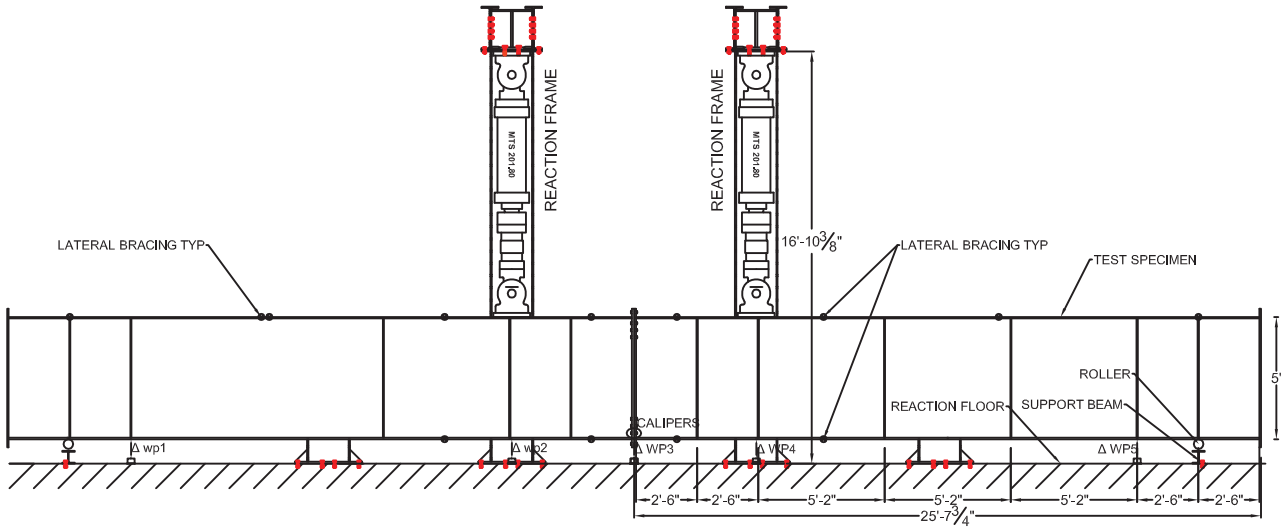

DEEP BEAM TEST SET-UP

NOTE: SPECIMENS WILL BE REUSED FOR A SECOND TEST BY ROTATING BEAM 180 DEGREES, FLIPPING OVER, AND CONNECTING THE UNTESTED END-PLATES

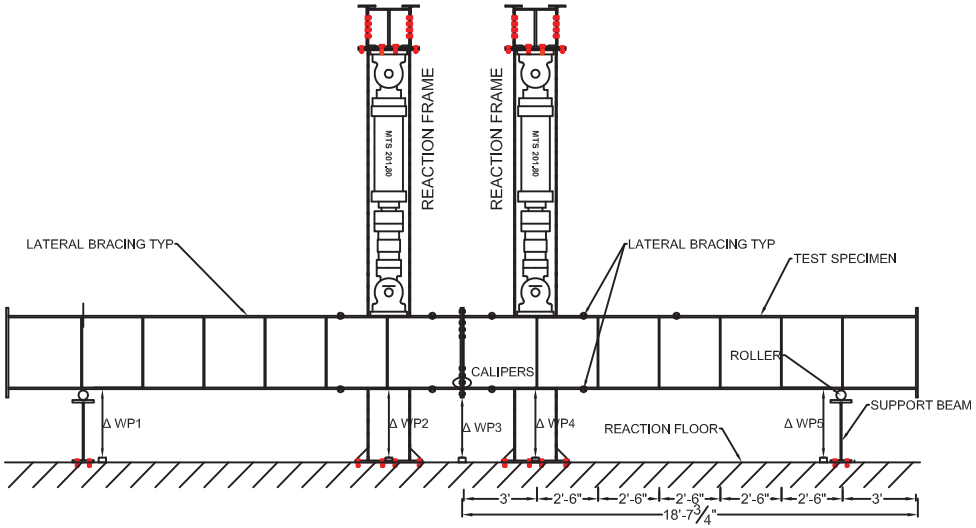

SHALLOW BEAM TEST SET-UP

VIRGINIA TECH	TITLE: TEST SET-UP ELEVATION		
PROJECT: MBMA END-PLATE MOMENT CONNECTIONS		05/09/14	SHEET 01

GIRDER SPECIMEN 01

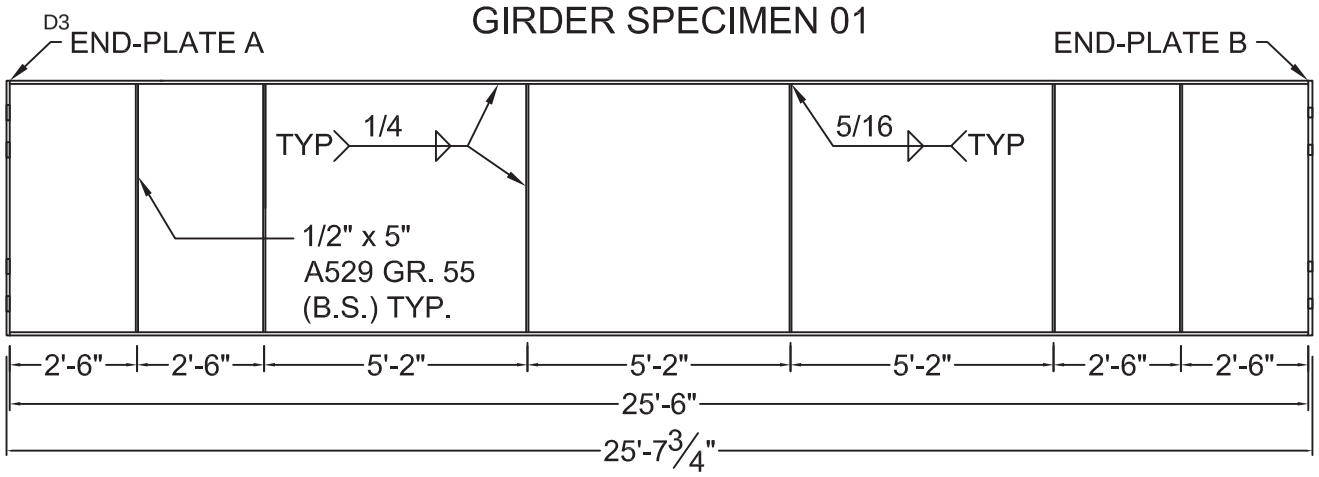

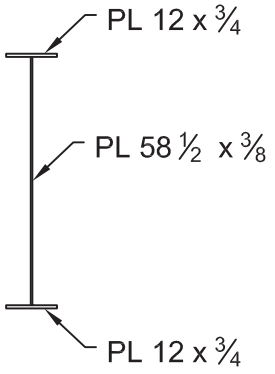

END PLATE A

THIN PLATE BEHAVIOR

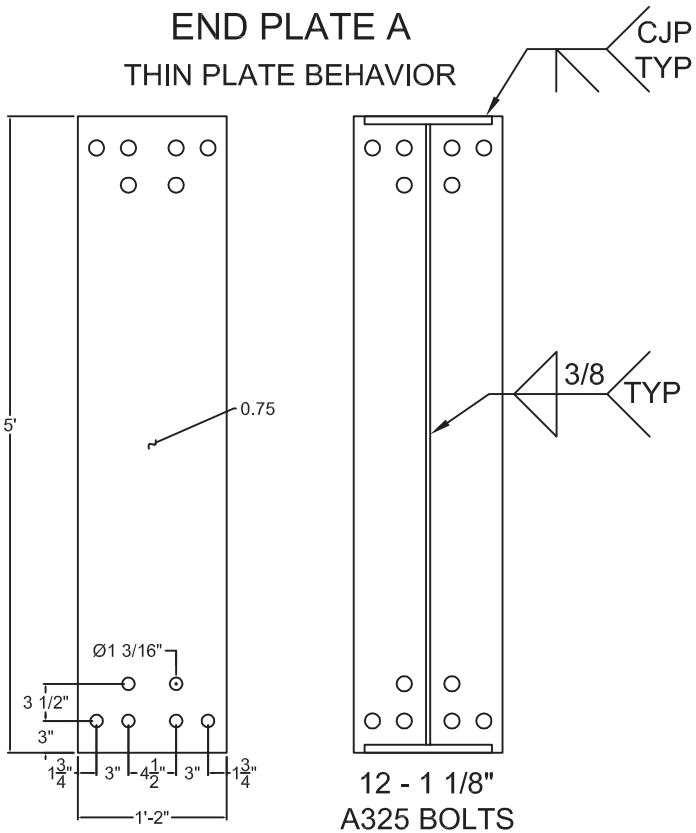

12 - 1 1/8"
A325 BOLTS

6B-4W/2W-1.125-0.75-60

END PLATE B

THICK PLATE BEHAVIOR

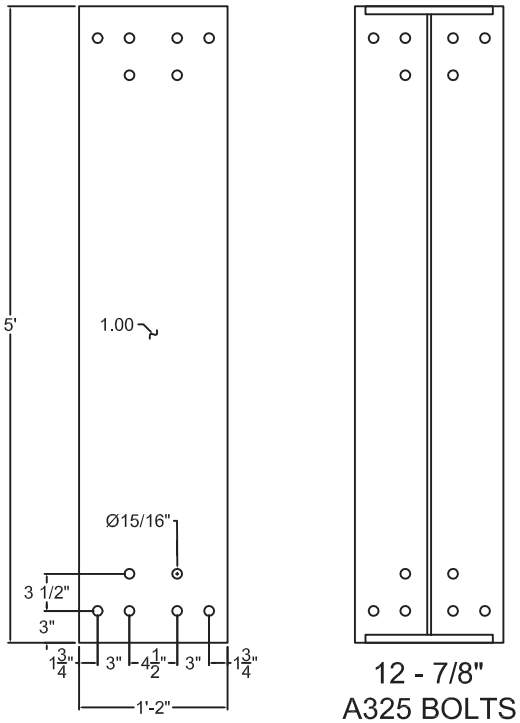

12 - 7/8"
A325 BOLTS

6B-4W/2W-0.875-1.00-60

QUANTITY: 2 EACH AND INCLUDE 18in x 14in COUPON FROM SAME HEAT OF MATERIAL AS END-PLATE. MATCH MARK COUPON AND END-PLATE FOR VERIFICATION

$F_{y\ end\text{-}plate}$ = 50 ksi ASSUMED

NO BLAST, NO PAINT

E70 ELECTRODES FOR ALL WELDS

VIRGINIA TECH	TITLE: SPECIMEN 01		
PROJECT: MBMA END-PLATE MOMENT CONNECTIONS		05/09/14	SHEET 02

GIRDER SPECIMEN 02

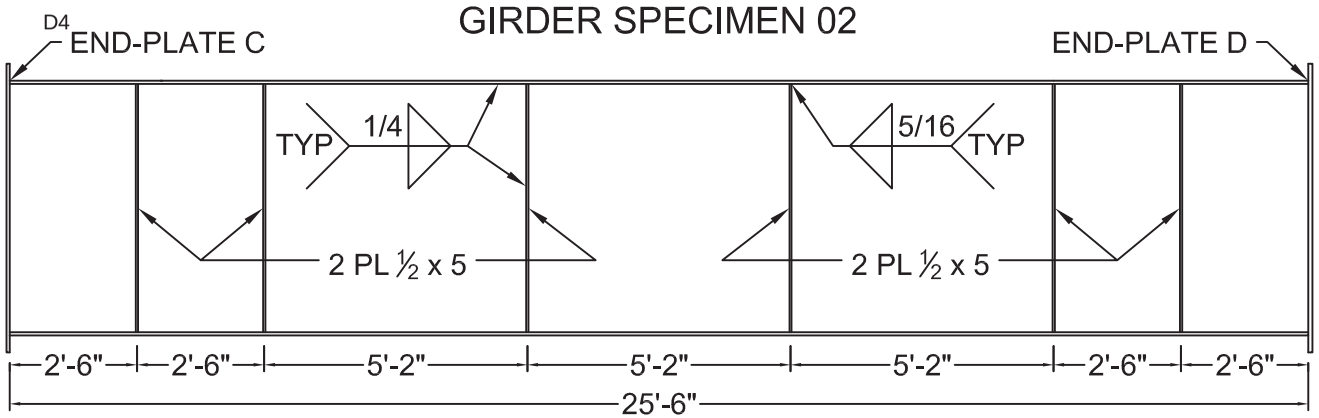

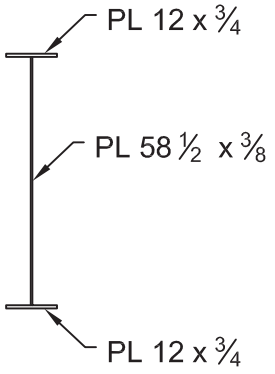

END PLATE C

THIN PLATE BEHAVIOR

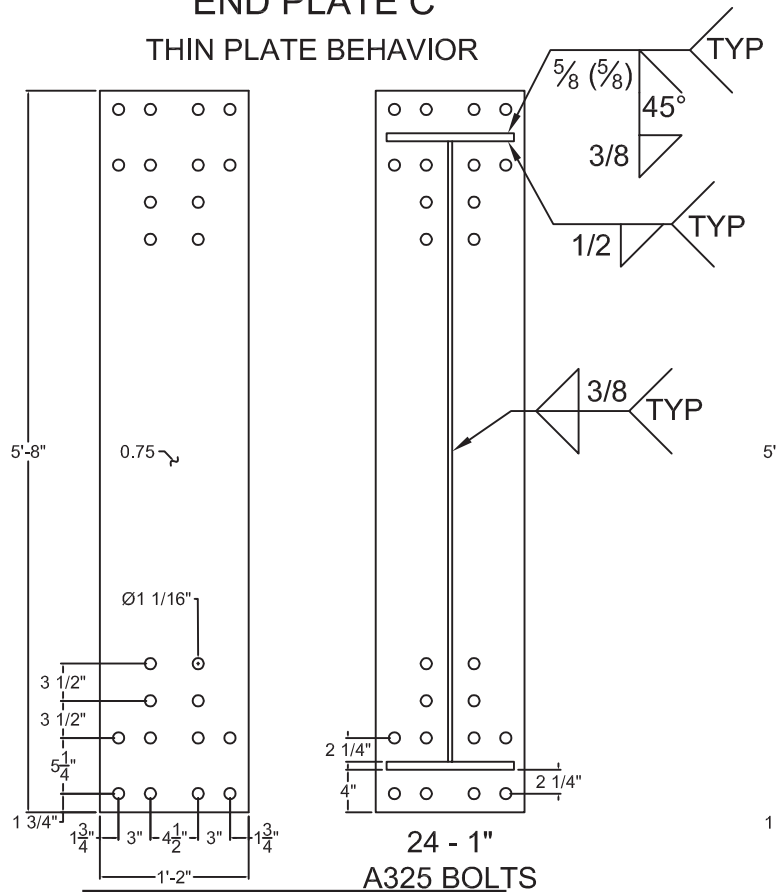

12B- MRE 1/3 -4W/2W-1.00-0.75-60

END PLATE D

THICK PLATE BEHAVIOR

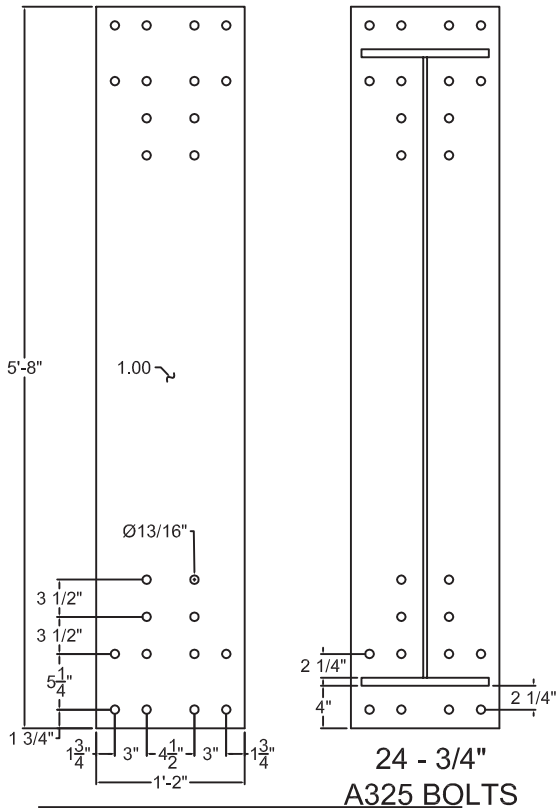

12B- MRE 1/3 -4W/2W-0.75-1.00-60

QUANTITY: 2 EACH AND INCLUDE 18in x 14in COUPON FROM SAME HEAT OF MATERIAL AS END-PLATE. MATCH MARK COUPON AND END-PLATE FOR VERIFICATION

$F_{y\ end\text{-}plate}$ = 50 ksi ASSUMED

NO BLAST, NO PAINT

E70 ELECTRODES FOR ALL WELDS

VIRGINIA TECH	TITLE: SPECIMEN 02	
PROJECT: MBMA END-PLATE MOMENT CONNECTIONS	05/09/14	SHEET 03

D5

GIRDER SPECIMEN 03

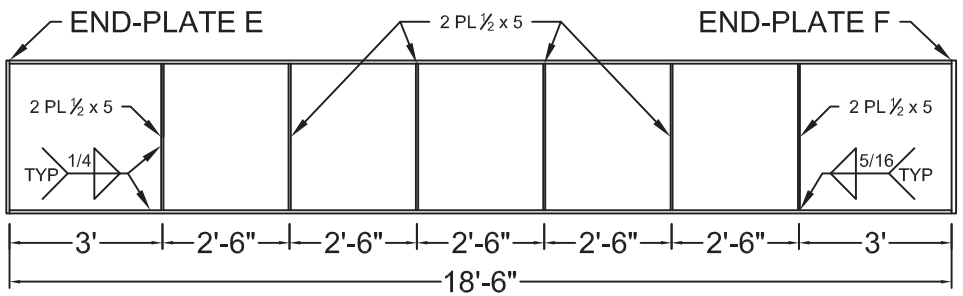

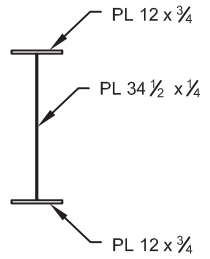

END PLATE E

THIN PLATE BEHAVIOR

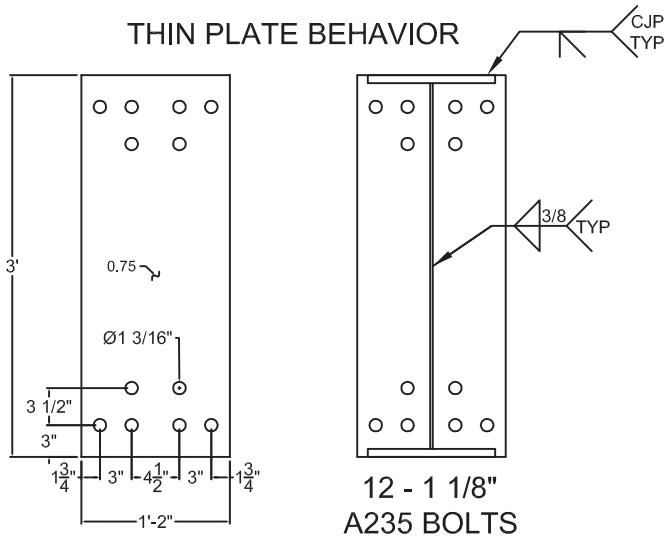

12 - 1 1/8"
A235 BOLTS

6B-4W/2W-1.125-0.75-36

END PLATE F

THICK PLATE BEHAVIOR

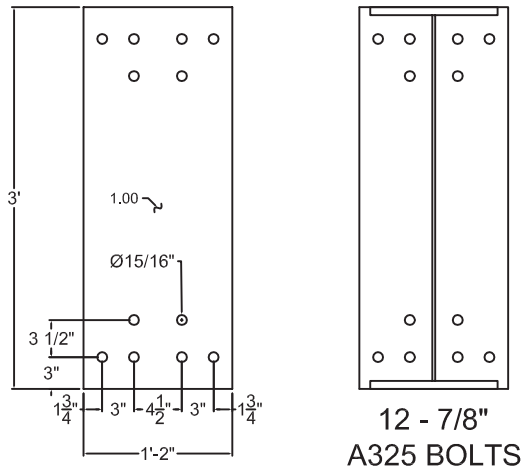

12 - 7/8"
A325 BOLTS

6B-4W/2W-0.875-1.00-36

QUANTITY: 2 EACH AND INCLUDE 18in x 14in COUPON FROM SAME HEAT OF MATERIAL AS END-PLATE. MATCH MARK COUPON AND END-PLATE FOR VERIFICATION

$F_{y\ end\text{-}plate}$ = 50 ksi ASSUMED

NO BLAST, NO PAINT

E70 ELECTRODES FOR ALL WELDS

VIRGINIA TECH	TITLE: SPECIMEN 03		
PROJECT: MBMA END-PLATE MOMENT CONNECTIONS		05/09/14	SHEET 04

GIRDER SPECIMEN 04

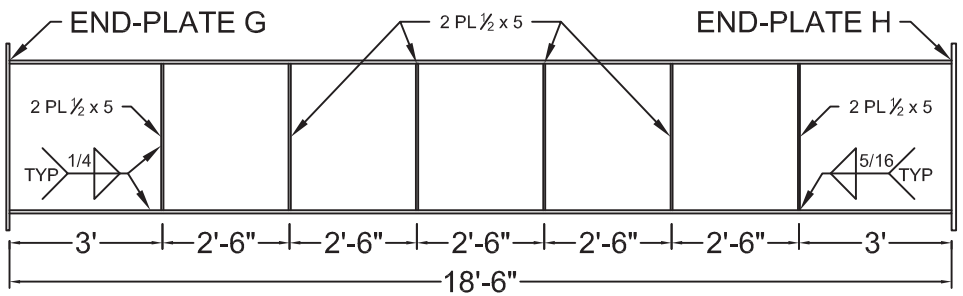

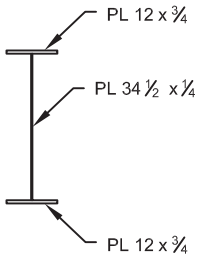

END PLATE G

THIN PLATE BEHAVIOR

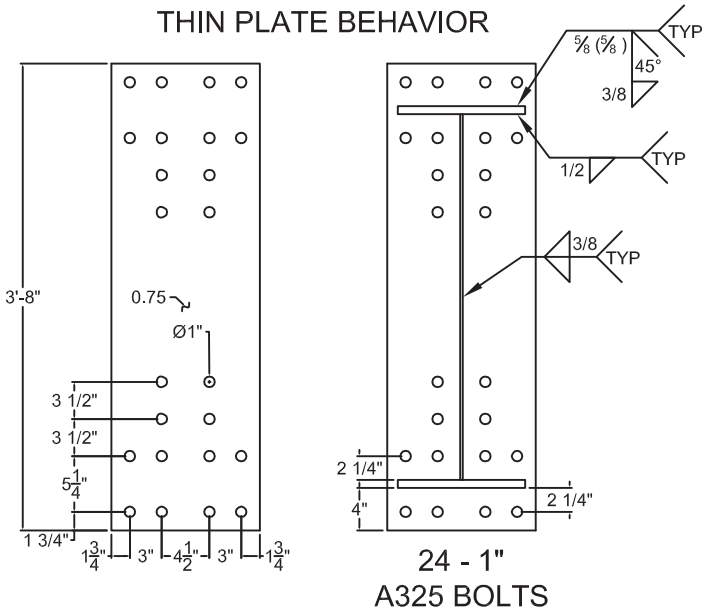

24 - 1"
A325 BOLTS

12B- MRE 1/3 -4W/2W-1.00-0.75-36

END PLATE H

THICK PLATE BEHAVIOR

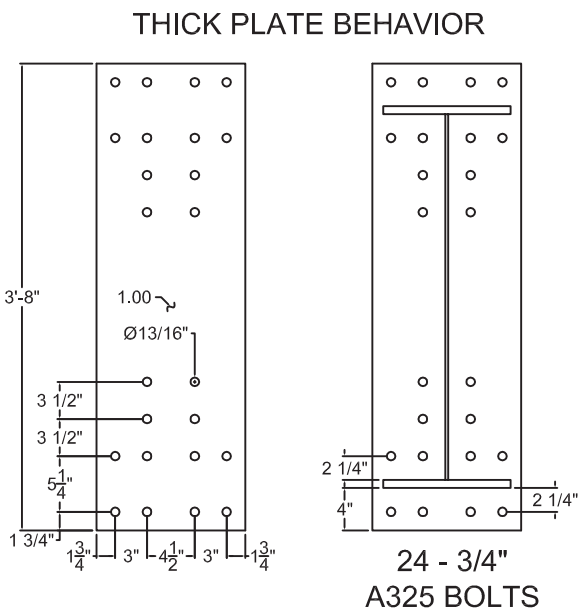

24 - 3/4"
A325 BOLTS

12B- MRE 1/3 -4W/2W-0.75-1.00-36

QUANTITY: 2 EACH AND INCLUDE 18in x 14in COUPON FROM SAME HEAT OF MATERIAL AS END-PLATE. MATCH MARK COUPON AND END-PLATE FOR VERIFICATION

$F_{y\ end\text{-}plate}$ = 50 ksi ASSUMED

NO BLAST, NO PAINT

E70 ELECTRODES FOR ALL WELDS

VIRGINIA TECH	TITLE: SPECIMEN 04		
PROJECT: MBMA END-PLATE MOMENT CONNECTIONS		05/09/14	SHEET 05

GIRDER SPECIMEN 05

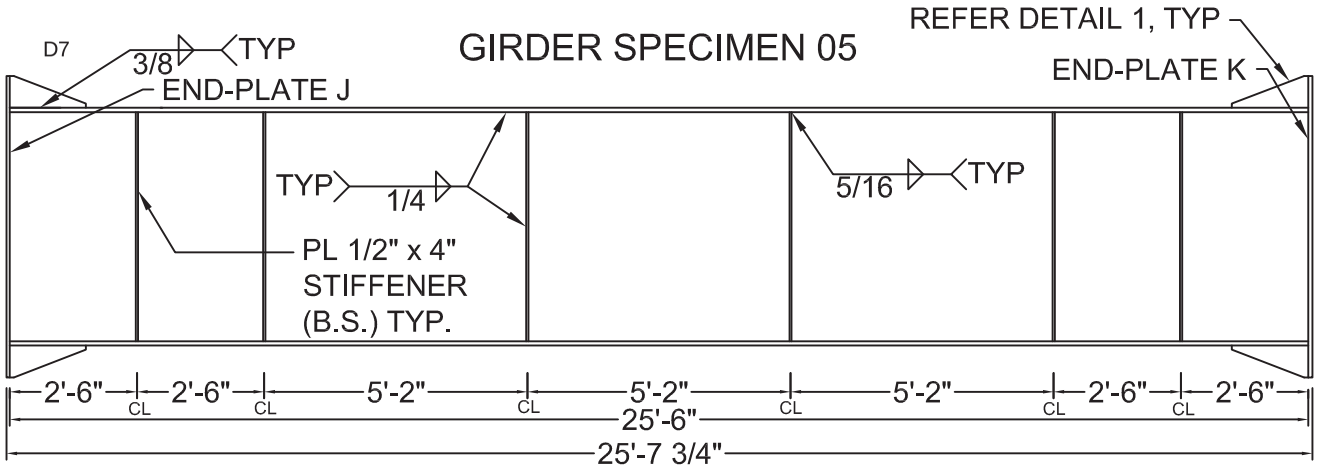

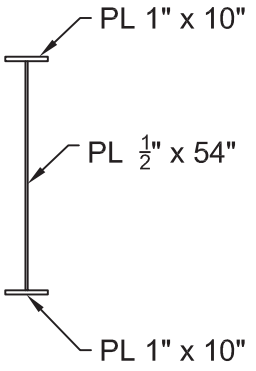

END PLATE J
(THIN PLATE BEHAVIOR)

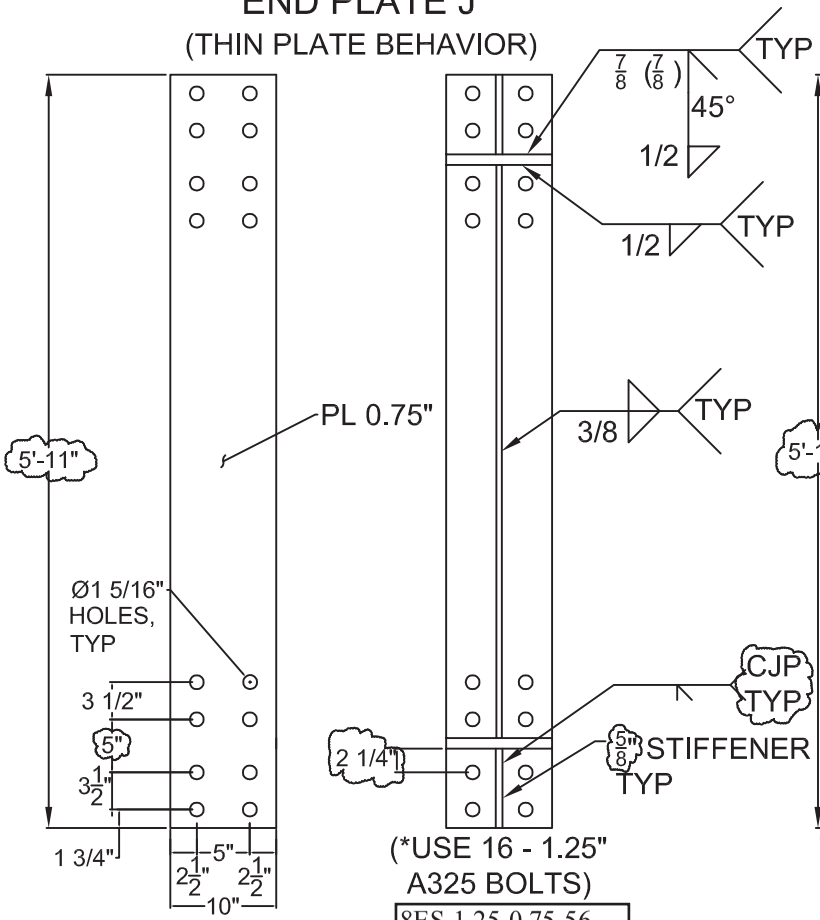

8ES-1.25-0.75-56

END PLATE K
(THICK PLATE BEHAVIOR)

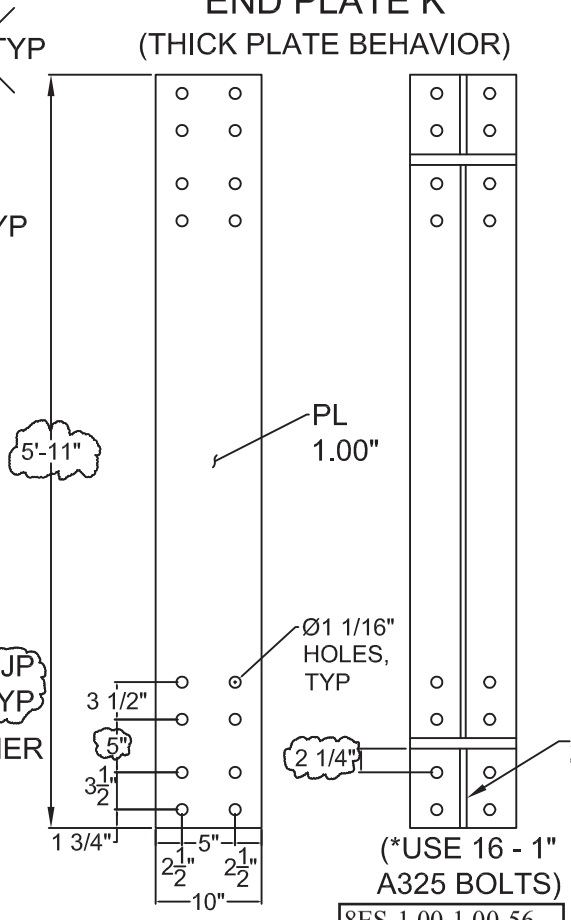

8ES-1.00-1.00-56

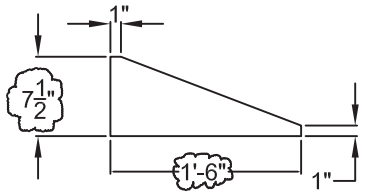

DETAIL 1

QUANTITY: 2 SPECIMENS EACH AND ALSO SHIP LOOSE ONE ADDITIONAL END PLATE OF EACH TYPE (J AND K) FROM THE SAME HEAT OF MATERIAL AS USED FOR THE SPECIMEN.

$F_{y\ end\text{-}plate}$ = 55 ksi ASSUMED

NO BLAST, NO PAINT

E70 ELECTRODES FOR ALL WELDS

NOTE: HOLE LOCATION ON OPPOSITE END OF PLATE ARE SYMMETRICAL

VIRGINIA TECH	TITLE: SPECIMEN 05	DRAWN BY: NJ, REV 1
PROJECT: MBMA END-PLATE MOMENT CONNECTIONS	11/19/14	SHEET 14

Appendix E Additional Data from Tests

6B-4W/2W-1.125-0.75-36

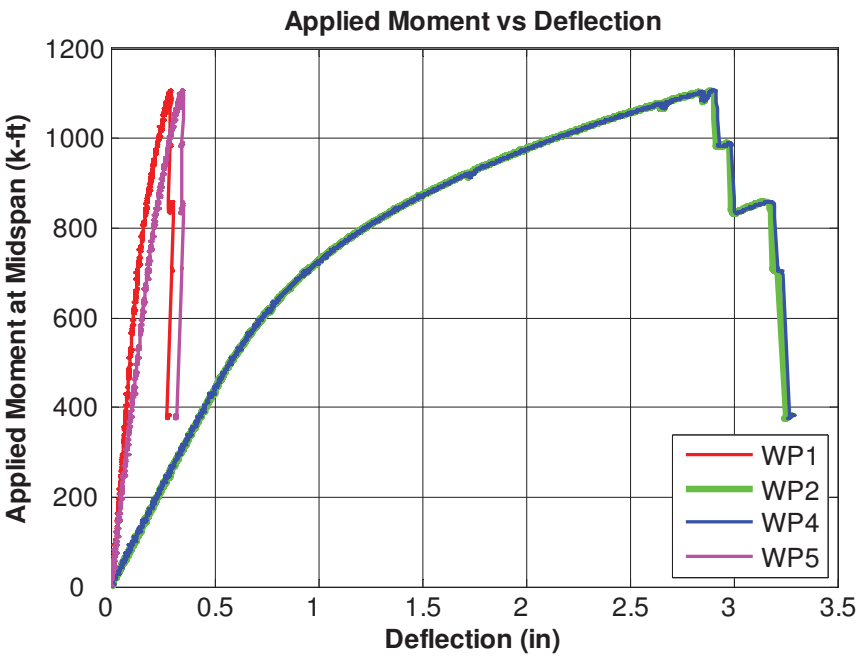

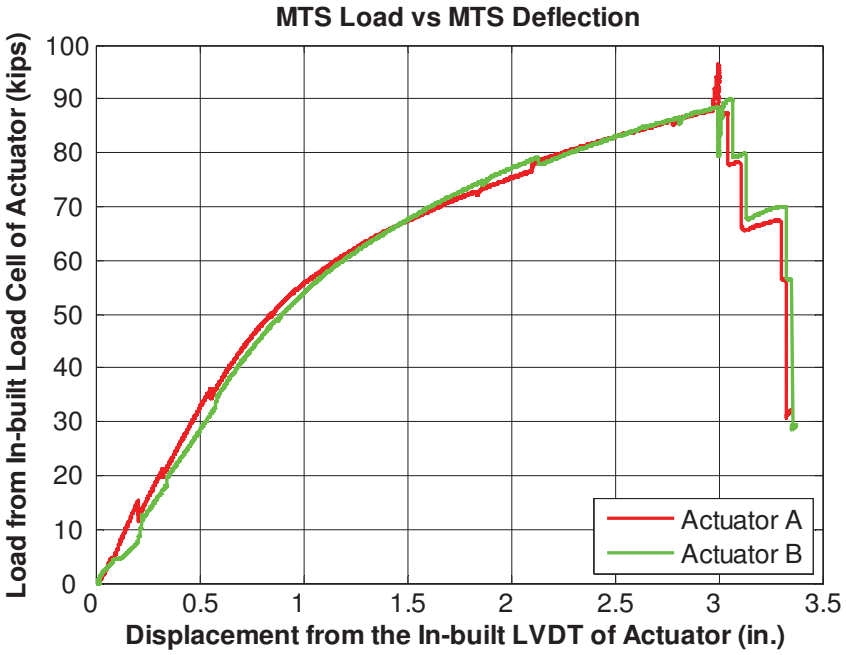

6B-4W/2W-0.875-1.00-36

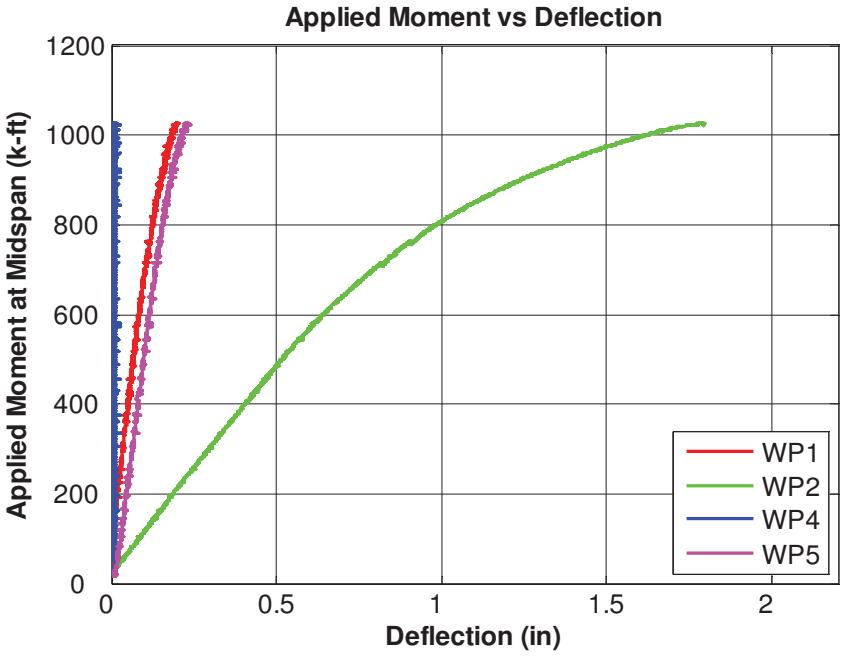

Note: WP4 didn't work

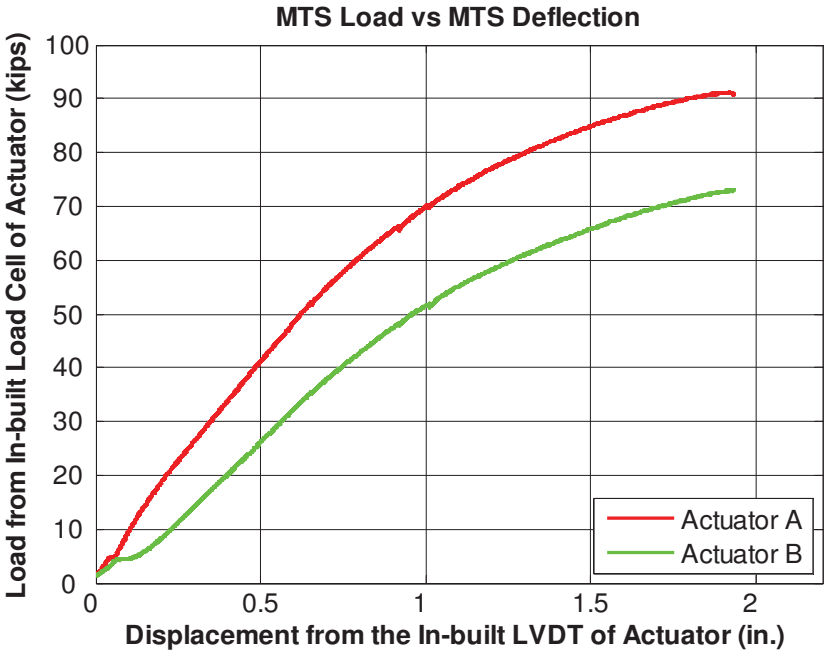

6B-4W/2W-1.125-0.75-60

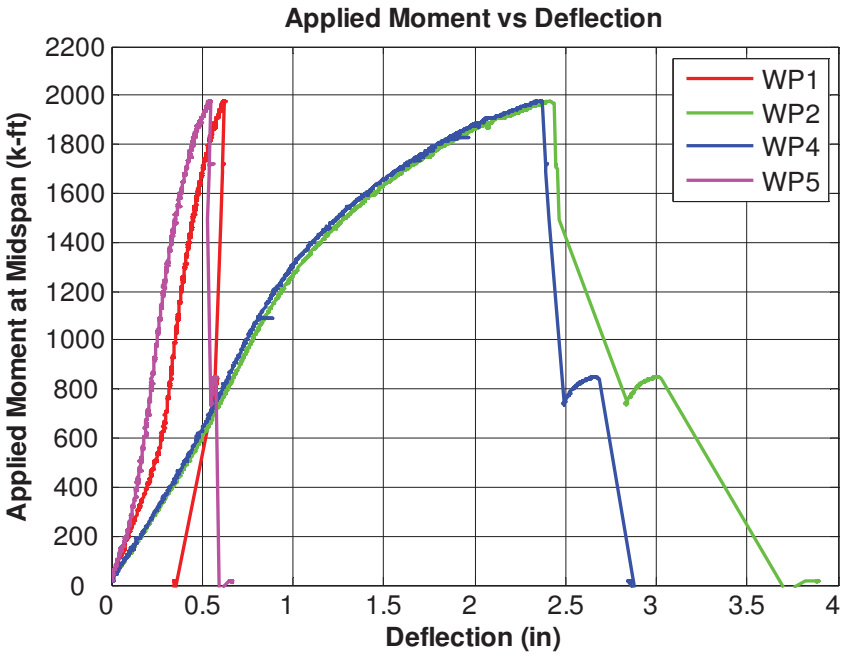

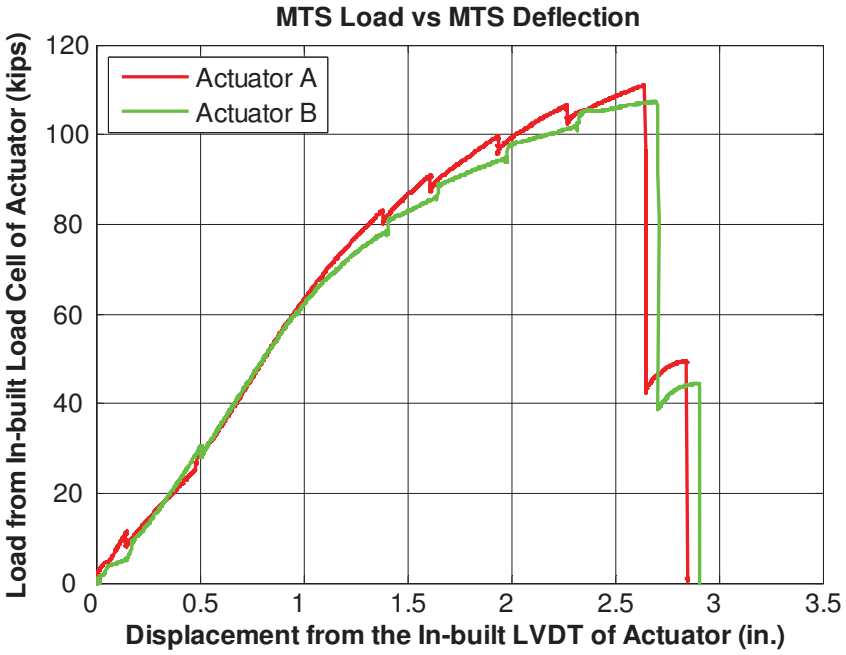

6B-4W/2W-0.875-1.00-60

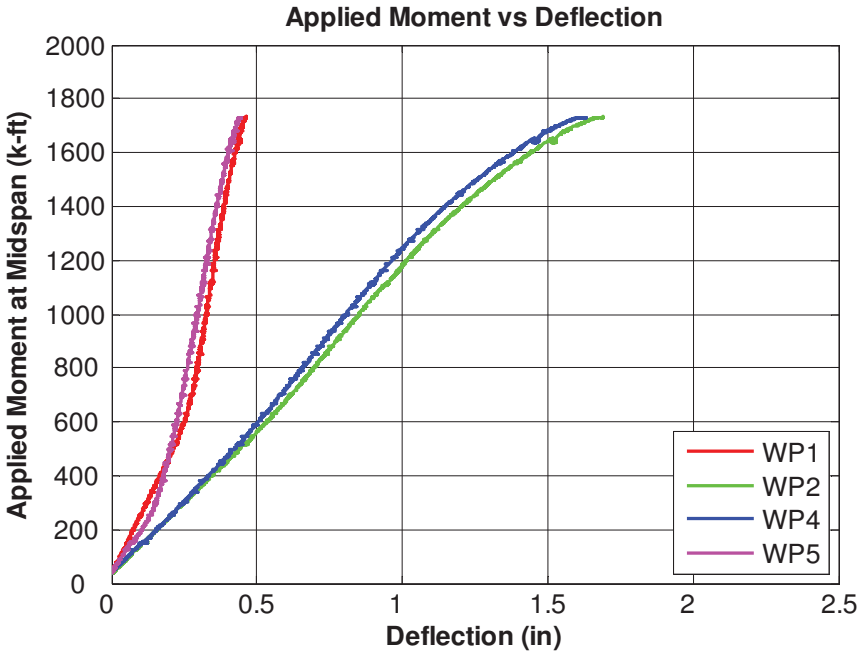

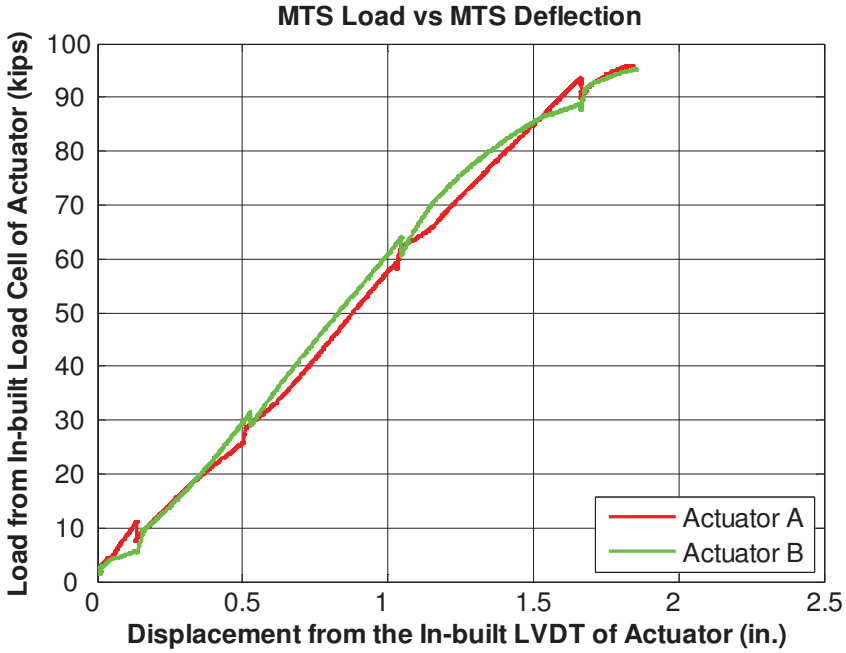

12B-MRE 1/3-4W/2W-1.00-0.75-36

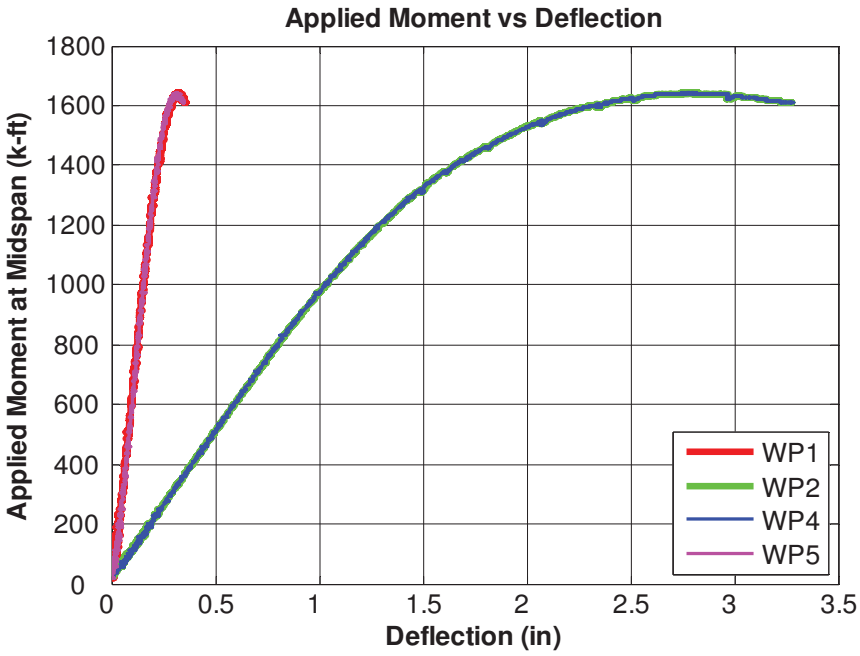

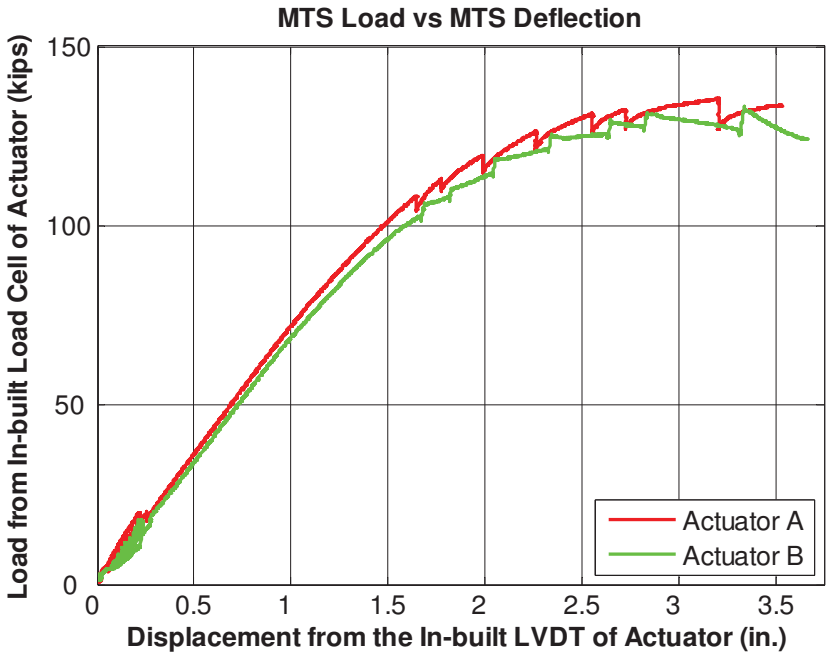

12B-MRE 1/3-4W/2W-0.75-1.00-36

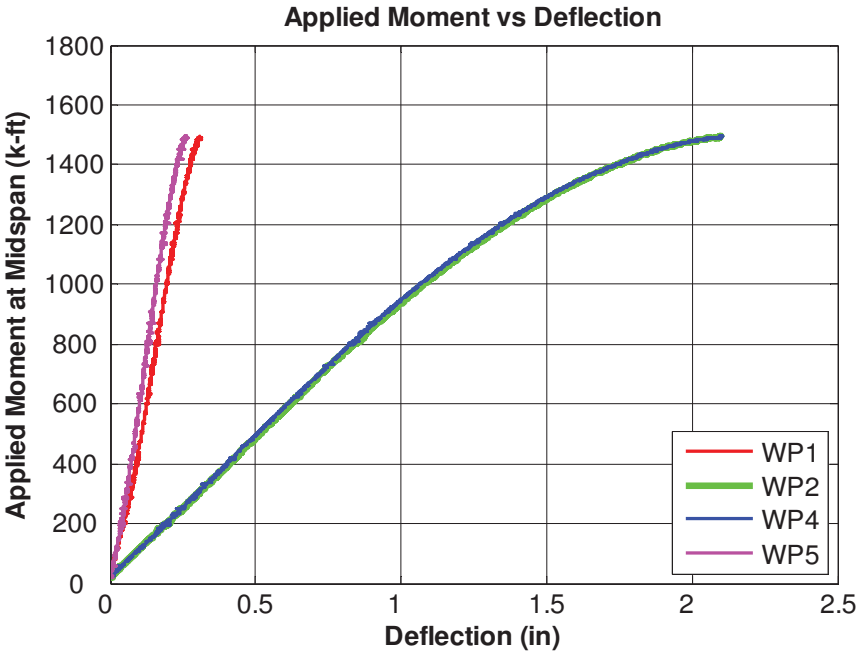

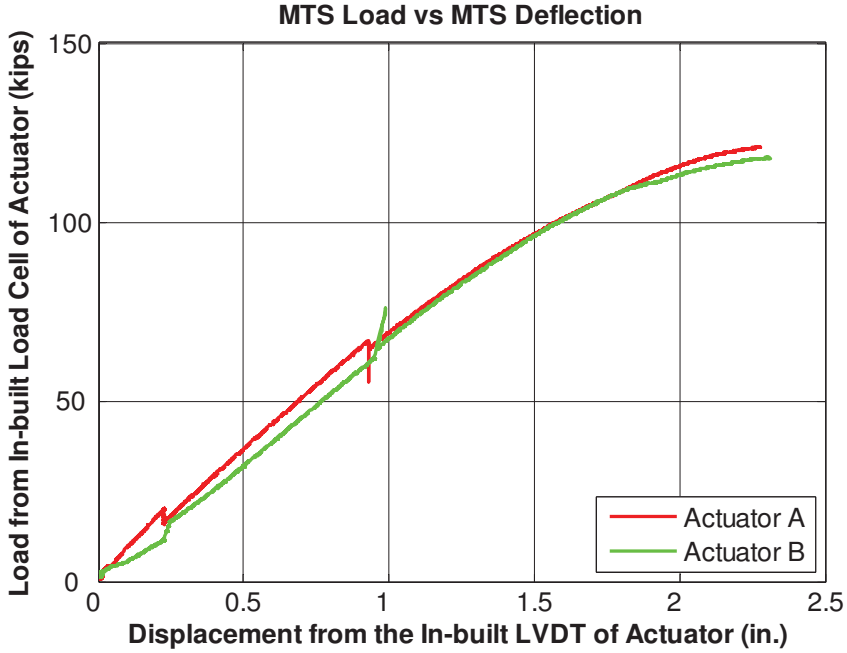

12B-MRE 1/3-4W/2W-1.00-0.75-60

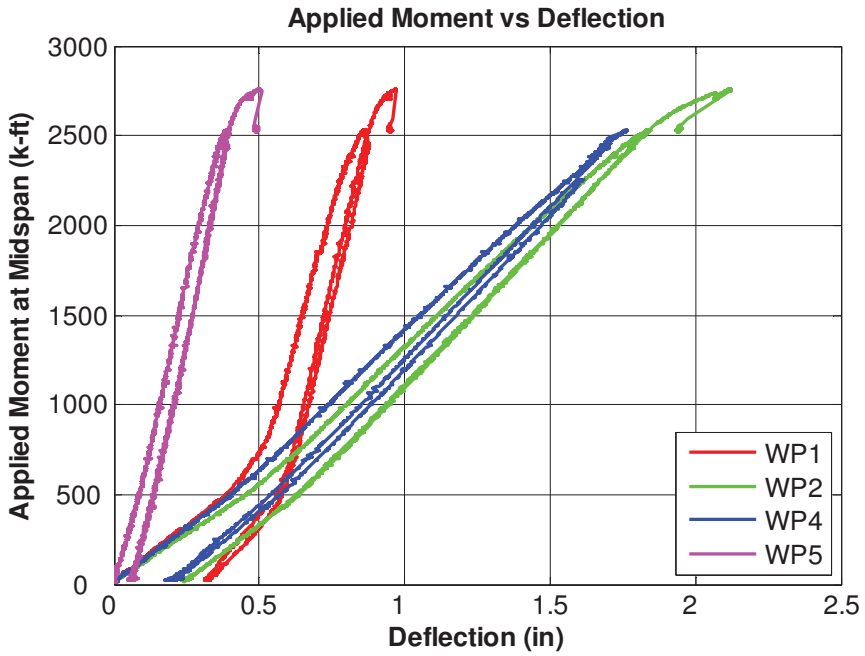

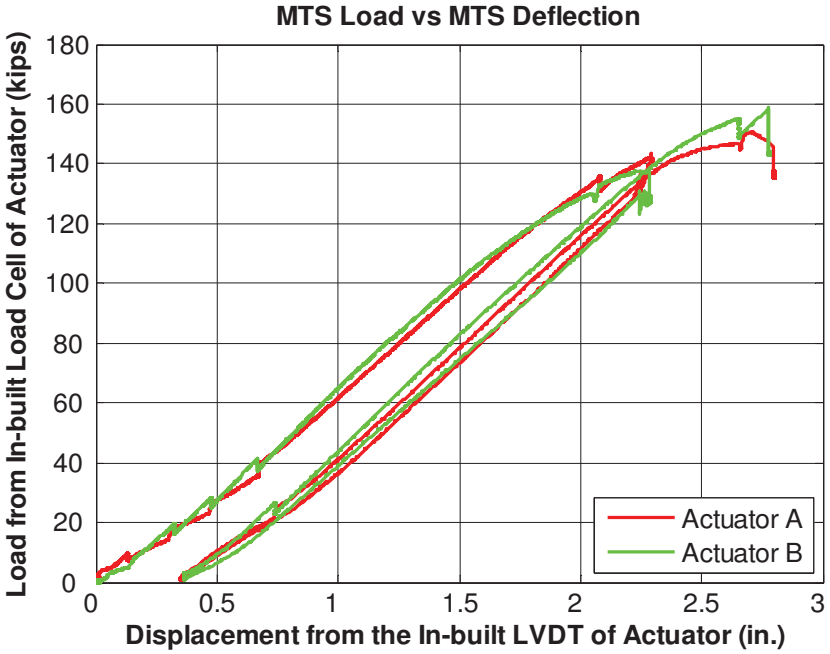

12B-MRE 1/3-4W/2W-0.75-1.00-60

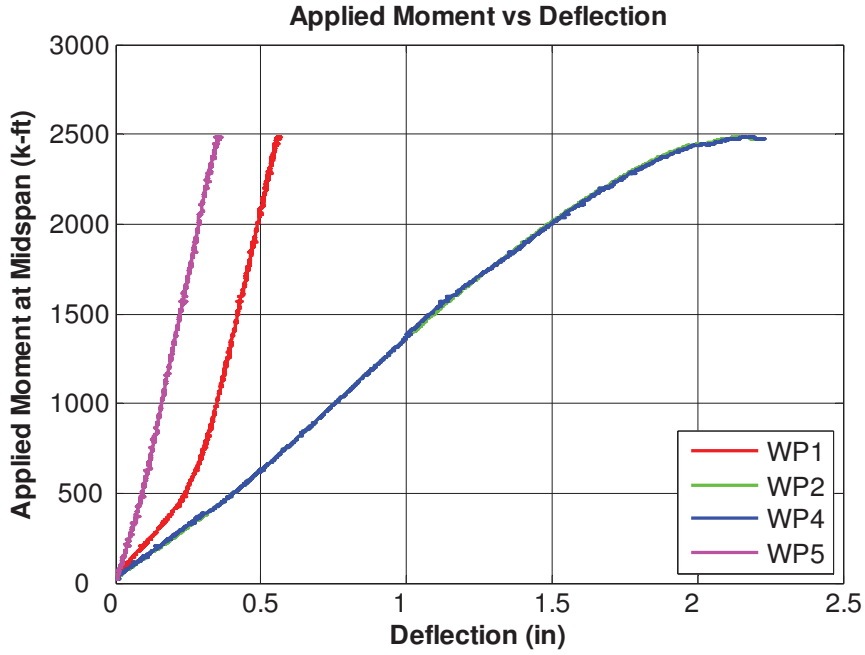

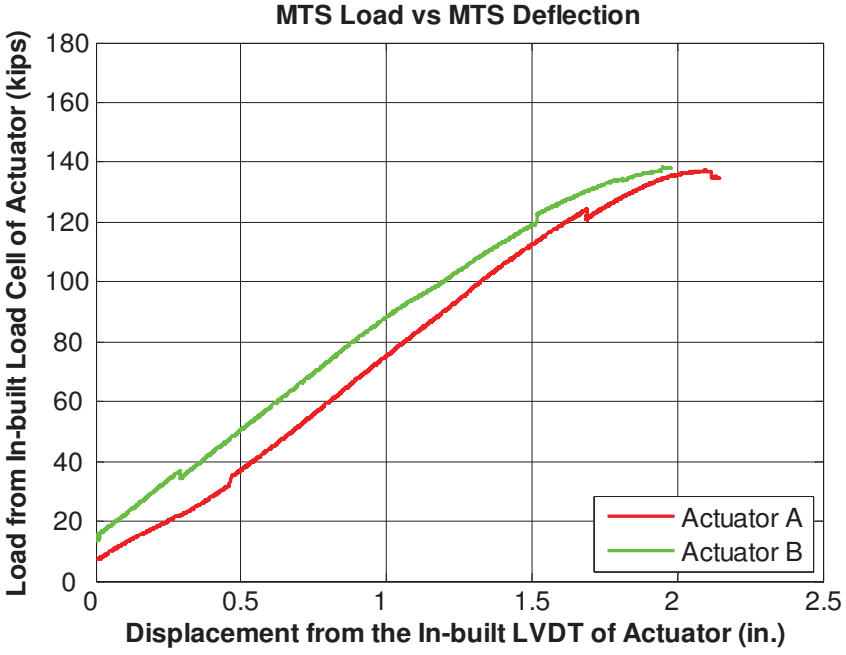

8ES-1.25-0.75-56

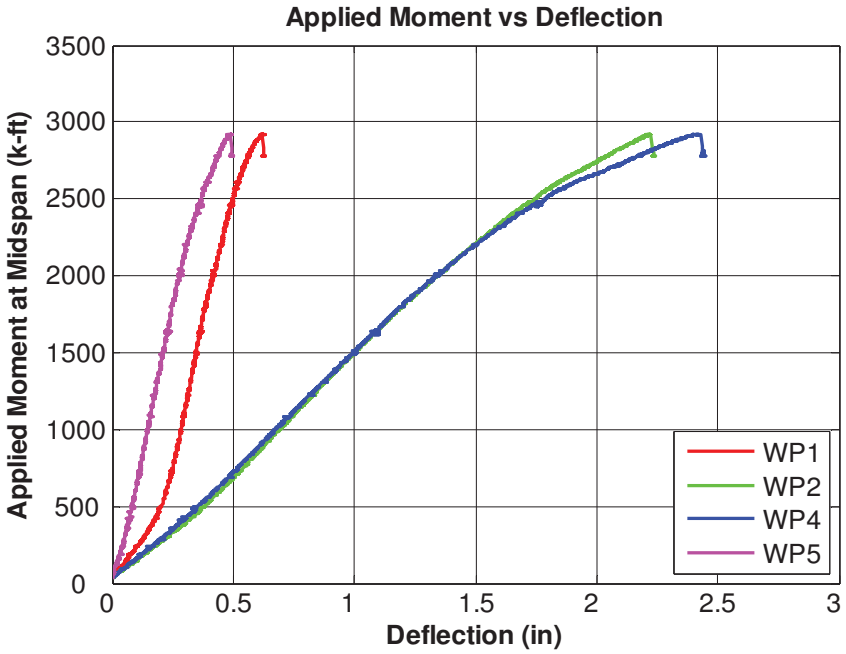

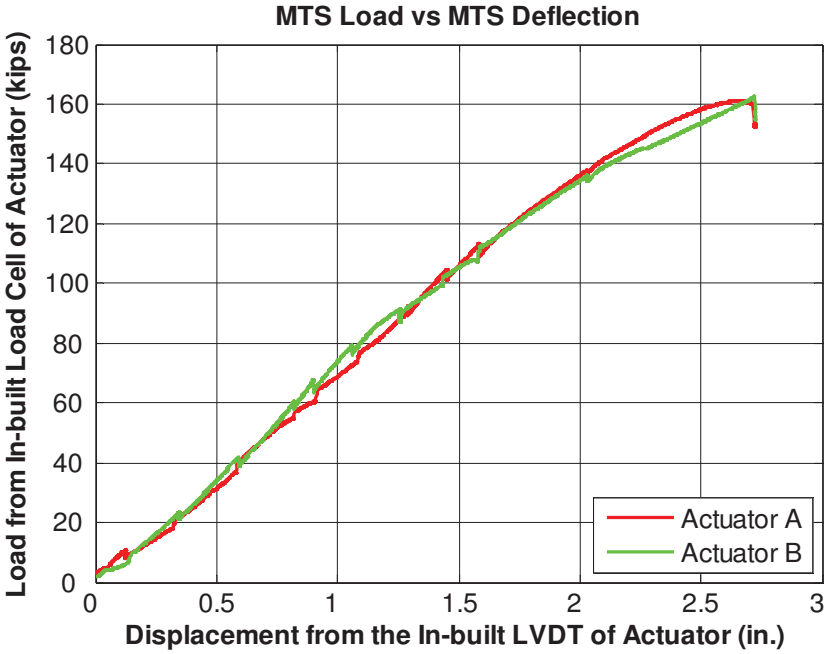

8ES-1.00-1.00-56